DOE/NASA/0043-2
NASA CR-159848
MTI 79TR76

HIGH TEMPERATURE SELF-LUBRICATING COATINGS FOR AIR LUBRICATED FOIL BEARINGS FOR THE AUTOMOTIVE GAS TURBINE ENGINE

Bharat Bhushan
Mechanical Technology Incorporated

April 1980

Prepared for
NATIONAL AERONAUTICS AND SPACE ADMINISTRATION
Lewis Research Center
Under Contract DEN 3-43

for
U.S. DEPARTMENT OF ENERGY
Conservation and Solar Applications
Transportation Energy Conservation Division

DOE/NASA/0043-2
NASA CR-159848
MTI 79TR76

HIGH TEMPERATURE SELF-LUBRICATING COATINGS FOR AIR LUBRICATED FOIL BEARINGS FOR THE AUTOMOTIVE GAS TURBINE ENGINE

Bharat Bhushan
Mechanical Technology Incorporated
968 Albany Shaker Road
Latham, New York 12110

April 1980

Prepared for
National Aeronautics and Space Administration
Lewis Research Center
Cleveland, Ohio 44135
Under Contract DEN 3-43

for
U.S. DEPARTMENT OF ENERGY
Conservation and Solar Applications
Transportation Energy Conservation Division
Washington, D.C. 20545
Under Interagency Agreement EC-77-A-31-1040

FOREWORD

The study reported herein, which was conducted by Mechanical Technology Incorporated under the NASA Contract No. DEN3-43, was performed under the program management of Mr. Harold E. Sliney, Head of Lubricants Section, NASA-Lewis Research Center. The author also wishes to thank Mr. S. Gray, Dr. G. J. Stelma, Mr. G. Pellissier from MTI; Mr. Frank Murray of RPI; and Mr. H. Sliney of NASA for useful discussions and recommendations during the program. The experiments were conducted by Mr. J. Wilson.

TABLE OF CONTENTS

TABLE OF CONTENTS (CONT'D)

TABLE OF CONTENTS (CONT'D)

TABLE OF CONTENTS (Cont'd)

LIST OF FIGURES

LIST OF FIGURES (cont'd)

LIST OF FIGURES (cont'd)

LIST OF FIGURES (cont'd)

LIST OF FIGURES (cont'd)

LIST OF TABLES

LIST OF TABLES (Cont'd)

EXECUTIVE SUMMARY

The objective of this program was to further develop the coating combinations identified in a previous program for compliant surface bearings and journals to be used in an automotive gas turbine engine. The coatings should be able to withstand the sliding start and stop contacts during rotor liftoff and touchdown under the representative loading of the engine of 14 kPa (2 psi) and up to 35 kPa (5 psi) if possible, and at a maximum temperature of 427°C-650°C. They should also be able to withstand occasional short-time, high-speed rubs at service temperature with a maximum loading of 6 g.

Some dozen coating variations of Cr_2O_3 (sputtered), CdO-graphite and Ag addition (air sprayed), and CaF_2 (plasma sprayed) were identified. Limited work was done on Cr_3C_2 (sputtered, detonation gun), $PbO-SiO_2$-Ag (fused), CaF_2-BaF_2-Ag (fused), HfN (ARE), TiC (ARE), CaF_2-ZrO_2 (plasma sprayed) and other proprietary Kaman DES and SCA coatings. Coatings application parameters were optimized. The coatings were examined for stoichiometry, metallurgical condition and adhesion.

As discussed later, sputtered Cr_2O_3 and air sprayed CdO-graphite-Ag coatings on bearing surfaces were particularly successful in screening tests.

Great care is required in the selection of optimum sputtering parameters to obtain adherent Cr_2O_3 coatings. Annealed substrates, metallic binders and interlayers have been investigated as a means of improving the ductility and the adherence of the coatings. Metallurgical examinations were conducted on the samples to screen out the good coatings. SEM photographs were taken up to 10,000X for examination of surface morphology. A 180° bend test, where coated foil samples were bent on themselves, was conducted to determine the coating adhesion and cohesion. Adhesion strength of the coating was measured using a tensile type tester. Flex tests on the coatings were done. An Auger electron spectroscopic analysis was conducted to determine the elemental composition of the surface and to determine uniformity through the coating. X-ray diffraction analysis was conducted to determine the structure of the materials.

Low pressure in the sputtering system, less target-substrate spacing, high power, water-cooled substrate and sputter-deposit mode improved the coating adhesion and its smoothness. Biased coatings were not as adherent as sputter-deposited coatings and had a lot of internal stresses. The cleanliness of the substrate, target, and the system was extremely crucial. The sputtering parameters had no influence on the coating composition. The optimized parameters for Cr_2O_3 coating in our sputtering system were:

Spacing mm	Power Watts	Chamber Pr Microns	Bias Sputter	Water Cooled Substrate	Coating Thickness µm (µin.)
41.3	390	6	No	Yes	1.02 (40)

The adhesion strength (in tension) was in excess of 68.9 MPa (10 ksi). The coatings as sputtered were amorphous after heat treatment, they crystallized and the structure was identified as Cr_2O_3.

Ni-Cr bonded Cr_2O_3 was found to have improved ductility as indicated by the bend tests but the coating did not perform very well during start-stop tests. The scratch resistance of the coating did not change from the Ni-Cr addition. Further optimizations are recommended.

In order to further improve the performance of CdO-graphite, Ag particles were added. A very fine silver grade (particle size 1 to 5 microns) was needed to obtain a uniformly dispersed coating which would not pull off easily during burnishing and the sliding.

The optimized coatings were first applied on flat test coupons (50 mm x 50 mm) which were subjected to static oven tests. The tests were conducted to screen out those coatings which could not stand the extended thermal exposure and thermal cycling. The tests consisted of exposure of material samples in an oven for 100 hours duration at service temperatures of 427°C, 540°C or 650°C, and exposure to 10 temperature cycles from room temperature of the service temperatures.

After the oven tests, the specimens were examined using the following techniques: flex bending test, tape test, scratch test, superficial hardness test, weight change and metallurgical examinations. The surface morphology of coatings was examined in the Scanning Electron Microscope (SEM). Microprobe analysis was utilized to determine the elemental composition.

The selected coatings were applied on the bearing and journal surfaces and were subjected to start-stop tests. The start-stop cycle tests consisted of testing partial-arc bearings at 14 kPa (2 psi) loading based on bearing projected area for 3000 start-stop cycles at maximum service temperature, 3000 start-stops at intermediate temperature and 3000 start-stop cycles at the room temperature, a total of 9000 start-stop cycles. Static and dynamic breakaway torques were recorded during the tests. Based on torque data, visual examinations and metallurgical examinations of the bearing surfaces, the following combinations were recommended:

Foil Coating	Journal Coating	Maximum Test Temperature °C (°F)
CdO-Graphite-Ag	Det. Gun and Ground	427
(HL-800-2)	Ni-Cr bonded Cr_3C_2	(800)
8-10 μm thick	60-90 μm thick	
Sputtered Cr_2O_3	Det. Gun and Ground	650
1 μm thick	Ni-Cr-bonded Cr_3C_2	(1200)
	60-90 μm thick	

Cr_2O_3 versus Cr_3C_2 coating combination was further successfully tested in full bearing tests to ensure that any wear debris generated would not give any problem. This coating combination has also been successfully tested for a total of 9000 start-stop cycles at a normal load of 14 kPa (2 psi) and at a maximum test temperature of 427°C (800°F).

Both the coating combinations were also tested during start-stop cycles at a higher normal load of 35 kPa (5 psi) loading. The coatings were able to survive for 3000 start-stop cycles at this load.

Finally, both the coating combinations were tested under shock loading with the journal running at 30,000 rpm. Contact resistance measurement between the bearing and the rotating journal verified that each shock level provided micro-contacts during shock application. Both the coatings survived 100 g's of impact and further testing was terminated because the foil bumps deformed at this loading level. It should be noted that the anticipated g level in the automotive gas turbine engine is six and this requirement was greatly exceeded.

I. INTRODUCTION

BACKGROUND

The U. S. Department of Energy has funded the development of an automotive gas turbine engine that will meet proposed Federal emission standards and demonstrate improved fuel economy over a comparable internal combustion engine. To enable future automotive gas turbine engines to achieve the performance requirements, the engine must be compact, operate at high rotational speeds, utilize high turbine gas temperatures, and be cost competitive. The high turbine gas temperatures will impose temperature requirements on turbine end support bearings that will impose serious design penalties upon the use of oil lubricated support bearing systems in these areas. The self-acting (hydrodynamic) air lubricated compliant journal bearing is a likely candidate to fill this requirement.

Potentially, the compliant air lubricated bearing offers the following advantages in the gas turbine engine:

- Higher cycle operating temperatures
- Elimination of oil requirements and limitations
- Greater accomodation of thermal distortions, assembly variations, and dynamic shaft motion because of bearing compliance
- Reduced frictional power loss at high speed
- Reduced rotor noise
- Lower bearing costs

MTI has designed, fabricated, and developed a 38 mm (1.5-inch) diameter, HYDRESIL^{TM}, air-lubricated, compliant journal bearing for use at the drive turbine end of the gas generator of the A-296 Upgraded Chrysler/ ERDA Automotive Gas-Turbine Engine, and this bearing is now used in the engine development program operating at up to 315°C (600°F) ambient temperature.

The basic construction of a Hydresil bearing is shown in Figure I.1. The bearing consists of a top foil and a bump foil in a cartridge assembly.

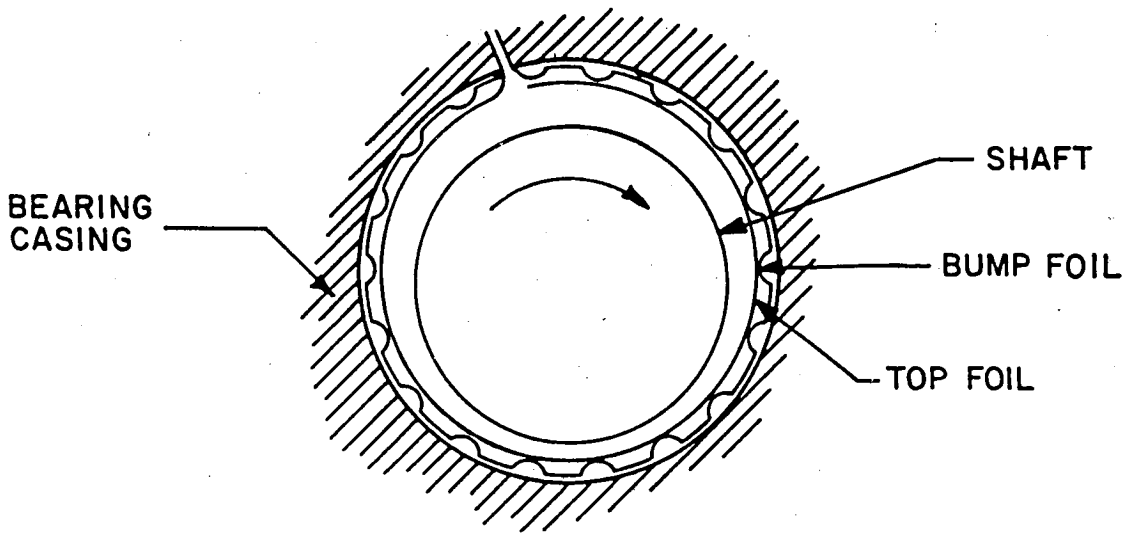

Fig. I.1 Basic Construction of a HYDRESIL Journal Bearing

The bump foil gives distributed elastic support for the top foil which provides the bearing surface. The elastic support provides resilience and frictional damping in the bearing. Both foil members are only 0.1 mm thick. Extremely important to the success of the hydrodynamic foil bearing, particularly when having to operate over a temperature range from below normal ambient up to 650°C (1200°F) and to speeds greater than 60,000 rpm, as anticipated in the advanced automotive gas turbine, is the selection of the journal and foil substrate materials and of wear resistant and lubricant coatings for the bearing foils. The materials and coatings must be suitable for the range of environmental temperatures, be capable of surviving the start-stop sliding contact cycles encountered before rotor liftoff and at touchdown, and survive occasional short-time, high-speed rubs.

In a recent two-part technology program, which was sponsored by NASA, the MTI Hydresil compliant hydrodynamic journal foil bearing was first extensively evaluated to achieve a greater understanding of the characteristics of the foil type of air bearing. The air film thickness around the bearing was measured from the rotating journal and the influence of end leakage of the air on bearing performance was determined. Then the maximum load capacity of the bearing in a 315°C (600°F) ambient was measured [1.1]*. Secondly, an intensive study was undertaken on a number of candidate materials and coatings. Static screening experiments and dynamic rig testing at temperatures up to 650°C (1200°F) were performed. The dynamic testing consisted of the simulation of start-stop sliding contacts [1.2]. In these studies, a baseline of coating performance was established at different operating temperature levels up to 650°C (1200°F).

In the program reported here, the major effort was applied to the most promising coating systems identified in the previous program. They were subjected to a careful review to determine what variables might be significant in effecting and improving long-life performance. Composition and techniques of coating application were developed or modified to improve coating systems life. Candidate materials were subjected to intensive static and dynamic tests at temperature. A parallel but minor effort was

* Numbers in brackets indicate references listed at the end of this report.

maintained to develop other promising coating candidates and introduce new coating systems for the advanced gas turbine into the program.

PROGRAM OBJECTIVE

The prime objective of the program was to develop bearing and journal materials and coatings suitable for use up to 650°C (1200°F). The approach was to further improve and develop the most promising material coating systems evaluated or identified in the previous program under NASA Contract NAS3-19427; these are Items (i), (ii), and (iii) in the following listing. In addition, Items (iv) and (v) were developed and tested.

	Foil (Inconel X-750)	Journal (A286)	Temperature Range
(i)	Cadmium oxide + graphite	Chrome carbide	Ambient to 370°C (700°F)
(ii)	Uncoated	Fluoride, silver compositions	Ambient to 540°C (1000°F)
(iii)	Chrome oxide (Sputtered & Kaman DES)	Chrome oxide (Sputtered & Kaman DES)	Ambient to 650°C (1200°F)
(iv)	Chromium carbide	Chromium carbide	Ambient to 650°C (1200°F)
(v)	Uncoated, preoxidized	Uncoated, preoxidized	Ambient to 650°C (1200°F)

A parallel effort on softer coatings for the 540-650°C (1000-1200°F) range was maintained because of potential problems with loose abrasive particles associated with hard particles. Soft coatings explored in this program were: $PbO-SiO_2$-Ag coating and CaF_2-BaF_2 eutectic-Ag coating.

The program consisted of a combined material process modification and experimental evaluation study.

PROGRAM APPROACH

The program approach, aimed at achieving improved coatings performance, was to subject selected candidates (and candidates with process modifications) to the following evaluation sequence:

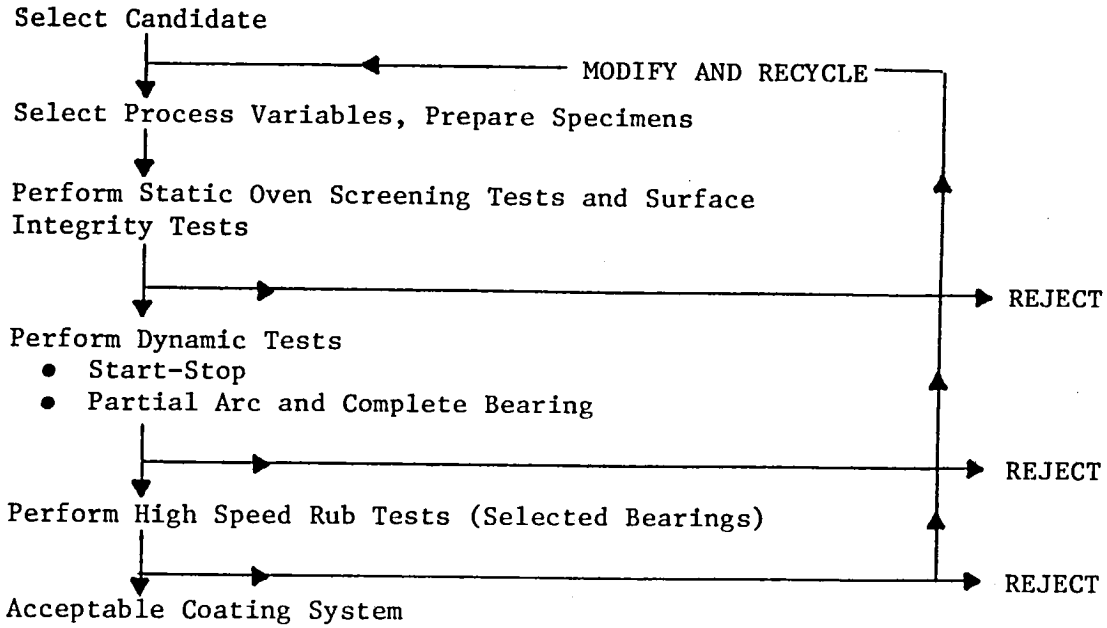

The plan provided means for recycling promising candidates for further refinement. From a practical point of view, program candidates were handled in groups.

Extremely important in the proposed program has been the effort to ensure the quality of specimens, care in screening, planning of the test matrices, and the quality of specimen analysis.

II. MATERIAL SURVEY AND SELECTION OF COATING MATERIALS

CONSIDERATIONS IN COATING SELECTION

When a hydrodynamic gas bearing starts or stops, the bearing and journal surfaces come in physical contact. Solid lubricants and/or hard wear resistant coatings are applied on the rubbing surfaces to minimize friction and wear.

The type of damage which is of primary concern is that which results from the successive adhesion and breaking of opposing micro-peaks or asperties in the surfaces. This is known as adhesive wear. If hard coatings are used, they can come off at places in the form of small particles and these particles trapped in the bearing clearance would lead to abrasive wear. In this event, every effort has to be made to remove the wear debris from the bearing. So our primary concern is to select materials which have low adhesive and abrasive wear and low coefficient of friction.

The conventional solid lubricants should have: low shear strength; good crystalline structure with preferred slip planes, e.g. layered lattice structure; good adhesion to the substrate; low hardness; and should be free from any abrasive contamination. The limitation of these lubricants is low temperature capability. For high temperature applications, hard wear resistant coatings are used which do not necessarily have low friction. These coatings should be extremely hard and, of course, should have good adhesion to the substrate.

Some reaction products with air provide effective lubrication in the temperature range they are formed [2.14]. In addition, many ceramic combinations can interact to form eutectic compounds which behave as low shear strength solid films. In most cases, such preferential interactions are limited to high-temperature or high-energy input conditions, but the possibility of deriving some benefit from this type of reaction should not be overlooked since this effect would be most evident during very severe operating conditions such as a high speed rub at high ambient temperatures.

There are several other properties which do not influence friction and wear properties directly, but are important in selecting an optimum coating:

- Mechanical Properties: The coating's yield strength and modulus of elasticity, and ductility should be compatible with the substrate in the temperature regime. The solid lubricants should be extremely ductile much more so than the substrate - for low shear strength and self-healing flow characteristics. The hard coatings should have high fatigue, impact, and tensile strength to follow substrate deformation without cracking.
- Thermal Stability: One of the advantages of solid lubricant coatings is their usability at temperatures higher than that of organic lubricants (<200°C). The coatings should be stable at elevated temperatures; i.e. should have adequate oxidation resistance.
- Thermal Conductivity: Frictional heat is generated at the interface during sliding. If the thermal conductivities of the sliding members are low, the heat cannot be dissipated and high surface temperatures are generated which can cause local melting and surface chemical reactions. Therefore, coatings should have high thermal conductivity to rapidly dissipate frictional heat from the interface except for the cases where the reaction products or localized melting enhance lubrication of the surface.
- Thermal Expansion: The coefficient of linear thermal expansion of the coating should be close to that of the substrate to minimize any interfacial stresses at temperature or during cooling and heating. The coating should also be dimensionally stable.
- Melting point: Solid lubricants lose much of their friction-reducing property above their melting point because their solidity is due to the strong lateral attraction between the molecular chains composing them which, combined with low shear strength, makes them effective, solid lubricants [2.1]. Above the melting point the lateral attraction is destroyed by thermal motion and the metal surfaces are no longer prevented from contacting and welding at high points.
- Corrosion resistance: The coating should not cause corrosion of the parts.

- Chemical Inertness: Solid lubricants should be inactive to the atmosphere, especially in the presence of high humidity. Inertness to reactive acids, alkalies, and to organic fluids is also a useful property under some conditions.
- Electrical Conductivity: High electrical conductivity is needed if the coatings are used to reduce wear of sliding contacts. When insulators are subjected to rubbing contact, a solid lubricant of low electrical conductivity must be used.
- Density: For solids which are applied in the form of dispersion in a liquid, low density material makes it easier to maintain a stable dispersion.
- Reactive replenishment: Coatings do wear. Oxidation of the substrate and the adjoining coating surface at high temperature during testing replenishes the oxide film continuously and thus protects the surface; this is known as reactive replenishment. This property is normally absent in solid lubricants.

SELECTION OF FOIL AND JOURNAL MATERIALS

The selection of foil and journal materials was made in the previous program [1.2] and the same materials are used here. Inconel X-750 was selected for foil bearings for the following reasons: prior favorable experience with the material, acceptable mechanical and thermal properties, ease of heat treatment, formability, availability in foil form, and cost. A-286 was selected for journals for the following reasons: acceptable mechanical and thermal properties at elevated temperatures, good machinability, availability, and cost. The properties of these materials can be found in Bhushan et. al. [1.2].

COATING MATERIAL SURVEY

A fairly large number of coatings and treatments for foil and journal surfaces were selected in a previous program [1.2, 2.2, and 2.3]. The materials consisted of solid lubricants, hard and wear-resistant coatings, diffusion treatments, and proprietary coatings. Due to a thin

substrate, the foil member could be coated only with these films by physical vapor deposition, resin bonding, and fusion processes. The materials were subjected to static oven tests and start/stop tests. Based on the tests, the following materials were recommended for further optimization:

FOIL COATING	JOURNAL COATING	MAXIMUM TEST TEMP. ^{o}C (^{o}F)
CdO-Graphite (HL-800)	Det. Gun - 25% Ni-Cr, 75% Cr_3C_2	370 (700)
Uncoated and Heat Treated	Plasma Sprayed NASA PS120 (20% CaF_2, 6% Tribaloy 400, 20% Ag)	540 (1000)
Kaman DES (Proprietary Cr_2O_3)	Kaman DES	650 (1200)

In the previous program, Kaman DES performed very well in the partial arc bearing tests, but the wear debris collected at the interface in the full bearing tests. This coating is primarily Cr_2O_3.

Murray [2.4] tested a number of materials for tilted pad gas bearing application. He conducted 1000 start/stop tests at 28kPa (4 psi) and high speed rub tests at speeds up to 60,000 rpm. Based on his tests at room temperature, plasma sprayed chrome oxide versus itself was the best combination. No significant work has been done to develop sputtered Cr_2O_3 coating. This coating was first developed by Perrot [2.5] for optical purposes. Later it was used in the foil bearing work, e.g. [2.2]. However, no systematic optimization of sputtering parameters has been done.

TiC and TiN deposited by sputtering, evaporation, and chemical vapor deposition techniques have been investigated in metal cutting tools, ball bearings, and other sliding applications [2.6 to 2.9]. The performance of rf-sputtered TiC was compared to sputtered coatings of TiB_2, Mo_2B_5, $TiSi_2$, $MoSi_2$, Mo_2C, and B_4C by Brainard et. al. [2.7].

Friction and wear results on rf-sputtered coatings at room temperature showed that the carbides, in general and TiC in particular provided the best wear performance. At very light loads (<1.0N), TiB_2 coatings showed good

wear properties and low friction. It should be noted here that TiC is stable below 540°C (1000°F). Sharma et. al. [2.6] investigated the CVD (chemical vapor deposition) coating for cemented carbide cutting tools. TiN has also been applied by CVD in metal cutting applications. The disadvantage of this process is that the deposition temperature is very high (about 900°C) which many times adversely affects the substrate heat treatment and subsequent machining is required because of some deformation during the process.

Brushan et.al. [2.8] have tested the cutting performance of cemented carbide tools coated with HfN and TiC by the activated reactive evaporation (ARE) process. The tool life of the HfN-coated tools was better than that of TiC-coated tools. However, the flank wear rate of the TiC-coated tools was better than that of the HfN-coated tools. Since crater wear is the primary mode leading to failure of the cutting edge, the HfN coating appears to be better than the TiC coating. TiC coated high speed steel tools [2.8] exhibited a tool life of 300-800% higher than the uncoated tools under continuous cutting conditions. Cutting forces also decrease by about 1/2 which indicated that the coefficient of friction must also markedly decrease.

TiC, TiN, and HfN all have a cubic crystal structure. They are all susceptible to oxidation above 540°C [2.10]. In fact, TiC is reported to oxidize at a significant rate above 430°C [2.11]. While oxidation products may protect the coating, because these materials form an adherent, protective oxide surface layer, one would be evaluating the TiO_2 or HfO_2 that is formed on the surface.

Nevertheless, these coatings were selected for evaluation because they perform well on cutting tools, but it should be noted that they are being used on very rigid, hard substrates (e.g. high speed steel and currented carbide tools). Since in our foil bearing application the substrate is soft and flexible, cracking is a potential problem.

WC + Co rf-sputtered coating has been investigated by Eser et. al. [2.12] for gas bearing application. It was believed that the presence of the

cobalt binder reduced both friction and wear because cementing action reduces granular separation and promotes a dense polished layer since it has low, shear strength forming properties. By adjusting the sputtering parameters they were able to obtain a wear-resistant coating. However, WC will not be stable at 650° C.

Plasma sprayed or detonation gun chrome carbide coatings have been used as a journal coating rubbing against solid lubricants; e.g. see Bhushan et. al.[2.3]. The detonation gun coating is very dense, and with care it can be ground to 0.025-0.05μm (1-2μin.) rms. It should be noted that chrome carbide is stable at 650°C. Another coating: plasma-sprayed Cr_2O_3 was too susceptible to thermal spalling above 540°C (e.g. see [2.2]) to be considered a viable candidate coating.

Sputtered Cr_3C_2, Cr_3Si_2, and $MoSi_2$ were deposited by sputtering techniques [15]. The coatings were well adhered to the substrate and during sliding, Cr_3Si_2 films exhibited a coefficient of friction two to three times lower than that of Cr_3C_2.

From this review it seems that hard coatings deposited by physical vapor deposition have a potential, and there is a need to optimize the coating parameters. Sputtering and evaporation techniques are especially attractive for foil surfaces because the coatings are too thin to adversely affect the foil properties. Therefore, heavy emphasis has been placed on the sputtered coating. The coating on a journal can be applied by almost all the processes. Cr_2O_3 was selected for sputtered coating development because Kaman DES (essentially Cr_2O_3 applied by a proprietary process) performed well in a previous program (see Bhushan et. al. [1.2]). Limited work was done on sputtered Cr_3C_2.

A parallel emphasis is placed on solid lubricants which are evaluated in this program. The lubricants are PbO coating system and CaF_2 coating system. The details on each coating system selected follows.

Chrome Oxide Coating Systems

(i) Kaman Cr_2O_3

In the previous program [1.2], Kaman DES coatings performed satisfactorily for 2000 start/stop cycles up to 650°C (1200°F). Kaman Sciences Corporation was consulted to explore other variations. They felt that the optimum thickness of Kaman DES coating is 1.3 to 13 μm (0.05-0.5 mil). In the previous program, the coating thickness on the foil was 1.3 to 3 μm (0.05-0.1 mil) and on the journal it was 8 to 13 μm (0.3-0.5 mil). The thickness of the coatings on the flexible member was kept low to avoid flaking of the coating and to minimize loose wear debris.

Kaman also produces the SCA 1002 coating which can be applied 13 to 51 μm (0.5-2 mils) thick. SCA 1002 is a cermet consisting primarily of Cr_2O_3 and small amounts of SiO_2, Al_2O_3, and a very small amount of metallic binder ZiO_2. According to the vendor, SCA has better bond strength and better wear resistance than DES. SCA bonds better on DES than on a metal substrate. SCA is too thick for the foil, but should be acceptable for the journal. One recommendation for the foil was to apply a thin coating of DES, about 3 μm (0.1 mil), and then coat with diluted solution of SCA to a total thickness of 13 μm (0.5 mil) and this would cover about 80% of the area by SCA. If this coating on the foil is well bonded, loose wear debris formation may be acceptable in spite of a thicker coating.

The following coatings were recommended and are listed with their thicknesses:

FOIL	JOURNAL
Kaman DES 1.3-3 μm*	Kaman DES 8-13 μm*
Kaman DES + Diluted SCA 1002 13 μm	Kaman SCA 1002 38-50 μm

(ii) Sputtered Cr_2O_3

A multi-layer coating concept was used in developing sputtered Cr_2O_3 coating systems.

*Was tested in a previous program. Selected here as a baseline and for endurance tests.

The following reasons may be given for lack of adherence in previous sputtered Cr_2O_3 coatings.

1. It may be difficult to obtain good coating adherence with the Inconel substrate due to its high hardness.
2. Due to its resilient construction, the foil has some high spots and during run-in period, contact occurs at the high spots and due to high contact stress, the coating comes off.
3. Since most of the coatings evaluated were ceramics and carbides, they came off due to lack of ductility. In brittle materials, it is easier to form a crack because coating cannot follow substrate deformation due to elasticity mismatch; and once a crack begins, it itakes almost no energy to propagate. In ductile materials, crack initiation and its propagation is more difficult.
4. Ceramics and carbides have low coefficients of thermal expansion compared to Inconel and, as a result, internal stresses are developed in the coatings at high temperature.

Since the substrate hardness may be responsible for poor coating adherence, the foils were coated in the annealed condition, then heat treated and coating adherence measurements were made to determine if there was any improvement. This technique can be used for coatings which can withstand 704°C (1300°F) exposure without any adverse effect.

Inconel was coated with an interlayer (a bond coat) of soft metal prior to deposition of chrome oxide. Metals are easy to coat and provide good interfacial bond and because of softer metal substrate, subsequent deposition of chrome oxide should also have good bond.

The ductility and the thermal expansion of the coating was improved by mixing 25% of Nichrome (80% Ni and 20% Cr) a metallic binder in the coating material. Nichrome has been used successfully as a component of other plasma sprayed coatings. Although Nichrome alone has poor gall resistance, experience shows that this mixed with hard materials works satisfactorily. Since cobalt is a good sliding material and it is used in cementing carbides, e.g., WC, it may be selected as a metallic binder later on.

In some cases an overlay of sacrificial coating of a softer lubricant which is stable at elevated temperatures (silver or gold or MoS_2) was applied over the hard coating to minimize wear of the hard coat during run-in. It was expected that soft lubricant would transfer to journal and lubricate. This coating, other than protecting the hard coating during run-in, would hopefully prolong coating life.

Coatings wear and it is the rate of wear which needs to be controlled. Inspite of an overlay to help during run-in, if there is excessive stress at some spot, the hard coating may come off. In that instance, the substrate should oxidize and replenish the coating by oxidation of chromium in the substrate to form chromium oxide (this process is defined here as reactive replenishment). Continuous oxidation of chromium in the substrate may deplete chromium in the subsurface layer. In order to prevent deficiency of the chromium in the Inconel surface resulting from reactive replenishment, a diffusion barrier can be applied to the Inconel surface prior to deposition of chrome oxide. The interlayer should also act as an oxidation barrier under final coatings of ceramics in case of substrates with poor oxidation resistance. Nickel base alloys usually do not require any interlayer because of adequate internal oxidation protection. The material of interlayer can be selected so that it acts as a supply of chromium, has low hardness, is easy to sputter, and resists oxidation at high temperatures. One such material recommended was Nichrome (80% Ni and 20% Cr). It is known to be a good bond coat material; it is soft, and easy to sputter and has adequate Cr.

The multi-layered coating concept is sketched in Figure II.1.

A parametric study was conducted to achieve optimum film properties. Some of the important parameters which influence the properties of a sputtered coating were varied in our sputtering optimization study and these are:

- Power level
- Gas pressure
- Substrate bias

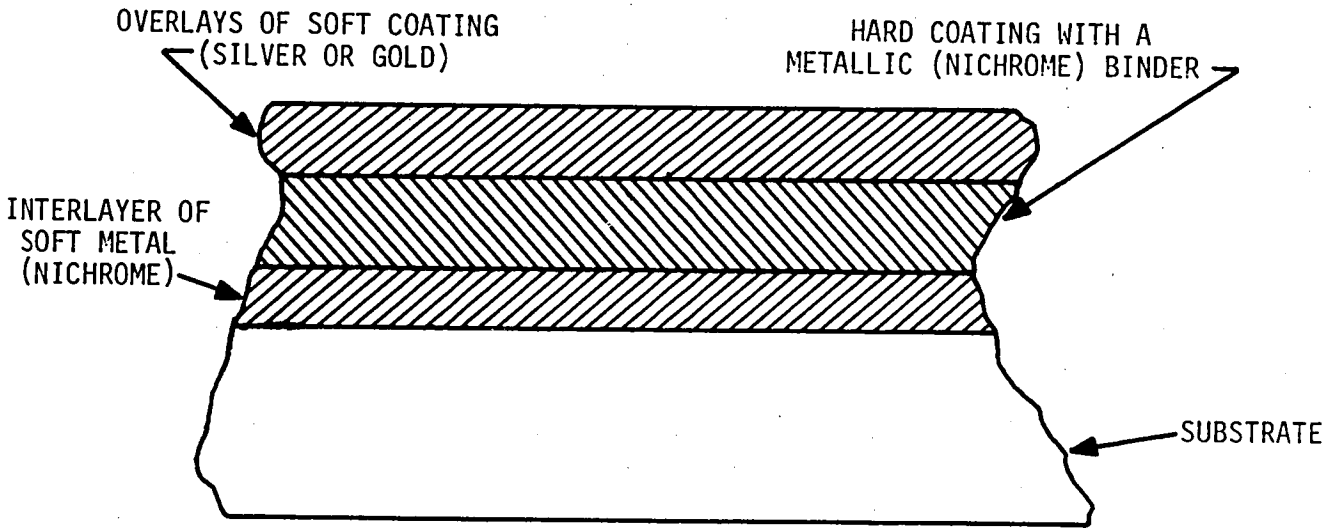

Fig. II.1 Proposed Approach to Improve Bond and Ductility of Hard and Wear-Resistant Sputtered Coatings

793300

- Target precleaning/sputter etching of substrate
- The thickness of the film deposited

The substrate in our system is water cooled and the substrate temperature can be changed somewhat by placing the substrate on a ceramic plate.

Prior experience at NASA Lewis shows that the optimum thickness of the coating is 5000 Å. The thickness of coating on HSS cutting tools is usually quite a bit higher, 10K-100K Å. In resilient bearings, there would be some initial out-of-flatness and the contact could be over a very small area resulting in high stresses. In these situations, thin coatings may not be forgiving as much as thicker coatings. Therefore, coating thickness is an important parameter and coatings developed were as thick as possible without loosing adherence.

Brainard [2.15] showed that adherence of refractory silicides, borides, and carbide coating on 440C substrate was promoted by the formation of an oxidized layer at the interface. Deliberate preoxidizing of the 440C produced enhanced adherence. This concept was tried in the program.

Cr_3C_2 was also recommended for limited study. Coatings and processing parameters for journal and foil to be tested in the program were:

Coating on Journal and Foil	Parameters
Cr_2O_3 (Baseline)	Power level/gas pr/bias/target cleaning/ substrate etching/pre-oxidation
Ni-Cr Bonded Cr_2O_3, Nichrome underlay and silver (or gold) overlay	Power level/gas pr/bias/target cleaning/substrate etching/pre-oxidation
NiCr bonded Cr_3C_2 Nichrome underlay and silver (or gold) overlay	Power level/gas pr/bias/target cleaning/substrate etching/pre-oxidation

(iii) Preoxidation

Preoxidation of Inconel X-750 (heating in air) produces a thin film of Cr_2O_3 and spinel compounds ($NiFe_2O_4$) on its surface. The thickness and composition of the oxide layer depends on the temperature, time and the

atmosphere. At the annealing temperature of Inconel (1065°C), a powdery form of oxide is formed and at heat treatment temperature (704°C), other oxides along with Cr_2O_3 are formed. A tenacious layer of Cr_2O_3 is formed on Inconel X-750 by heating to 870°C (1600°F) for four hours. Preoxidation of A286 (journal material) at 650°C (1200°F) also produces Cr_2O_3 and other beneficial oxides. Tests of preoxidized foil against a preoxidized journal were conducted as a baseline. Durability was expected to be poor at room temperature, but fair (possibly) at 650°C. Any coating system has to be better than the simply preoxidized specimen to be worthy of further consideration.

Solid Lubricants

(i) CdO-Graphite Coating System

A coating consisting of cadmium oxide-graphite mixture (1 to 3 by weights of CdO and graphite) has performed well up to 370°C (700°F). Graphite is stable in air up to 430°C (800°F). Therefore, some tests were planned at 430°C (800°F) to establish its temperature limit. Silver and gold have proven to be good lubricants at lower temperatures, for example, silver has been used in NASA PS 101 coating to improve its lubricity in RT-500°F range [2.16] and gold has been used in MLF-5 coatings to improve wear [2.17]. Silver was found to be a good lubricant at high temperature (316 to 982°C) by Peterson et. al. [2.18]. Therefore, it is believed that Ag should lubricate well in the entire temperature range. Ag was added to the cadmium oxide-graphite coating to possibly improve the lubricity (friction and wear performance) of the coating in the entire temperature regime and increase its temperature limit.

The bond strength is higher if the coating is thinner. If the coating is sprayed thick, the water at the bottom of the coating does not dry up as rapidly as at the top resulting in poor adherence. But, the coating should be thick for increased life. Therefore, a trade-off has to be made of the thickness to get optimum bond strength and wear life. New techniques can be used to improve the bond strength. One proposed approach is to apply the coating in thin layers (2.5-4 μm) and cure each time until the coating builds up to 12 to 18 μm. Since at each time a thin coating is

applied, the adhesion may be improved. One important parameter determining the improved adhesion would be whether or not the coating adheres better on the coating itself than on the substrate.

The literature indicates that the preoxidation of stainless steel [2.15 and 2.19] improves the coating bond; but our experience with Inconel substrate shows that the oxide layer weakens the coating bond.

It is very difficult to pretreat the foil without causing distortion. Therefore, it is preferred that the coating be applied on the journal and foil be left bare. Even coated foil against coated journal combination may have improved life. The CdO-graphite coatings were therefore applied on a relatively porous Metco chrome carbide coated journal.

The recommended changes were: CdO-graphite with additions of silver coating; application in thin layers; coating journal with solid lubricant.

(ii) Fluorides Coating System

Coatings consisting of CaF_2 and other constituents have been developed by H. Sliney at NASA Lewis [2.20], and have been used in aircraft air frame bearings of the oscillating type. PS101 coating included 25% calcium fluoride, 30% silver, 30% nichrome, and 15% sodium-free glass. CaF_2 is chemically and thermally stable and has thermal expansion close to that of metals and provides lubrication at elevated temperatures. Glass was added for oxidation protection at high temperatures. Ag was added to improve lubrication properties below 260°C. Nichrome metal enhanced strength and improved ductility. This coating (PS101) was found to wear excessively in foil bearings [1.2] and was modified.

A variation of this coating, PS 120 consisting of 60% Tribaloy 400, 20% silver, and 20% CaF_2 was tested satisfactorily at 540°C in a previous program [1.2]. More work at NASA was conducted to improve coating hardness and reduce porosity. The new combinations which were recommended were: CaF_2 with more Tribaloy 400 and CaF_2-ZrO_2 coating.

ZrO_2 has been used in high temperature applications and has a good hardness. One recommendation was also to fill the coating pores with CdO-graphite coating. Although this filling will eventually oxidize at 540°C, it may provide some lubrication and prevent damage during the run-in period which is crucial to the ultimate coating survival.

The CaF_2-BaF_2 eutectic coating with binder have performed well in the temperature range 260-815°C [2.21]. Silver can be added to improve the room temperature properties [2.22]. Further studies were conducted for this program by NASA to evaluate if development of CaF_2-BaF_2 with silver addition would be useful.

The following fluoride coating tests were recommended:

NASA PS 120 (60% Tribaloy 400, 20% CaF_2, 20% Ag) on journal	Processing variations in plasma spraying
NASA PS 122 (80% Tribaloy 400, 10% CaF_2, 10% Ag) on journal	Processing variations in plasma spraying
CaF_2-ZrO_2 coating on journal	Processing variations in plasma spraying
OSF-6 (CaF_2-BaF_2 eutectic, calcium-silicate and Ag) on foil and journal	Composition and processing variations

(iii) PbO-SiO_2 Coating System

PbO-SiO_2 coating (95% by weight PbO and 5% by weight SiO_2) has worked satisfactorily in the temperature envelope of 260°C-676°C (500°-1250°F) on 440 C substrate. About 5% by weight SiO_2 was used to stabilize PbO against transformation to Pb_3O_4 which is not a good lubricant. When the PbO-SiO_2 was applied on a substrate which does not form Fe_3O_4 during firing of the coating, the coating adherence was poor. It was observed that the iron oxide increases the fluidity of PbO which becomes homogeneous more readily than a highly viscous one, and this is reflected in improved uniformity after solidification resulting in better bond. Also the presence of iron-oxide rich transition layer at the ceramic-metal interface is helpful in improved bond [2.23]. Ten percent by weight Fe_3O_4 was added to the coating mixture when the coating was applied to

the substrate not forming Fe_3O_4 during firing, for example, 304 stainless and Inconel X.

The coating melts from the frictional heat at the points of sliding contact and ambient temperature and forms a low shear strength film. This melting may be very localized and of very short duration with the surface film in the molten condition only at the contacting asperities during the time that they are in sliding contact. Some tests by Sliney [2.21] have shown that at higher speeds, $PbO-SiO_2$ works well even at low temperatures because interface temperature may be high due to frictional heat alone. In our application, the surface speed at lift-off is about 7.62 $m.s^{-1}$ (1500 fpm) and at this speed, the $PbO-SiO_2$ may work fairly well at low temperature.

The coating for application on Inconel X-750 was applied with and without Fe_3O_4. The addition of silver in the mixture was planned to further improve its low temperature properties. Past experience indicates that a large amount of silver becomes lumpy during milling and coating solidification. A coating with $PbO-SiO_2$ mixture and 10% to 20% silver by weight was tried. The $PbO-SiO_2$ coating was fired at 900°C (1650°F) for 6-7 minutes. The mixture with silver was fired at a temperature slightly below the melting point of silver (960°C) so that silver does not flow and make lumps. Since the melting point of $PbO-SiO_2$ is 760°C (1400°F), the mixture can be fired at temperature slightly higher than 760°C (1400°F) and the firing time depends on the substrate weight. A thin substrate like Inconel foil may only take a minute to heat up and melt the mixture.

Effect of surface preparation and pretreatments on the coating bond was also planned to be examined. In their work with $PbO-SiO_2$, Murray and Peterson [2.19] found that the preoxidizing of the substrate had influence on the coating bond. This was further explored in this program.

Other Potential Candidates Using ARE Process

Professor R. F. Bunshah acted as a consultant on the program. He was contacted to make some recommendations based on his experience of hard coatings applied on metal cutting tools to improve their life. He

recommended superhard materials like TiC, TiN, and HfN. All of these coatings have a cubic structure. These hard coatings and similar other hard coatings have been deposited by the Activated Reactive Evaporation Process and by the Sputtering Process for several years now. Some of these coatings are being used in Japan (for improving the scratch resistance of watch cases, for cutting tools, experimentally for bearing applications in the Mechanical Engineering Laboratory by Dr. Enamoto). He has found in his own tests that the cutting forces decrease by about 1/2 which shows that the coefficient of friction must also markedly decrease. According to him, one of the great advantages of the ARE-type process for deposition of these coatings is the ability to vary the microstructure as well as the composition (carbon to metal ratio or nitrogen to metal ratio) of these coatings. This enables one to tailor the structure and properties of the coating to a particular application since change in these properties should also change the fracture toughness of the material. He felt that these would be excellent coatings for the foil of our foil bearings. Moreover, the severity of the loading is much less for the foils than for the tool applications. Since these coatings have performed successfully on high speed steel tools, he saw no reason why they would not perform equally well or better in bearings. Another benefit of the ARE process is the ability to lay down mixed carbides, or mixtures of carbides or nitrides, carbonitrides, oxycarbides, etc. This demonstrates the versatility of the process.

The coatings TiC (ARE), TiN (ARE), and HfN (ARE) are all susceptible to oxidation above 540^{o}C [2.10]. In fact, TiC is reported to oxidize at a significant rate above 430^{o}C [2.11]. TiN is very poor at temperatures at or higher than 540°C and is not selected. The oxidation products form an adherent protective oxide surface layer which may provide a lubricating function.

Summary

A summary of selected coating compositions and process variables for static oven screening tests is given in Table II.1. Relevant properties of the selected coatings are shown in Table II.2. The data are based on [2.9, 2.11, and 2.24] and bulletins available from Metco, Inc.

TABLE II.1

SELECTION OF COATING SYSTEMS AND PROCESS VARIABLES

Coating Combination	Development Source	Composition and Process Variables
Chrome Oxide Coating Systems		
(i) (Cr_2O_3 proprietary process)	Kaman Sciences Co.	a. Try Kaman DES + diluted SCA overlay on foil.
		b. Try Kaman SCA 1002 on journal.
(ii) Sputtered Cr_2O_3 (and limited work on Cr_3C_2)	MTI	a. Make following changes: Interlayer of Nichrome to improve bond and provide oxidation resistance, 25% Nichrome binder to improve ductility of the coating, better match thermal expansion and overlays of Ag and Au to provide run-in lubricant.
		b. Optimize following parameters: Power level/gas pressure/substrate bias/target precleaning/substrate etching/preoxidation.
(iii) Preoxidation	MTI	a. Evaluate preoxidized Inconel against preoxidized A286.
Solid Lubricant Systems		
(i) CdO and graphite	MTI	a. Add silver to study effect on lubricity, improved oxidation resistance and maximum temperature capabilities.
		b. Spray CdO-graphite on a porous hard journal and test against bare foil.
(ii) CaF_2 and BaF_2 coating system	NASA	a. Vary composition and processing parameters to improve hardness and porosity of the NASA PS 120 coating.
		b. Develop CaF_2 - BaF_2 eutectic + Ag coating on foil.
(iii) $PbO-SiO_2$	MTI	a. Develop $PbO-SiO_2$ + Ag coating
Other Potential Candidates		
(i) Commercial hard coatings by ARE and sputtering processes	UCLA Quad Group	Test TiC, and HfN coatings applied by ARE and sputtering processes.

TABLE II.2

RELEVANT PROPERTIES OF COATING COMPOSITIONS

Compound	Crystalline Structure	Density gm/cc	Melting Point °C	Hardness[a]	Ultimate Tensile Strength MPa	Linear Coefficient of Thermal Expansion x 10^{-6}/°C	Oxidation (Decomposition) Temperature °C	Most Stable Oxidation Products	Thermal Conductivity Cal. $s^{-1}.cm^{-1}.C^{-1}$ RT	Thermal Conductivity Cal. $s^{-1}.cm^{-1}.C^{-1}$ Temp.°C
Inco X-750 (sheet)	FCC	8.30	1390-1426	33-Rc	1233	12.53 (93°C) 15.14 (650°C)		NiO	0.029	0.046 (540)
A-286 (bar)	FCC	7.92	1371		1005	16.50 (93°C) 17.78 (650°C)		NiO-Cr_2O_3	0.036	0.057 (600)
Nickel (Ni)	FCC	8.91	1455	90-120 R_B hot rolled	413-585	13.32		NiO	0.195	0.13 (327)
Chromium (cr)	BCC/FCC	7.20	1843			6.12		Cr_2O_3	0.22	0.17 (627)
Iron (Fe)	bCC/FCC	7.86	1539	69 Bhn (ann.)		11.7		Fe_2O_3	0.17	0.125 (327)
Cobalt (Co)	HCP	8.86	1495	138 Bhn	758	12.24		CoO	0.165	-
Nichrome Powder (80% Ni & 20% Cr)	-	7.11	1400	90 R_B	158	17		NiO and Cr_2O_3	-	-
Silver	FCC	10.49	960	50-150 Bhn (plated)	152 (ann.)	19.62		No stable oxide at high temperature	1	1 (127)
Gold	FCC	19.32	1063	25 Bhn (ann.)	131 (ann.)	14.22		No stable oxide	0.72	0.65 (327)
Chrome carbide powder (Cr_3C_2)	Orthorhombic	5.59	1890	91 R_A 2650 $Knoop_{50}$		11.52		Cr_2O_3		0.018 (275)
25% Ni-Cr, 75% Cr_3C_2				Macro-R_c 54 Micro-$knoop_{50}$ 950 DPH_{300} 700						
Chrome oxide powder (Cr_2O_3)	HCP	5.20	2435	Macro-R_c 65-72 Micro DPH_{300} 1000-1200		5.4		Fully oxidized material		
Titanium carbide (TiC)	FCC	4.93	3037	93 RA 2000-2750 $Knoop_{50}$	241-275	7.56	540	TiO_2	0.041	-
Aluminum oxide (Al_2O_3)	α form HCP	3.98	3720	3000 VPH	255	7.92	-	-	0.082	-
Titanium Nitride (TiN)	FCC	5.43	2950	1950 VPH	-	8.1	540	TiO_2	0.050	-
Hafnium Nitride (HfN)	FCC	13.92	3300	1650 VPH	-	6.5	540	HfO_2	0.051	-
Cadmium oxide (CdO)	FCC	8.14	1500		-	-	980	-	-	-

(a) Actual values of coatings very dependent on method of preparation porosity and purity.

TABLE II.2 (CONTINUED)

Compound	Crystalline Structure	Density gm/cc	Melting Point °C	Hardness	Ultimate Tensile Strength MPa	Linear Coefficient of Thermal Expansion x 10^{-6}/°C	Oxidation (Decomposition) Temperature °C	Most Stable Oxidation Products	Thermal Conductivity $Cal.s^{-1}.cm^{-1}.C^{-1}$	
									RT	Temp.°C
Synthetic graphite	HCP	1.99	3480		-	-			-	0.2-0.5 (100)
Sodium sillicate	Amorphous glass		1088				Melts at 1040	-	-	0.02 (225)
Calcium fluoride (CaF_2)	FCC	~3.0	1330				Stable	-	0.02	0.006 (600)
Barium fluoride (BaF_2)	FCC	~5.0	1282				Stable	-	0.026	0.025 (127)
CaF_2-BaF_2 eutectic	Amorphous glass	~4.0	1020				Stable	-	-	-
Tribaloy 400	Laves phase is hexagonal	9.36	1232-1593	51-58 R_c	1895 (compressive)	13.41	980	CoO, MoO_3 Cr_2O_3 and SiO_2	0.035	-
PbO-SiO_2 (95% by wt PbO and 5% by wt SiO_2)	Glass	~9.3	760		-		760	SiO_2 Stabilizes PbO - straight PbO decomposes to Pb_3O_4	4 PbO.SiO_2 0.03 (RT)	

Based on the results from oven tests, the coatings were then selected for start/stop tests.

SELECTION OF COATING COMBINATIONS

Referring to Table II.1, several potential coatings have been selected for journal and foil members. In soft-hard combinations, the hard coating was put on the journal to minimize the possibility of any damage since the cost of repairing and balancing a journal may be very high. It is also noted that low shear strength solid lubricant films are usually more effective on a hard substrate. An additional consideration when the foil and the journal are coated with two different materials (e.g., putting coating A on the foil and coating B on the journal) is that reversing these coatings may have a significant effect on the results. The underlying cause of this difference is thermal in nature. When the journal is rubbing in contact with the foil, the contact area on the foil is fixed and all of the frictional heat is concentrated in one area, while the contact on the journal is continuously changing with the shaft rotation; and the temperature rise is much more gradual. Also, if the coating on the journal is worn, the worn part does not come in contact all of the time; but if it is on the foil, it does.

Thus, material transfer and frictional behavior are markedly different with certain combinations of materials, depending on their relative positions on the foil or on the journal. This effect would be particularly important in the case where a soft metal film, such as silver or gold, was being used to protect one of the surfaces or in the case of the solid lubricant films like CdO-graphite.

Table II.3 shows the preliminary selection of coating combinations recommended for the static oven test and the partial arc bearing start/stop tests with criteria for selection. Table II.4 shows the selected combinations in a matrix form.

TABLE II.3

SELECTED COATING COMBINATIONS FOR START-STOP TESTS

(Subjected to Successful Completion of Static Screening Tests)

	Foil Coating or Treatment	Journal Coating or Treatment	Test Temperature °C (°F)	Comments
1.	Graphite-cadmium oxide with and without Ag (A.S.)	Cr_3C_2(D.G.)	430(800)	Expand data bank for bonded graphite
2.	Graphite-cadmium oxide (A.S.)	Graphite-cadmium oxide (A.S.)	430(800)	Effectiveness of solid lube against itself
3.	Graphite-cadmium oxide (A.S.)	Graphite-cadmium oxide (A.S.) on Metco chrome carbide	430(800)	Effectiveness of solid lube against itself
4.	Preoxidized foil	Preoxidized A286	650(1200)	Baseline data
5.	Preoxidized foil	Heat treated PS 120 (P.S.)	540(1000)	Check data reproducibility
6.	Preoxidized foil	Graphite-CdO filled, heat treated PS120 (P.S.)	540(1000)	Employ graphite to fill surface porosity
7.	Preoxidized foil	Heat treated PS122 (80 Tribaloy 400-10 Ag-10 CaF_2) (P.S.)	540(1000)	Composition modification to reduce silver transfer
8.	Preoxidized foil	CaF_2-ZrO_2 (P.S.)	650(1200)	Upgrade PS coating to 650 C°
9.	Kaman DES (C.A.)	Kaman DES (C.A.)	650(1200)	Endurance test
10.	Kaman DES SCA (C.A.)	Kaman DES (C.A.)	650(1200)	Improve DES coating
11.	Kaman DES or DES, SCA (C.A.)	Kaman SCA (C.A.)	650(1200)	Per Kaman recommendation
12.	Chrome oxide and nichrome bonded Cr_2O_3 (sp.)	Cr_3C_2 (D.G.)	650(1200)	To compare with no. 9 and investigate ductile matrix concept
13.	Nichrome bonded Cr_2O_3 with Ni-Cr interlayer and Ag overlay (sp.)	Cr_3C_2 (D.G.)	650(1200)	Investigate effect of multilayers
14.	Nichrome bonded Cr_3C_2 (sp.)	Cr_3C_2 (D.G.)	650(1200)	Investigate ductile matrix concept.
15.	Cr_2O_3 or Cr_3C_2 (sp.)	Cr_2O_3 or Cr_3C_2 (sp.)	650(1200)	To compare with no. 12 to no. 14
16.	TiC (ARE)	Cr_3C_2 (D.G.)	540(1000)	Effectiveness of ARE process
17.	HfN (ARE)	Cr_3C_2 (D.G.)	540(1000)	Effectiveness of ARE process
18.	Preoxidized foil	OSF-6 (F.C.)	650(1200)	Effectiveness of Ag in FS-Ag
19.	OSF-6 (F.C.)	Preoxidized A286	650(1200)	Effectiveness of Ag in FS-Ag
20.	PbO-SiO_2-Ag (F.C.)	Preoxidized A286	650(1200)	Effectiveness of Ag in PbO-SiO_2
21.	Preoxidized foil	PbO-SiO_2-Ag (F.C.)	650(1200)	Effectiveness of Ag in PbO-SiO_2

A.S. - Air sprayed; P.S. - plasma sprayed; D.G. - detonation gun; Sp. - sputtered, ARE - activated reactive evaporation; F.C. - fused coating; C.A. - chemically adherent.

TABLE II.4

SELECTED COATING COMBINATIONS IN MATRIX FORM FOR START-STOP TESTS

(Subject to Successful Completion of Static Screening Tests)

Foil \ Journal →		1	2	3	4	5	6	7	8	9	10	11	12	13
		Cr_3C_2 (D. G.)* preox.	Graphite - CdO (A. S.)	Metco Cr_3C_2 (P.S.) Graphite-CdO filled	Preox.* journal	NASA PS 120 (P.S.)* preox.	NASA PS 120 (P.S.)* preox., graphite-CdO filled	NASA PS 122 (P.S.)* preox.	NASA CaF_2-ZrO_2 (P.S.)* preox.	Kaman DES (C.A.)	Kaman SCA 1002 (C.A.)	Nichrome Bonded Cr_2O_3 or Cr_3C_2 (sp.)	OSF-6 (F.C.)	PbO-SiO_2-Ag (F.C.)
A.	CdO-graphite (A. S.) std., addition of Ag and process change	(1a,b) (430°C)	(2) (430°C)	(3) (430°C)										
B.	Preox. foil**				(4) (650°C)	(5) (540°C)	(6) (540°C)	(7) (540°C)	(8) (650°C)				(18α) (650°C)	(21) (650°C)
C.	Kaman DES (C. A.)									(9α) (650°C)	(11) (650°C)			
D.	Kaman DES, SCA (C. A.)									(10α) (650°C)				
E.	Cr_2O_3 (Sp.) and nichrome bonded Cr_2O_3 (Sp.) two thicknesses	(12a,b,c) (650°C)										(15) (650°C)		
F.	Nichrome bonded Cr_2O_3 with nichrome interlayer and silver overlay (Sp.)	(13) (650°C)												
G.	Nichrome bonded Cr_3C_2 (Sp.)	(14α) (650°C)												
H.	TiC (ARE)	(16β) (650°C)												
I.	HfN (ARE)	(17β) (650°C)												
J.	OSF-6 (F.C.)				(19) (650°C)									
K.	PbO-SiO_2-Ag (F.C.)				(20) (650°C)									

*650°C/4 hours **870°C/4 hours

α - cancelled due to poor processing

β - cancelled due to poor thermal oxidation resistance

III. COATING PREPARATION AND PROCUREMENT

CHEMICALLY ADHERENT CHROME OXIDE COATING

Journal and foil samples were coated by Kaman Sciences Corporation, Colorado Springs. The journals were to be coated with Kaman DES (8 to 13 μm thick) and Kaman SCA 1002 (38 to 50 μm thick) coatings. The foils were to be coated with Kaman DES (1.3 to 3 μm thick) coatings. Based on surface examination, the coated DES foils were acceptable. DES and SCA coated foils had a coating about 0.025 mm thick, which cracked during rolling for bearing formation. Therefore, test consisting of this coating, numbered 10 in Table II.4, was cancelled. The coated journals were very rough (1.22 μm CLA) and were returned for reprocessing.

Kaman Sciences had a problem in getting a surface finish of about 0.25μm (10μin.) which they provided in a previous program. They made several runs in order to achieve the desired hardness and surface finish. Since the coating was stripped off after each bad run, the journal became out of round during successive runs. These journals were checked at MTI using the Gould machine, and journals were found to be out of round 12 to 35μm. These were then ground at MTI to get them within 5μm. During grinding, either the coating was stripped off entirely at places or it became very thin. None of the DES journals were acceptable for tests and only one SCA journal had adequate coating with a surface roughness of 0.81μm(23μin.). Although this surface roughness was believed to be high, this is the best which could be obtained. Since there was no good DES journal available, the test No. 9 in Table II.4 had to be dropped.

CHROME CARBIDE COATING

Detonation gun chrome carbide coating was applied on the journal by Linde Division of Union Carbide. The coating is LC-1C which consists of 25% Nichrome (20% Ni, 5% Cr) and 75% Cr_3C_2. The coating was sprayed about 175-200μm (7 to 8 mils) thick and was ground to a thickness of 62-88μm (2.5 to 3.5 mils) with a surface roughness of 0.038-0.051μm (1.5 to 2μin. CLA).

A porous, plasma sprayed Cr_3C_2 coating was also applied on a journal for subsequent spraying of CdO-graphite. The coating was sprayed using Metco 81-NS powder consisting of 75% Cr_3C_2 (-140 + 10 microns) and 25% Nichrome (-106 + 10 microns).

CALCIUM FLUORIDE BASED COATING

Plasma Sprayed Coatings

Three compositions of CaF_2 based coatings were plasma sprayed on the test journals at NASA-Lewis. The coatings were the following: PS120 consisting of 60% Tribaloy 400, 20% silver, and 20% CaF_2; PS122 consisting of 80% Tribaloy 400, 10% silver, and 10% CaF_2. The coatings were generally rough in the range of 0.84-1.53μm (33-60μin.) CLA. One of the PS120 journals were coated with CdO-graphite coating about 3-5μm to fill the pores.

Fused Coating

CaF_2-BaF_2 eutectic based coatings designated OSF-6 were applied on the journal and the foils at NASA-Lewis. The coating composition was 58.5% fluoride eutectic (31% CaF_2 and 69% BaF_2), 35% silver, and 6.5% CaO-SiO_2. The OSF-6 powders were mixed in a 4:1 mixture of lacquer and thinner and sprayed with a paint sprayer on a precleaned substrate.

After baking in a vacuum oven overnight at 225°C to remove volatiles, the coatings were fused in an argon furnace at 995°C for 20 minutes. After 20 minutes cooling in argon, the coating was hand sanded with wet 600 grit paper to a final thickness of 10 $\pm$ 2.5μm (0.6 $\pm$ 0.1 mil).

In case of coating of foils, they deformed during fusing of coating and were flattened by reverse bending on a 38 mm diameter cylinder. The coated journal, as received from NASA, was rough. It was ground to clean off the coating, the coating was penetrated by taking off only 7.5μm. Also it was found that the journal was out of round; about 15μm. Since the journal was out of round, it could not be used and the test No. 18 in Table 11.4 was dropped.

TITANIUM CARBIDE AND HAFNIUM NITRIDE COATINGS

ARE Processed Coating

Professor R. F. Bunshah at UCLA coated foils with two variations of TiC and two variables of HfN. The variations were in the microstructure and stoichiometry resulting in a change in hardness. First of all, two foils were coated with TiC coating about 10μm (0.4 mil) thick. The foils became curled due to the residual stresses between the coating and the substrate. The curling could not be removed by rolling; in fact, the coating cracked during rolling.

In the next batch, a thinner (2μm thick) and a softer coating was applied. The foils still became curled, but not as much as in the previous batch. A piece of the coated foil was vacuum annealed at 1000°C to remove the curl without success. At this stage, it was decided to test the foils as they were. If the coating had the potential, one could go back and do further optimization to avoid curling.

The foils were also coated with hafnium nitride coating about 2μm thick. The residual stresses in this case were much smaller than TiC coating. The processing parameters are given below.

The substrate temperature in each case was 500°C. In the case of TiC, the substrates were coated by evaporation of titanium from a rod-fed electron beam heated evaporation source in the presence of partial pressure of C_2H_2 of 4×10^{-4} Torr. The details for HfN are:

Evaporation Rate, g/min	Gas Pressure, Torr	Expected Stoichiometry
0.49	3.8×10^{-4}	$HfN_{1.0}$
0.49	2.6×10^{-4}	$HfN_{0.80}$

Sputtered TiC Coating

The foils were sputter coated with TiC by R. P. Riegert of Quad Group located at Santa Barbara, California. This was primarily used to compare results with ARE coated TiC. Prior to coating, the foils were cleaned ultrasonically in toluene, acetone, and 2-propanol of reagent

grade and blown dry with nitrogen. The parts were coated immediately after cleaning. The process used was their standard Romelus hard coat process and the thickness of the coating was 1200 ± 100A (5 ± 0.5μin.). The coating adherence in tension was reported to be in excess of 35 MPa (5000 psi).

CdO-GRAPHITE BASED COATING

CdO-Graphite Coating on Journal

A journal with Metco Cr_3C_2 undercoating and an uncoated journal were sprayed with CdO-graphite (HL-800) coating. The journal was held in a lathe and was rotated during spraying. The nozzle of the air brush was held perpendicular to the journal axis and it was moved at a speed of 12 to 25 $mm.s^{-1}$ (0.5 to 1 in. per sec.) from one end to another. Two passes had to be made to get 12-15μm (0.5 to 0.6 mil) thick coating. If the journal was rotated slowly at a speed of 60 rpm, the coating had a spiral-type appearance because the "feed" was too fast. If the journal was rotated too fast, there was danger of coating being thrown off. A speed was selected which was fast enough to avoid the spiral effect. The optimum speed was about 120 rpm. Following baking, the sprayed coating was burnished to a thickness of 7 to 10μm (0.3 to 0.4 mil).

CdO-Graphite-Ag Coating (HL-800-2)

High purity (99.99% pure)-230 mesh (0.062 mm sieve opening) Ag was obtained from the Materials Research Corporation. Cdo was 99.9% pure (commercially pure) material with 95% of the particle sizes finer than 200 (95-200). The graphite was a 99.9% pure electric furnace synthetic graphite (KS-2) having an average particle size of about 2μm, and it was made by Joseph Dixon Crucible Company, New Jersey. Sodium silicate (water glass), made by Philadelphia Quartz was 99% pure. Wetting agent used was Absol 895 with a cloud point of 65°C. A composition consisting of 10% Ag by weight was prepared using essentially the procedure as described in the previous report [1.2]. A coating consisting of 15% by weight CdO, 45% by weight graphite, 10% by weight Ag, and 30% by weight sodium silicate (8.9% Na_2O, 28.7% SiO_2 and balance water) excluding water content, was sprayed on the foil. It was suspected that if Ag was ball milled too long, it

may become lumpy because it is soft. To optimize the technique of mixing, in one case CdO-Graphite mixed in distilled water were ball milled for two hours; then Ag was added and milled for thirty minutes and the standard technique was used for spraying. In the second case, CdO-graphite was ball milled for two hours, Ag was added, and the mixture was agitated in a magnetic stirrer for thirty minutes. Examinations showed that the Ag particle density and distribution were about the same in either case. The coating involving mixing with a magnetic stirrer, probably had a slightly better mix. Therefore, all future runs were made by mixing silver in a magnetic stirrer.

During burnishing, the -230 mesh silver particles were being pulled out because of their relatively large particle size and the soft matrix. A very fine Ag powder with a particle size of 1 to 5 microns was obtained for further preparations. The next run was made using the fine Ag powder. After burnishing slightly with an Emery 600 paper, randomly-distributed, silver particles could be seen on the surface. A better technique of burnishing was to roll a dowel pin to press in the high spots and smoothen the surface. With this method, there was no Ag particle pull out.

Metallurgical Examination: The coating was examined under SEM. The representative photographs of the coating and a photograph of CdO-graphite for comparison are shown in Figure III.1. The CdO and Ag particles were randomly distributed. Particles were milled down fine during ball milling. There were some large silver particles with a maximum size of 10μ (see Figure III.1) which were confirmed by electron microprobe analysis. Overall, the coating seemed fairly uniform and the constituents were well distributed.

The coating was analyzed using X-ray diffraction techniques. The diffraction data are provided in Table III.1. The analysis proved to be inconclusive. Five peaks were identified although not conclusively. Peaks at 38.7 ± 0.5^{o}, 66.4 ± 0.2^{o}, and 85 ± 0.8^{o} seem to correspond to graphite and peaks at 50.1 ± 0.2^{o}, 57.2 ± 0.2^{o}, and 85.0 ± 0.8^{o} appear to be CdO.

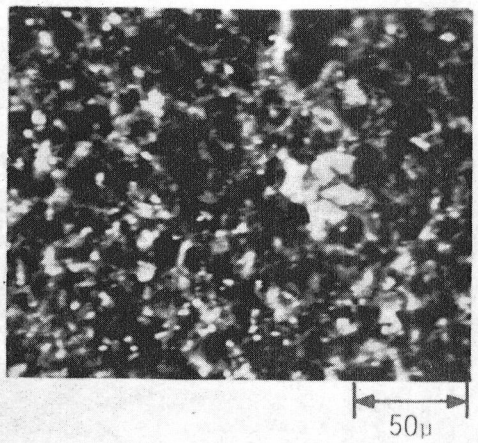

CdO-GRAPHITE-Ag COATING

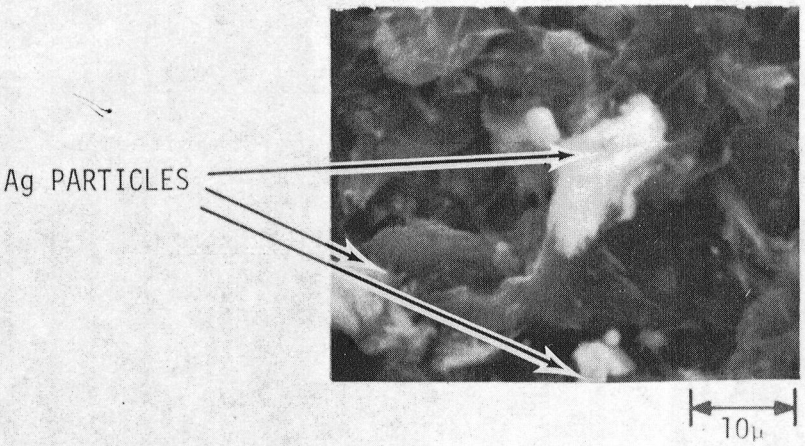

CdO-GRAPHITE-Ag COATING

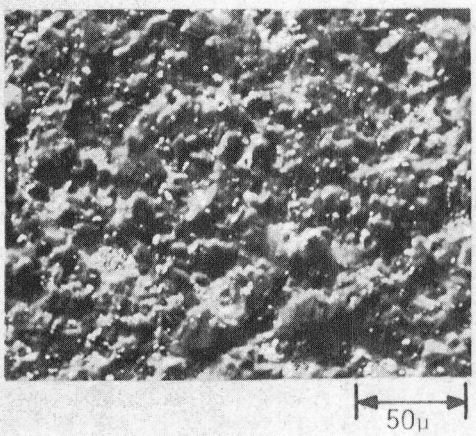

CdO-GRAPHITE COATING

Fig. III.1 SEM Photographs of Graphite Based Coatings

793275

TABLE III.1

X-RAY DIFFRACTION DATA FOR CdO-GRAPHITE-Ag-SILICATE COATING

X-Ray Run for Inconel X-750 Substrate using Cr Target with Vd Filter

2θ (degrees)	Intensity (arbitrary units)	d (Angstroms)	hkl
39.45	1.0	3.39	
43.95	5.0	3.06	
51.20	2.2	2.65	
67.60	Off Scale (>10)	2.06	111
75.30	2.4	1.87	
79.90	8.5	1.78	200

X-Ray Run for Inconel X-750 Substrate with CdO, Ag, Graphite, and Sodium Silicate (HL-800-2), using Cr Target with Vd Filter

2θ (degrees)	Intensity (arbitrary units)	d (Angstroms)	hkl
22.9	7.5	5.77	
25.4	Off Scale	5.20	
27.0	1.0	4.90	
37.1	2.1	3.59	
38.7	Off Scale	3.45	
42.8	7.6	3.13	
48.8	1.8	2.77	
50.1	2.0	2.70	111
53.7	1.2	2.53	
57.2	4.7	2.39	200
66.4	8.2	2.09	
74.1	2.0	1.90	
78.6	6.5	1.80	
85.0	4.5	1.69	220
90.7	1.5	1.60	

Substrate Preparation and Process Variation

The HL-800-2 coating was sprayed on foils with different surface preparations which were: foil heat treated in air, heat treated in nitrogen atmosphere, and electro-etched as described by Bhushan [3.1]. The surface heat treated in air had a lot more oxide buildup than in nitrogen. The coating was applied in four passes with a 30-second interval between each pass to give some time for the coating to dry.

All coated foils were bent 180° upon themselves with the coating on the outside of the bend, then unbent and photographed (see Figure III.2). It was found that electro-etched foil coated in a single pass gave the best adherence; in all other cases, the coating cracked at the bend.

PbO-SiO_2 BASED COATING

Coatings consisting of PbO, SiO_2, Ag, and with and without Fe_3O_4 were prepared. PbO (lead monoxide) used was yellow in color, 99.999% pure, and with particle size less than -100 mesh. It should be noted that if PbO is exposed to air for a long time, it forms red lead (Pb_3O_4) which is abrasive, So it should be assured that PbO is yellow in color. SiO_2 (silicon dioxide) was 99.99% pure, reagent grade and -325 mesh size. Fe_3O_4 (ferrous oxide) was 99.9% pure with an average particle size less than half a micron. The Ag was 99.99% pure and 1 to 5 microns in size. All chemicals were purchased form the Materials Research Corporation, Orangeburg, New York.

Sliney and Johnson [3.2] reported that lead silicate (4 PbO-SiO_2) and lead monoxide (PbO) are at equilibrium for compositions with less than 6.7 wt. % of PbO. If SiO_2 is more than 6.7%, only lead silicates are formed. PbO with 5% SiO_2 (m.p. $\sim$ 760°C) was considered optimum; it protects against oxidation of PbO as well as insuring that free PbO is available for lubrication at temperatures above 500°C.

A mixture of 75% PbO, 5% SiO_2, and 20% Ag (SiO_2% in PbO-SiO_2: SiO_2 - 6.23%) was sprayed and baked (Trial No. 1). The process involved ball milling the PbO and SiO_2 in a quantity of water for one hour then adding

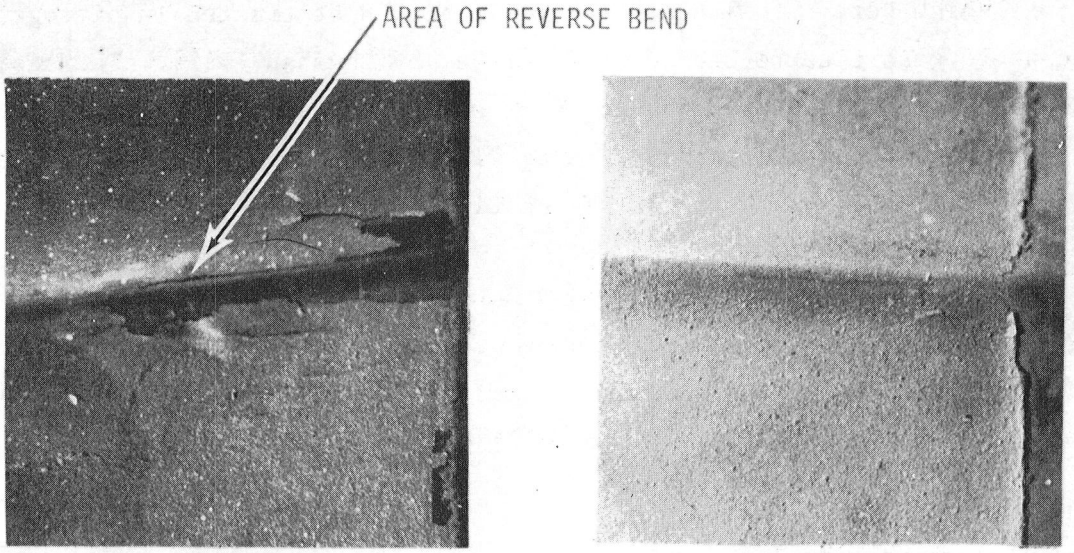

FOIL HEAT TREATED IN AIR PRIOR TO COATING

FOIL HEAT TREATED IN NITROGEN PRIOR TO COATING

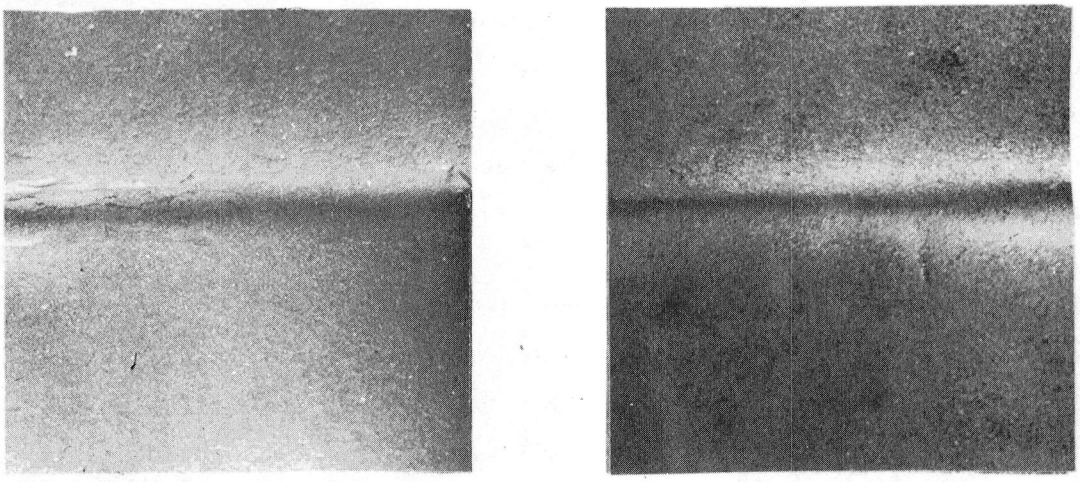

COATING APPLIED IN FOUR COATINGS PASSES WITH 30 SEC INTERVAL ON ELECTRO-ETCHED FOIL

COATING APPLIED IN A SINGLE PASS ON ELECTRO-ETCHED FOIL

Fig. III.2 Photographs of the Coated Foils After Reverse Bending

silver and mixing in a magnetic stirrer for 30 minutes; then a drop of Absol 895 was added. The coating was sprayed on Inco X-750 foil preoxidized and foils heat treated in nitrogen and preoxidized A286 coupons. One foil was fired at 982°C (1800°F) to see if melting of silver had any positive effect. In this case, silver became lumpy and the coating was nonuniform.

The sprayed coating was heated at 93°C (200°F) to remove water and then fired at 900°C (1650°F) for one minute after it melted. It took about 20 seconds for the foil coating to melt and about two minutes for A286 coupon coating to melt.

The coating on the foil did not flow well and was very nonuniform, whereas, on the journal coupons it was all right. It has been observed by Sliney et. al. [3.2] that PbO-SiO_2 coating material applied to substrates which did not form Fe_3O_4 during firing, did not flow well. The coating was very hard, probably due to excess 4 PbO·SiO_2 which is abrasive. In the next preparation, the amount of SiO_2, was reduced to 4.2% in PbO-SiO_2.

The composition after adding silver was 3% SiO_2, 72% PbO, and 25% Ag (trial No. 2). When the coating was burnished, red powder (Pb_3O_4) came off which meant that there was not enough SiO_2 to stabilize PbO. In this preparation, cellulose Nitrate lacquer (120-140 CPS, No. 2012) and lacquer thinner butyl acetate were used instead of water because lacquer holds Ag particle better. When thinner was added just before spraying to get proper fluidity, it gelled. Therefore, all other mixtures were prepared in water.

In the next preparation, SiO_2 was increased so that SiO_2 was about 5% of PbO-SiO_2 mix. The composition in this preparation was 4% SiO_2, 71% PbO, and 25% Ag (trial No. 5). The coating on the journal looked good. It was better on a preoxidized A286 coupon than on a clean A286 coupon. Coating again did not flow well on foil.

In the next preparation, some Fe_3O_4 was added to improve coating uniformity on the Inconel foil. The composition consisted of 25% Ag, 3.5% SiO_2, 61.5% PbO, and 10% Fe_3O_4 (trial No. 6). The coating on the preoxidized foil looked well bonded.

The trial No. 5 and 6 were selected for journal and foil, respectively. Both substrates were preoxidized when sprayed. As sprayed coating thickness on the journal was 75-88μm (3 to 3.5 mil) and it was burnished to about 25μm by grinding. As sprayed coating on the foil was 38-50μm (1.5to 2 mil) and it was burnished by a 600 grit emery paper to a thickness of 15-20μm (0.6 to 0.8 mil). The coatings looked smooth after burnishing.

As it will be explained in the next section, the coating did not perform well in the start/stop tests, and it was felt that it was due to high Ag content in the coating. At this time, two runs were made with reduced silver content. Coating consisting of 75.8% PbO, 4.2% SiO_2, 10% Ag, and 10% Fe_3O_4 was sprayed on preoxidized Inconel foil (trial No. 7) and a coating with 85.2% PbO, 4.8% SiO_2, 10% Ag was sprayed on preoxidized and clean A286 journal coupons (trial No. 8). The photographs of selected coupons are shown in Figure III.3a. It shows that the coating as sprayed on preoxidized foil is quite smooth. Comparison of coating on clean and preoxidized A286 coupons show that the coating on preoxidized coupon is smoother and, hence, is selected here.

Metallurgical Examination: An SEM study of PbO-SiO_2-Fe_3O_4-Ag coating on Inconel X-750 foil (trial No. 7) was conducted to examine surface appearance and particle distribution. The coating seemed fairly smooth (see Figure III.3b) and although silver was not distinctly visible, electron microprobe detected that Ag was uniformly distributed (see Figure III.3b). Ag particles were probably coated with PbO-SiO_2 during firing.

X-ray diffraction analysis was carried out of trial No. 7. A General Electric diffractometer was used for all measurements made at room temperature. The measurements covered the range $10^o<2\theta<90^o$ using a Cr target with a Vd filter. Four peaks were yielded. Three of these were located at 43.9 ± 0.6^o, 46.4 ± 0.4^o, and 49.2 ± 0.4^o with d-spacings of 3.06 (hkl;110), 2.90 (hkl;002), and 2.74Å (hkl;200), respectively. These three peaks correspond to PbO. The fourth peak was at 29.2 ± 0.80, corresponding to the d-spacing of 4.54 Å, characteristic of an Ag-Fe- sili-

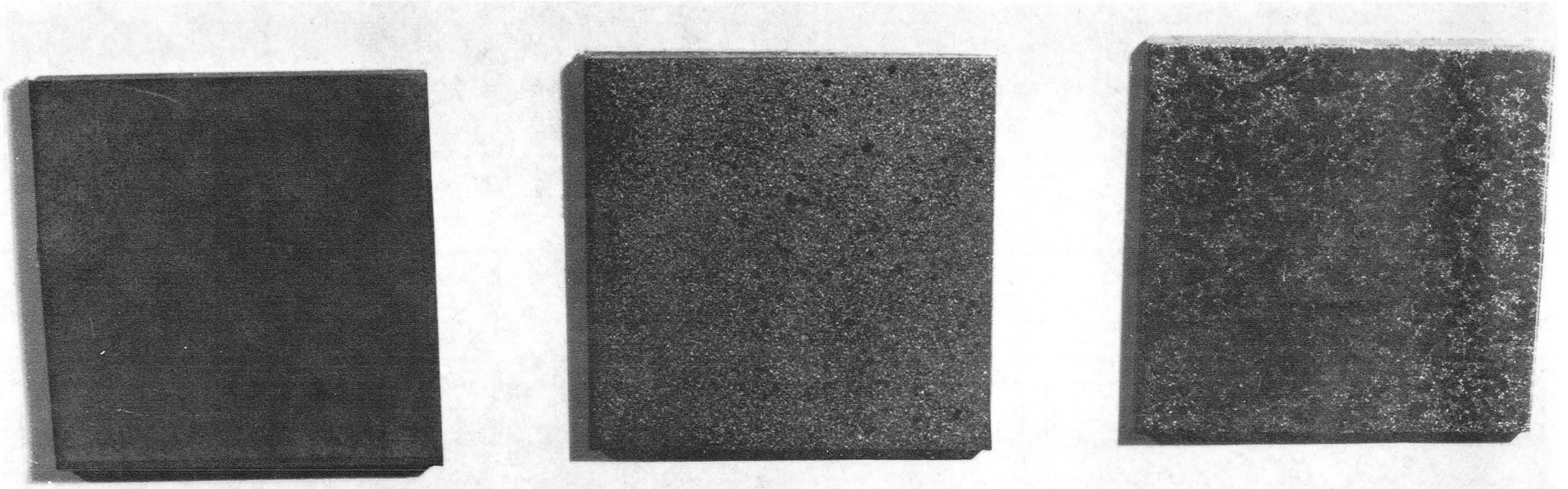

RUN NO. 7 ON PREOXIDIZED INCO X-750 FOIL

RUN NO. 8 ON PREOXIDIZED A-286 COUPON

RUN NO. 8 ON CLEAN A-286 COUPON

Fig. III.3a Photographs of A-286 and Inco X-750 Coupons Coated With $PbO-SiO_2-Ag-Fe_3O_4$

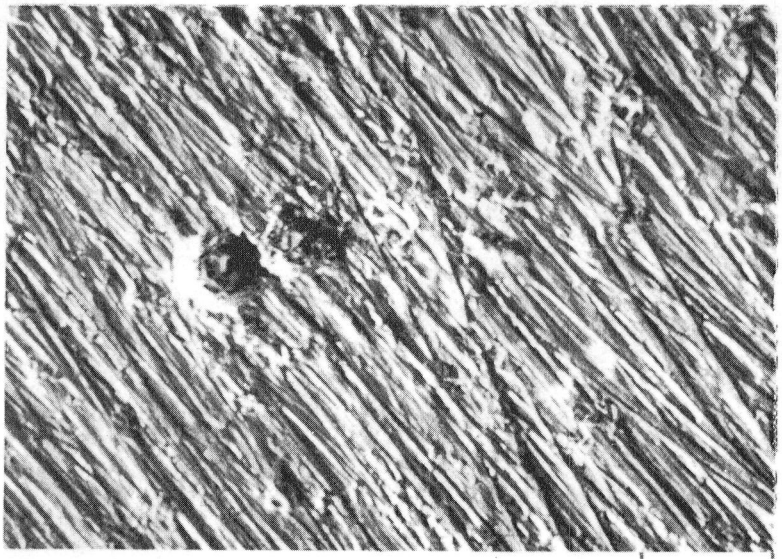

SURFACE MICROGRAPH

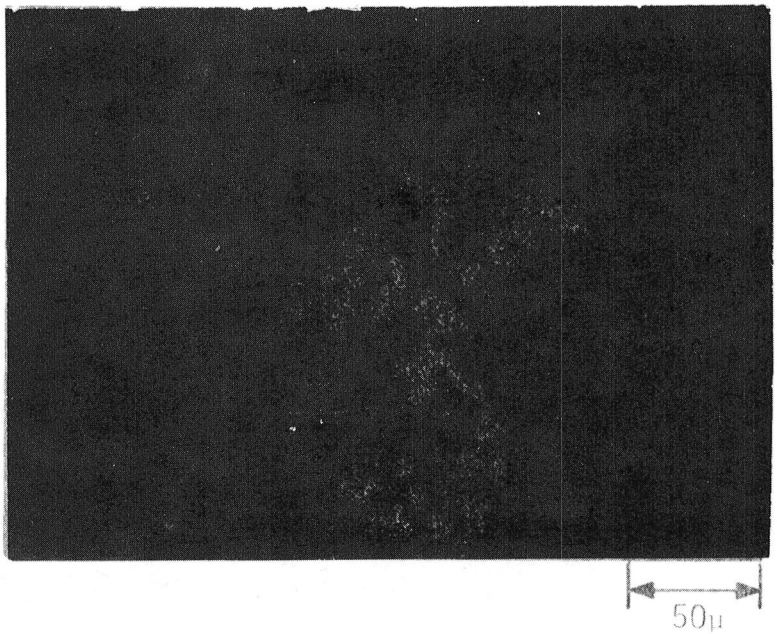

X-RAY MAPPING OF SILVER

Fig. III.3b SEM Micrograph and X-Ray Image of $PbO-SiO_2-Fe_3O_4-Ag$ Coating on Inconel X-750 Foil

cate system. No other patterns were detected. It should be noted that 4 $PbO-SiO_2$ is amorphous and has no diffraction pattern. The analysis shows that the coating has free PbO available which is a good high temperature lubricant.

SPUTTERED Cr_2O_3 COATINGS

Introduction

The primary objective here was to develop Cr_2O_3 coating for a 0.1 mm thick Inconel X-750 foil by sputtering techniques and to optimize sputtering parameters. Then this coating was applied on an A286 journal surface. This section describes the test apparatus and procedure, optimization of parametric study, and the results of metallurgical analysis.

Sputtering Apparatus and Procedure:

Sputtering was done using a commercial rf-diode sputtering apparatus operating at 13.56 MHz (mfg. by Perkin Elmer, Ultek Inc., Palo Alto, California, Model 3140-6J) powered by a 1/2 KW rf-generator. A schematic of the machine is shown in Figure III.4a and a photograph is shown in Figure III.4b. The material to be sputter deposited (normally called the target) is in the form of a hot pressed, disc-shaped compact, 152 mm in diameter and 4.75 mm thick which was commercially purchased from Materials Research Corporation, Orangeburg, New York. The target is mounted on a water cooled rf electrode. The specimen to be coated is placed directly below the target on a table connected to a water-cooled J arm which can swing out from under the target for easy loading of the specimens. The spacing between specimens and target can be varied from 38 mm to 125 mm. The spacing can be further reduced by adding stock on the table, but the sputter etching option becomes inoperative due to the close spacing between the specimen and the shutter. Polarity can be reversed and the specimen can be sputter-etched. A folding shutter is placed between the target and the substrate. Although the specimen table is water cooled, the temperature of specimen during sputtering at full power (500 W) may be as high as 250°C and at half power (250 W) the temperature may drop by 40%. The temperature of the specimen can be

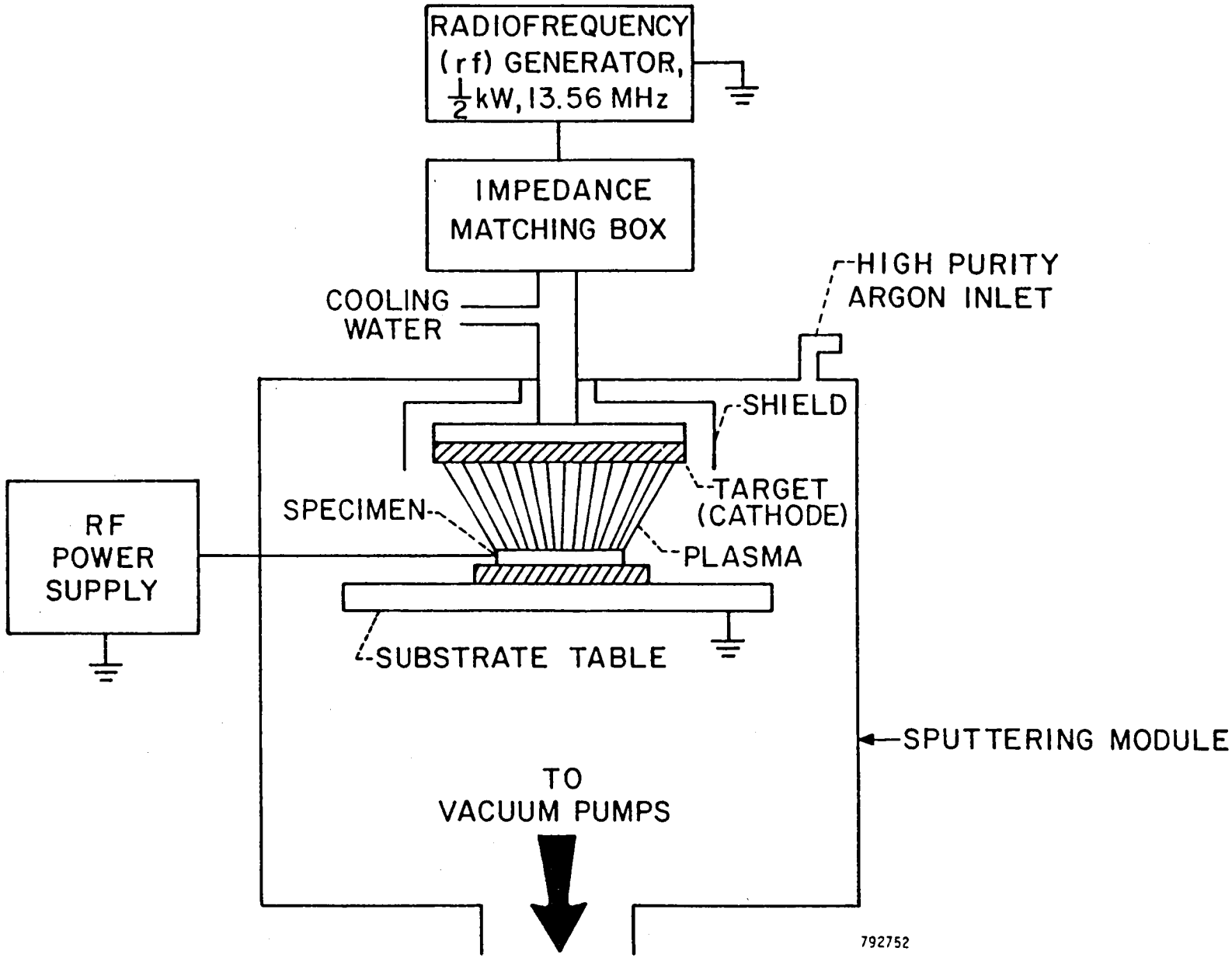

Fig. III.4a Schematic of Radio Frequency Sputtering Apparatus

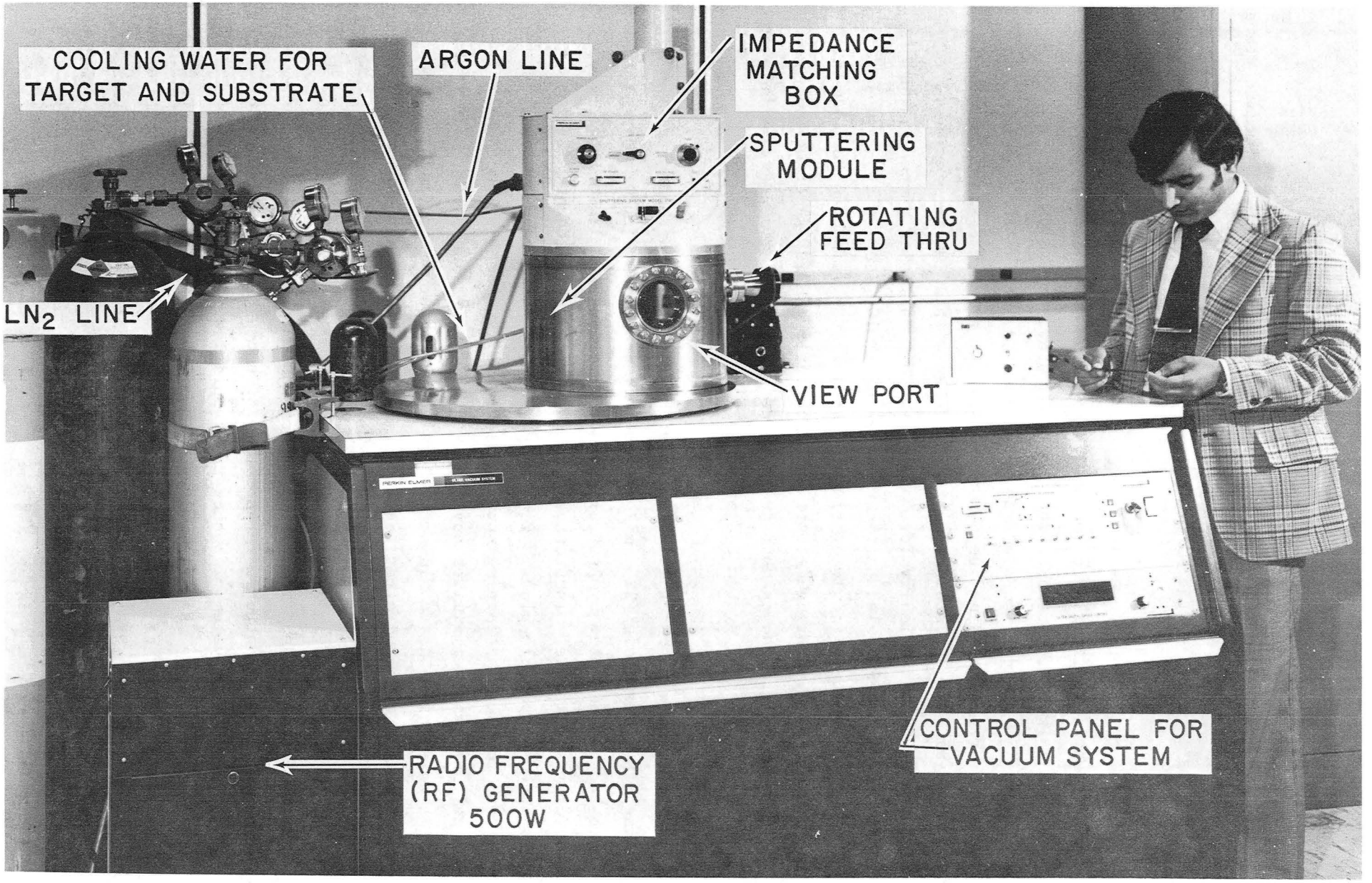

Figure III.4b Photograph of Radio Frequency Sputtering Apparatus

further increased if so desired by 30-40% by inserting a 4 mm ceramic plate between the specimen and the table. The temperatures cited here are the estimates supplied by the manufacturer.

A fixed ten percent of total rf power going to the sputtering module can also be applied directly to the specimen during film deposition. If the specimen is round, it can be mounted on a rotating feed through and rotated at low speed by an electric motor located outside the vacuum. The entire system comprising the diode (target and the table) is contained in a 375 mm diameter stainless steel chamber with a 100 mm viewing port. The system is mechanically fore pumped and oil duffusion pumped through a liquid nitrogen cooled baffle to between 5×10^{-7} to 7×10^{-8} Torr. The argon is bled a couple of times and the system is pumped down again to low pressure. During deposition, high purity (99.999%) argon was bled continuously into the chamber and a predetermined dynamic pressure balance between the pumping system and argon leak was maintained.

The specimens were carefully cleaned with anhydrous isopropanol alcohol using lint-free cloth (225 mm X 225 mm Poly Jean knitted from polyester yarn and washed, mfg. by Lens Clean Inc., Clifton, New Jersey) to remove any dirt and grease. Isopropanol was preferred over methanol due to outgassing. Disposable plastic gloves were worn during cleaning to avoid any finger prints. The coating surface is generally smooth if the substrate is polished which minimizes any preferential nucleation sites. Since the foils were thin, they could not be polished without distorting them and were coated as rolled after heat treatment in nitrogen atmosphere or as received in the annealed condition.

Prior to starting deposition, the target was outgassed overnight in a vacuum, then pre-sputtered for a couple of hours to clean the surface and help rid the system of background impurities. If the target was either new or had not been used for a long time, it was sputtered with a shutter in place for about eight hours or more before coating application to ensure removal of any surface oxides; otherwise, the target was sputter cleaned at full power ($\sim$400 W) until the level of reflected power stabilized which

was about 30 minutes for a Cr_2O_3 target. (Color of the plasma also gives indication if the system is clean. Pink-purple represents water vapor present and blue represents sputtering of Cr_2O_3.) Following target cleaning, the polarity was reversed and the specimen was etched with a shutter in place for about 30 minutes at an rf power level of 100 W and 950 volts. The low power was selected so that the specimen temperature would not warp it. After target cleaning and sputter etching, the system was pumped down to high vacuum to remove any contamination resulting from outgassing of the hot target and hot substrates. After about five minutes, Argon was bled and a predetermined pressure was again maintained. Then the sputter deposition was carried out in most cases at about 400 W or 220 W/mm^2 for about one hour. The voltage at the target at full power was about 1600 V and voltage at the specimen during bias sputtering (about 10% of total power) was about 100 V. The power in each case was increased slowly to avoid thermal shock of the target. After sputter deposition, the specimen was left inside the chamber to cool off for about 30 minutes before it was taken out.

Optimization of Cr_2O_3 Coating for Foil

The sputtering parameters have to be optimized for each coating system in order to obtain a smooth and dense coating with best adherence and desirable mechanical properties. In the case of a rough coating, the peaks may break off and debris would build up progressively during wear. Once a crack develops, it takes almost no energy to propagate. Therefore, smoothness of the coating is extremely important. The desired structure of the coating is either a uniformly columnar structure or as an equiaxed structure. A structure characterized by tapered crystallites with domed tops is not preferred because of its inferior strength and ductility due to high porosity of tapered crystallites. Porosity decreases as one changes from tapered to equiaxed structure.

Movchan and Demchishin [3.6] found that the grain size and structure depended on the sputtering conditions (see Figure III.5). It was later confirmed by Thornton [3.7] for thick copper coatings.

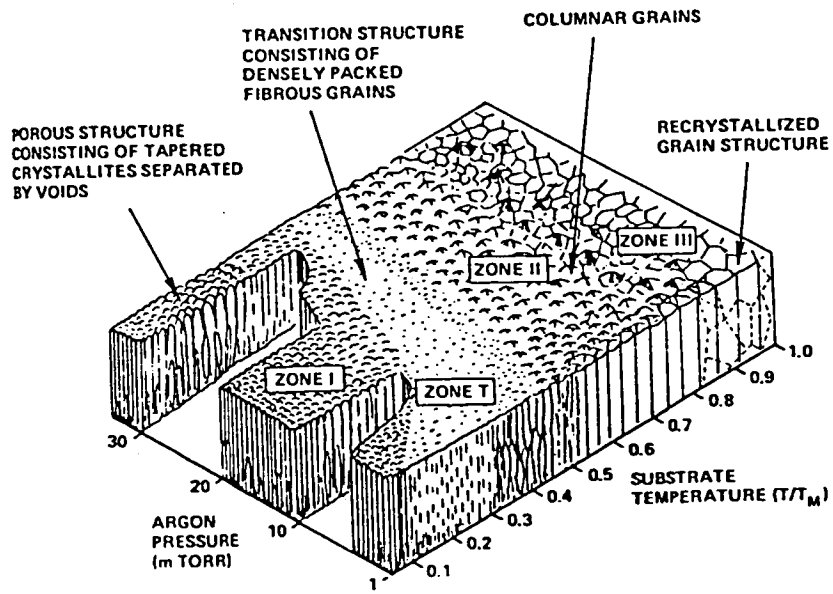

Fig. III.5 Influence of Substrate Temperature and Pressure on Microstructure of Sputtered Metallic Coatings (from Ref. 3.6). Numbers refer to Movchan-Demchishin zones.

793254

According to Taylor [3.8] the tensile strength and hardness of nitride, oxide, and carbides are low for tapered crystallites with dome tops (ZoneI) and high for equiaxed grains (Zone III). He also pointed out that attempts to deposit the Zone III type of coating at high temperatures have generally been unsuccessful in that the resulting coatings have high hardness but tend to spall due to the differential thermal expansion of the coating and substrate during cooling of the coating after deposition.

The parameter variations during the program were: chamber pressure, target to specimen spacing, power level, biasing, substrate temperature, substrate hardness, and coating thickness. The coatings were applied on 0.1 mm thick Inco X-750 foils, two glass slides making a step, and a carbon planchet. A coating step on the glass slide was measured using a Taylor-Hobson profilometer in order to determine the coating thickness. The coating on carbon planchets was applied for electron-microprobe analysis in order to eliminate substrate interaction. The optimization of sputtering parameters was done on Cr_2O_3 coating. These parameters were then used to develop other Cr_2O_3 based coating.

The foil samples were examined under SEM up to 10,000X for surface morphology. This consisted of vapor depositing about 200 Å of gold-palladium alloy (60-40) onto the surface of each sample to enhance electron image contrast of the surface.

A 180° bend test to determine the coating adhesion and cohesion was conducted on sections of the samples trimmed to rectangles approximately 25 mm X 5 mm in size. Each strip was then bent back upon itself at the center of the long dimension. The coating was on the outside of the bend. The bend sample was then placed inside the SEM, and photographed in a direction normal to the outside of the bend at a magnification of 700X. X-ray diffraction and Auger Electron Spectroscopy (AES) analysis were carried out on selected samples. The samples were analyzed by X-ray diffraction over a 2θ range of 10° to 90° employing chromium radiation and a vanadium filter. The specimens were cleaned by sputter etching prior to obtaining the AES data.

Adhesion strength of the coatings was measured using a coating adherence tester manufactured by Quad Group, Santa Barbara, California. The coated specimens were mounted with an epoxy on a stud whose other end was pulled by motor and the pull stress was continuously recorded. In the case of Inconel foil, a glass backing plate was epoxied to the surface in order to prevent any deflection of the foil. The stress required to pull the coating was thus measured. The stress capability of the unit is 68.9 MPa (10,000 psi).

Flex tests on the coating were conducted using a commercially available bending fatigue machine. The settings were: maximum peak-to-peak amplitude - 12 mm, frequency - 1200 cpm, and specimen length - 50 mm.

Effect of Target-to-Substrate Spacing: Generally, sputtering rates are inversely proportional to the electrode spacing and the coating is non-uniform at excessive spacing because the sputtering atoms are diverted and some of the kinetic energy is lost by interactions with ionized gaseous particles and other contaminants. The coating sometimes also becomes contaminated resulting in poor adhesion. Four spacings were tried--63.5 mm, 50.8 mm, 41.3 mm, and 38 mm. The coating was non-uniform and very thin when the spacing was 63.5 mm (Sample No. 1, Table III.2). Coating with a spacing of 50.8 mm (Sample No. 2) exhibited considerable crazing and flaked off during the bend test. With a 38 mm spacing, the sputter-etching feature could not be used because the shutter was too close to the specimen table and the run was stopped. The coating with 41.3 mm spacing (Sample No. 5) was uniform and exhibited less crazing than Sample No. 2. Small cracks with a width on the order of 0.15μm ran transverse to the bend. Little flaking of the coating was also apparent. The other parameters, coating thickness and adhesion, and comments are shown in Table III.2 (Sample Nos. 1, 2, and 5) and SEM photographs of coated and bend surfaces shown in Figure III.6. Based on the metallurgical examination, Sample No. 5 (i. e., spacing of 41.3 mm) was considered optimum.

Effect of Pressure: As the pressure in a sputtering system is raised, the ion density and, therefore, the sputtering-current density increases. Therefore, for constant power input, the deposition rate increases

TABLE III.2

TEST DATA OF Cr_2O_3 SPUTTER-COATED SAMPLES

Sputtering Time = 1 hour

Sample No.	Spacing mm	Power Watts	Chamber Pr Microns	Bias Sputter	Water Cooled Substrate	Foil Heat Treated	Thickness μm (μin.)	Adhesion† MPa (ksi)	Comments
1	63.5	390	10	No	Yes	Yes	0.46 (18)	36.5 (5.3)	Coating - nonuniform
2	50.8	390	10	No	Yes	Yes	0.61 (24)	70.3+ (10.2+)	Coating - nonuniform
5	41.3	390	10	No	Yes	Yes	1.02 (40)	54.9+ (7.97+)	Round globules 0.2 μm on top of a slight grainy surface.
6	41.3	390	5	No	Yes	Yes	0.89 (35)	54.6+ (7.93+)	Grainy surface (grains - 0.1 μm) with large globules 0.5 μm in diameter.
7	41.3	390	20	No	Yes	Yes	1.27 (50)	70.3+ (10.2+)	Jagged globules ~0.5 μm in diameter on field of the small (~.1 μm) grains.
8	41.3	390	30	No	Yes	Yes	1.52 (60)	63.9+ (9.28+)	Much grainier or even porous structure. Pores ~0.2 μm in diameter.
9	41.3	200**	10	No	Yes	Yes	1.40 (55)	70.3+ (10.2+)	Grainy appearance (0.1-0.2 μm diameter). Larger (~.5 μm) globules scattered.
12	41.3	390	10	Yes	Yes	Yes	-	66.4 (9.64)	Some coating came off in handling. Smoother appearance with scattering of 0.2 μm grains.
13A	41.3	390	10	No	Yes	No (annealed)	1.02 (40)	70.3+ (10.2+)	Smoothest with an extremely fine structure.
13B	41.3	390	10	No	No*	Yes	1.02 (40)	70.3+ (10.2+)	Like 13A but large globules (~0.5 μm) scattered.
14	41.3	390**	10	No	Yes	Yes	2.16 (85)	-	Coating peeled off.
16	41.3	390***	10	No	Yes	Yes	1.65 (65)	40.0 (5.81)	Porous looking with ~0.2 μm grains.

* Specimen placed on ceramic plate

** Sputtered for two hours

*** Sputtered for 1.5 hours

† + Indicates that either limits of the machine (68.9 MPa) was exceeded or epoxy fractured.

Repeat runs numbered 29, 50, 51, 55, and 56 were made using sputtering parameters used in sample No. 13A.

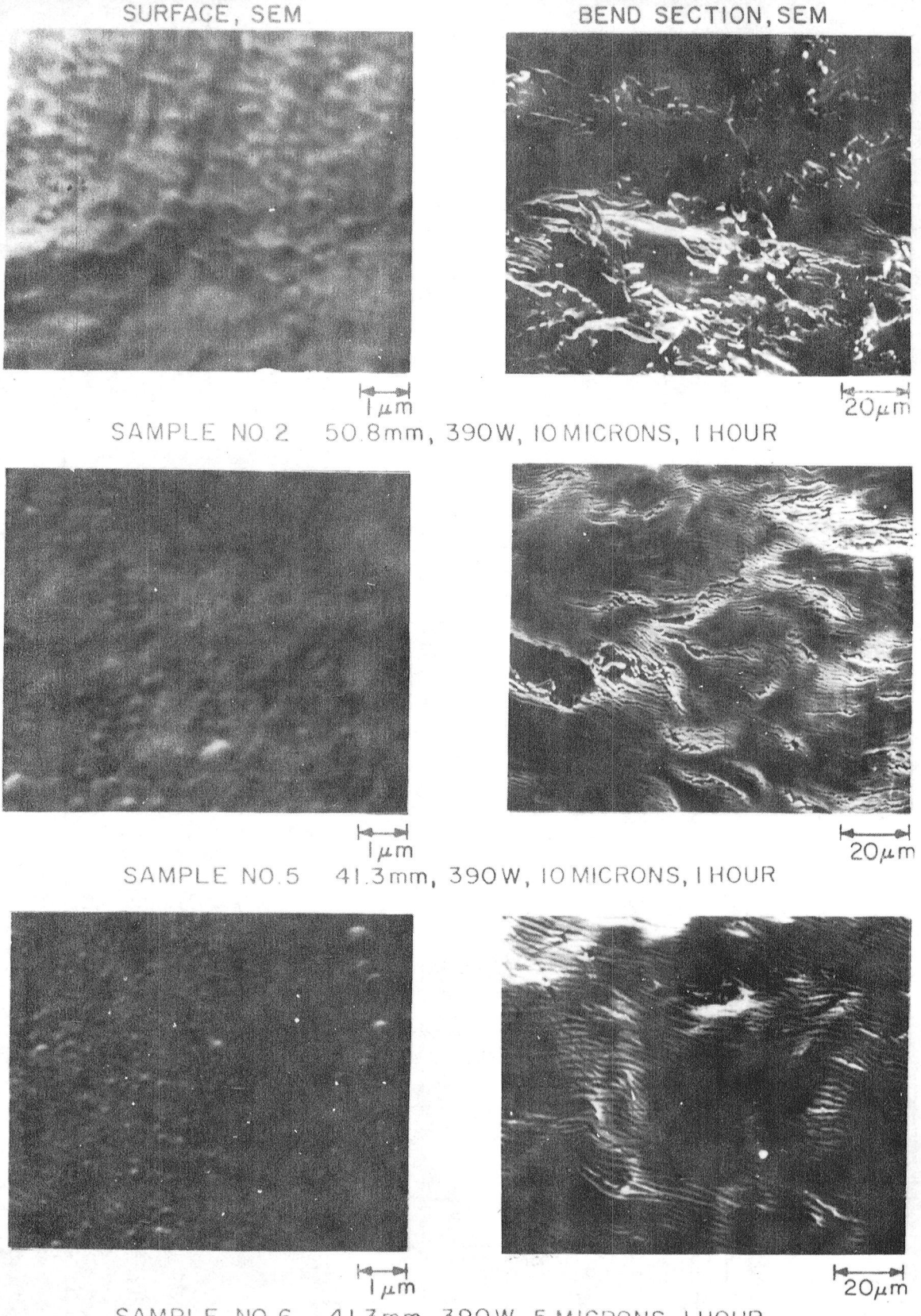

Fig. III.6 SEM Micrographs of Cr_2O_3 Deposited at Various Sputtering Conditions. Following conditions were used: water cooled substrate, foil-heat treated, and sputter-deposit mode.

linearly with pressure provided the latter is not too high. At high pressures, higher than 130 microns (mTorr), a fraction of the sputtered deposit returns to the cathode by back diffusion and the deposition rate goes down (see Maissel and Glang [3.3]). Normally, the coating becomes rough at high pressure due to increased thickness. Results of Sample Nos. 5 to 8 reported in Table III.2 show that the sputtering rate increases with increase in pressure. Figures III.6 and III.7 show that the coating is smoothest when the pressure is lowest (5μ). When the pressure is high, there is increased diffusion of argon gas in the coating and other contaminants present in the gas which make the coating rough and less adherent. Sample No. 6 exhibited considerable crazing with hardly any flaking. Sample No. 7 exhibited crazing and minor flaking, and Sample No. 8 exhibited crazing and had wide separations in the coating. Based on these examinations, a pressure of 5 to 10μ is considered optimum for this coating.

Effect of Power and Substrate Temperature: The effect of power and substrate temperature are interrelated. If power is increased, both the target and the substrate temperatures increase. It has been observed that at high substrate temperatures the coating sometimes outgasses, and there is desorption of impurities during sputtering. Hence, this can provide cleaner deposition surface and thereby an adherent film. In some cases, heating of the substrate may aid the formation of an intermetallic interface layer which facilitates adhesion (see Greene et. al. [3.4]). High Cathode (target) temperature can degas and desorb the surface rapidly.

In case of multi-component films, the components with the highest sputtering rates will come off faster; but a so called "altered region" soon forms at the surface of the cathode. This region becomes sufficiently deficient in the higher-sputtering yield component to compensate for its greater removal rate; so subsequent deposits have the compositon of the parent metals. If the cathode temperature is too high, not only can this cause diffusion into the altered layer, but one or more of the components of the system may have a significant vapor pressure under this condition which might lead to its evaporation from the cathode. Therefore, the level of power becomes crucial (for more details, see Maissel and Glang [3.3]).

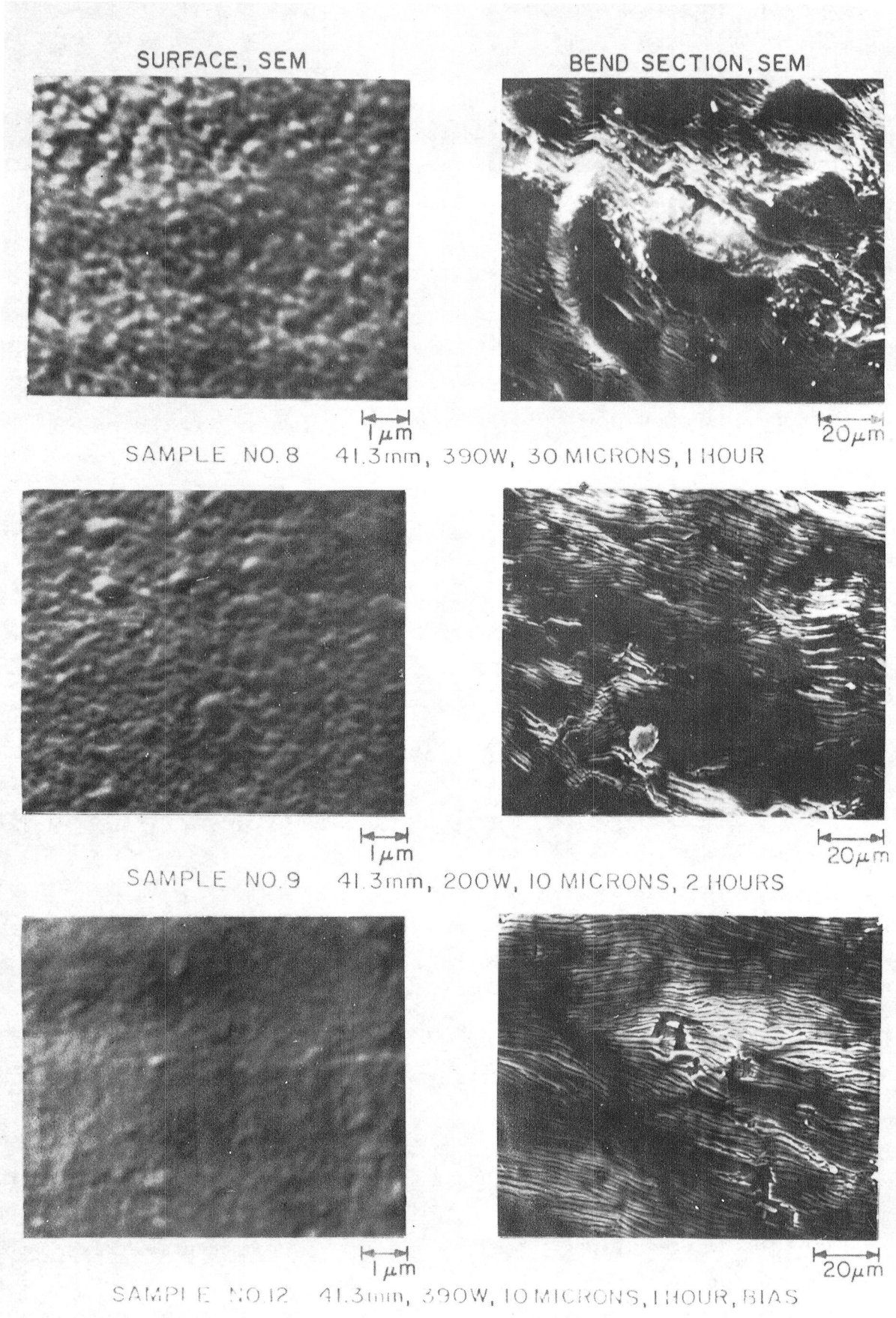

Fig. III.7 SEM Micrographs of Cr_2O_3 deposited at various sputtering conditions. Following conditions were used unless otherwise specified: water cooled substrate, foil-heat treated, sputter-deposit mode.

Examination of results reported in Table III.2 (Samples Nos. 5, 9, and 13B) and SEM micrographs in Figures III.6 to III.8 show that coating at half power (Sample No. 9) is not as good as coating at 390 W (Sample No. 5). Sample 9 exhibits a surface of long parallel cracks, many of which extend across the entire field of view of the micrograph. Coatings applied at high substrate temperature (Sample No. 13B) are also rough and crazed more in the bend test with numerous patches in which there are large separations ($\sim$11μm) in the coatings. Probably insulation by the ceramic plate develops some bias which further increases the temperature and the coating cracks or builds up stresses during cooling after sputtering. Sputtering conditions of full power (390 W) and a water-cooled substrate are recommended for an optimum coating.

Effect of Bias: The use of a negative bias is generally found to be beneficial in the cleaning technique. Surface ion bombardment removes impurities in the coating occurring by chemisorption and condensation. It is believed that during re-sputtering (due to bias voltage), most impurities should be preferentially removed from the atoms of the main film. Whether or not impurities are removed depends on the relative strengths of the metal-to-impurity and the metal-to-metal bonds.

In the run with chrome oxide using bias (Sample No. 12), the coating exhibited crazing with long parallel cracks (see Figure III.7). The coating peeled off because of intrinisic film stresses. Also, the temperature of the substrate is usually higher during bias than sputter deposit, therefore, the biased coating probably could crack during cooling after sputtering because of thermal stresses. As observed in the analysis reported later, one reason for poor adherence in biased chrome oxide coatings was absence of a naturally occurring oxide layer at the interface.

Effect of Substrate Hardness: Substrate hardness has a significant effect on the coating adhesion. If the substrate is soft, the sputtering atoms are expected to penetrate more deeply into the surface and provide adherent film. If the substrate is very hard, the coating adhesion can be improved if it is coated in the annealed condition and then heat treated provided the coating can withstand heat treatment cycle. Also, the heat treatment

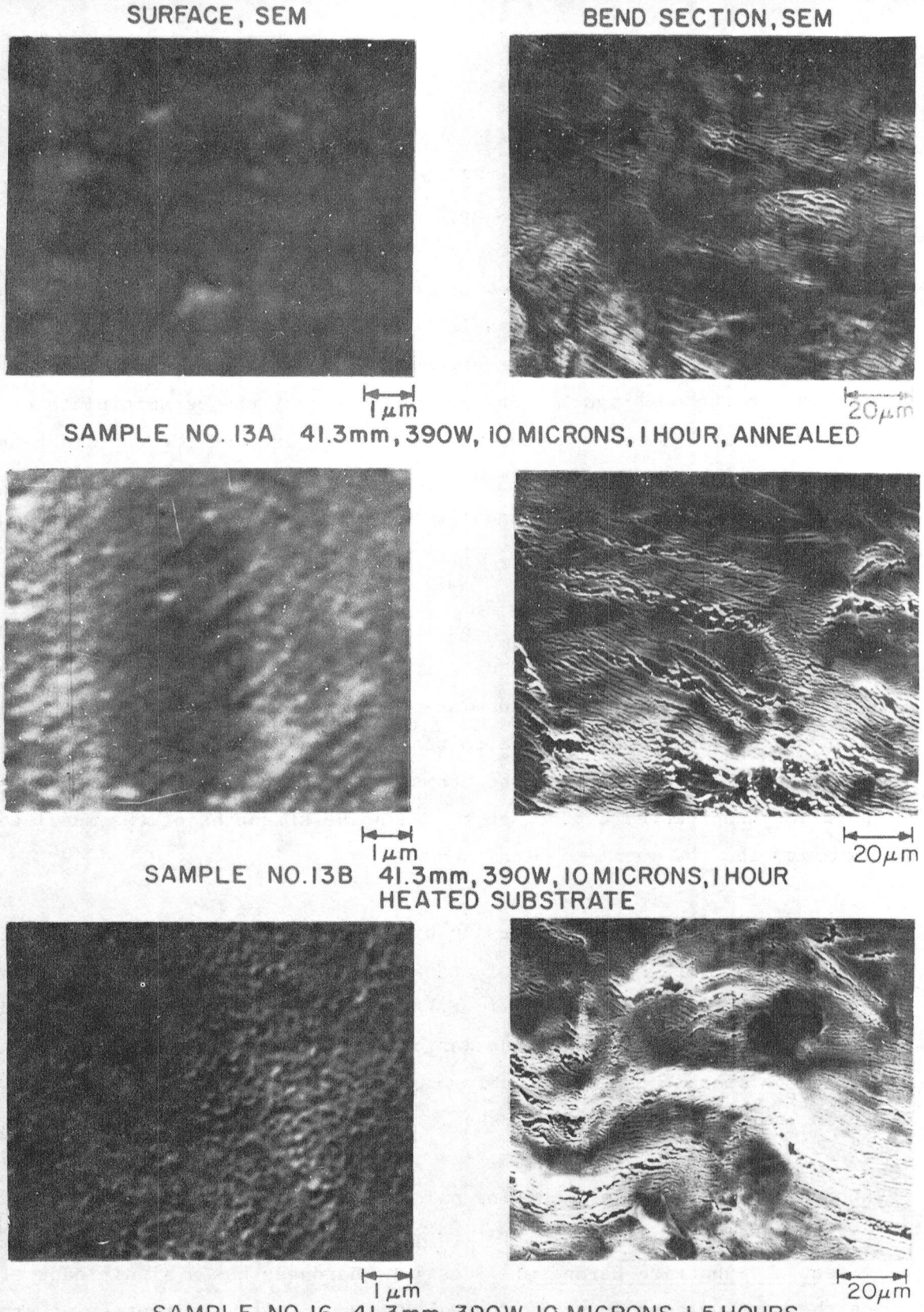

Fig. III.8 SEM Micrographs of Cr_2O_3 deposited at various sputtering conditions. Following conditions were used unless otherwise specified: water cooled substrate, foil-heat treated, and sputter-deposit mode.

can promote diffusion at the interface which normally provides a stronger bond.

A foil was coated in the annealed condition (Sample No. 13A). Bend tests showed that the coating suffered the least amount of damage during the test; SEM surface photographs also show that the coating is smooth. Consequently, coating annealed material is recommended (see Figure III.8).

A fatigue test on the coated foil was conducted for 72 hours and the samples were examined in the SEM. No cracking was observed in the test samples. The coated foil would have to be heat treated before installing in the bearing. A coated sample was heat treated using the Inconel X-750 heat treatment procedure (704°C/20 hours). Metallurgical tests on the heat treated sample showed that there was no significant change in the surface appearance and coating adhesion from the heat treatment.

Effect of Coating Thickness: During sliding contact, coatings wear and coating life can sometimes be increased if the coatings are thick. However, if the sputtered coatings are too thick, they spall. The thickest coatings were obtained in Sample 14 and 16. The coating thickness was 2.16μm (85μin.) in Sample No. 14 and the coating spalled. At one-half this coating thickness (Sample Nos. 5 and 6) spalling did not occur, and the coating looked smoother than the thicker coating. This is normal. As coatings grow in thickness, they get rougher due to the influence of preferential nucleation sites. A coating thickness of about 1μm (40μin.) is smooth and well bonded and is considered an optimum for this coating-substrate combination.

Effect of Substrate Surface Topography: A smoother coating would have improved wear life because high spots in a rough coating can easily be knocked off during sliding resulting in catastrophic failure. The smoothness of the coating considerably depends on smoothness of the substrate. A coated glass slide (which is considerably smoother than Inco X-750 foil) from Sample No. 13A was examined under SEM which showed that the coating on slide was smoother than that on Inco X-750 (see Figure III.9). Therefore, results reported here are only valid for the Inconel foil and if

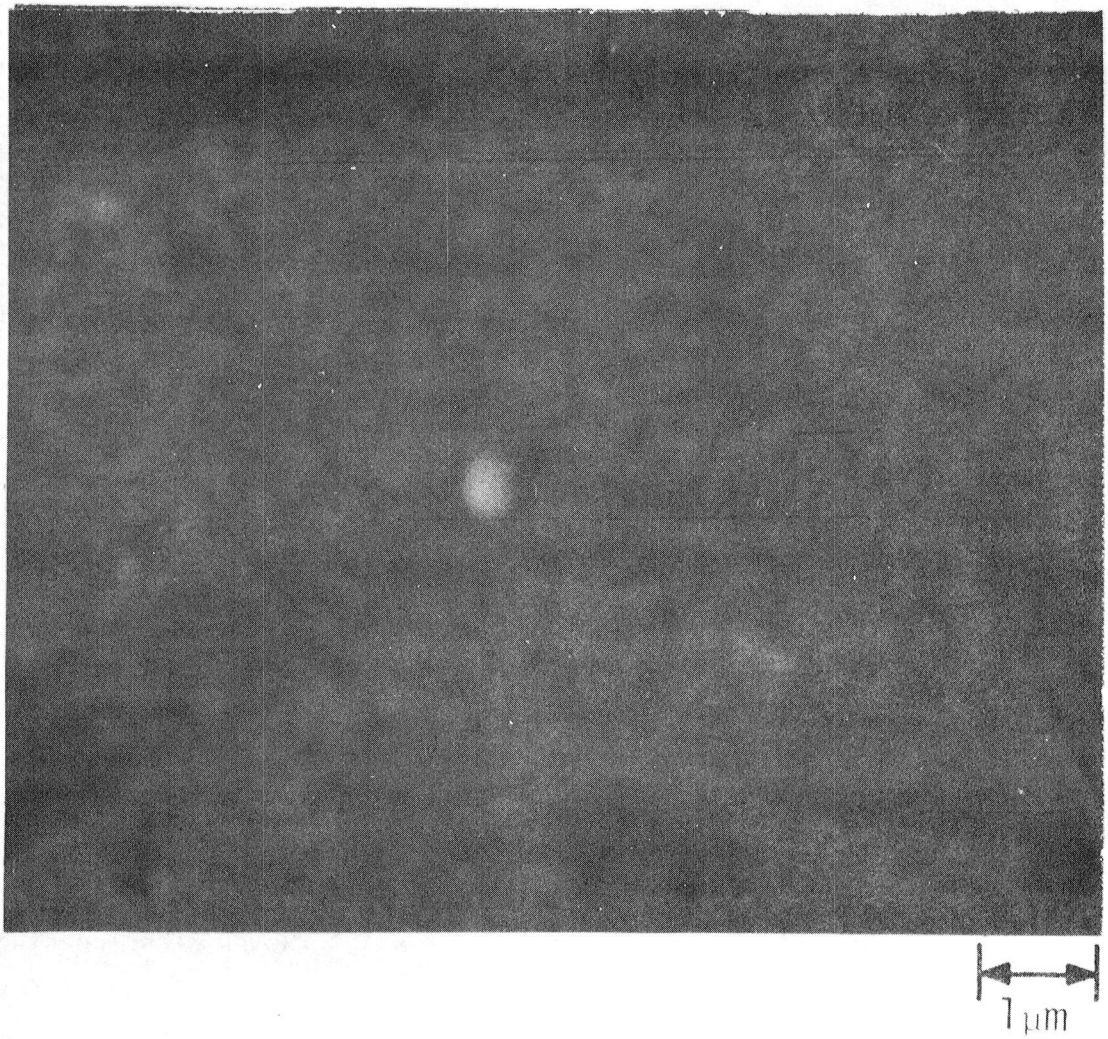

SAMPLE No. 13A 41.3 mm, 390 W, 10 MICRONS
1 HOUR

Fig. III.9 SEM Micrograph of Sputtered Cr_2O_3 Coating on a Glass Slide

793274

the substrate roughness, etc., is changed, coating morphology would be changed.

Analysis of Selected Samples: Surface composition studies of selected samples (Nos. 2, 5, 8, 9, 12, 13A, and 13B) and a chip from Cr_2O_3 target were made by Auger Electron Spectroscopy (AES)(for details see Appendix A). The Auger spectra showed the expected peak for Cr and O, and in addition very small peaks for S, Cl, and C, presumably as surface impurities. There were minor variations in peak heights on different areas of the coating, indicating good coating uniformity. The results indicate that all the samples show essentially the same atomic ratio of O to Cr indicating that the coating composition did not change significantly with the indicated change in sputtering parameters.

Concentration versus depth profiles were conducted on the following Sample Nos.: 5, 12, and 13A after heat treatment at 704°C/20 hours/AC. The sample No. 5 had a native chromium rich oxide layer on the substrate, prior to film formation. This probably accounts for better bond than in Sample No. 12 (bias sputtered). In Sample No. 13A (heat treated), there was some diffusion of Fe at the coating interface during heat treatment which probably improved the bond. As discussed earlier, the coating on annealed foil (as sputtered 13A) was also well bonded probably because of the soft substrate.

X-ray diffraction studies of Samples 5, 12, and 13A after heat treatment show that the coatings as sprayed are amorphous with microcrystalline structure of Cr-O; but after heat treatment, the coating crystallizes and is made of Cr_2O_3.

Auger analysis on the contrary show that it is CrO with some oxygen deficiency. There is no convincing reason for this difference except that the atoms could rearrange to Cr-O in the top atomic layers of the coating because of its lowest energy configuration. It has been mentioned earlier that in case of sputtering of multi-component materials if the sputtering rates of the components are different, the very first time that sputtering is performed from a multi-component cathode, the component with the highest

sputtering rate will come off faster; but a so called "altered region" soon forms at the surface of the cathode. This region becomes sufficiently deficient in the higher sputtering yield component to compensate for its greater removal rate; so subsequent deposits have the composition of the parent material. With subsequent sputtering the altered layer is maintained. The thickness of the altered layer varies and was found to be about 40 Å for sputtering of $AuCu_3$ alloy from bombardment by 400-eV ions (see Maissel and Glang [3.3], p. 4-39). It is very possible that Auger measured the composition of this altered layer rather than the bulk of the coating.

An X-ray diffraction study examines the bulk of the coating and is more reliable for composition. Auger is a good tool to get relative measurements and to get depth profiles. Therefore, it is concluded that the bulk of the coating is Cr_2O_3.

Conclusions: Chrome oxide, a hard refractory coating, can be sputtered successfully on Inconel foil and an acceptable adhesion and smoothness can be achieved using optimum sputtering parameters. The substrate hardness has some influence on the coating adhesion. Softer material substrates have been found to have improved adhesion.

Low pressure in the sputtering system, high power, and water cooled substrate improve the coating adhesion and its smoothness. Biased coatings were not as adherent as sputter-deposited coatings and had a lot of internal stresses. One reason could be absence of naturally occurring chrome oxide layer present at the interface in biased coatings which may be responsible for increased adhesion. The optimum thickness of the coating was found to be about 1μm (40μin).

The deposited coatings were amorphous as sputtered. After heat treatment the coatings were crystallized and made of Cr_2O_3. The coating recommended for bearing tests was the coating as applied in Run #13A.

Cr_2O_3 Coating for A286 Journal

The optimized Cr_2O_3 coating was applied on the A286 journal (38 mm O.D. and 38 mm long). The journal was clamped on the rotating feed through. The journal was rotated at 1 rpm by an electric motor coupled to gear reduction unit. Because of the apparatus limitation, the journal could not be sputter etched before coating application. The mimimum distance between the top of the journal and the target was fixed to 50.8 mm and was used. All other parameters and coating procedures were the same as described in the previous section for Sample No. 13A. The journal was ground and lapped to about 0.076μm (3 μin) before coating.

An A286 flat coupon (about 3 mm thick) was placed next to the journal for metallurgical examinations and adhesion tests. About 6 mm wide foil was wrapped on the dummy journal and held tight by a thin wire wrapped over the foil. This created a step on the journal which could be measured by the Talysurf. Thus, coating thickness could be determined. It took about four hours to get 2μm (80μin) thick coating.

Two coating thicknesses 2μm (80μin) and 1.25μm (50μin) with sputtering times of four hours and three hours, respectively, with 300 W power, were prepared. The thick coating was scratched by a scriber held at about a 45° angle to the plane to be tested, but the thin coating was not. There was no damage whatsoever of the thin coating when rubbed with 600 grit emery paper. Therefore, the thin coating was selected (Run No. 54). The adhesion of the coating was in excess of 68.9 MPa (10,000 psi).

Any bend tests could not be performed because the A286 coupon was very thick. SEM examination of the coupon was conducted and the coating was found to be fairly smooth with some randomly scattered globules (see Figure III.10).

SPUTTERED Cr_2O_3 COATING WITH NICHROME BINDER

Optimized parameters for straight Cr_2O_3 were used for development of Cr_2O_3 coating with nichrome metallic binder. The target consisted of 25% nichrome (80% Ni, 20% Cr) and 75% Cr_2O_3. All the runs were made

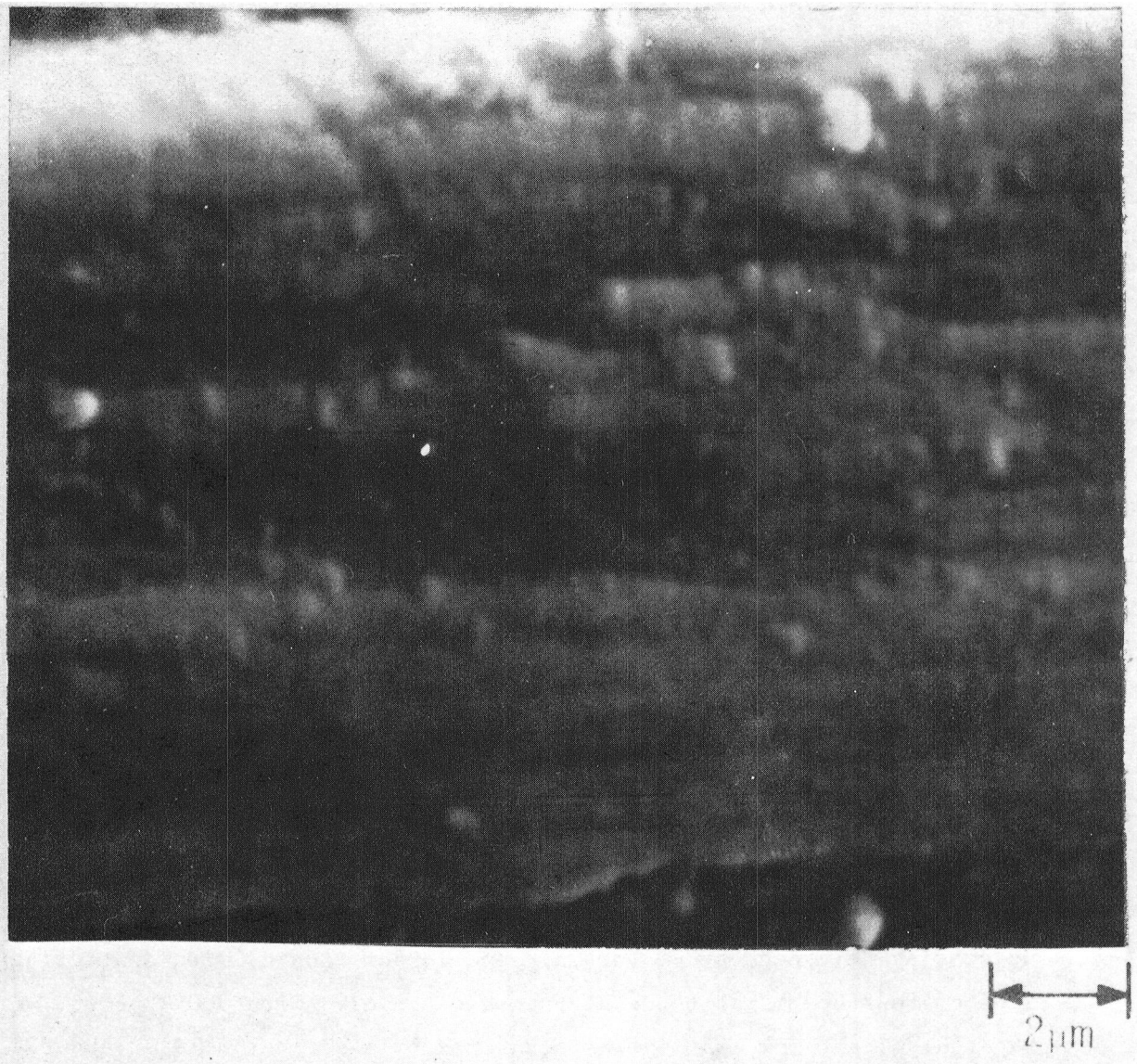

SAMPLE NO. 54 50.8 mm, 300 W, 6 MICRONS, 3 HOURS

Fig. III.10 SEM Micrographs of Sputtered Cr_2O_3 on A-286 Coupon

with a target-substrate spacing of 41.3 mm, at full power of 390 W and a chamber pressure of 10μ. Later during the program, it was realized that a smoother coating could be obtained at pressures of 6μ and some runs were prepared at this pressure. The substrate and the target were water-cooled.

The variations studied were: sputtered deposit/bias mode, coating thickness, and heat treated/annealed substrate.

Heat Treated Foil

The first four runs (Sample Nos. 20 to 23) were made on the heat treated foils consisting of two coating thicknesses in sputter-deposit and bias sputter modes. Selected SEM micrographs of the surface and bend samples are shown in Figure III.11 and the coating thicknesses, adhesion strengths, and comments on surface appearances are given in Table III.3. The thicker coating (1.14μm) applied in sputter-deposit mode was rougher in appearance than a thinner coating (0.76μm). Bend tests showed that Sample No. 21 exhibited considerable crazing and severe flaking off of the coating. Sample No. 20 performed slightly better. Therefore, a thin coating of about 0.76μm thickness is preferred. A coating 1.14μm thick was applied in bias-sputter mode and it loosened in spots during handling. Even thinner coating (0.89μm thick, Sample 23) flaked off badly in the bend tests. This coating was slightly rougher than that coating in the sputter deposit mode (Sample 20). Poorer performance of bias sputtered Ni-Cr-Cr_2O_3 is consistent with that of Cr_2O_3 coating.

It should be noted that the crazing of Ni-Cr-Cr_2O_3 is coarser than that of straight Cr_2O_3 which implies that this coating is more ductile.

Annealed Foil

Next the coating was applied on annealed foil in sputter deposit mode since bias sputtered coating had tremendous residual stresses and were not as adherent. After coating application, the foil was heat treated. SEM micrographs of the coating surfaces and of bend section are shown in Figure III.12 and other data are presented in Table III.3. The coating

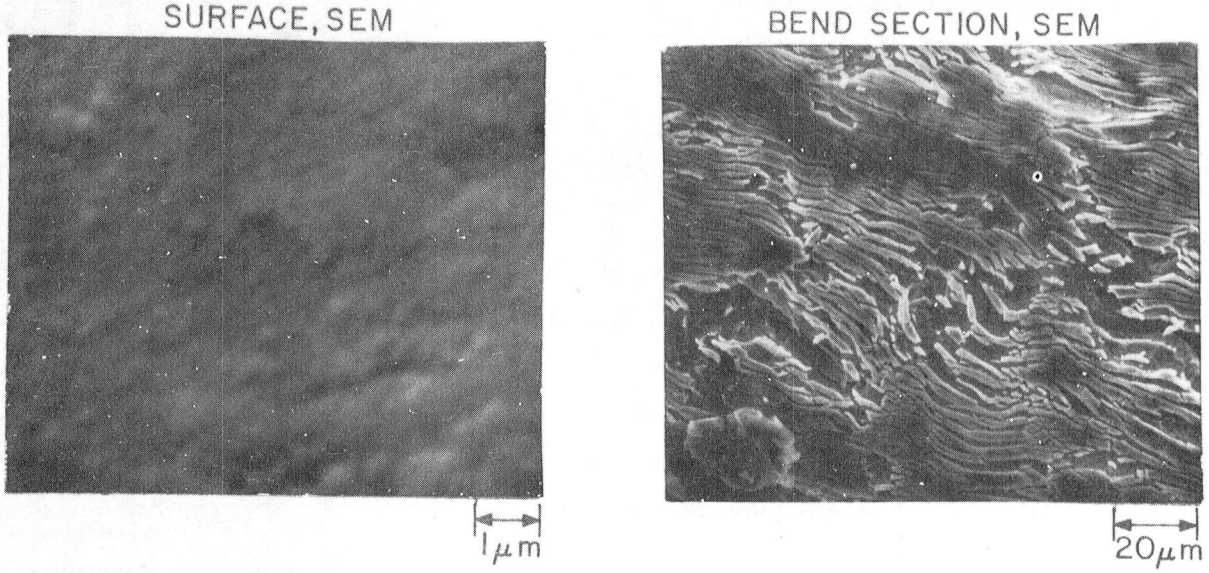

Sample No. 20 41.3 mm, 390 W, 10 Microns, 40 Minutes, Sp. Deposite

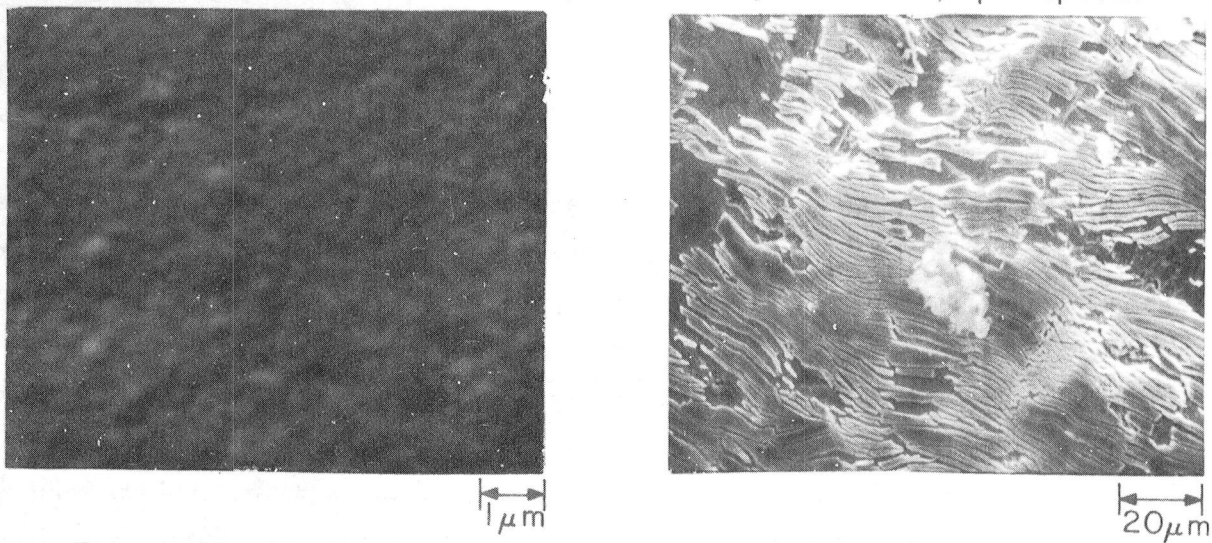

Sample No. 21 41.3 mm, 390 W, 10 Microns, 1 Hour, Sp. Deposite

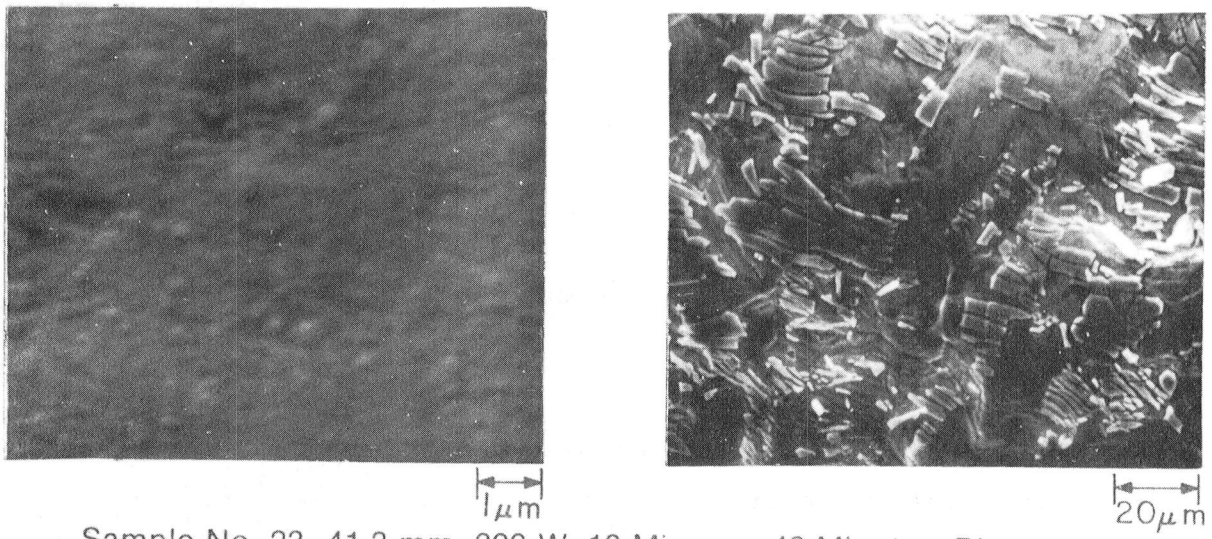

Sample No. 23 41.3 mm, 390 W, 10 Microns, 40 Minutes, Bias

Fig. III.11 SEM Micrographs of Ni-Cr-Cr_2O_3 Deposited for Various Sputtering Conditions on Heat Treated Inco X-750 Foil.

TABLE III.3

TEST DATA OF Ni-Cr-Cr_2O_3 SPUTTER COATED SAMPLES

Spacing = 41.3 mm, Power 390 W
Substrate - Water Cooled

Sample No.	Bias Sputter	Foil Heat Treated	Chamber Pressure Microns	Sputtering Time Min.	Thickness μm(μin.)	Adhesion† MPa (ksi)	Comments on Surface Appearance	Comments on Bend Test
20	No	Yes	10	40	0.76 (30)	70.3+ (10.2+)	Uniformly grainy surface (grains ~0.1-0.2 μm)	Exhibited considerable crazing and severe flaking
21	No	Yes	10	60	1.14 (45)	67.7 (9.82)	Grainy surface same as sample 20 but has patches of larger globules ~0.8 μm	Same as sample 20
22	Yes	Yes	10	60	1.14 (45)	65.7 (9.54)	Some coating peeled off in handling	-
23	Yes	Yes	10	40	0.89 (35)	70.3+ (10.2+)	Resembles sample 21 except larger globules are smaller ~0.4 μm	Most of the coating flaked off
30	No	No (annealed)	10	60	1.14 (45)	70.3+ (10.2+)	Uniformly grainy appearance (grains ~0.1-0.2 μm)	Exhibited considerable crazing but very minor amounts of flaking
38	No	No (annealed)	6	40	0.76 (30)	70.3+ (10.2+)	Grainy appearance (grains ~0.1 μm)	Exhibited crazing and very little flaking
47	No	No (annealed)	6	30	0.58 (23)	70.3+ (10.2+)	Coating smooth	Exhibited crazing with no flaking
31*	Yes	No (annealed)	10	60	1.14 (45)	70.3+ (10.2+)	Grainy appearance (grains ~0.1 μm) and patches of larger grains ~0.3 μm	Resembles sample 30
34*	No	Yes	10	60	1.02 (40)	56.5 (8.20)	Grainy appearance with patches of grains ~0.2 μm	Exhibited much crazing and some flaking off
32	No 3 min. Yes 57 min.	Heat treated + annealed	10	60	1.14 (45)	65.6 (9.52)	Coating peeled off in handling on all foils	-

† + Indicates that either limit of the machine (68.9 MPa) was exceeded or epoxy fractured
* Substrate not etched prior to coating

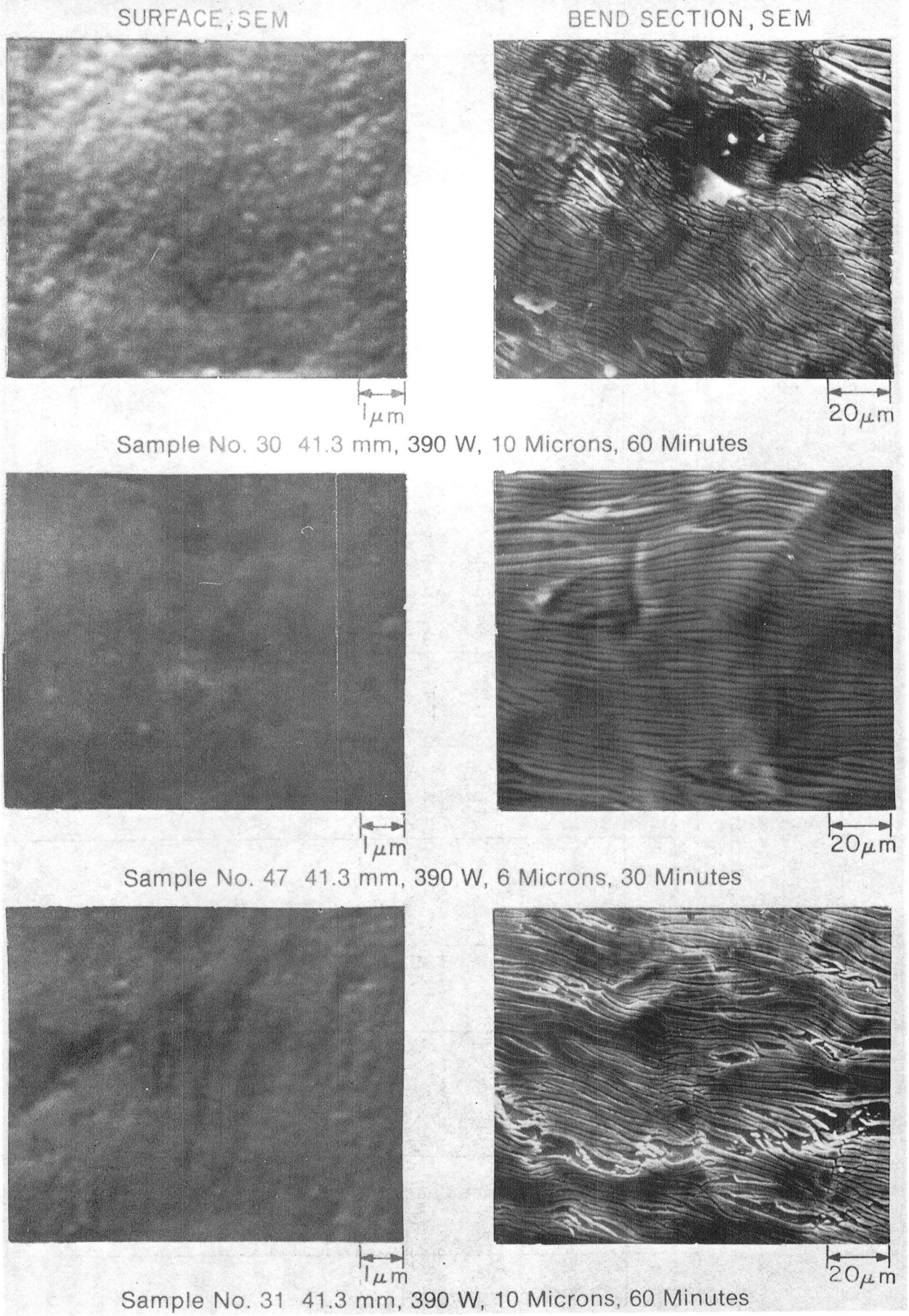

Fig. III.12 SEM Micrographs of Ni-Cr-Cr_2O_3 Deposited for Various Sputtering Conditions on Annealed Inco X-750 Foil. The coating was applied in sputter deposit mode.

792860

thickness in Run No. 30 applied was 1.14μm (45μin) thick. This coating had the least crazing compared to heat treated foils after coating and was selected for start/stop tests. This coating had slight spalling and more runs (Nos. 38 and 47) were made with reduced coating thicknesses. The coating, 0.58μm thick (Sample #47) had no spalling during bending and the surface was very smooth and was selected for wear tests.

Effect of Surface Preparation

Brainard [3.5,2.7] during the investigation of Mo_2C, Mo_2B_5, and $MoSi_2$ films on 440C substrate found that sputter etching substrates prior to coating deposition gave poorer adhesion because of removal of interfacial oxide layers. Deliberately preoxidizing the substrate prior to coating produced significant gains in coating adherence. The improved adherence was believed to be due to the formation of a mixed oxide interface. Substrate biasing in some cases also adversely affected adhesion by removing interfacial oxide layers although it produced improved bulk properties. To examine if this would hold true for Cr_2O_3 coating with Inconel X-750 as substrate, three additional runs (Nos. 31, 34, and 32) were made.

The first run No. 31 consisted of coating the annealed foil in bias sputter mode with no sputter etching. This run was made to examine the effect of surface oxides in bias sputtering. Run No. 34 consisted of coating heat treated foil in sputter-deposit mode with no sputter etching. This run was made to examine the effect of interfacial oxides present due to heat treatment on sputter-deposit mode. In a third run, No. 32, the coating was applied for three minutes in sputter-deposit mode on annealed and heat treated foils so that oxides were not removed, and then coating was applied in bias sputtered mode to provide hopefully more stoichiometric coating with improved bulk properties. The results show that the coating in Run No. 32 peeled off in handling probably due to intrinsic film stresses so there was no advantage of initial sputter deposit. Also, coatings in Run Nos. 31 and 34 peeled off more than in Run No. 30 during bend tests (see Figure III.12).

Analysis of Selected Samples

Surface analyses of Sample Nos. 30 (as coated), 30 (after heat treatment), 31 (as sputtered), and the target chip were done and the details are reported in Appendix B. The Cr: O: Ni ratio of the coating 30 (as sputtered) was very close to the theoretical value with some deficiency of oxygen and nickel. The heat treatment of the coatings did not change the concentration ratio of Cr and O, but Ni concentration appears to have reduced. X-ray diffraction shows that the coating as sputtered is amorphous, but crystallizes to nichrome bonded Cr_2O_3 after heat treatment. Bias sputtered coating (Sample 31, as sputtered) was found to be deficient in oxygen and nickel. The oxygen level in this specimen was slightly smaller than that in Sample 30 which makes sense because bias sputtering reduces the oxygen contamination and in case of oxide sputtering can preferentially sputter some of the oxygen available from the target material.

Conclusions:

It is concluded that bias sputtered coatings are not well adhered due to intrinsic film stresses. The sputter deposit mode and sputter etching provides more adherent coatings. The crazing network after bend tests, in most of the samples, was coarser than that in straight Cr_2O_3, indicating that the nichrome binder improved the ductility of the coating. The coatings produced in run Nos. 30 and 47 were best based on SEM studies of the surfaces and bend samples. The metallurgical examinations show that the coating sputtered is Ni-Cr-Cr_2O_3.

SPUTTERED MULTI-LAYERED NICHROME BONDED Cr_2O_3

Nichrome and Ag Layers

The nichrome (80% Ni, 20% Cr) and Ag were developed to be used as interlayers and overlays, respectively, for Ni-Cr-Cr_2O_3 coatings. Parameters used were the same as used in Ni-Cr-Cr_2O_3: target - substrate spacing - 41.3 mm, substrate - water cooled, power - 390W (full), background pressure = 10μ. The results are presented in Table III.4. The sputtering rates for Ni-Cr and Ag were 380 Å/min and 1280 Å/min, respectively. The coatings were very smooth and no sign of cracking or flaking of Ni-Cr

TABLE III.4

TEST DATA OF MULTI-LAYERED SPUTTER COATED SAMPLES

Sputter Deposit Mode, Substrate - Water Cooled
Spacing = 41.3 mm, Power = 390 W

Sample No.	Chamber Pressure, μ	Foil Heat Treated	Sputtering Time Min.	Thickness μm(μin.)	Adhesion† MPa (ksi)	Comments
Nichrome Coating						
33	10	Yes	20	0.76(30)	50.15+ (7.28+)	Smoothest coating. No sign of cracking or flaking during bend test.
Ag Coating						
25	10	Yes	5	0.63(25)	70.21 (10.19)	Coating very smooth. No bend test conducted.
Ni-Cr-Cr_2O_3 with Ni-Cr Underlayer						
26	10	Yes	7+40	0.18(7) +0.71(28)	68.7 (9.97)	Seems rather smooth, very few large globules. Most of the coating flaked off in pieces in bend test.
39	6	Yes	10+40	0.38(15) +0.76(30)	70.3+ (10.2+)	Most of the coating flaked off during bend test.
40	6	No	10+40	0.3 (12) +0.69(27)	70.3+ (10.2+)	Crazing much coarser than Ni-Cr-Cr_2O_3 coating and some flaking off during bend test.
Ni-Cr-Cr_2O_3 with Ni-Cr Underlayer and Ag Overlay						
27	10	Yes	7+40+2	0.20(8) +0.69(27) +0.30(12)	49.2 (7.14) Silver layer torn	Grainy appearance (grains ~0.1-0.2 μm). Most of the coating flaked off in ~14 μm wide flakes during bend test.
41	6	No	10+40+2	0.20(8) +0.69(27) +0.20(8)	55.8 (8.1)	Most of the coating came off loose during bend test.

† + Indicates that either limit of the machine (68.9 MPa) was exceeded or epoxy fractured.

was found during bend tests. No bend tests on Ag were conducted because the coating was expected to be good.

AES and X-ray diffraction analyses of nichrome was conducted to assure that stoichiometry was maintained. The results are reported in Appendix C. AES analysis showed that the composition of the coating was very close to that of the target. X-ray diffraction analysis also verified it.

Ni-Cr-Cr_2O_3 with Ni-Cr Interlayer

Next, three runs were made of Ni-Cr-Cr_2O_3 coating with Ni-Cr as interlayers. The first two runs (Nos. 26, 39) were made on heat treated foils with 10μ and 6μ background pressure because earlier tests indicated that lower pressure might provide a smoother coating. In both cases, the coating flaked during tests (see Table III.4 and Figure III.13). The third run (No. 40) was made on the annealed foil. The coating flaked off very little during bend test and was fairly well adhered. This sample was selected for wear tests.

Ni-Cr-Cr_2O_3 with Ni-Cr Interlayer and Ag Overlay

Two runs (Nos. 27 and 41) were made with Ni-Cr-Cr_2O_3 coating with Ni-Cr underlay and Ag overlay on the heat treated and annealed foils. In both cases, the coating came off loose during bend tests. Further work will have to be done in a future program to develop this coating system.

SPUTTERED NICHROME BONDED CHROME CARBIDE

Nichrome bonded chrome carbide was sputtered using the optimized parameters for chrome oxide coating. The sputtering parameters were: chamber pressure = 6μ, target-to-substrate spacing = 41.3 mm, substrate water cooled. The coating was applied using the sputter-deposit and bias-sputter modes and the heat treated and annealed foils. It was also sputtered at half power (200 W). In all cases, the coating came off entirely during bend tests (for results see Table III.5). In each case, the coating even cracked with slight bending. The coatings probably had high intrinsic internal stresses. An X-ray diffraction study indicated an amorphous

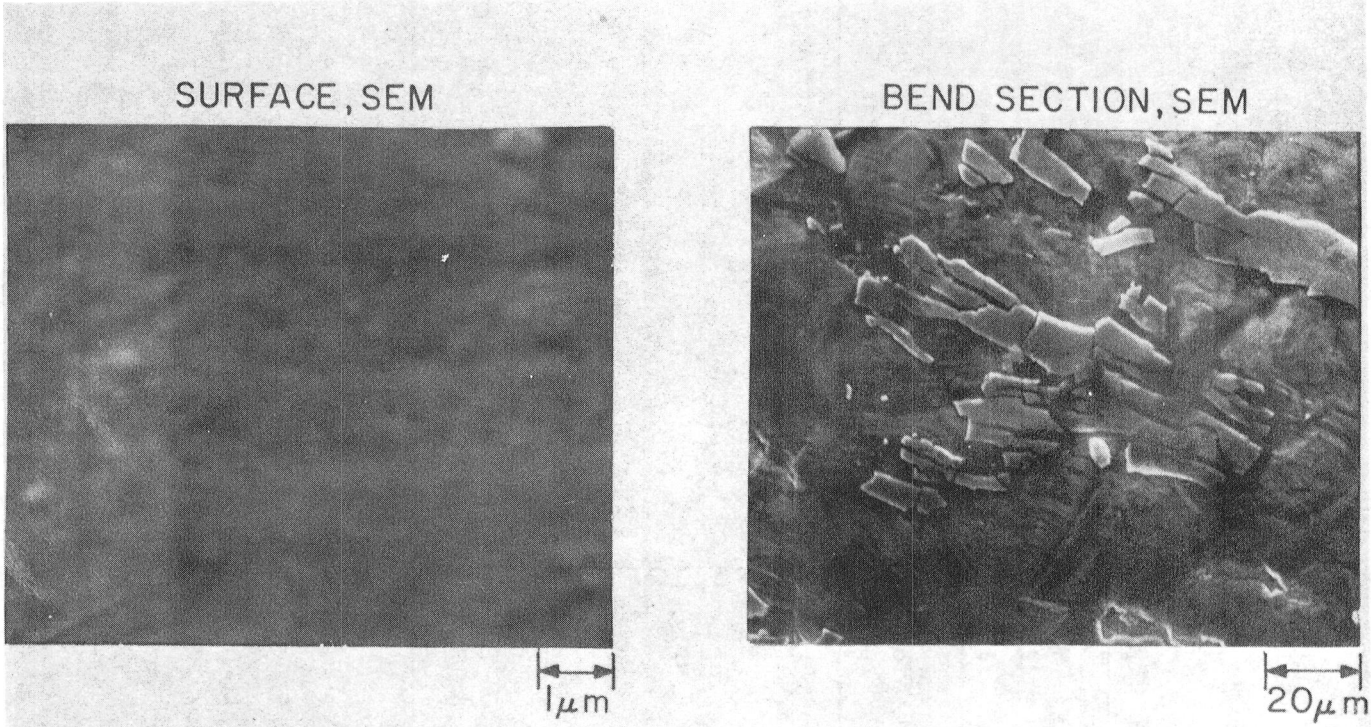

Sample No. 26 41.3 mm, 390 W, 10 Microns, 47 Minutes, Heat Treated Foil

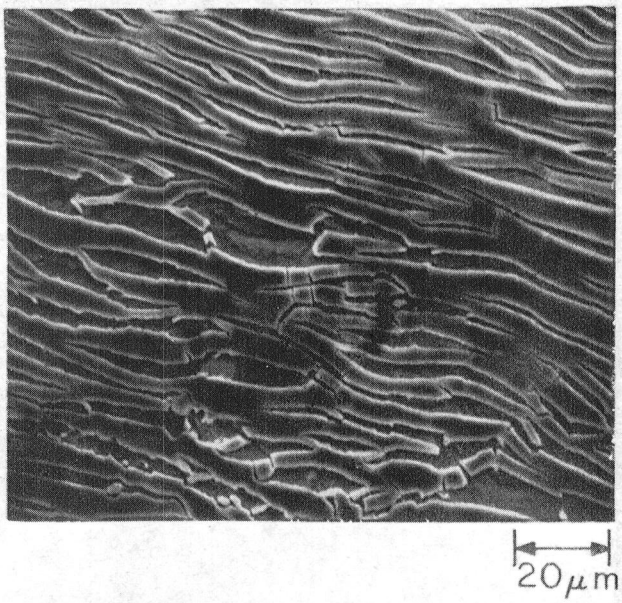

Sample No. 40 41.3 mm, 390 W, 6 Microns, 50 Minutes, Annealed Foil

Fig. III.13 Micrographs of Ni-Cr-Cr_2O_3 Coating with Ni-Cr Underlay on Inco X-750 Foil. The coating was applied in sp. deposit mode.

TABLE III.5

TEST DATA OF Ni-Cr-Cr_3C_2 SPUTTER COATED SAMPLES

Chamber Pressure = 6μ, Substrate - Water Cooled
Spacing = 41.3 mm, Power = 390 W

Sample No.	Bias Sputter	Foil Heat Treated	Sputtering Time Min.	Thickness μm(μin.)	Adhesion† MPa (ksi)	Comments on 180° Bend Test
42	No	Yes	60	1.14(45)	32.65 (4.74)	Coating came off entirely at bend
43	Yes	Yes	60	1.14(45)	33.90 (4.92)	Coating came off entirely at bend
44	No	Yes	120 at 200 W power	1.27(50)	32.38 (4.70)	Coating came off entirely at bend
45	No	No	60	1.14(45)	42.58 (6.18)	Most of the coating came off at bend.

†The coating cracked in each case with slight foil bending.

coating, and Auger analysis showed the coating was close to the composition of the target. The details are presented in Appendix D.

It is felt that the sputtering parameters, found to be optimum for Cr_2O_3 system, necessarily are not optimum for Cr_3C_2 and a parametric study has to be conducted in a future program to develop Cr_3C_2 coating system.

Since a reasonable coating could not be developed, coating combination No. 14 was dropped from Table II.4.

SCRATCH TEST OF SELECTED COATINGS

The objective of the test was to evaluate the relative scratch abrasion resistance of the selected sputtered coatings of straight Cr_2O_3 and with metallic binders and Cr_3C_2. A series of tests were run using the Taber Model 502 Shear/Scratch Tester with a number 139-58 diamond tool as the cutting tool. In this test, the specimen is mounted on a motor driven turntable which rotates at a speed of about 0.6 rpm. The diamond tool, which is the corner of a cube with three sides and edges converging at 90° to a point, is mounted on a calibrated scale beam. The load is applied, and varied, by sliding a weight along the beam. Loads from 10 grams to 1000 grams can be applied.

Four sputtered Inconel X-750 foil specimens were evaluated. These included:

1. Cr_2O_3 as sputtered on annealed foil - Sample 13A
2. Cr_2O_3 sputtered on annealed foil then heat treated - Sample 13A
3. Ni-Cr-Cr_2O_3 sputtered on annealed foil then heat treated - Sample 47
4. Ni-Cr-Cr_3C_2 as sputtered on annealed foil - Sample 44

Preliminary tests showed that a 50 gram load on the diamond tool was capable of making a visible scratch in all of the foil surfaces although most of the coatings still appeared to be intact. The scratches were apparently due to substrate deformation. Successive tests were run at loads of 50, 100, 150,

and 200 grams. The results are shown in Figure III.14 which is a plot of scratch width - in μm, against load in grams.

Based on the microscope examination of the scratches, the least amount of the material was distributed in the foil that was sputtered with Cr_2O_3 and then heat treated (Sample 13A). The Ni-Cr plus Cr_2O_3 sputtered on annealed foil then heat treated (Sample 47) was comparable. The Cr_2O_3 , as sputtered, (Sample 13A) was slightly less effective. Diffusion at the interface during heat treatment might have improved adhesion somewhat. Although the Ni-Cr plus Cr_3C_2 on annealed foil (Sample 44) showed the narrowest scratch width at all loads, it should be noted that there was a disturbed zone on each side of the scratch which probably indicates that if the coating was being constantly abraded, a significant amount of material would be removed very rapidly.

Description of the Scratch

The Cr_2O_3 coated foils all showed similar scratch characteristics at each load. Under reflected light, it was relatively easy to determine if the coating had been removed at the bottom of the scratch groove because the appearance of the chrome oxide is dark and the appearance of the substrate metal is light. With the Cr_3C_2 coated foil, the coating and the substrate are both metallic and, therefore, appear light.

Cr_2O_3 Scratch

The scratch produced from the 50 gram load had isolated areas of coating removed which were less than 5% of the entire scratch length. The scratch produced by the 100 gram load had areas of coating removed ranging from 5% to 10% at the bottom of the scratch groove. With the 150 gram load, approximately 80 to 100% of the coating had been removed, while 100% of the coating was removed at the bottom of the scratch with the 200 gram load.

The scratch edges showed little deformation with no sign of perpendicular cracking. It appeared as though the coating was removed in fine particles, and in some cases, these particles had deposited on the surface next to the scratch.

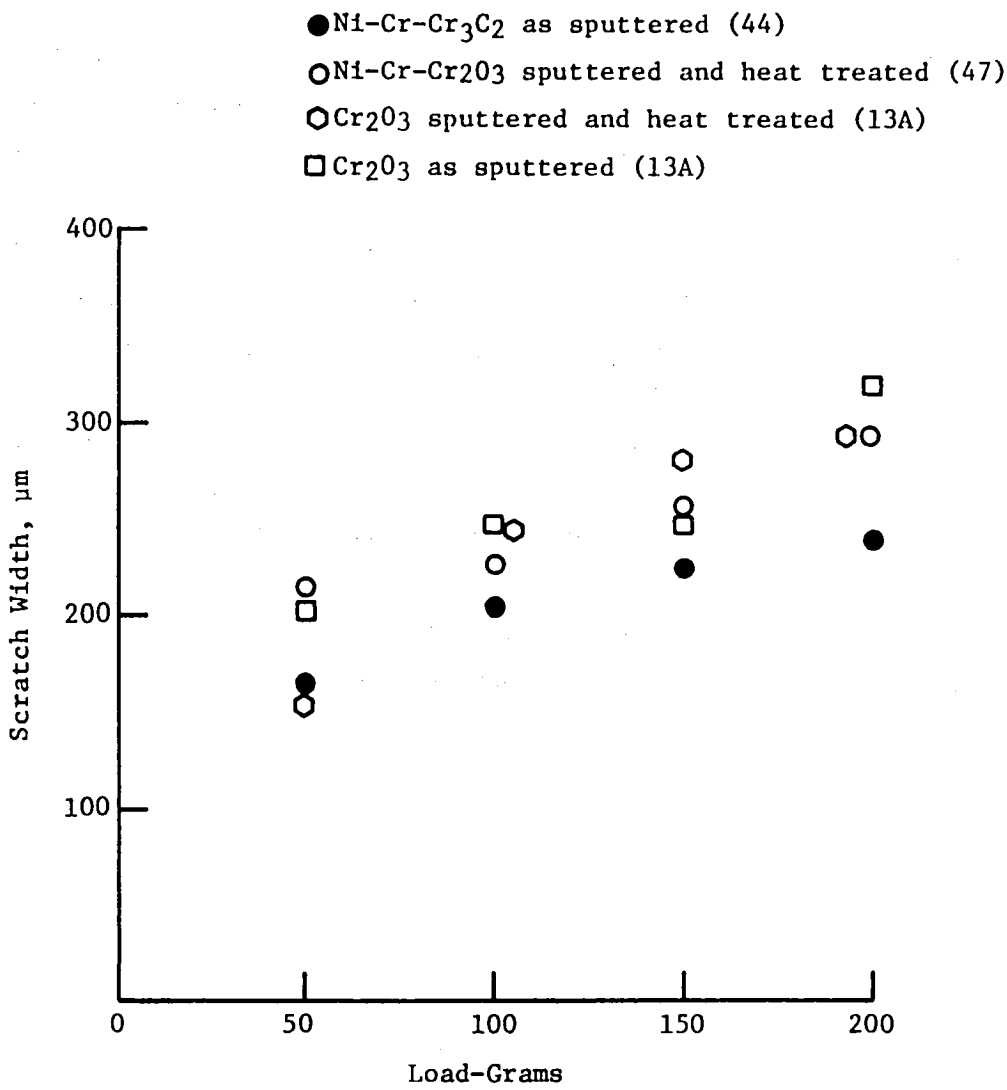

Fig. III.14 Scratch Width versus Load for Selected Sputtered Coatings

792854

In conclusion, the Cr_2O_3 coatings seemed well adhered and Ni-Cr-Cr_2O_3 was comparable to Cr_2O_3 in scratch abrasion resistance.

Cr_3C_2 Scratch

The existence of coating still bonded to the substrate was not well defined from observations made under the microscope. However, the scratch edges showed deformation which appeared to be more severe as the load increased. Essentially, the coating was lifting from the substrate in flakes but was still bonded to the undisturbed coating adjacent to the scratch. Hence, if the coating was removed it would separate in flakes rather than fine particles as was the case with the Cr_2O_3. The width of the disturbed material was greater than 0.5 mm (0.020 in) at the highest load. Therefore, the graph shows the scratch width for the Cr_3C_2 to be lower than with the Cr_2O_3; but the overall damage produced by the diamond tool is considerably greater. It should also be noted that there were several cracks in the deformed coating which ran perpendicular to the scratch.

It is recommended that SEM studies be made in a future program to elaborate on the points mentioned in the above discussion.

IV. EXPERIMENTAL COATING SYSTEM (ECS) EVALUATION TESTS

ECS evaluation tests included static screening tests, partial arc start/stop tests, full journal bearing start/stop tests, and high-speed rub tests. ECS coupons failing or performing poorly at any step in the sequence above were recycled for further refinement within the scope of the program. Post test examination including light microscopy, scanning electron microscopy, microprobe, Auger, and diffraction analyses were used in studying and evaluating samples after testing.

STATIC MATERIAL SCREENING TESTS

Sample Preparations

The selected specimens were in the form of small foil samples approximately 50 mm X 50 mm (2 in. X 2 in.) square and 100μm (0.004 in.) thick and small journal samples approximately 50 mm X 50 mm (2 in. X 2 in.) square and 2.6 mm (0.102 in.) thick each with the appropriate coatings as described in the previous section. Thin sheet coupons of journal were selected so that weight change could be detected more accurately. They were selected to be flat for ease in sectioning for metallurgical examinations. Three sets of each coating were prepared. Two sets were to go through the oven test and the third set was retained for comparisions. Duplicate specimens were used to ensure repeatability.

Oven Screening Tests

Static screening tests were conducted on coated coupons suitable for operation over three temperature ranges:

1. Room temperature to 427°C (800°F)
2. Room temperature to 540°C (1000°F)
3. Room temperature to 650°C (1200°F)

The test consisted of exposure of material samples in an oven (oxidizing environment) for 100 hours at the maximum service temperature (427°C, 540°C, or 650°C) and 10 temperature cycles from room temperature to the maximum service temperature. The specimens were cooled from maximum service temperature to close to room temperature in about 20 minutes.

The specimens were subjected to standard physical and metallurgical surface examinations prior to and after test for further screening. The foil coupons were tested under flex bending. All of the shaft and foil coupons went through a surface adhesion tape test, and a scratch test under microscope examination. Selected specimens were examined using scanning electron microscope and other analytical techniques. Superficial Rockwell hardness tests were performed on the thicker coatings. The weight and the thickness of the coupons, before and after the oven tests, were recorded. The coupons before and after the oven tests were mounted side by side for visual comparisons. The coatings selected from these tested were then tested in dynamic tests.

Discussion of Results

The results of the static oven and the thermal cycle tests are presented in Appendix E. The results were very encouraging since most of the promising candidate materials survived these screening evaluations. The photographs of the coupons before and after tests are shown in Figures IV.1 to IV.5. The results are reviewed in Table IV.1 and IV.2. Not much change was seen from oven tests.

CdO-graphite-Ag coating became yellowish. The microprobe analysis was done to find out what the yellowish matter was. It revealed the presence of chlorine over most of the surface. Based on our NaCl standard for Cl, the average amount present in the coating was 1.3 w/o.* The spots which showed concentrated areas of chlorine counts on an X-ray map for chlorine were parts of the silver particles of the coating. It was believed, therefore, that AgCl has formed on some of the silver of the coating, giving

*The net number of X-ray counts/sec obtained for chlorine from the standard is 17936. Chlorine makes up 60.66% by weight of the material in NaCl. Therefore, 17936 c/s is the number of counts from a material whose concentration of chlorine is 60.66 w/o. Back calculating to the number of counts which would be emanating from a pure chlorine standard is 29568 c/s. The chlorine of the coating gave a net count of 382. Computing, we get:

$$\frac{382}{29568} \times 100\% = 1.3 \text{ w/o Cl}$$

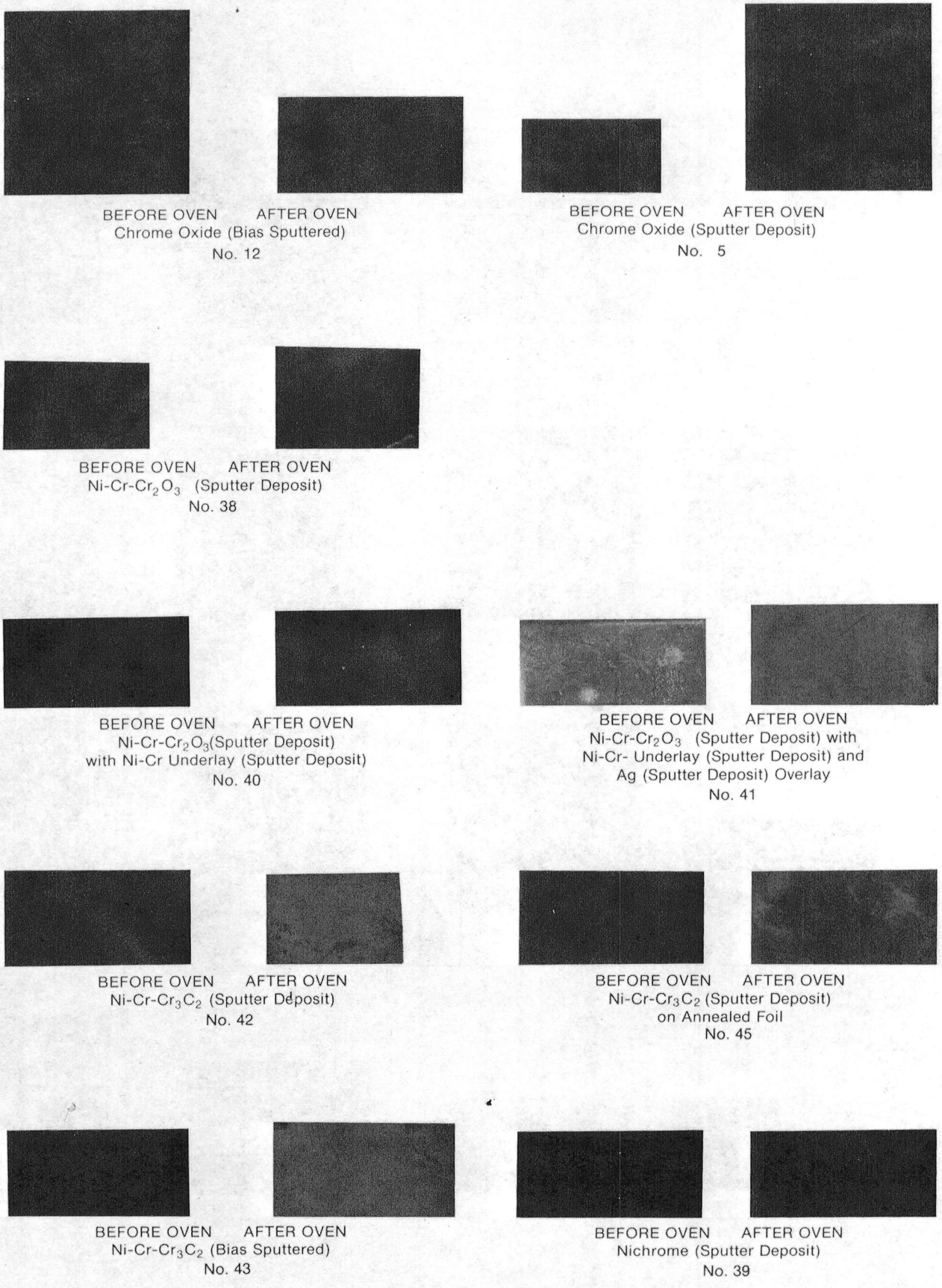

Fig. IV.1 Photographs of Coatings Before and After Oven Test

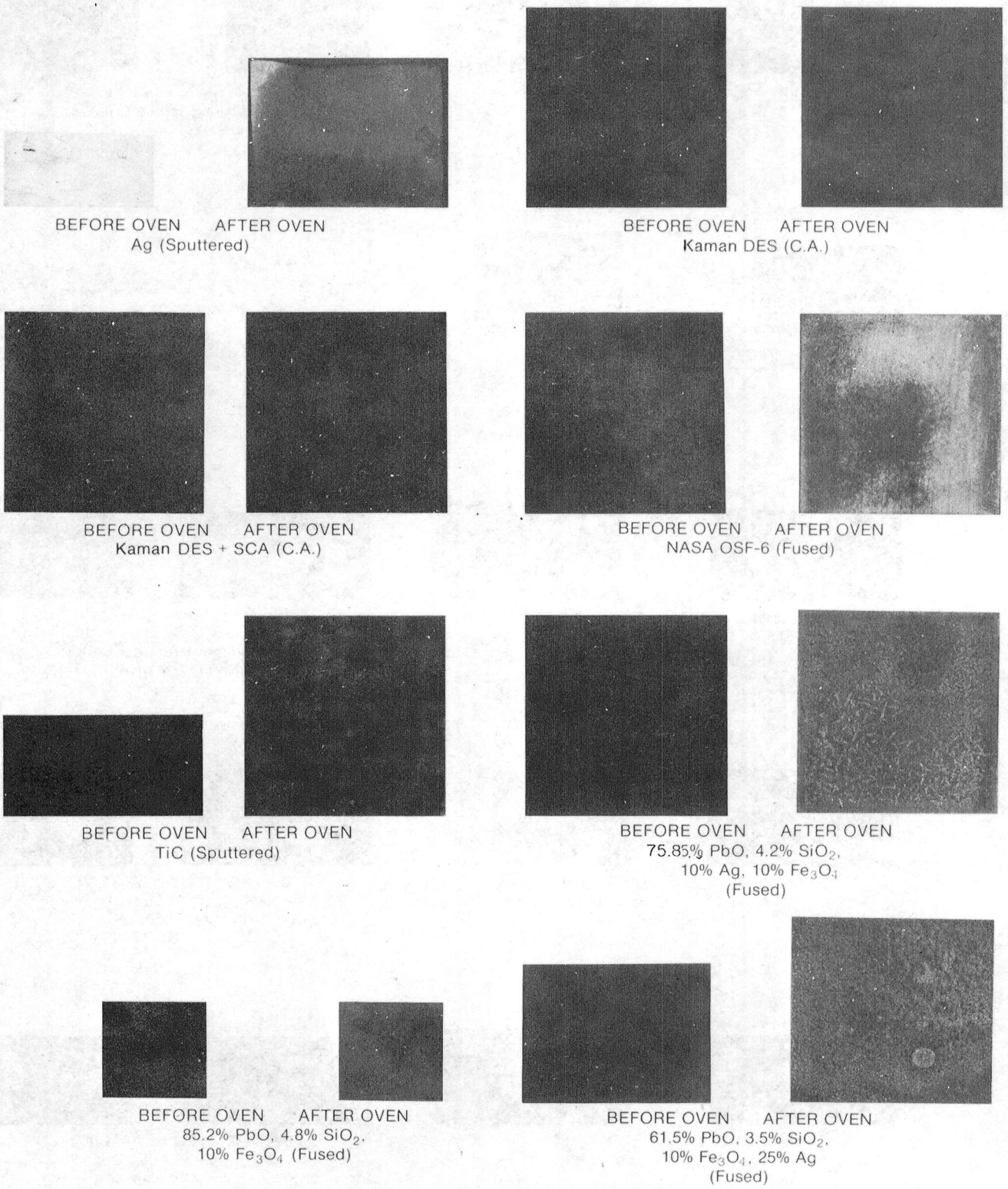

Fig. IV.2 Photographs of Coatings Before and After Oven Test

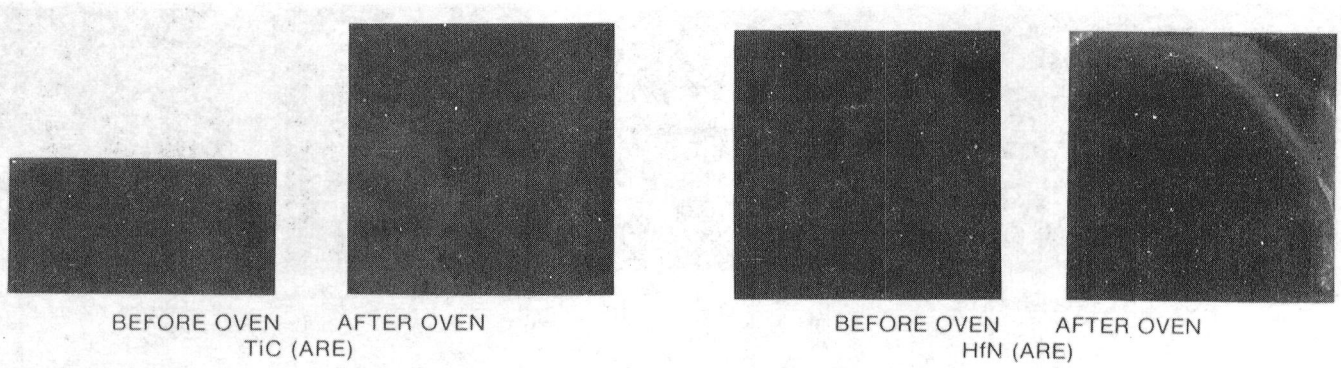

Heat Treated Inconel X-750 Foils (540°C)

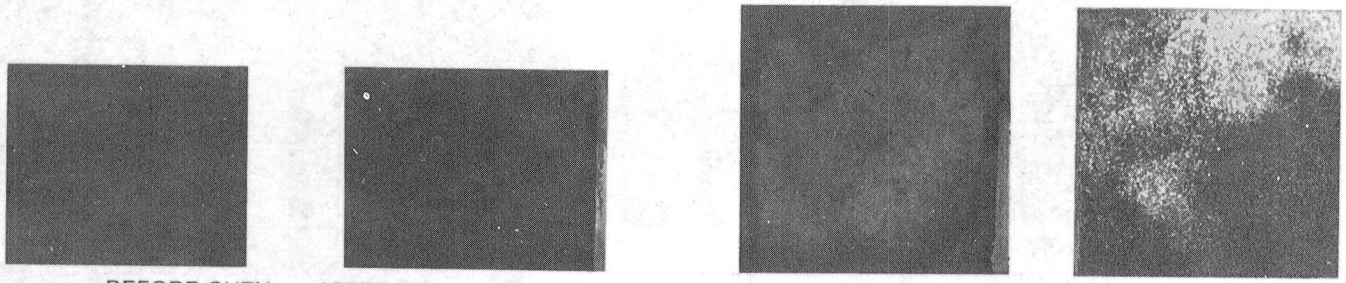

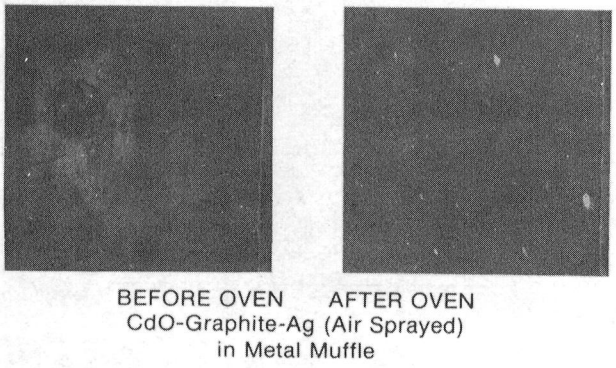

Heat Treated Inconel X-750 Foils (427°C)

Figure IV.3 Photographs of Coatings Before and After Oven Test

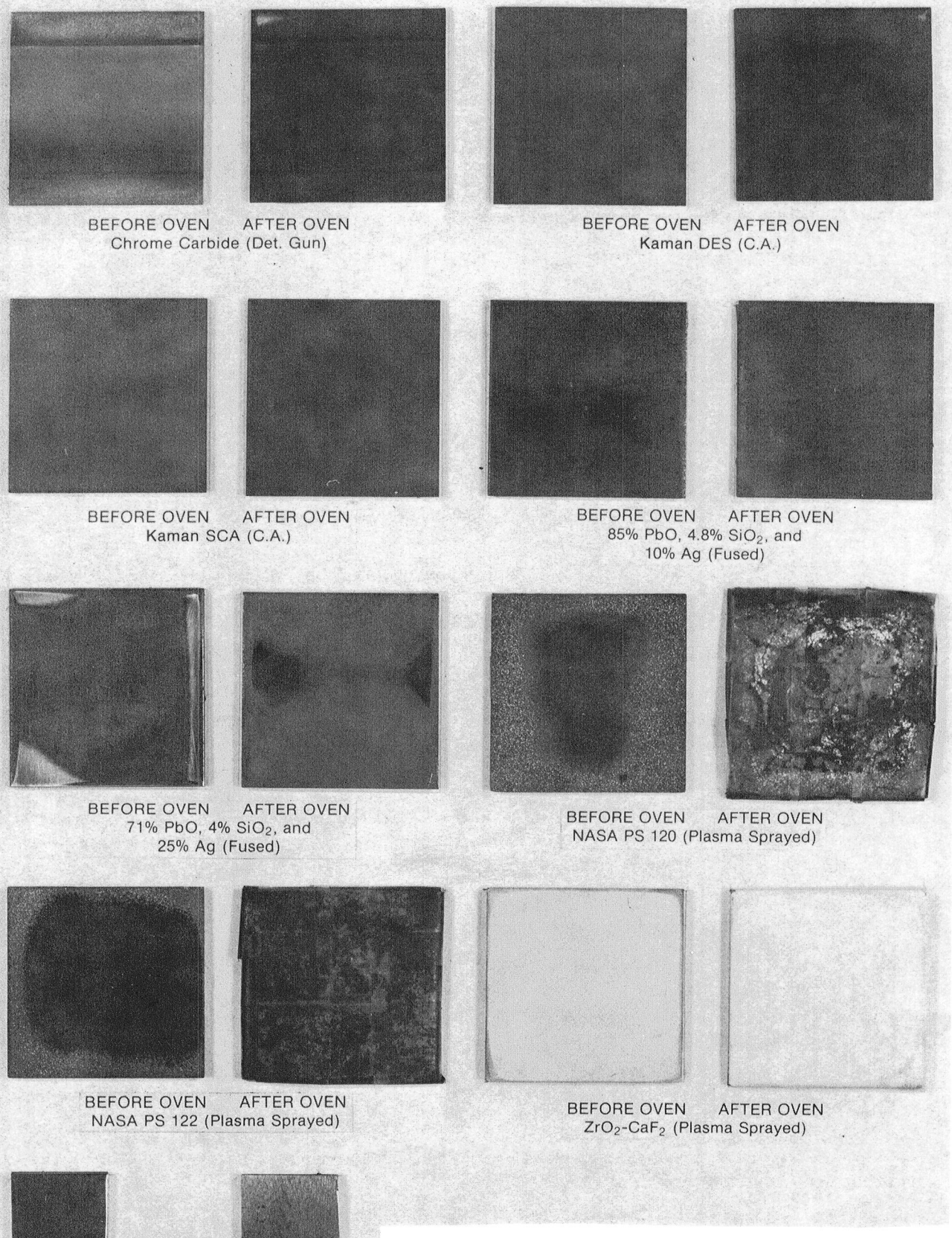

Figure IV. 4 Photographs of Coatings Before and After Oven Test

Heat Treated A-286 Coupons (650° C)

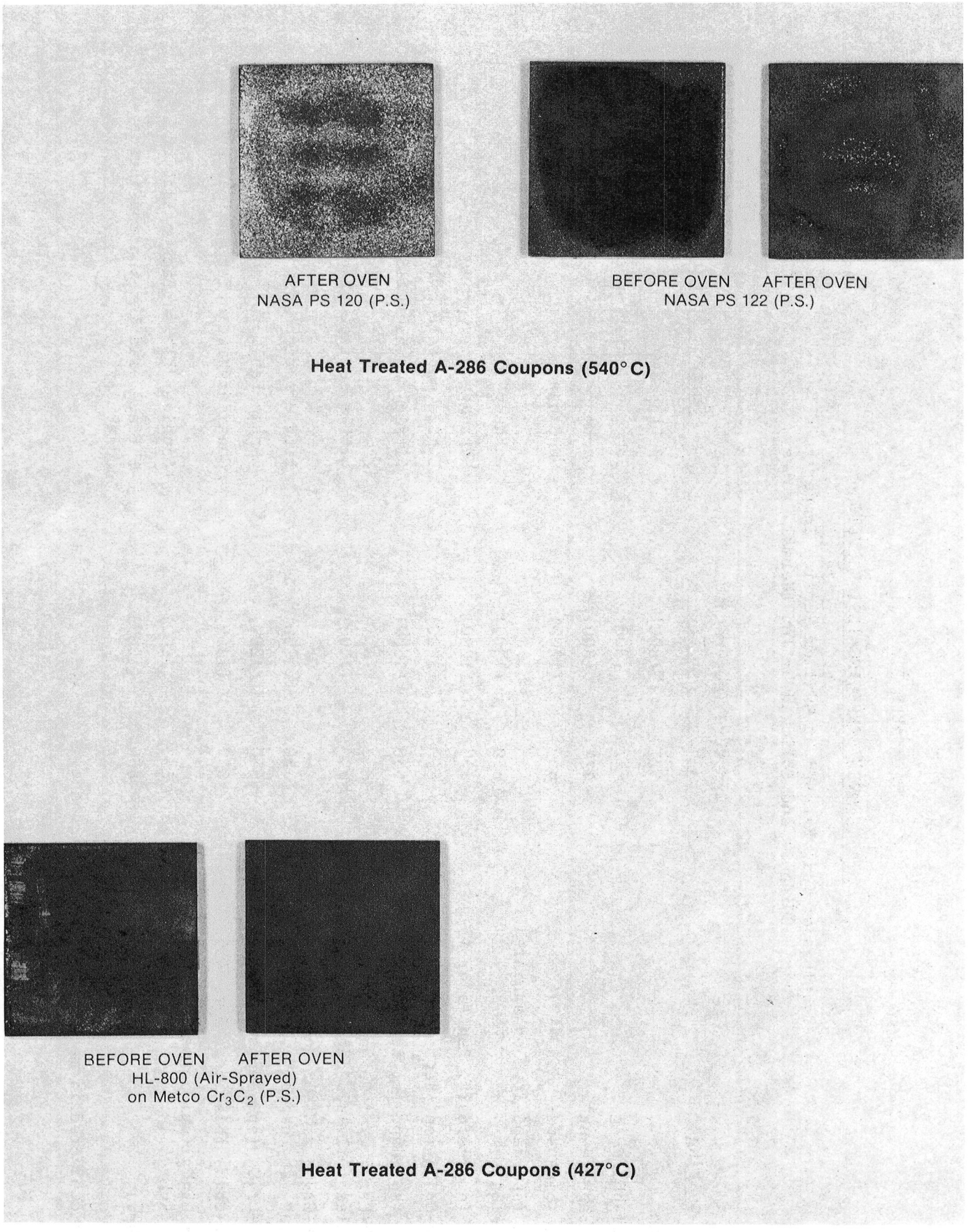

Figure IV.5 Photographs of Coatings Before and After Oven Test

TABLE IV.1

STATIC OVEN SCREENING TEST RESULTS

Coatings of Foil Exposed at Maximum Service Temperature for 100 Hours and Followed by Ten Thermal Cycles

Coating	Exposure Temperature (°C)	(°F)	Surface Appearance
HL-800	427	(800)	Unchanged
CdO-graphite-Ag	427	(800)	Some yellowish spots on foil
CdO-graphite-Ag*	427	(800)	Unchanged
Cr_2O_3 (bias sp., Run #12)	650	(1200)	Unchanged
Cr_2O_3 (sp. deposit) on annealed foil (Run #13A)	650	(1200)	Unchanged
Cr_2O_3 (sp. deposit, Run #5 or 15)	650	(1200)	Unchanged
Ni-Cr-Cr_2O_3 (sp. deposit, Run #30)	650	(1200)	Little surface oxidation
Ni-Cr (sp. deposit, Run #39)	650	(1200)	Little surface oxidation
Ni-Cr-Cr_2O_3 w/Ni-Cr underlay on annealed foil (sp. deposit, Run #40)	650	(1200)	Little surface oxidation
Ni-Cr-Cr_3O_3 w/Ni-Cr underlay and Ag overlay (sp. deposit, Run #41)	650	(1200)	Little surface oxidation
Ni-Cr-Cr_3C_2 (sp. deposit, Run #42)	650	(1200)	Considerable surface oxidation
Ni-Cr-Cr_3C_2 (bias sp., Run #43)	650	(1200)	Considerable surface oxidation
Ni-Cr-Cr_3C_2 (sp. deposit) on annealed foil (Run #45)	650	(1200)	Considerable surface oxidation
Ag (sp.)	650	(1200)	Surface oxidized Coating intact underneath

*Test conducted in metal muffle inside furnace.

TABLE IV.1 (cont'd)

Coating	Exposure Temperature (°C)	(°F)	Surface Appearance
Kaman DES	650	(1200)	Unchanged
Kaman DES + SCA	650	(1200)	Unchanged
TiC (sp.)	650	(1200)	Coating oxidized
TiC (ARE)	540	(1000)	Coating oxidized
HfN (ARE)	540	(1000)	Coating oxidized
61.5% PbO, 3.5% SiO_2, 10% Fe_3O_4, 25% Ag	650	(1200)	Surface oxidized, coating underneath intact
75.8% PbO, 4.2% SiO_2, 10% Ag and 10% Fe_3O_4 (fused, Run #7)	650	(1200)	Coating recrystalized at the surface, it melted and flowed. After polishing could recover original coating.
85.2%, PbO, 4.8% SiO_2, 10% Fe_3O_4 (fused, Run #9)	650	(1200)	Unchanged
CaF_2-BaF_2-Ag (OSF-6)	650	(1200)	Unchanged

TABLE IV.2

STATIC OVEN SCREENING TEST RESULTS

Coatings on Journal Exposed at Maximum Service Temperature
for 100 Hours and Followed by 10 Thermal Cycles

Coating	Exposure Temperature °C	(°F)	Surface Appearance
HL-800 on Metco Cr_3C_2	427	(800)	Unchanged
Cr_2O_3 (sp. deposit, Run #54)	650	(1200)	Unchanged
Kaman DES	650	(1200)	Unchanged, became greener
Kaman SCA	650	(1200)	Unchanged, became greener
Cr_3C_2 (D.G.)	650	(1200)	Unchanged
NASA PS120 (P.S.)	650	(1200)	Coating flaked off
NASA PS122 (P.S.)	650	(1200)	Coating flaked off
NASA PS120 (P.S.)	540	(1000)	Unchanged
NASA PS122 (P.S.)	540	(1000)	Unchanged
ZrO_2 - CaF_2 (P.S.)	650	(1200)	Unchanged
71% PbO-4% SiO_2 - 25% Ag	650	(1200)	Surface oxidized, coating underneath intact
85.2% PbO, 4.8% SiO_2 and 10% Ag (fused, Run #8)	650	(1200)	Surface oxidized, coating underneath intact

rise to the peculiar pale yellow film. No chlorine was found on the reference as sprayed coating before the oven test. The source of chlorine is unknown; it might either come from water or the outgassing of the brick furnace. The next run was made with distilled water and the oven test was conducted in a metal muffle. There was no yellowish spots this time. Care should be taken to use distilled water so that no chlorine is added in the coating.

TiC, HfN, and Ni-Cr-Cr_3C_2 coatings on the foil oxidized and were dropped from the test matrix. NASA PS120 and PS122 coatings on the journal coupon spalled at 650°C, but were intact in 540°C tests. All coatings other than TiC and HfN (coating combinations 16 and 17 in Table II.4) were recommended for dynamic tests. It should be noted that coating combination numbered 10, 14, and 18 in Table II.4 were cancelled due to the lack of good DES and SCA coated foils, Ni-Cr-Cr_3C_2 foils, and OSF-6 coated journal.

TEST FACILITY AND INSTRUMENTATION

Start/Stop Test Apparatus Description

An existing test apparatus which was used in the previous NASA program was used to run start/stop tests. It was automated to run unattended. Program time switches (mfg. by Dayton, Model SPDT W/96 on-off at 15 s intervals) were used to turn the heaters on and off. A temperature control unit was used to maintain the bearing temperature to a desired level. The test rig was further modified to allow hot air to go through the bearing in full bearing tests. It was also modified to have the capability to run high speed rub tests. The test apparatus used for start/stop tests is shown in Figures IV.6 and IV.7. Figure IV.8 shows the close up of the apparatus.

The support shaft was made of A286 to match the material of the test journals and supported on two preloaded angular contact ball bearings. The shaft incorporated an integral heat dam consisting of a 28.4 mm (1.12 in) long section, 1.6 mm (.063 in) thick which extended into the hot zone. The test journal was a light interference fit onto the shaft. The pilot

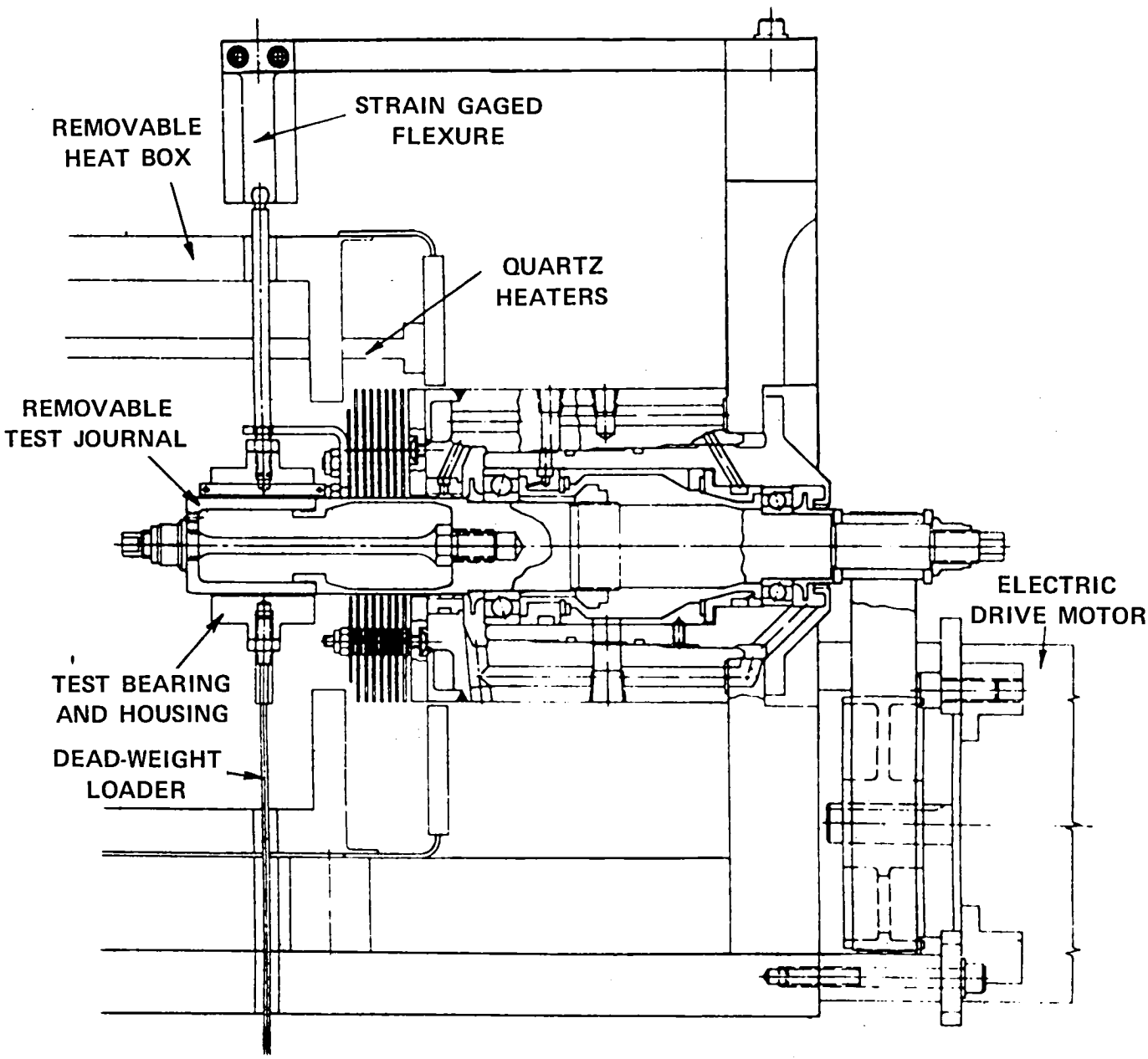

Figure IV.6 Foil Journal Bearing Materials Test Rig

MTI-17620

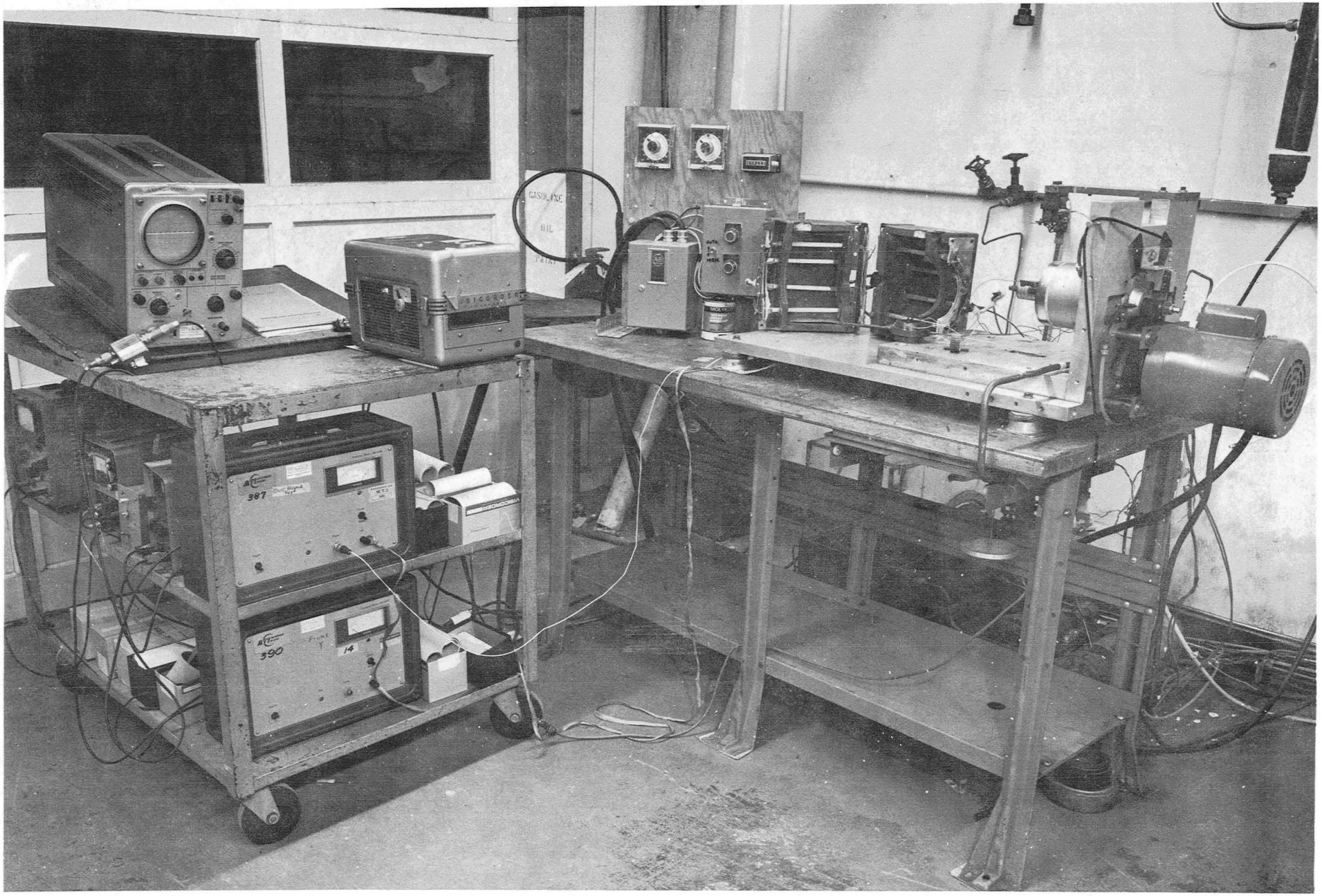

Figure IV.7 Foil Journal Bearing Materials Test Facility

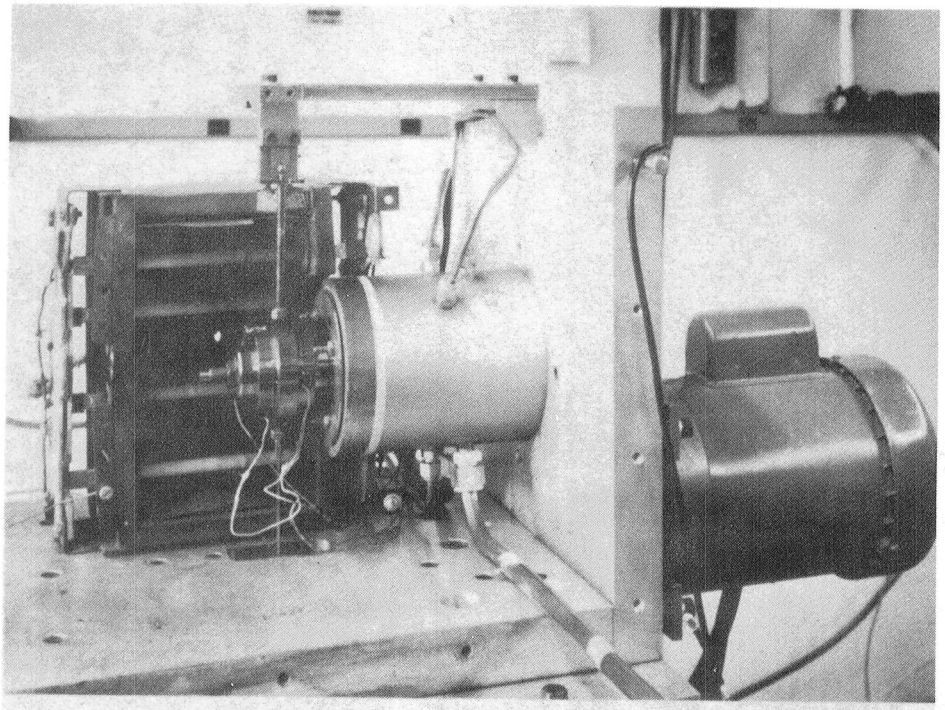

Figure IV.8 Foil Journal Bearing Materials Test Rig

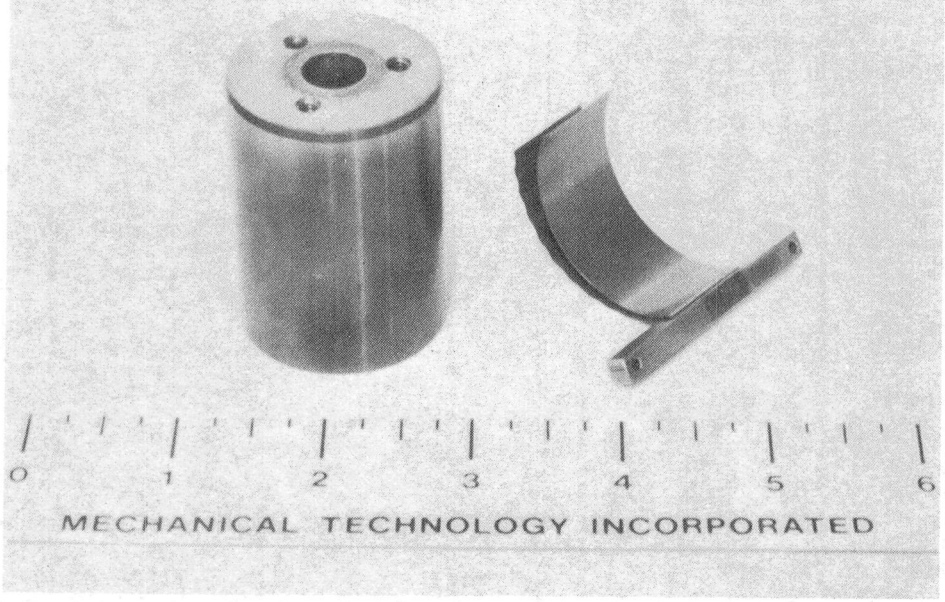

Figure IV.9 Partial Arc Foil and Journal Test Specimens

diameter for the interface was coated with a 5-10μm (.0002-.0004 in.) thick layer of nickel-chromium applied by the Electrolizing Company. The test journal was held in place with a tie bolt, also made of A286, which was threaded into the shaft. Heat baffles mounted to the support housing interrupted the flow of heat out of the hot zone. In addition a 6.4 mm (.250 in) thick Mycalex 500 disk acted as an insulator between the heat baffles and the support housing.

Oil for lubricating and cooling the support ball bearings was supplied through two oil jets 180^{o} apart at each bearing. A water cooled heat exchanger in the oil supply loop removed heat from the oil. A water jacket in the support housing assisted in removing heat from the test end support ball bearing.

A double laybrinth seal with pressurized air supplied between the seals prevented the oil from traveling down the test shaft into the test bearing area.

The test spindle was driven by a 1 hp and 3450 RPM electric motor. The motor was attached to the main vertical support plate and connected to the spindle with a flat drive belt. A pulley ratio of 4:1 was used to obtain a 13,800 RPM spindle speed. The on-off cycle rate was controlled by adjustable timers. The spindle was turned on for 4s and turned off for 7s. The time was selected so that the bearing fully lifts off during on cycle and the spindle is completely stopped during the off cycle. An impulse counter was used to count each cycle.

A heater box consisting of eight 500-watt quartz lamps was used to heat the test chamber to the required temperature. The test temperature was manually controlled by use of variacs to vary the voltage to the quartz lamps.

Measurements and Instrumentation

Rotor Speed: Rotational speed was measured by an MTI Fotonic Sensor^{TM} fibre optic probe which responds to the once per revolution passing of a dark band painted on the test shaft. The output of the Fotonic Sensor was displayed on one channel of a two-channel visicorder.

Test Temperature: The test bearing housing temperature was monitored using four (4) Type K, Chromel-Alumel thermocouples. The thermocouples were mounted on the outside of the housing 90^{o} apart, then covered with a heat shield to prevent direct radiation from the quartz lamps. These thermocouples were used to monitor the test temperature. It had been determined during initial rig checkout that the test bearing temperature was essentially the same as that recorded on the bearing housing after the housing had been allowed to soak at the test temperature for 15 minutes. The output of the thermocouples were recorded on a Honeywell multipoint chart recorder.

Frictional Drag: The mechanical arrangement used to measure the breakaway frictional drag of the test bearing during starting and stopping is shown in Figure IV.6. The floating foil bearing housing is restrained from rotation by a torque arm connected to the test bearing housing, and a flexure in the vertical plane acting through the bearing centerline. Bearing frictional drag causes deflection of the flexure which is measured by a capacitance proximity probe. The range of the capacitance probe used in the system was 0.254 mm (0.010 inch). The output of the capacitance probe was recorded on one channel of a visicorder.

The kinetic friction coefficient was also measured during the tests. The belt was removed from the support shaft and it was rotated by a variable speed drill at about 60 rpm or less. A plastic sleeve was inserted over rotating member of the drill, which was pressed against the shaft to get better contact. The continuous output was recorded through the visicorder as described earlier.

The static breakaway torque was measured by using an arm with a pan perpendicular to the support shaft. The pan was loaded gradually until the journal slips. This gives the friction of the assembly. Then the bearing is installed and the test is repeated. The difference between the two gives the static friction of the bearing.

Test Bearing Load:

The test bearing loading was accomplished by applying calibrated dead weights to the test bearing housing.

Test Bearing and Test Journal

The test bearing selected was a partial arc 38.1 mm (1.5 in) diameter Hydresil™ Journal Bearing. The test bearing and test journal are shown in Figure IV.9. The bearing diameter and mechanical design were based on the bearing used in Part I of this program. The bearing consists of a bump foil and a top or smooth foil. The smooth foil receives the coating to be evaluated. The two foils are individually attached to a "key" by spot welding and are separated by a spacer block. The key then fits into a slot in the floating bearing housing and is secured in place by tapered pins. This method of attaching the foils to the housing is not typical for hydresil applications, but did greatly facilitate changing test specimens while having the fewest number of test components.

To properly evaluate each coating combination, a newly coated foil was run against a clean journal surface which had not been tested against other foil coatings. To reduce the number of test journals required, a bearing of 19.05 mm (.75 in) wide was used which allowed the 44.5 mm (1.75 in) wide journal surface to be used with two (2) foil coatings. The test bearing housing was indexed axially along the test sleeve to locate the test bearing over the appropriate section of the test journal.

A partial arc bearing was used rather than a complete bearing to simplify bearing fabrication and testing. The test bearing had a pad arc of approximately 186^{o}. Through testing, it was determined that a pad of less than 180^{o} resulted in rough bearing operation. The test bearing had one bump more than one half the total number of bumps in a complete circular bearing, which resulted in the 186^{o} pad arc. Rotation of the journal was from the loose end into the weld. A complete L/D = 1, 360^{o} pad bearing was used to evaluate the most promising coating combination identified from the partial arc testing.

Final machining of the journals was completed after the plasma sprayed coatings were applied and before the fused and sputtered coatings were applied. The journals were ground to be 5μm (.0002 in) round and 2.5μm

(.0001 in) straight over the test area. Typical static and dynamic run-outs of the test journal surface after installation on the shaft were approximately 7.5μm (.0003 in).

Modifications for Full Bearing Tests

The modification was to introduce air flow through the full bearing (38 mm in diameter and L/D - 1) in a manner representative of the engine. This air could help in removing the wear particles generated at the sliding interface. The air flow in a current engine system is about 0.027 N.s-1 (0.006 lb/s); and about half of it flows through the bearing. Therefore, about 0.009-0.013 N.s-1 (0.002-0.003 lb/s) air goes through the bearing. An air flow setting of 0.012 N.s-1 (0.00275 lb/s or 2.2 ft^3/min) was established in the rig at room temperature and at 5-10 psig. This air was passed through a heavy duty hotwatt heater (#HAS224, 1500 W @ 120 V) then through a 6.4 mm O. D. 304 stainless steel coil inside the quartz heater (used to heat up the bearing) to the bearing interface. In case higher flow than needed for the bearing has to be provided so that heater would not burn up, a bleed off valve was placed to discharge the extra air flow. The required air flow turned out to be sufficient for the heaters.

The temperature of the air coming out of the heater was only about 315°C (600°F). But air heated up considerably in the coil and the temperature of air coming out of the coil was about 593°C (1100°F) which is only 55°C (100°F) lower than of the bearing in 650°C tests. The air probably heated up slightly more during about 6 mm travel from the coil outlet to the bearing inlet. In 427°C tests, the air temperature could be raised to the same level as the bearing temperature, e.e., 427°C. The set up is seen in the high speed rub test facility shown in the next sub-section (Figure IV.10).

Modifications for High Speed Rub Tests

High speed rub tests consisted of dropping weights from a predetermined height on the bearing running at a high speed - 30,000 rpm. The turbine drive was installed to be able to run the test rig at 30,000 rpm. A loading mechanism was also installed to be able to apply the desired g's in a shock load. It consisted of a vertical Inco 625 rod, which penetrated the top of the furnace and was sitting on a hemispherically ended and MoS_2 coat-

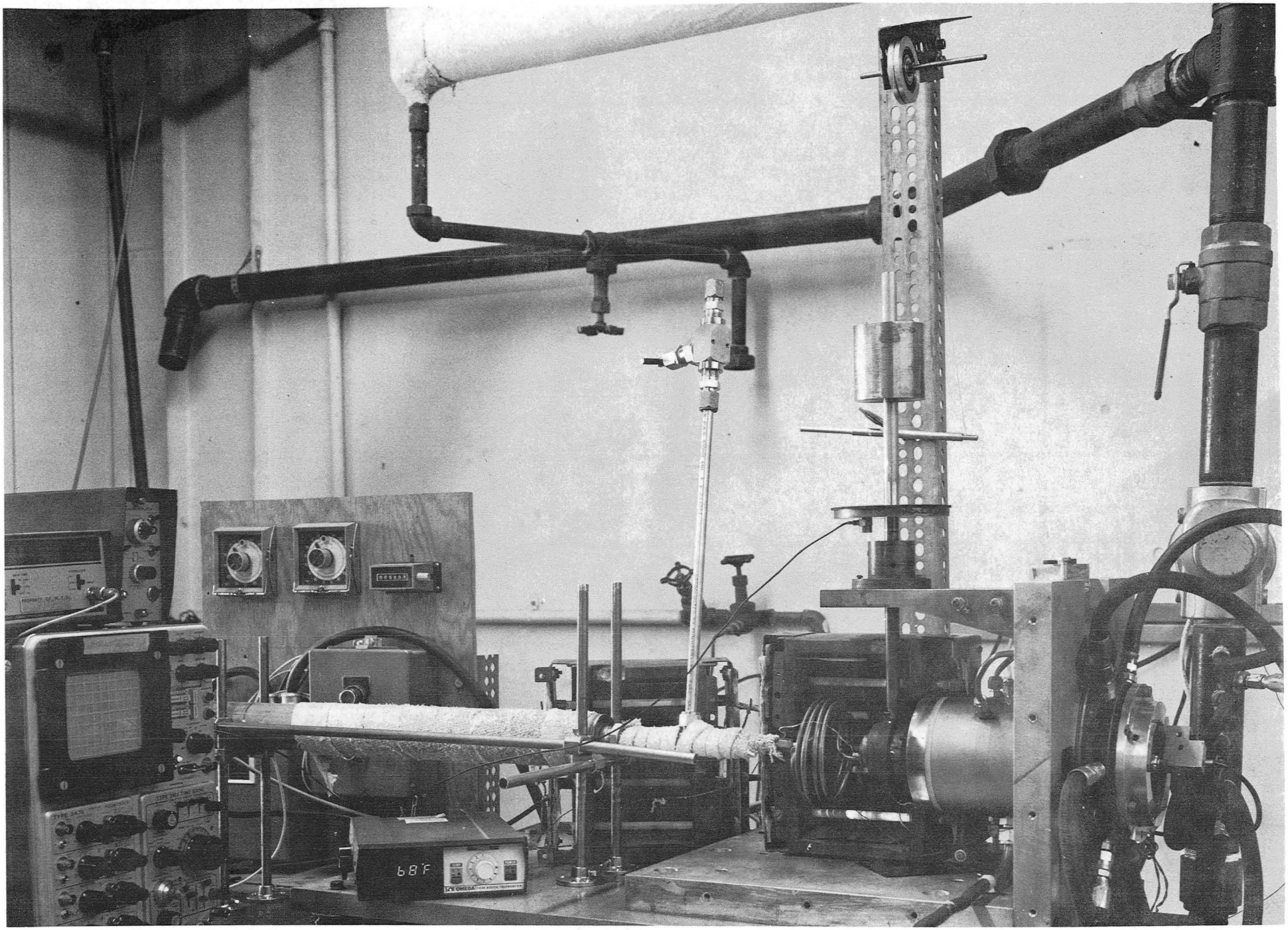

Fig. IV.10 Photograph of High Speed Rub Testing Facility

ed pin screwed to the bearing housing which was used to transmit the shock load. A pan was mounted on the vertical rod. To impose an impact load on the bearing, a known load was dropped from a known height and impacting the pan connected to vertical rod. The rod transmitted the impact load to the housing and the test bearing. A photograph of the test rig is shown in Figure IV.10.

If the load was dropped directly onto a metal pan connected to the bearing housing, the shock was extremely high. A 6.3 mm thick elastomer was placed over the pan and it gave flexibility of generating a range of lower g's levels. An accelerometer (Type 4333, mfg. by Bruel and Kjaer, Denmark) was mounted on the bottom of the pan near the center. Its output was fed to the storage oscilliscope through a charge amplifier. A Krohn-Hite filter, low pass 100 Hz, 12 db/octave was used to remove low frequency noise. By dropping different loads, the load-acceleration curve was generated at room temperature.

A thermocouple was welded to the upper surface of the bump foil at one end in the loaded zone. The output of the thermocouple was fed to a digital voltmeter with a meter scan time of 0.4 s. If there is significant rubbing, it would increase the transient ambient temperature and it could be recorded. This was used as an indication of any rubs or bearing failure.

Measurement of Number of Contacts During Rub:

Contact resistance between the bearing and rotating shaft was also measured to determine if there was any physical contact during each shock load test. A slip bronze brush was used to make contact with the rotating shaft. The bearing housing was isolated from the ground.

An electronic circuit was built to detect any physical contact and measure the number of contacts. A simple voltage comparator was built that had an adjustable threshold or sensitivity feature that enabled evaluation of contact at selectable resistance levels. At any instance when the resistance changed from a value greater than a selected level (e.g. 12,000 Ω) to a value less than the selected level, a contact was registered. Initial resistance measurements of the bearing indicated approximately five ohms of static

contact resistance and more than 100,000 ohms of resistance when rotating at 30,000 rpm. Accordingly, circuit component values were selected that allowed adjustment throughout the range of 1000 to 50,000 Ω of contact resistance to trigger the voltage output level of the detector. The output voltage, which could swing from 0 volts at low or touch resistance to 5 volts at the high or open circuit condition, was used to accumulate counts instantaneously on a Hewlett Packard Pulse Counter Model 5216A which operated as a total counter with a manual reset to zero.

In operation, the counter would acquire a number of pulse or touch counts on start up and would cease counting when stable rotational conditions were recorded. At this time, application of pressure or dropping of weights on the bearing would result in additional counts being accumulated and further counts were acquired when the shaft slowed down as a result of turning off the turbine.

The circuit is shown in Figure IV.11 assuming a sensitivity around 100 k Ω is desired. At 100 kΩ the voltage at E, will be 4.54 volts as a result of the voltage divider effect of the 10KΩ fixed resistor and the 100 kΩ assumed value of foil to shaft resistance. If the voltage at E_2 is adjusted by means of the 10 kΩ potentiometer to 4.54 volts, then any change of resistance of the foil bearing to the shaft results in an output voltage change of zero to five volts which can be used to trigger a pulse counter. Calibration to any desired value of resistance sensitivity is accomplished by disconnecting the foil bearing leads and inserting a fixed value resistor between point E and ground. Measure at the output with a voltmeter and adjust the 10 kΩ trimpot until the setting is found that just causes the output voltage to swing between +5 volts and zero volts DC. Leave the adjustment set at zero volts DC output. A little hysterisis was placed in the circuit by means of 560 kΩ of feedback which helps remove the normal ambiguity of the circuit at or near the voltage crossover point. The 1.2 kΩ output resistor is simply a pull up for the oven collector transistor in the LM 311 voltage comparator. Since no attempt to slow down the frequency response of the sensing circuit was made, the unit will respond to touch times in the order of 10 to 15 microseconds.

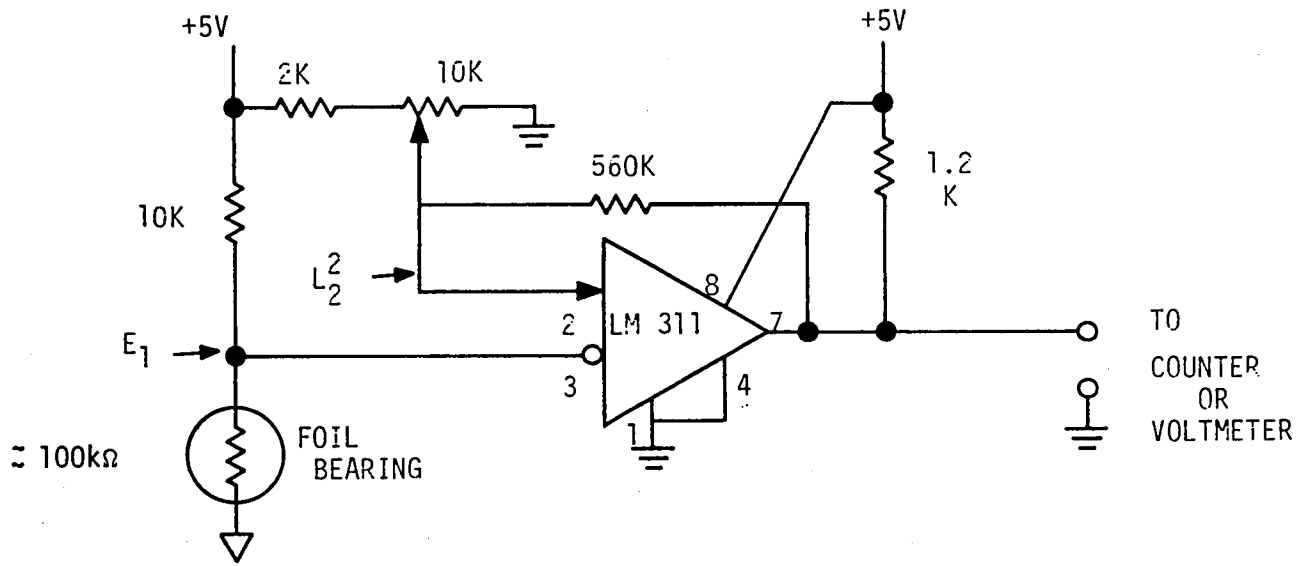

Fig. IV.11 Schematic of the Electronic Circuit used for Counting Number of Contacts during High Speed Rub Tests

793301

START-STOP TEST RESULTS AND DISCUSSIONS

Testing and Screening Technique

The start-stop tests were conducted with the facilities described in the previous sub-section with one-third the number of test cycles at a test chamber temperature of 427°C (800°F), 540°C (1000°F) or 650°C (1200°F), one third at the intermediate temperature and the other third at room temperature. The test format for the test specimens coated with hard coatings was as follows:

1. Five hundred cycles* at maximum temperature; 4 seconds on and 7 seconds off,
2. Five hundred cycles at controlled temperature program, RT to maximum temperature.
3. Five hundred cycles at room temperature
4. Repeat steps 1, 2, and 3 in the sequence until coatings fail up to a total of 9000 start-stop cycles.

In a previous program it was found that in case of hard coatings, if the tests were run at high temperature first, the coating performed better (reactive replenishment concept). Therefore hard coatings were tested at high temperature first. In the case of solid lubricant coatings (CdO-Graphite-Ag) the test sequence was reversed (Steps 3, 2, 1) because preoxidating of the bearing surfaces was not needed.

Time elapsed for 500 cycles was about 1.5 hours. If the heater was turned off after 500 cycles at maximum temperature, it took about 1.5 hours for the bearing to cool off, which matched with the time needed for 500 cycles. So, 500 cycles at intermediate temperature could be conducted while the bearing was cooling off. A typical temperature-time curve is shown in Figure IV.12.

During tests, the following test conditions were monitored and recorded:

- Serialization of specimens to include: materials, vendors, processing, and finishing data.
- Visual inspection of coatings before and after each 500 cycle period.

---

* One cycle consists of one start and one stop.

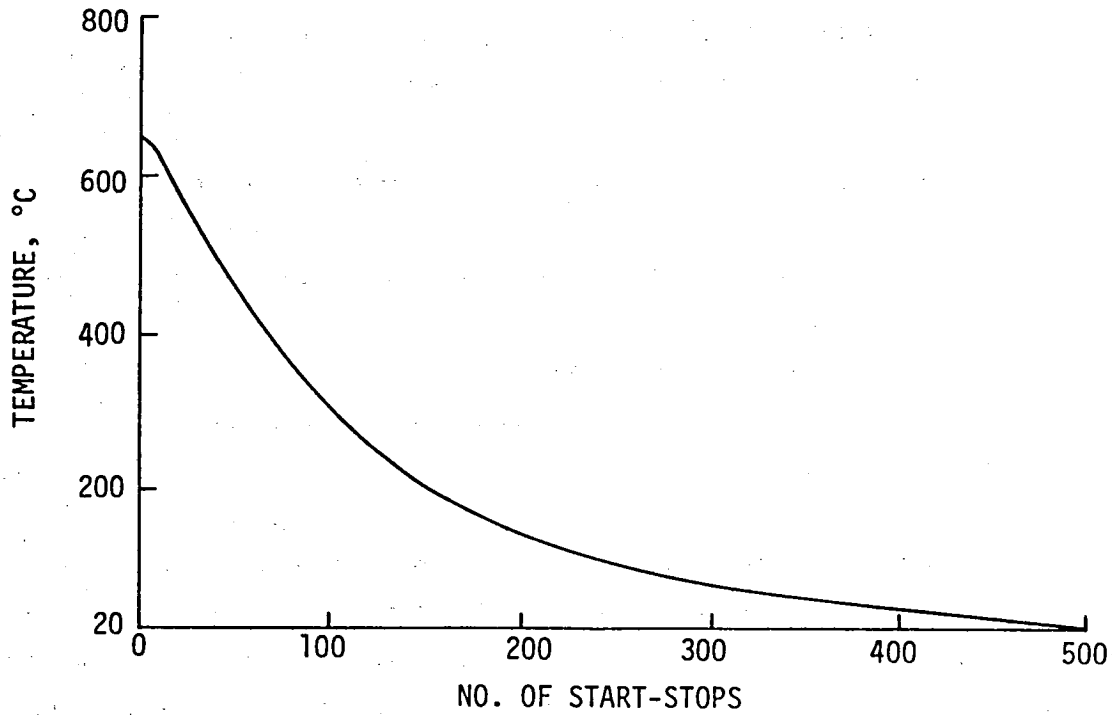

Fig. IV.12 Cooling Curve of the Bearing from 650°C when the Heater is Turned Off

793297

- Dynamic breakaway friction and kinetic friction of the bearing at the start and conclusion of each 500 cycles.
- Static breakaway torque at the beginning and end of the test.
- Ambient temperature.
- Maximum speed of spindle.
- Static and dynamic runout of test spindle.
- Unit loading

After every 500 test cycles a recorded trace of dynamic friction torque as a function of rotating speed during acceleration and deceleration was obtained for the purpose of estimating the general condition of the rubbing surfaces. The acceleration and deceleration of the drive motor was too fast to estimate the lift-off and touch-down speeds.

Initially, partial arc bearing tests on all of the test combinations selected from static oven screening tests were made and tested to the maximum of 9000 start-stop cycles at approximately 14 KPa (2 psi) based on projected area. This was followed by partial arc bearing start-stop tests at increased loading with the most promising material combinations, the unit projected specimen load in this test being 35 kPa (5 psi). Finally, start-stop tests of the most promising material combinations resulting from partial arc tests were made using a complete foil bearing.

The following criteria were used to screen the start-stop test results:

- Static and dynamic breakaway friction and kinetic friction at the start and conclusion of each 500 cycles.
- Visual inspection of the journal and the foil before and after each 500 cycles.
- Microscopic examination of the journal and the foil.

If the friction torque increased or the surfaces showed significant loss of coating or wear, the bearing was considered failed and the testing was terminated. Certain subjective judgment was required. Photographs of the bearing surfaces after the test and sometimes during the test were taken.

Partial Arc Bearing Tests at 14 kPa (2 psi) Loading

As explained earlier, foil bearing pads with a width of 19 mm (3/4 in.) and a pad arc of 186° were made. This made it possible to conduct two separate tests on each journal (38 mm, bearing width) using parallel contact tracks. The results of the coating combinations tested are reported in Table IV.3. The table shows the dynamic and static breakaway friction coefficient and kinetic friction coefficient, surface roughness of the journal before and after tests, and comments on the surface appearance of the journal and bearing after test.

Baseline Test: First test consisted of detonation gun Cr_3C_2 on the test journal and Hohman M-1284 (MoS_2 dry film) on the foil. This test was used as a baseline reference in evaluating rig performance. At the end of the 1500 start-stop cycle sequence which included: 500 cycles at room temperature; 500 cycles at 274°C (525°F); and 500 cycles at intermediate temperature, both coatings were still in a serviceable condition with only light transfer of the dry film to the journal occurring.

Preoxidized Surfaces: Next, preoxidized foil versus preoxidized journal were tested at a maximum temperature of 650°C (Test No. 4, Table IV.3). After 1500 cycles, foil and journal had numerous scratches and the surfaces galled. It demonstrated the need for coating foil and journal surfaces to minimize wear and damage of the rubbing areas.

CdO-Graphite Coating System: Air sprayed CdO-Graphite on foil versus detonation gun Cr_3C_2 on journal was tested at a maximum temperature of 427°C. After 6000 start/stops at HT, IT, and RT, the foil coating was polished and there were no bare spots. The journal was lightly coated with graphite which reduces further wear. In the next 3000 cycles, the journal was virtually unchanged, but the foil had some wear bands. For photographs of surfaces after test, see Figure IV.13a.

Air sprayed CdO-Graphite coating on both foil and journal (Test No. 8) was tested at a maximum temperature of 427°C. After 3000 cycles, the coating was worn and the test was stopped. The test was repeated with new journal and foil pieces and the same results were obtained. Although CdO-Graphite

TABLE IV.3

START-STOP TEST RESULTS OF COATING COMBINATIONS

Partial Arc Bearings

Load = 14 kPa (2 psi) Based on Bearing Projected Area

Test No.	Coating Combination	Foil and Journal Coatings	Maximum Test Temp. °C (°F)		At Start	Friction Coefficient After 499 Cycles	After 999 Cycles	After 1499 Cycles	After 5999 Cycles	After 9000 Cycles	Surface Roughness of Journal μm (μin.) Before	After	Comments
1*	None assigned (Baseline Test)	Air sprayed MoS_2 (Hohman 1284) versus Det. Gun Cr_3C_2	274 (525)	S[1]	0.13	0.13		0.16			0.33 (13)	0.33 (13)	Completed 1500 cycles at RT, HT and IT. Both surfaces serviceable after test. Rated - successful.
				D[2]	0.15			0.19					
				K[3]				0.22					
4**	4	Preoxidized†† versus preoxidized†	650 (1200)	S	0.27						0.46 (18)	1.32 (52)	500 cycles each at HT, IT and RT - Foil and Journal had numerous scratches and surfaces galled badly. Rated - unsuccessful.
				D	0.48	0.33	0.56	0.56					
				K	0.48			0.44					
2*	1a	Air sprayed CdO-Graphite (HL-800) versus Det. Gun Cr_3C_2	427 (800)	S	0.20			0.22		0.35	0.04 (1.7)	0.13 (5)	2000 cyc. each at RT, HT and IT-Foil coating polished, journal lightly coated with graphite. After next 3000 cycles-journal unchanged, foil coating worn along six bumps in the loaded zone. Both surfaces serviceable. Rated - Acceptable.
				D	0.22	0.22	0.22	0.22	0.29	0.59			
				K	0.22	0.22	0.24	0.24	0.29	0.59			
8*	2	Air sprayed CdO-Graphite versus Air-sprayed CdO-Graphite	427 (800)	S	0.13			0.22	0.23 (3000)				500 cycles each at RT, HT and IT - Foil and journal deeply polished at one edge. Fine polishing throughout both. After next 1500 cycles, one edge of journal and foil was worn. Rated - unsuccessful.
				D	0.22	0.3	0.41	0.19	0.45 (3000)				
				K	0.22			0.19	0.44 (3000)				
5*	3	Air sprayed CdO-Graphite versus Air sprayed CdO-Graphite with Metco Cr_3C_2 undercoat	427 (800)	S	0.18							0.89 (35)	500 cycles each at HT, IT and RT - Journal polished, foil had bare spots in loaded zone. After next 1500 cycles - journal had several wear bands and foil had several wear zones at the bumps in the loaded zone. Rated - unsuccessful.
				D	0.3	0.26	0.52	0.15	0.22 (2000)	0.56 (3000)	-		
				K	0.18	0.26	0.37			0.41 (3000)			
3*	1b	Air sprayed CdO-Graphite-Ag versus Det. Gun. Cr_3C_2	427 (800)	S	0.21				0.26 (3000)				500 cyc. each at RT, HT and IT-Foil polished uniformly, journal unchanged. After next 1500 cycles-silver smeared into bands on foil and some graphite-CdO came off in the bands. Journal lightly coated with silver corresponding to silver bands on foil. Rated - unsuccessful.
				D	0.26	0.29	0.29	0.26	0.41 (3000)		0.04 (1.7)	0.38 (15)	
				K	0.24			0.26	0.41 (3000)				

TABLE IV.3 (cont'd)

Test No.	Coating Combination	Foil and Journal Coatings	Maximum Test Temp. °C (°F)		Friction Coefficient At Start	After 499 Cycles	After 999 Cycles	After 1499 Cycles	After 5999 Cycles	After 9000 Cycles	Surface Roughness of Journal µm (µin.) Before	After	Comments
11*	1b	Air sprayed CdO-Graphite-Ag† versus Det. Gun Cr_3C_2	427 (800)	S	0.16	0.18		0.12	0.23	0.26			1000 cycles each at HT, IT and RT - Foil polished, journal unchanged. After 6000 cycles, foil coating worn slightly with two bands on edges. After 9000 cycles, journal smooth and shiny. Foil worn some over bumps in the loaded zone. Rated - successful.
				D	0.33	0.44	0.44	0.44	0.44	0.63	0.11 (4.5)	0.13 (5)	
				K	0.3	0.37	0.3	0.3	0.44	0.60			
12**	11	Kaman DES versus Kaman SCA	650 (1200)	S	0.22								500 cycles each at HT, IT, Journal polished. Foil coating worn considerably over bumps and over edges. Rated - unsuccessful.
				D	0.81	0.89	1.0				0.81 (23)	0.30 (12)	
				K	0.44 RT 0.81 (650)		1.0						
13**	5	Preoxidized versus Plasma sprayed NASA PS120	540 (1000)	S	0.22								500 cycles each at HT, IT, RT - Journal polished. Silver transferred to foil. Friction too high. After next 1500 cycles, lot of transfer of silver on foil. Journal diameter loss 18 µm (0.7 mil). Bearing running rough. Rated - unsuccessful.
				D	0.96	0.96	0.96	0.81	1.04 (3000)		1.07	0.46	
				K	0.37 (RT) 0.81 (540)		0.81	0.74	0.89 (3000)		(42)	(18)	
14**	6	Preoxidized versus Plasma sprayed NASA PS120 with CdO-Graphite Topcoat	540 (1000)	S	0.23								50 cycles at HT-Graphite disappeared resulting in high friction, friction too high. 500 cycles each at HT, IT, and RT-journal polished. Silver transferred on foil. After next 1500 cycles - more silver transferred on the foil, journal diameter loss = 10 µm (0.4 mil). After 4500 cycles-foil in loaded zone coated with Ag, Journal diameter loss-20 µm (0.8 mil) Squeal during running. Stick slip seen in kinetic friction reading. Rated - unsuccessful.
				D	0.51	0.89	0.89	0.89	1.0 (3000)	0.89 (4500)	0.91 (36)	0.36 (14)	
				K	0.26			0.89	0.89 (3000)	0.89 (4500)	Before CdO-Graphite Coating		

TABLE IV.3 (cont'd)

Test No.	Coating Combination	Foil and Journal Coatings	Maximum Test Temp. °C (°F)	Friction Coefficient	At Start	After 499 Cycles	After 999 Cycles	After 1499 Cycles	After 5999 Cycles	After 9000 Cycles	Surface Roughness of Journal µm (µin.) Before	After	Comments
15**	7	Preoxidized versus Plasma sprayed NASA PS122	540 (1000)	S	0.20								1000 cycles each at HT, RT, IT - Silver transferred on foil over bumps. Journal polished and diameter under 8 µm (.3 mil). Friction too high. After next 1500 cycles, foil coated with Ag over bumps in loaded zone. Journal under 10 µm (0.4 mil). Rated - unsuccessful.
				D	0.81	0.96	0.96	0.96	0.96 (3000)	0.96 (4500)	0.84 (33)	0.28 (11)	
				K	0.22 RT 0.74 (540)		0.78	0.85	0.89 (3000)	0.89 (4500)			
26	8	Preoxidized versus Plasma sprayed ZrO_2 - CaF_2	650 (1200)	S	0.18		0.83 (600)						500 cycles at HT, and 100 cycles at RT journal coating became smoother somewhat. Bearing running very rough test stopped. Rated - unsuccessful.
				D	0.59	1.04	1.04 (600)				1.52 (60)	1.14 (45)	
				K	0.59	0.81	1.0 (600)						
9**	20	Fused 61.5% PbO-3.5% SiO_2-25%-Ag-10% Fe_3O_4 versus preoxidized	260 (500)	S	0.21		0.43				0.46 (18)	0.86 (34)	Kinetic friction was too high at high temperature. Test temperature lowered to 260°C After 500 cycles each at HT and IT - foil had some wear on outer edges, journal polished. Bearing ran rough at starting, ran smooth at maximum speed. Rated - unsuccessful.
				D	0.67	0.74	0.74						
				K	0.67	0.78	0.70						
10**	21	Preoxidized versus fused 71% PbO, 4% SiO_2, 25% Ag	260 (500)	S	0.22		0.60				0.28 (11)	0.46 (18)	Test temperature lowered to reduce friction. After 500 cycles each at HT and IT journal uniformly worn. Foil had polished marks at edges. Rated - unsuccessful.
				D	0.96	0.89	0.89						
				K	0.19	0.81	0.81						
				S									
				D									
				K									
17**	20	Fused 75.8% PbO, 4.2% SiO_2, 10% Ag, 10% Fe_3O_4 versus Preoxidized	260 (500)	S	0.25								50 cycles at HT-friction went up after 20 cycles. Coating probably melted and increased friction. Bearing running unstable. Bearing surfaces unchanged. Rated - unsuccessful.
				D	0.09	1.03 (50)					0.23 (9)	0.33 (13)	
				K	0.15	1.03 (50)							

TABLE IV.3 (cont'd)

Test No.	Coating Combination	Foil and Journal Coatings	Maximum Test Temp. °C (°F)	Friction Coefficient						Surface Roughness of Journal μm (μin.)		Comments
					At Start	After 499 Cycles	After 999 Cycles	After 1499 Cycles	After 5999 Cycles	After 9000 Cycles	Before	After	
18**	21	Preoxidized versus Fused 85.2% PbO, 4.8% SiO_2, 10% Ag	260 (500)	S	0.22	0.70 (100)					0.51 (20)	0.94 (37)	100 cycles at HT-friction went up considerably after 60 cycles. Bearing running unstable. Similar results obtained at 244°C (400°F). Rated - unsuccessful.
				D	0.15	1.03 (100)							
				K	0.15	1.03 (100)							
21**	20	Fused 85.5% PbO, 4.5% SiO_2, 10% Fe_3O_4 versus Preoxidized	370 (700)	S	0.24	0.84 (150)					0.33 (13)	0.41 (16)	150 cycles at HT-Foil surfaces unchanged. Friction too high through the test. Coating melted and was sticking to the journal Rated - unsuccessful.
				D	0.88	0.88 (150)							
				K	0.88	0.88 (150)							
16**	19	Fused CaF_2-BaF_2-Ag (OSF-6) versus Preoxidized	650 (1200)	S	0.28	0.50 (100)					0.23 (9)	1.78 (70)	100 cycles at HT-journal and foil both badly scored. Wear debris did not permit bearing liftoff. Friction too high. Rated - unsuccessful.
				D	0.80	1.03 (100)							
				K	0.59	1.03 (100)							
6**	12a	Sputtered Cr_2O_3 (Run #29) versus Det. Gun Cr_3C_2	650 (1200)	S	0.19					0.28	0.046 (1.8)	0.56 (22)	500 cycles each at HT, IT and RT - polishing of foil coating over bumps in the loaded zone. Journal had fine scratches. After another 1500 cycles - journal looks the same, foil had more polishing spots. After 9000 cycles - journal looks the same. Foil had several wear spots in the center and at outer edges, but the spots were reoxidized. Rated - successful.
				D	0.26	0.22	0.45	0.56	0.45	0.40			
				K	0.26	0.22	0.45	0.56	0.45	0.40			
19**	12	Sputtered Cr_2O_3 (Run #29) versus Det. Gun Cr_3C_2	650 (1200)	S	0.15				0.27	0.58	0.05 (2)	0.38 (15)	Repeat Test 2000 cycles each at HT, IT, and RT-coating slightly worn in bands in the loaded zone, journal unchanged. After next 3000 cycles more coating worn in the loaded zone and substrate reoxidized. Rated - successful.
				D	0.41	0.41	0.51	0.56	0.51	0.71			
				K	0.41	0.41	0.51	0.56		0.67			

TABLE IV.3 (cont'd)

Test No.	Coating Combination	Foil and Journal Coatings	Maximum Test Temp. °C (°F)	Friction Coefficient						Surface Roughness of Journal µm (µin.)		Comments
					At Start	After 499 Cycles	After 999 Cycles	After 1499 Cycles	After 5999 Cycles	After 9000 Cycles	Before	After	
7**	12b	Sputtered Ni-Cr-Cr_2O_3 (Run #30) versus Det. Gun Cr_3C_2	650 (1200)	S	0.12			0.37	0.6 (3000)		0.046 (1.8)	0.61 (24)	500 cycles each at HT, IT and RT - foil had three bands of deep polishing in loaded zone. Journal evenly polished. After 3000 cycles - journal looks same. Foil had 4 wide and several small wear bands. Rated - marginal.
				D	0.26	0.40	0.40	0.40	0.52 (3000)				
				K	0.26	0.26		0.40	0.44 (3000)				
22**	13	Sputtered Ni-Cr-Cr_2O_3 (Run #47) versus Det. Gun Cr_3C_2	650 (1200)	S	0.13			0.78			0.13 (5)	0.20 (8)	500 cycles each at HT, IT, and RT - foil coating worn significantly in the loaded zone. Journal looks the same. Rated - unsuccessful.
				D	0.50	0.44	0.74	0.88					
				K	0.48	0.37		0.88					
20**	13	Sputtered Ni-Cr-Cr_2O_3 with Ni-Cr undercoat (Run #40) versus Det. Gun Cr_3C_2	650 (1200)	S	0.08				0.72 (3000)		0.05 (2)	0.31 (12)	500 cycles each at HT, IT, RT journal unchanged. Foil worn some over bumps in loaded zone. After next 1500 cycles - journal O.K. Foil worn in the loaded zone. Some scratched in worn area. Rated - marginal.
				D	0.41	0.50		0.81	0.81 (3000)				
				K	0.41			0.81	0.81 (3000)				
24**	15	Sputtered Cr_2O_3 (Run #50) versus Sputtered Cr_2O_3 (Run #54)	650 (1200)	S	0.19				0.72 (3000)		0.076 (3)	1.02 (40)	500 cycles each at HT, IT, and RT - foil coating polished, journal coating deeply polished. After next 1500 cycles-coatings on foil polished over bumps, journal coating worn. Rated - unsuccessful.
				D	0.51			0.70	0.81 (3000)				
				K	0.44	0.59		0.70	0.81 (3000)				

* Test cycle sequence - 500 RT, 500 HT, 500 IT, repeated

**Test cycle sequence - 500 HT, 500 IT, 500 RT, repeated

† - 1800°F/1 hour/AC polished + 1325/16 hours/AC

†† - 1600°F/4 hours/AC + 1300°F/20 hours/AC

1 - Static breakaway at RT

2 - Dynamic breakaway at test temperature

3 - Kinetic at test temperature

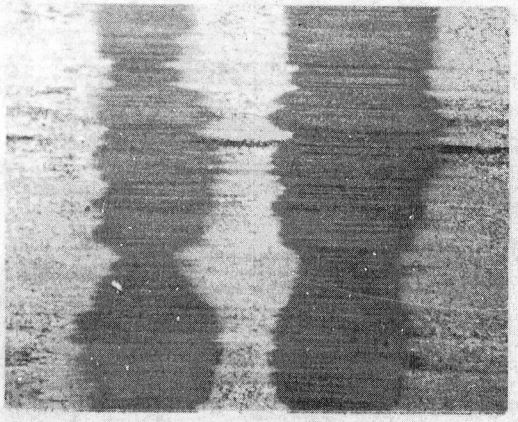

7X

CdO-GRAPHITE ON FOIL

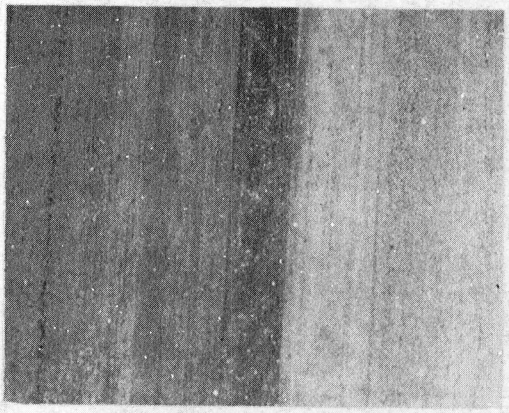

7X

Cr_3C_2 ON JOURNAL

(a)

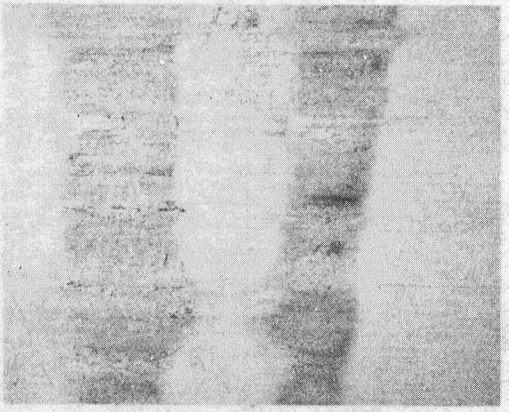

7X

CdO-GRAPHITE-Ag ON FOIL

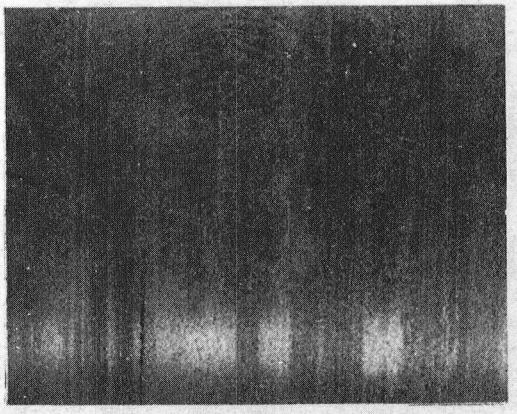

7X

Cr_3C_2 ON JOURNAL

(b)

Fig. IV.13 Photographs of Surfaces After Test for 3000 Cycles Each at 427°C, Intermediate Temperature and Room Temperature
(a. Test No. 2, b. Test No. 11)

on foil versus hard Cr_3C_2 coating on journal has worked well, CdO-graphite against itself failed catastrophically.

In a parallel work done by Heshmat and Bhushan [4.1], CdO-graphite coatings when applied on both journal and the foil worked satisfactorily when tested at 274°C. This probably means that CdO-graphite versus itself is a good lubricant system if tested below 427°C so that some interface temperature increase due to decreased coupled thermal conductivity does not exceed the temperature limit.

In the next test (numbered 5), the CdO-graphite coating was applied on a coarse Metco Cr_3C_2 pre-coated journal. After 3000 cycles, the foil and the journal coatings were worn (for photographs see Appendix F). The undercoating of the journal was selected to be porous so that graphite coating had better adhesion. However, when graphite wore it exposed the sharp Cr_3C_2 particles which damaged the foil surface which led to coating failure. A smoother undercoating of Cr_3C_2 is recommended for future tests.

Next test (numbered 3, Table IV.3) was conducted with CdO-graphite-Ag coating (HL-800-2) on foil versus detonation gun Cr_3C_2 coating on the journal. Ag used in the coating preparation had a particle size of 230 mesh. After 1500 cycles, foil was polished and more silver was exposed on the surface. After another 1500 cycles, the silver was collected in pockets and most of the graphite came off and a lot of Ag collected in bands in the loaded zone. The journal was lightly coated with Ag where silver bands on foil were riding. The test was stopped after 3000 cycles (for photographs see Appendix F). The silver particles were rather large (0.062 mm max.). It was therefore considered worthwhile to examine the effect of reducing the particle size.

New CdO-graphite-Ag coatings were made using very fine silver particles having a particle size of 1 to 5 microns. This coating on foil was tested against det. gun Cr_3C_2 on the journal (numbered 5, Table IV.3). After 3000 cycles, the coating was lightly polished and not worn at all. After an additional 3000 cycles, the foil coating was worn slightly with two wear bands on the outer edges. After 9000 cycles, the journal was smooth and

shiny (shiny because of the light silver transfer) and the foil was worn over bumps in the loaded zone. In the last 3000 cycles (from 6000 to 9000), the friction went up due to some bare spots on the foil. The photographs of the surfaces after the test are shown in Figure IV.13 and the Talysurf traces of journal surfaces before and after the test are shown in Figure IV.14.

Comparing this test (numbered 11) with CdO-Graphite coating test (numbered 5), we find that the CdO-graphite coating with fine particle size Ag experienced less wear than the coating without Ag. Therefore CdO-graphite-Ag is recommended for 427°C maximum temperature applications.

Kaman Coating: Kaman DES coating versus itself had completed 1000 cycles at 540°C, 1000 cycles at 650°C, and 2000 cycles at room temperature in the previous program [1.2]. Endurance testing of this coating combination was planned in the present program. After 500 cycles each at HT (650°C), IT and RT, the journal and the foil had substantial wear. The surface roughness of the coated journal in this program was 1.22 μm (48 μin.) CLA and in the previous program it was only 0.28 μm (11 μin.) CLA. It is believed that poor performance was due to the rough journal coating. All Kaman DES and SCA journals then were returned to the vendor for reprocessing.

As mentioned in Section III, adequate surface finish could not be provided by the vendor on the DES journals. The only acceptable (marginally) journal was SCA. The journal was very rough and was considered marginal for an air bearing application because previous experience has shown that air film thickness and load capacity is reduced in a porous journal. This coating was tested against Kaman DES on foil (Test No. 12, Table IV.3). The friction of the coating was low at room temperature, but it rose to a very high value (0.81) at maximum temperature. After 1000 cycles, the foil coating was worn considerably and the wear particles filled up the journal surface making it smooth during testing. Due to excessive wear the test was discontinued. The photographs of bearing surfaces after the test are shown in Figure IV.15a. As indicated in section III, DES and SCA coating on the foil was unacceptable and the combinations number 10 in Table II.4 was dropped.

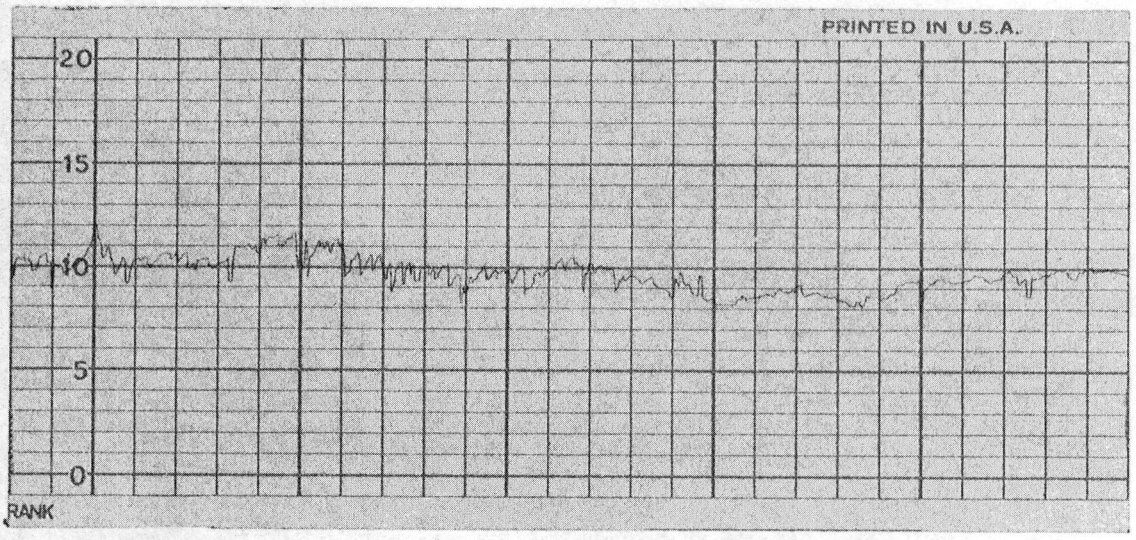

BEFORE TEST

CLA = 0.11μm (4.5μin.)
VERTICAL MAG.: EACH SMALL DIV. = 0.25μm

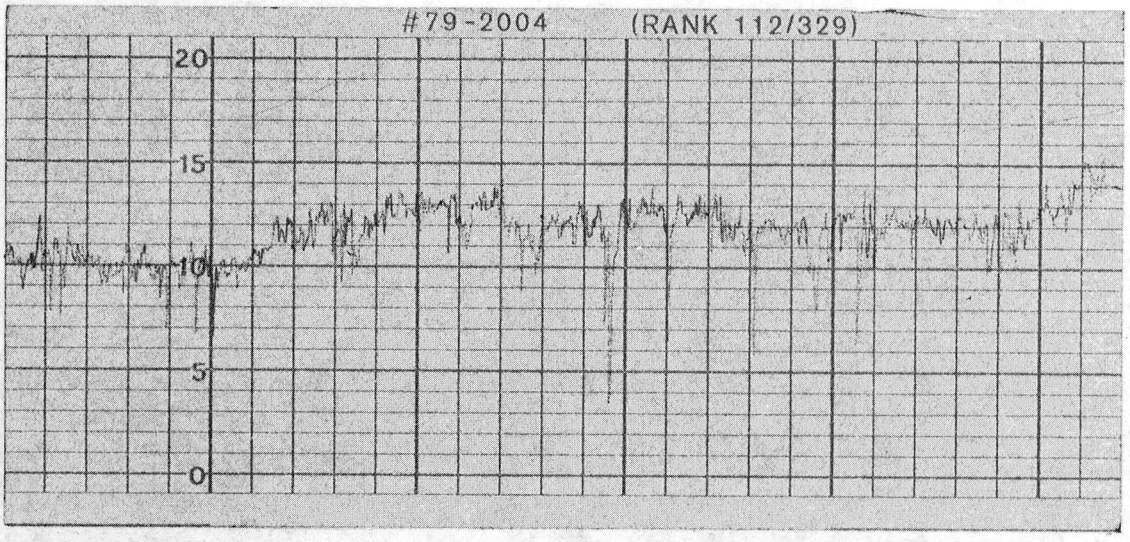

AFTER TEST

CLA = 0.13μm (5μin.)
VERTICAL MAG.: EACH SMALL DIV. = 0.13μm
HORIZONTAL MAG: EACH SMALL DIV. = 250μm

Fig. IV.14 Talysurf Traces of Det. Gun Cr_3C_2 Coated Journal Tested Against CdO-Graphite-Ag Coated Foil for 3000 Cycles Each at 427°C, IT and RT (Test No. 11)

793271

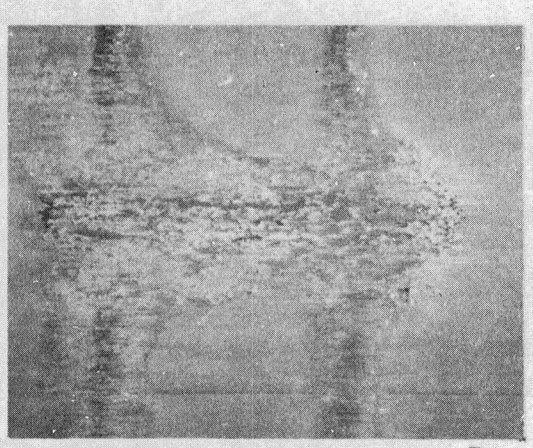

7X

KAMAN DES ON FOIL

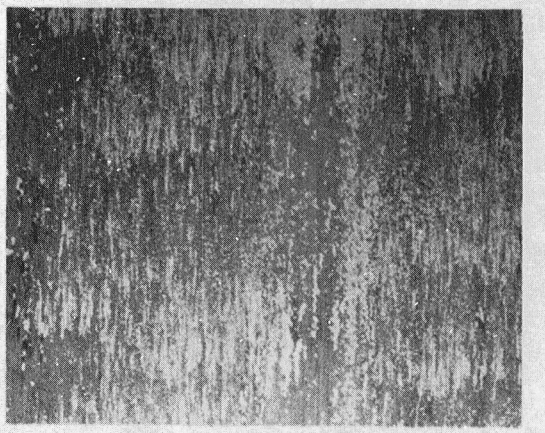

7X

KAMAN SCA ON JOURNAL

(a)

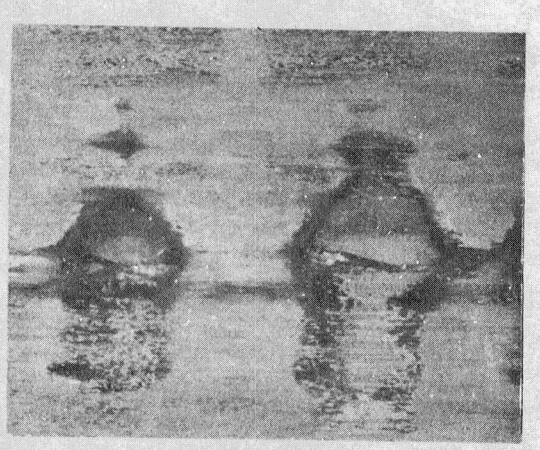

7X

PREOXIDIZED FOIL

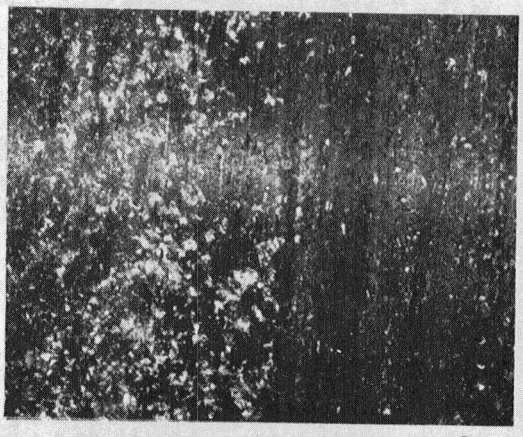

7X

NASA PS12C + CdO-GRAPHITE ON JOURNAL

(b)

Fig. IV.15 Photographs of Surfaces After Test
(a. Test No. 12, b. Test No. 14)

793261

NASA PS Coatings: NASA PS120 on journal against uncoated foil was successfully tested for 1000 cycles at 540°C and for an additional 1000 cycles at RT. This test was repeated here (Test No. 13, Table IV.3). The journal supplied in this program was quite a bit more porous, 1.07μm compared to 0.53μm in the previous program. At start, the kinetic friction at room temperature was low, but it became high at the maximum temperature. The coefficient of friction was considered too high for the application. During the first 1500 cycles, silver from the journal coating was transferred to the foil. In the next 1500 cycles, there was diametral loss of journal size of about 18μm (0.7 mil)(for photographs of surfaces after test Appendix F). This was considered unacceptable because this would have a twofold effect. First it will open up the bearing clearance, resulting in a reduction in load capacity. Second, the hard wear particles in a full bearing would not eject easily and would act as an abrasive and do damage as seen in the case of Kaman DES versus itself in the previous program (see Bhushan et. al. [1.2]).

The next test (No. 14) consisted of the same PS120 coatings, except the journal had CdO-graphite coating over NASA PS120 coating. Graphite oxidized in the first 50 cycles at 540°C and the friction increased. Then the coating behaved the same as in the previous test (numbered 13). After 4500 cycles, the loss in the journal diameter was 20 μm (0.8 mil) which was considerable and the test was discontinued. The photographs of surfaces after the test are shown in Figure IV.15b.

Next a test with preoxidized foil versus journal coated with NASA PS122 (No. 15) was conducted. This coating was rough. The coefficient of friction in this coating was also high and the journal was worn about 10μm (0.4 mil) after 4500 cycles. There was silver transfer to foil from the journal. Although the wear of the journal in this test is less than that in the previous test (No. 14) it is considered too high. The high friction aggrevates the situation.

The next test (No. 26) consisted of plasma sprayed ZrO_2-CaF_2 coating on the journal and preoxidized foil. The friction was high at 650°C after 500 cycles. After another 100 cycles during cooling, the friction got

very high and the bearing started running very rough. The test was stopped after 600 cycles (for photographs of bearing surfaces after test see Appendix F).

PbO-SiO_2-Ag-Fe_3O_4 Coatings: Fused 61.5% PbO-3.5% SiO_2-25% Ag-10% Fe_3O_4 coating on foil was tested against preoxidized journal (No. 9). Kinetic friction initially went down with an increase in temperature up to roughly 260°C and then it started to climb. During cooling, the friction did not change significantly (see Figure IV.16). The initial decrease in friction has already been reported in the literature and it is probably due to melting of PbO-SiO_2. The later increase in the friction is surprising and it may be that silver contents stick at higher temperatures and results in the high friction. The test was conducted at 260°C because friction was lowest at this temperature. The bearing ran very rough and the test was stopped after 1000 cycles. In additional tests, silver contents were reduced to study its effect on friction.

Fused 71% PbO-4% SiO_2-25% Ag on journal was tested against preoxidized foil. The test was run at 260°C maximum temperature where the friction was lowest. In the first cycle, the dynamic breakaway torque went up considerably. The bearing ran rough during starting. The journal was significantly though uniformly worn after 1000 cycles. The test was stopped. For photographs of the bearing surfaces after the test, see Appendix F.

The next test consisted of 75.8% PbO-4.2% SiO_2-10% Ag-10% Fe_3O_4 coating (with reduced Ag content) on foil versus preoxidized journal (Test No. 17). The kinetic friction was measured during heating. The friction was lowest (0.15) at 315°C (600°F), and at 370°C (700°F) it went up to 1.03. During cooling, friction stayed high (for plot see Figure IV.17). The coating melted at 370°C and got stuck to the journal and damaged the surfaces. It was felt that since friction is low in the 260-315°C range, another test should be conducted with new surfaces. The test temperature was selected to be 260°C so that there is some margin for frictional heating. The friction went up after only 20 cycles, and it was very high (kinetic - 1.03) after 50 cycles. The test was discontinued after 50 cycles.

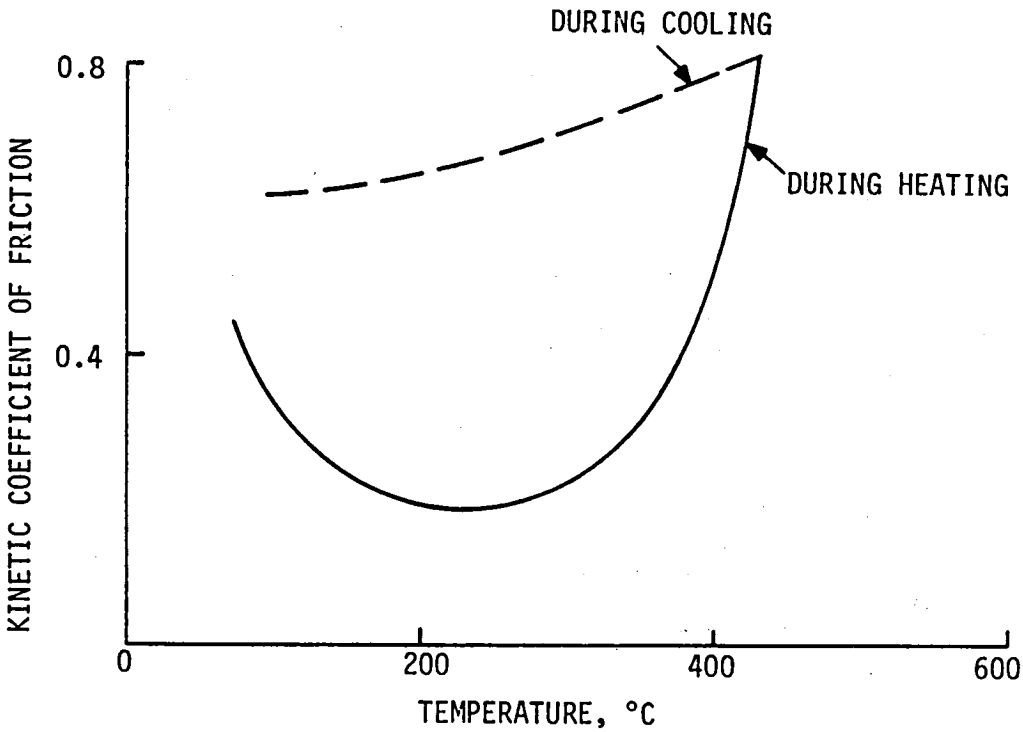

Fig. IV.16 Kinetic Friction versus Temperature for Fused 61.5% PbO-3.5% SiO_2-25% Ag-10% Fe_3O_4 on Foil and Preoxidized Journal (Test No. 9)

793293

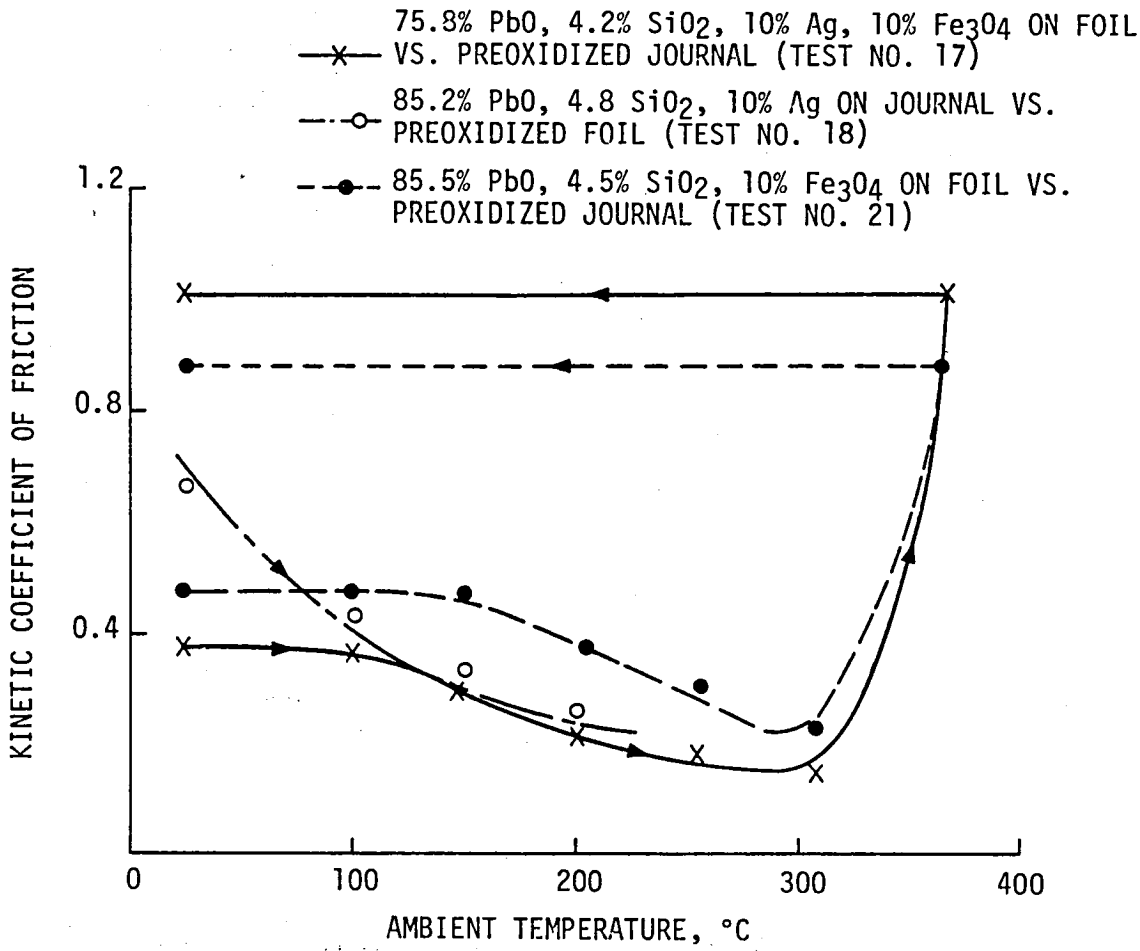

Fig. IV.17 Kinetic Coefficient of Friction versus Ambient Temperature for Fused PbO-SiO_2 Coating System with Additives

793302

In the next test (No. 18) - 85.2% PbO-4.8% SiO_2-10% Ag coating versus preoxidized foil were tested. The test was conducted at 260°C (500°F). The kinetic friction initially was low and it remained so up to 60 cycles; then it rose to 1.03 after 100 cycles. The test was discontinued after 100 cycles.

It was believed that the coating had a low melting point. A phase diagram of Pb-Ag shows that its eutectic melts at 304°C. To the investigator's knowledge, no PbO-Ag phase diagram is available. From the experimental data, it seems that PbO-Ag reduces to Pb-Ag system or forms a eutectic which melts at almost the same temperature as Pb-Ag. In that case, the Ag addition would not be too beneficial.

A test of 85.5% PbO-4.5% SiO_2-10% Fe_3O_4 with no Ag addition was planned next to reproduce some of the work done in pin on disk studies at NASA-Lewis in the late fifties [2.23]. The kinetic friction went down with temperature increasing from 25°C up to 315°C, then it rose at 371°C (see Figure IV.17). The test was conducted at 371°C. The coefficient of friction was high at running, and the test was stopped after 150 cycles.

This coating has worked in a rigid bearing application, but does not work in compliant foil bearings. It is felt that due to localized melting, the thin foil is distorted and makes the bearing run rough.

CaF_2-BaF_2-Ag Coating: Fused CaF_2-BaF_2-Ag (OSF-6) coating on the foil versus preoxidized journal (Test No. 16) was tested at 650°C. The kinetic friction rose to 0.8 in only the first four cycles and kept going up to 1.03 after 100 cycles. There was wear debris collected at the interface which did not permit the bearing to liftoff. After 100 cycles, the journal had deep grooves and the foil was deeply worn. The test was discontinued after 100 cycles.

Cr_2O_3 Based Sputtered Coatings: Optimized Cr_2O_3 coating on the foil was tested against detonation gun Cr_3C_2 coating on journal (Test No. 6). The friction at the maximum test temperature (650°C) was lower than that at RT through the cycle (see Figure IV.18). It is noted that in all previous tests, the

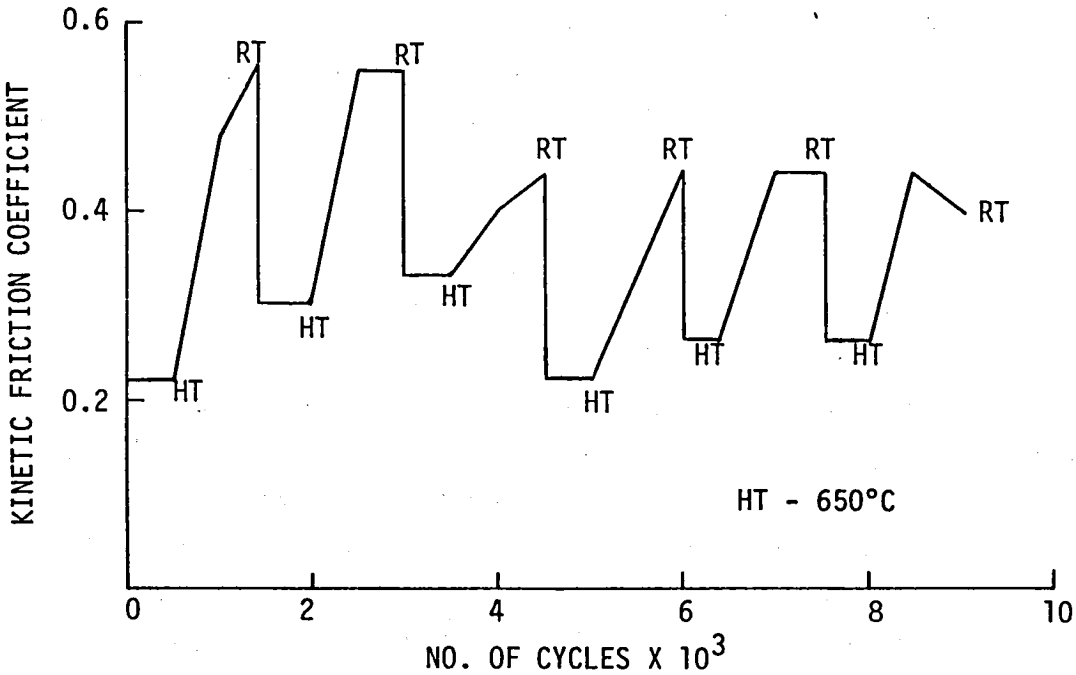

Fig. IV.18 Kinetic Friction Coefficient at Test Temperature versus Number of Cycles for Cr_2O_3 sp. on Foil versus Det. Gun Cr_3C_2 on Journal (Test No. 6)

793298

friction was not dependent on the temperature. The coating combination successfully completed the test sequence. The wear of the sputtered coating was very low and the friction was fairly repeatable with the temperature. The photographs of bearing surfaces after the test and Talysuf traces of the journal before and after tests are shown in Figures IV.19 and IV.20, respectively. A representative visicorder trace showing the friction versus time at the end of the test is shown in Figure IV.21. A repeat test (No. 19) was conducted and the coating again completed the test sequence. The friction in this test was higher than the previous test, but the friction versus temperature trend was the same.

Next, Ni-Cr-Cr_2O_3 coating on foil was tested against detonation gun Cr_3C_2. This coating combination did not perform so well. The coatings were worn after 3000 cycles.

Next Ni-Cr-Cr_2O_3 was applied thinner at lower chamber pressure (Trial No. 47, Table III.3) and it was tested against Cr_3C_2 (Test No. 22). After 1500 cycles, the foil coating was worn in the loaded zone and the test was stopped. For photographs of surfaces after the test, see Figure IV.22.

Test No. 20 consisted of sputtered Ni-Cr-Cr_2O_3 with Ni-Cr undercoat on annealed foil (then heat treated) versus detonation gun Cr_3C_2. The coating ran well initially, then the friction increased. After 3000 cycles, the foil was worn in the loaded zone. It is believed that the Ni-Cr-Cr_2O_3 coating (top layer) may have become slightly soft due to the high content of Ni-Cr. In a future program, the coating with the reduced amount of Ni-Cr or other metallic binders, e.g., cobalt, should be tried; and since this concept has a potential, the coating is rated marginal. The photographs of the surfaces after the tests are shown in Figure IV.22. It should be noted that we have demonstrated in Section III that nichrome improves the ductility of the coating which is very much needed. Once an optimum mix of metallic binder is available and further parametric study is done, it should behave better than straight Cr_2O_3.

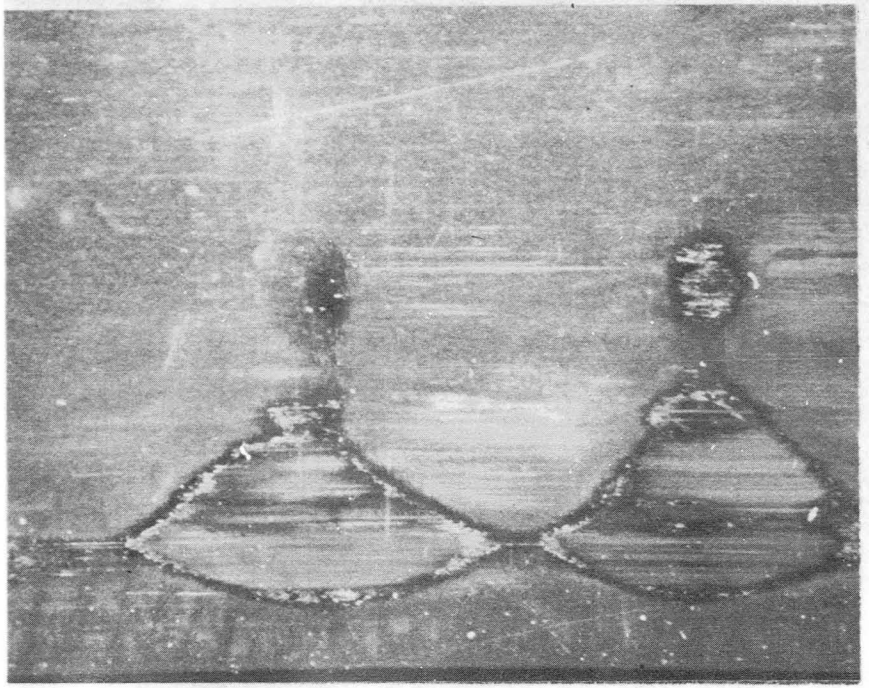

7X

Cr_2O_3 ON FOIL

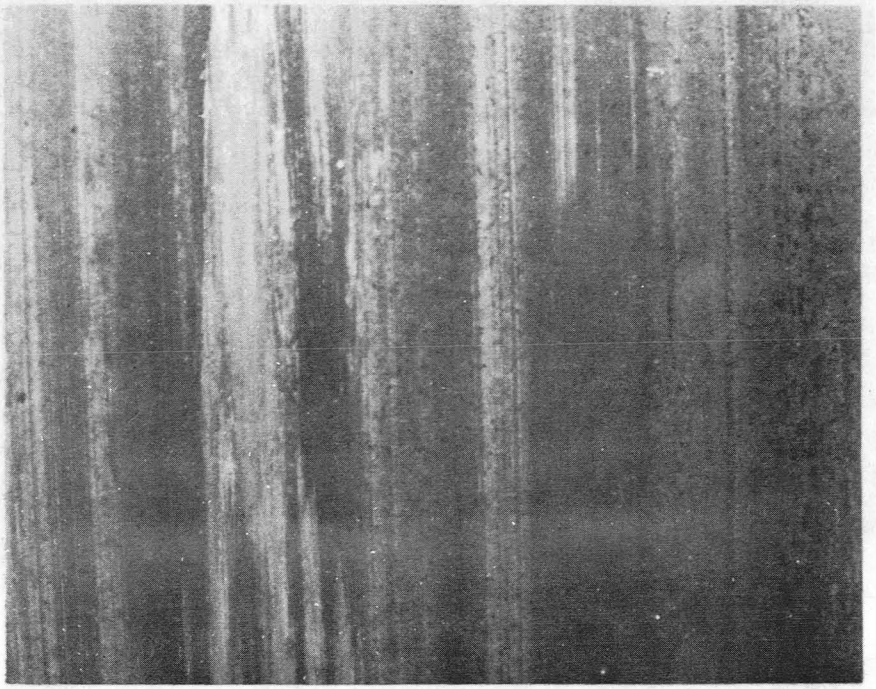

7X

Cr_3C_2 ON JOURNAL

Fig. IV.19 Photographs of Surfaces After Test for 3000 Cycles Each at 650°C, IT and RT
(Test 6)

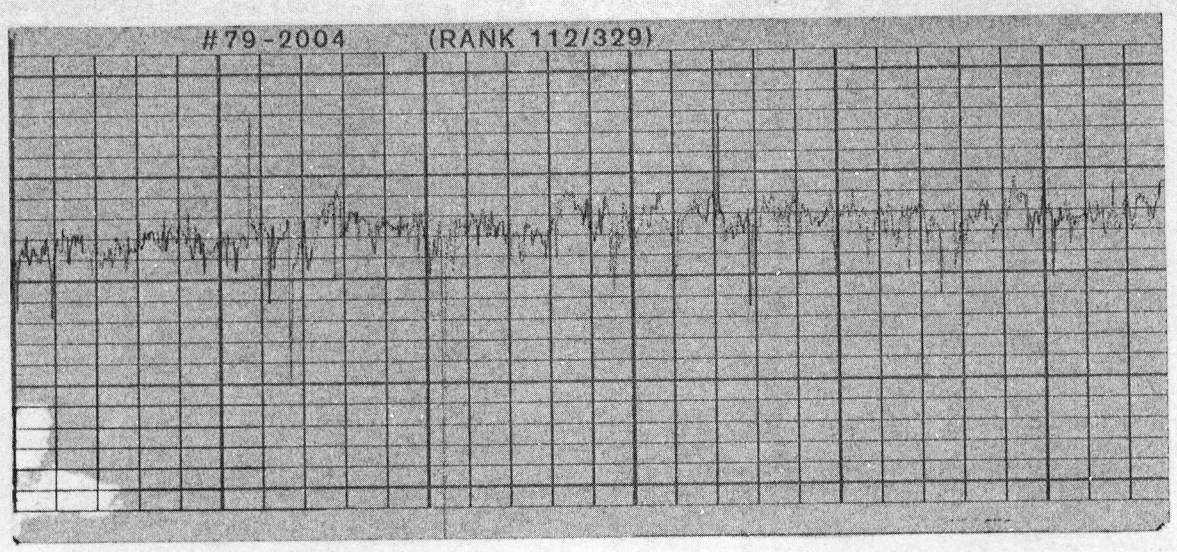

BEFORE TEST

CLA = 0.0 46 μm (1.8 μin.)

VERTICAL MAG.: EACH SMALL DIV. = 0.05μm

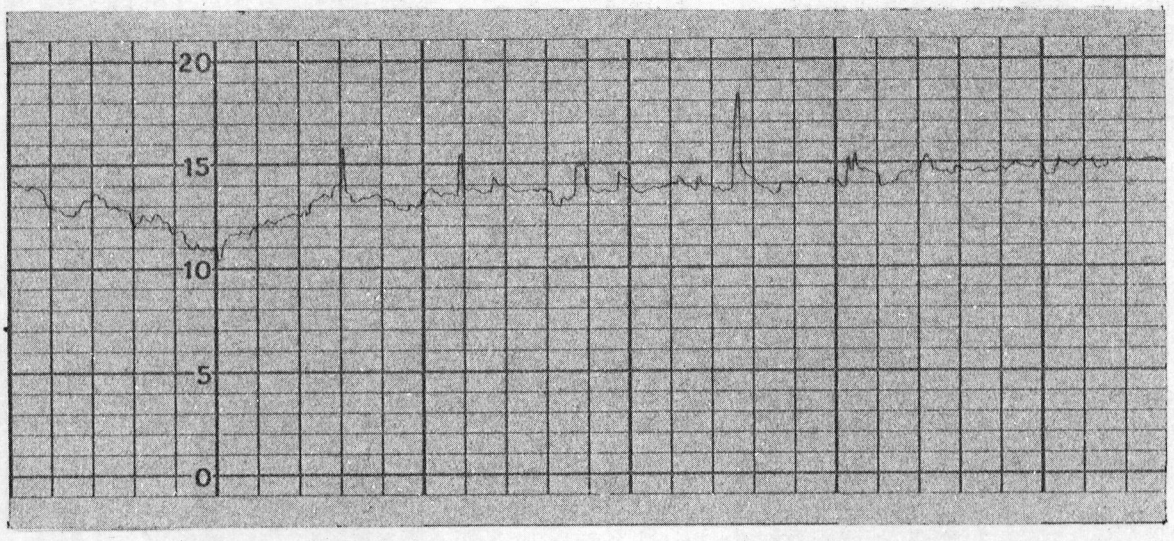

AFTER TEST

CLA = 0.56μm (22μin.)
VERTICAL MAG.: EACH SMALL DIV. = 0.5μm
HORIZONTAL MAG.: EACH SMALL DIV. = 250μm

Fig. IV.20 Talysurf Traces of Det. Gun Cr_3C_2 Coated Journal Tested Against Sputtered Cr_2O_3 Foil for 3000 Cycles Each at 650°C, IT and RT (Test No. 6)

793259

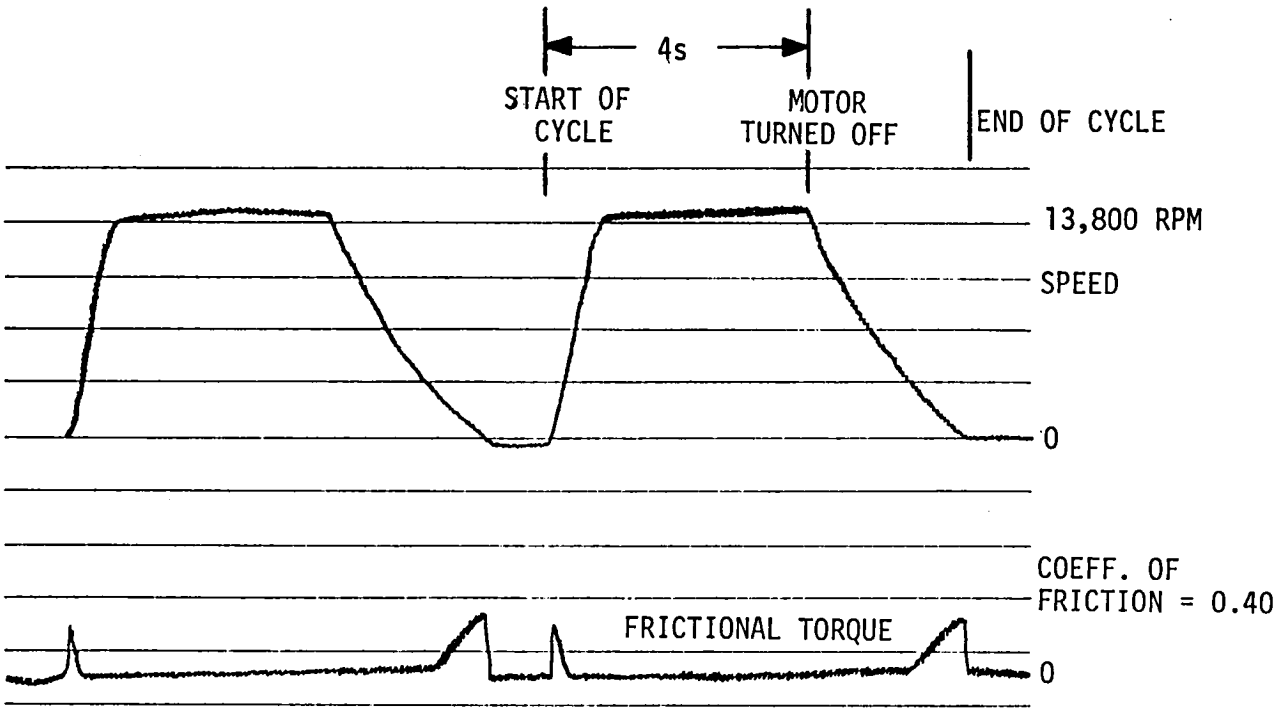

Fig. IV.21 Visicorder Trace of Coating Combination Sputtered Cr_2O_3 on Foil versus Det. Gun Cr_3C_2 on Journal after Test for 9000 Cycles with 3000 Cycles each at 650°C, IT and RT (Test No. 6)

793299

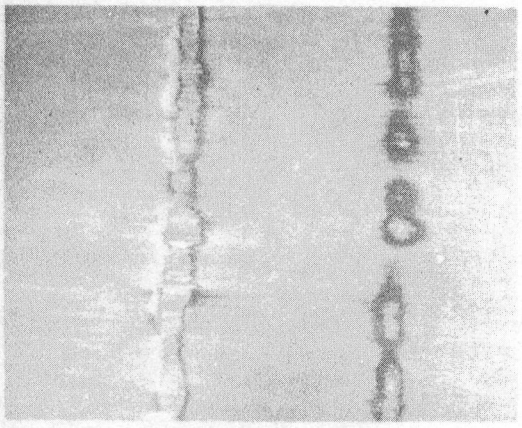

7X

$Ni-Cr-Cr_2O_3$ WITH Ni-Cr UNDERCOAT ON FOIL

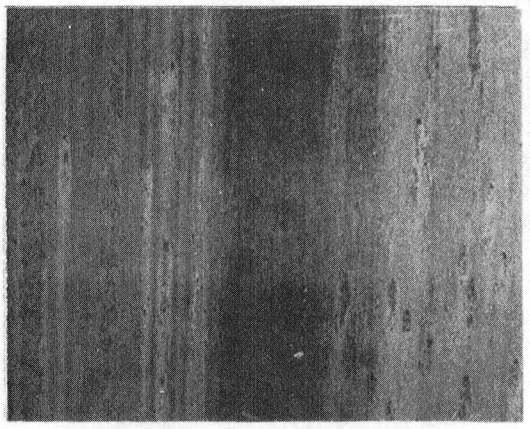

7X

Cr_3C_2 ON JOURNAL

(a)

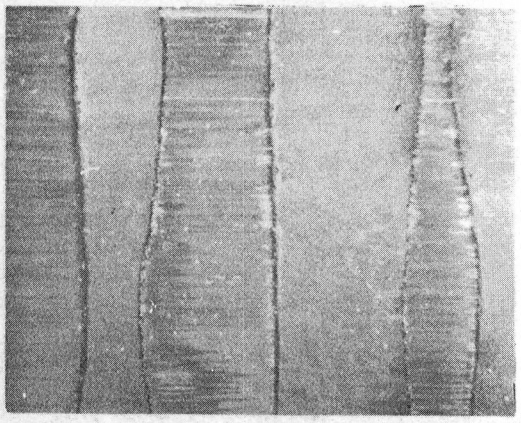

7X

$Ni-Cr-Cr_2O_3$ ON FOIL

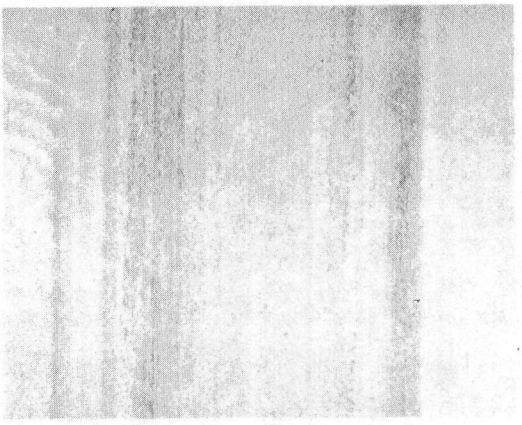

7X

Cr_3C_2 ON JOURNAL

(b)

Fig. IV.22 Photographs of Surfaces After Test at 650°C, IT and RT (a. Test No. 20, b. Test No. 22)

793267

The next test (No. 24) consisted of sputtered Cr_2O_3 on the journal and on the foil. The journal coating was significantly worn after 3000 cycles. The test was discontinued. This test was repeated (No. 25) and the same results were obtained. Adhesion tests and crude abrasion tests on the journal coating indicated the coating was well bonded. This lack of coating life could be due to the following variations from the foil coating: (a) the journal could not be pre-cleaned because a rotating feed through is not capable of sputter-etching in our system, (b) substrate has been changed to A286, and (c) the A286 journal has to be heat treated at 980°C; this temperature is too high for the coating because it can build up some scaling. Therefore, the journal was coated after it had been heat treated. Note that the best results were obtained with Inconel foil coated in the annealed condition, (d) the spacing between the top of the journal and the target had to be changed to 50.8 mm from 41.3 mm (for Inco foil work) due to machine limitations.

Partial Arc Bearing Tests at 35kPa (5 psi) Loading

The most promising coating combinations at 14kPa loading were: sputtered Cr_2O_3 versus detonation gun Cr_3C_2 (Test No. 6) and air sprayed CdO-graphite-Ag versus detonation gun Cr_3C_2 (Test No. 11). These coating combinations were further tested at 35kPa (5 psi) loading. The test results are shown in Table IV.4. Initially, the coatings were tested at 14kPa for 100 cycles, then the load was increased to 35kPa.

After 3000 cycles, the sputtered Cr_2O_3 coating on the foil in (Test No. 23) was significantly worn and the journal coating was unchanged. The friction was up high and the test was discontinued. The photographs of bearing surfaces after the test are shown in Figure IV.23. It is concluded that the coating combination can function a maximum of 3000 start/stops and further development is needed for improved life.

After 500 cycles each at RT, HT, and IT, the CdO-graphite-Ag coating on the foil (Test No. 27) was worn in the loaded zone and the journal was polished and shiny. The friction coefficient also went up about 35%. After the next 1500 cycles, the initial foil coating was completely worn in the loaded zone but had a light transfer of lubricant film. The journal

TABLE IV.4

START-STOP TEST RESULTS OF COATING COMBINATIONS

Partial Arc Bearings

Load = 34.5 kPa (5 psi) Based on Bearing Projected Area

Test No.	Foil and Journal Coatings	Max. Test Temp. °C(°F)	Friction Coefficient						Surface Roughness of Journal μm (μin.)		Comments
			At Start	After 499 Cycles	After 999 Cycles	After 1499 Cycles	After 2999 Cycles	After 4500 Cycles	Before	After	
23**	Sputtered Cr_2O_3 (Run #50) versus Det. Gun Cr_3C_2	650 (1200)	S[1] 0.19				0.66		0.13 (5)	0.13 (5)	500 cycles each at HT, IT, and RT-coating on foil worn over bumps in loaded zone. After next 1500 cycles coating on foil worn significantly in the loaded zone, journal unchanged, Rated - Marginal.
			D[2] 0.49	0.59	0.86	0.98	0.95				
			K[3] 0.42	0.50		0.95	0.95				
27*	Air sprayed CdO-graphite-Ag† versus Det. Gun Cr_3C_2	427 (800)	S 0.19			0.27	0.41	0.41	0.11 (4.5)	0.31 (12)	500 cycles each at RT, HT and IT-journal polished and shiny, foil worn in the loaded zone. After next 1500 cycles-initial coating completely worn in the loaded zone, but had coating transfer, journal same. After 4500 cycles - foil coating completely worn. Rated - Marginal.
			D 0.29	0.35	0.38	0.38	0.50	0.71			
			K 0.29	0.35	0.41	0.41	0.47	0.80			

* Test Cycle Sequence - 500 RT, 500 HT, 500 IT, repeated

**Test Cycle Sequence - 500 HT, 500 IT, 500 RT, repeated

† This run was made with fine silver powder.

1 - Static Breakaway at RT

2 - Dynamic Breakaway at Test Temperature

3 - Kinetic at Test Temperature

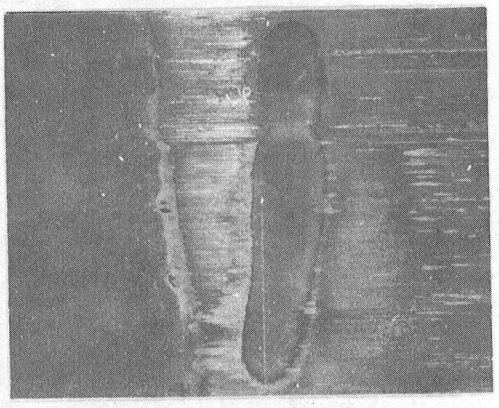

7X

Cr_2O_3 ON FOIL

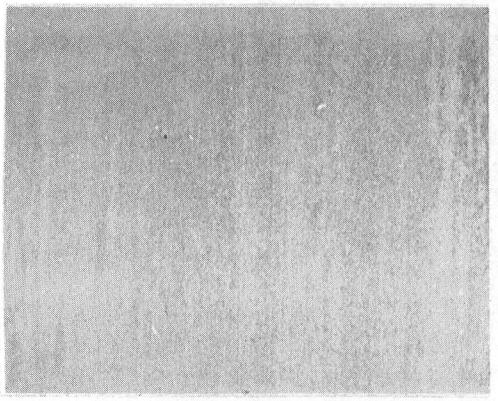

7X

Cr_3C_2 ON JOURNAL

(a)

7X

CdO-GRAPHITE-Ag ON FOIL

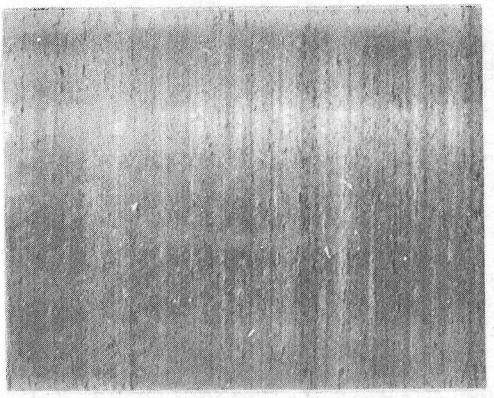

7X

Cr_3C_2 ON JOURNAL

(b)

Fig. IV.23 Photographs of Surfaces After Test at a Load of 34.5 kPa (a. Test 23, b. Test 27)

793265

was unchanged. The coefficient of friction went up indicating loss of lubricant film. It was believed that this was the end of the useful life of the coating. However, the tests were continued to determine the limit of the coating. In another 1500 cycles, the foil coating was completely worn and the journal looked the same. The friction coefficient went up drastically by more than a factor of two. The test was discontinued after 4500 cycles. The photographs of the bearing surfaces after the test are shown in Figure IV.23. It is concluded that the CdO-graphite-Ag coating has a useful life of 3000 start/stops.

Full Bearing Tests at 14kPa (2 psi) Loading

The successful coating combination, sputtered Cr_2O_3 versus detonation gun Cr_3C_2, was tested in a full bearing to examine if wear debris would give any problem because ejection of wear debris is more difficult from full bearings than from partial arc bearing. This combination was tested in a full bearing with hot air flowing through it. The results are reported in Table IV.5. After 3000 cycles, the bearing was taken apart and there was polishing over the bumps on the outer edges. No worn spots were apparent. After a total of 9000 start/stops, the foil coating was polished over bumps and a few spots were worn. The journal coating was unchanged. The photographs of the bearing surfaces after the test are shown in Figure IV.24. The friction again was low at HT and high at a low temperature. The curve for friction versus cycles is shown in Figure IV.25.

Worn spots could be detected by measuring the resistance across the foil. Since the coating is an insulator, the coating area measures ∞ resistance and worn area would have a very low number. If a thin layer of coating is present, it will measure a moderate value of resistance.

After a successful test at 650°C, a question was raised if the coating would work as well at a maximum temperature of 427°C which possibly may be the maximum temperature in some engines instead of 650°C. A test was conducted to measure friction at RT to 650°C in number of steps. The data are plotted in Figure IV.26. The friction at 427°C is not significantly higher than that at 650°C; and it was believed that the bearing should perform reasonably well in tests at a maximum temperature of 427°C.

TABLE IV.5

START-STOP TEST RESULTS OF COATING COMBINATIONS

Full Bearings

Load = 14 kPa (2 psi) based on bearing projected area

Test No.	Foil and Journal Coatings	Max. Test Temp. °C(°F)	Friction Coefficient						Surface Roughness of Journal μm (μin.)		Comments
			At Start	After 499 Cycles	After 999 Cycles	After 1499 Cycles	After 5999 Cycles	After 9000 Cycles	Before	After	
28**	Sputtered Cr_2O_3 (Run #51) versus Det. Gun Cr_3C_2	650 (1200)	S[1] 0.22					0.88	(0.051) (2)	(0.076) (3)	1000 cycles each at HT, IT and RT - coating polished over bumps on outer edges. After next 6000 cycles, coating deeply polished over bumps and few spots were completely worn. Journal polished slightly. Rated - successful
			D[2] 0.37	0.37	0.59	0.66	0.88	0.81			
			K[3] 0.37	0.37	0.59	0.66	0.88	0.81			
29**	Sputtered Cr_2O_3 (Run #55) versus Det. Gun Cr_3C_2	427 (800)	S 0.24					0.92	(0.102) (4)	(0.127) (5)	3000 cycles each at HT, IT and RT - coating polished over about eight bumps only part of the way. Journal virtually unchanged. Rated - successful
			D 0.41	0.41	0.59	0.77	0.77	0.81			
			K 0.41	0.41	0.59	0.77	0.77	0.81			

**Test Cycle Sequence - 500 HT, 500 IT, 500 RT, repeated

1 - Static Breakaway at RT

2 - Dynamic Breakaway at Test Temperature

3 - Kinetic at Test Temperature

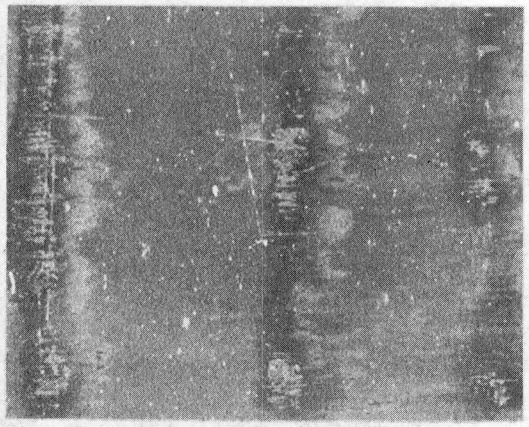

7X

Cr_2O_3 ON FOIL

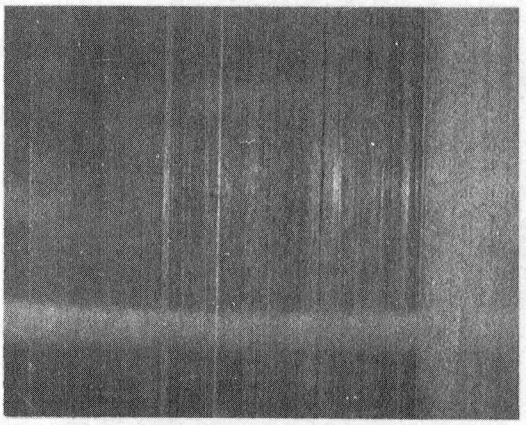

7X

Cr_3C_2 ON JOURNAL

MAX. TEST TEMPERATURE = 650°C

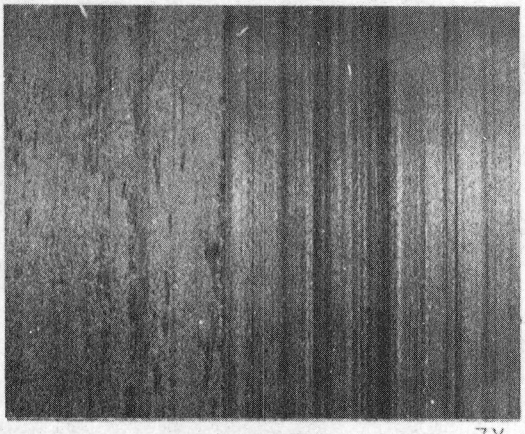

7X

Cr_2O_3 ON FOIL

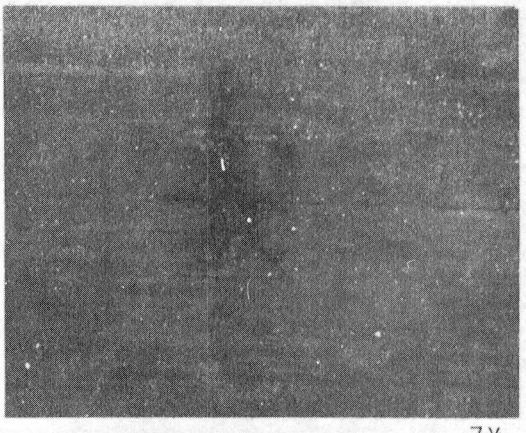

7X

Cr_3C_2 ON JOURNAL

MAX. TEST TEMPERATURE = 427°C

Fig. IV.24 Photographs of Surfaces After Full Bearing Test for 3000 Cycles Each at Max. Temperature, IT and RT

793268

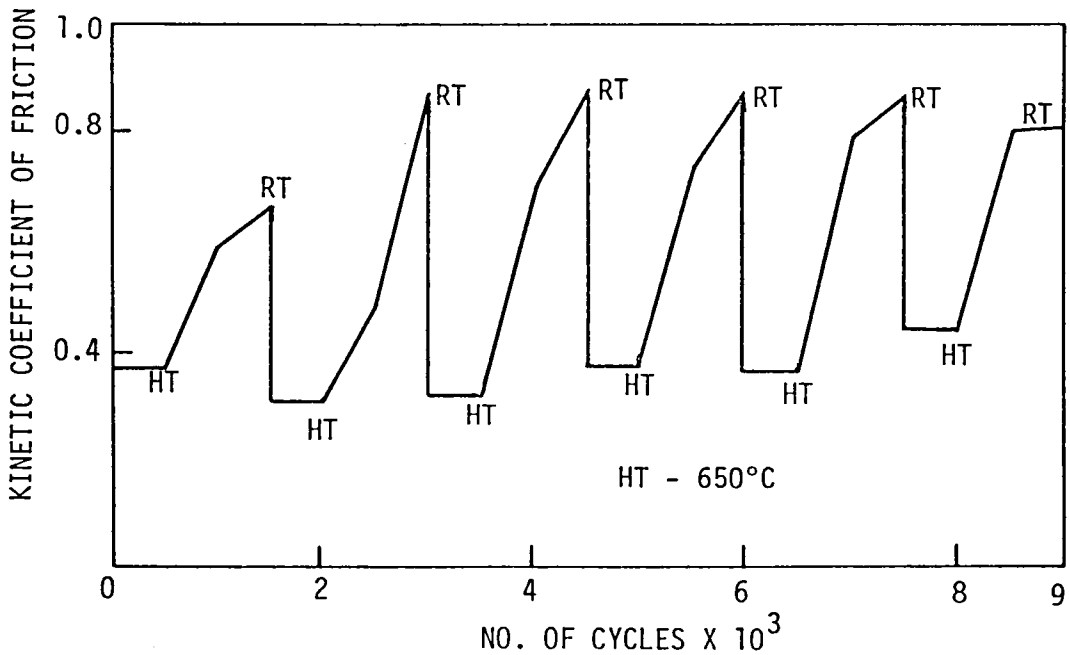

Fig. IV.25 Kinetic Friction at Test Temperature versus Number of Cycles for Cr_2O_3 Sputtered on Foil versus Det. Gun Cr_3C_2 on Journal (full bearing tests - test No. 28)

793296

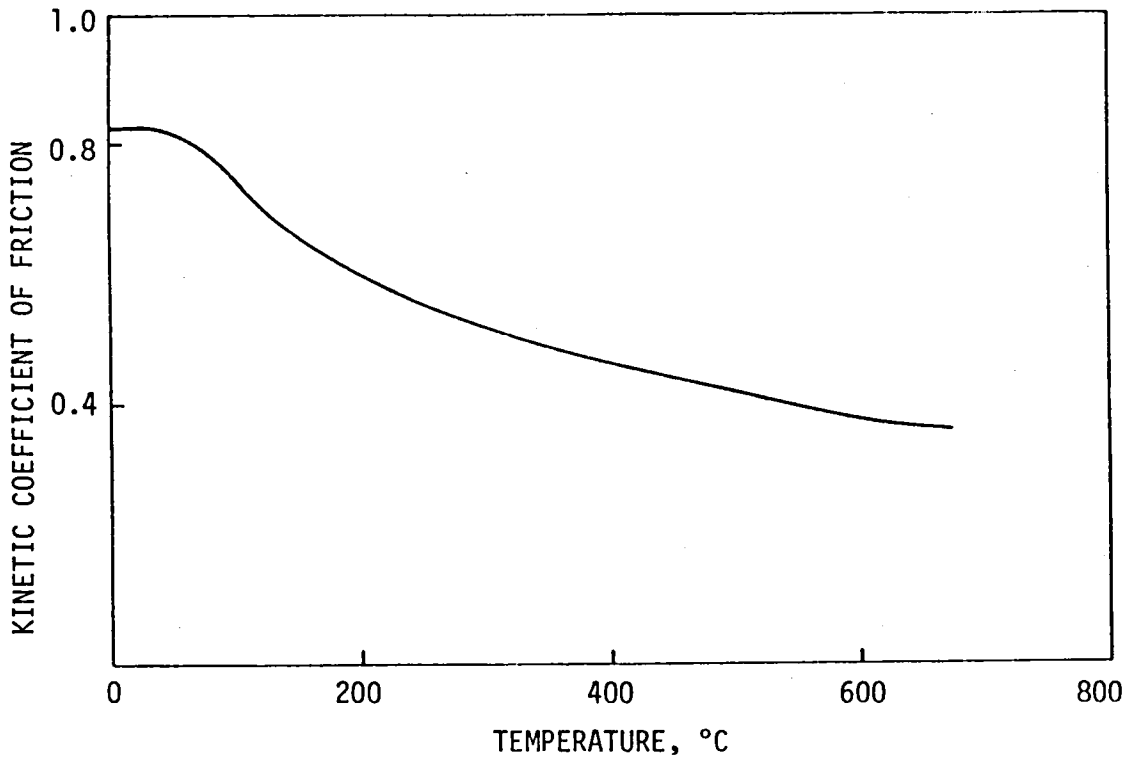

Fig. IV.26 Kinetic Friction versus Temperature for Cr_2O_3 (sp.) Coating on Foil versus Det. Gun Cr_3C_2 on Journal (Test No. 28)

793295

The next test was conducted at 427°C IT and RT, and the results are shown in Table IV.5. The coating wear and polishing in this case was less than that of Test No. 28 at 650°C. The photographs of the bearing surfaces after the test are shown in Figure IV.24. The coating successfully completed 9000 start/stops and this could have experienced many more cycles since the friction pattern was unchanged during testing (Figure IV.27).

HIGH SPEED RUB TESTS

Shock Load-Acceleration Calibration

The shock load-acceleration data were obtained at room temperature. An accelerometer was mounted underneath the pan close to the centre point. The load was applied when either the shaft was stationary or running at 30,000 rpm with an air turbine drive. Load-acceleration data are presented in Table IV.6. A shock up to 101 g could be generated. Representative acceleration-time pictures are shown in Figure IV.28. The anticipated g's level in the engine mounted in a vehicle is only six.

Contact Measurement During Shock Loading

Using the technique described earlier, the number of contacts between the bearing and the journal were measured during the shock test. An electrically-conductive coating combination CdO-graphite-Ag on the foil versus Linde Cr_3C_2 on the journal was used. This technique was first used to measure the number of contacts during normal start/stops. Under a 14kPa (2 psi) loading, there were from 5000 to 30,000 counts or contacts* in each start/stop when the cut off resistance was 12,000 Ω. When the cut off resistance was changed to 1000 Ω, there were only 2 to 4 contacts during each start/stop cycle. It shows that the majority of the contacts are very minute and there are few severe rubs.

A bearing running at 30,000 rpm under steady-state condition, started making microscopic contact under a normal load of 28kPa (4 psi). At the load slightly above 28kPa, there were about 1000 contacts per second or two contacts/revolution (at cut-off resistance of 12,000 Ω). At cut-off

*A contact was registered at an instance when the resistance between the bearing and the shaft changed from a value greater than the selected cut-off resistance to a value less than the cut-off resistance.

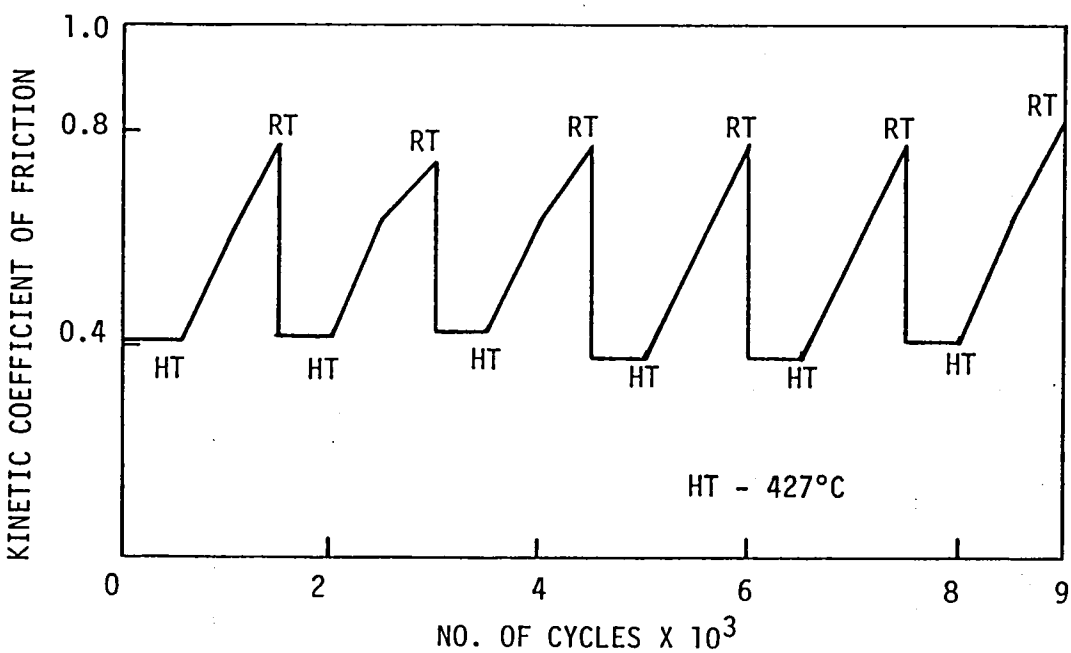

Fig. IV.27 Kinetic Friction at Test Temperature versus Number of Cycles for Cr_2O_3 (sp.) on Foil versus Det. Gun Cr_3C_2 on Journal (Full Bearing Test No. 29)

793294

TABLE IV.6

LOAD - ACCELERATION (g's) DATA FOR HIGH-SPEED RUB TEST APPARATUS

Load N(lb)	Height mm (in.)	Stationary/Running	g's
4.5(1)	25(1)	Stationary	5
		Running	6
4.5(1)	50(2)	Stationary	12
		Running	12
13.4(3)	25(1)	Running	15
22.3(5)	25(1)	Stationary	21
22.3(5)	50(2)	Running	27
31.2(7)	50(2)	Running	40
40.1(9)	50(2)	Running	45
48.9(11)	25(1)	Running	64
48.9(11)	50(2)	Running	101

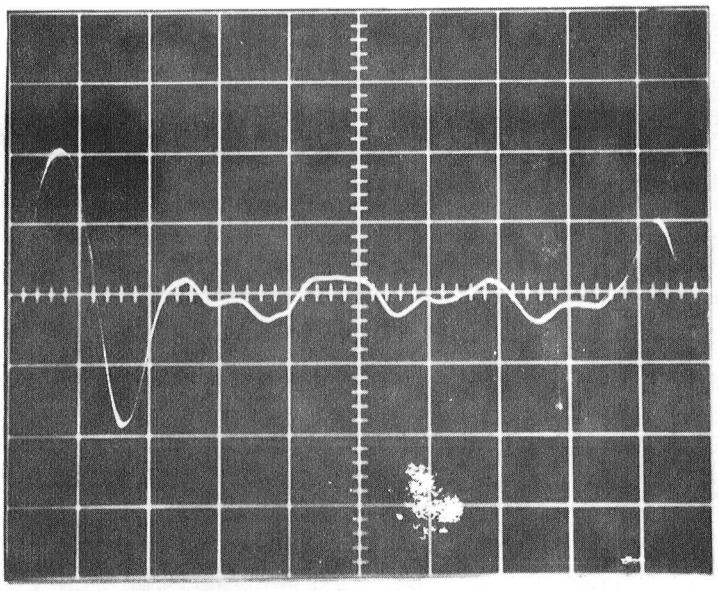

LOAD 13.4N
HEIGHT = 25 mm
SWEEP 5 ms/cm
VERTICAL MAG: 0.1V/cm;
18.8 mV/c

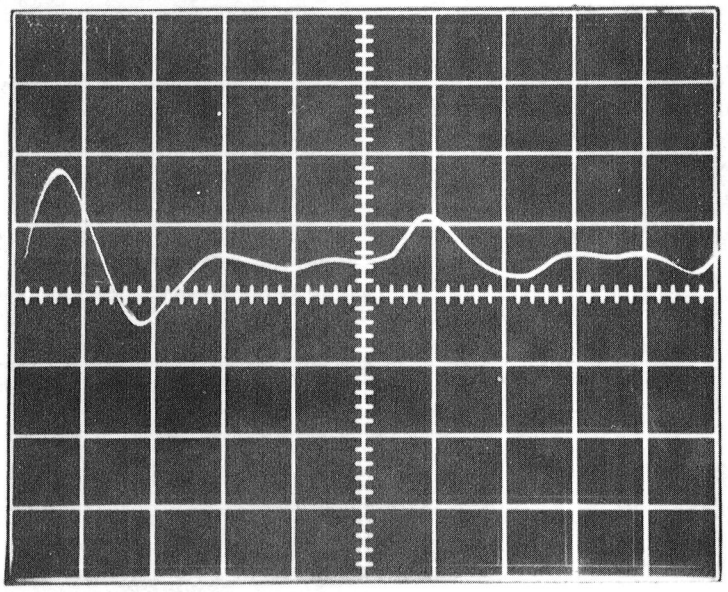

22.3 N x 50 mm
0.5V/cm

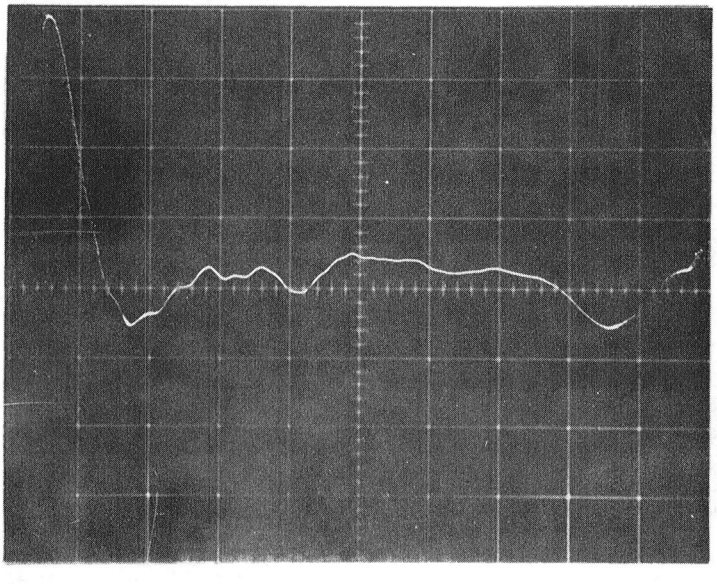

48 N x 50 mm
0.5V/cm

Fig. IV.28 Typical Oscilloscope Traces for Shock Load Calibration

793269

resistance of 1000 Ω, there were no contacts up to 55kPa (8 psi) tested. It shows that there probably would be no large contacts up to at least 55kPa (8 psi), but microscopic contacts occur under loads as low as 28kPa. These contacts result from vibration of the bearings and bearings having no hydrodynamic air pressure at the ends. In a real application, the bearing is rigid so fewer contacts are expected.

Next the shock load was applied. It was found that 4.5N dropped from 25 mm height gave about 40 to 100 contacts when the cut off resistance was 12,000 Ω. The number of contacts increased with increase in shock. If the cut off resistance was reduced to 1000 Ω, no contacts were observed even at 40.1N (9 lbs.) dropped from 50 mm height. Again it is observed that shock produces only microscopic contacts. Even the mildest shock produces microscopic contacts.

Test Procedure

The shaft was run at 30,000 rpm and the bearing assembly was heated to the maximum temperature of the coating. The following load sequence was used; loading was stopped if the bearing did not perform satisfactorily.

a. Impact the bearing against journal fifty times by dropping a 4.5N(1 lb.) weight from a height of 25 mm (1 in.) against the elastomer on top of the vertical steel rod which is coupled to the bearing housing.

b. Impact the bearing twenty times by dropping a 13.4N (3 lb.) weight from a height of 25 mm (1 in.).

c. Impact twenty times by dropping a 13.4N (3 lb.) weight from a height of 50 mm (2 in.).

d. Impact twenty times by dropping a 22.3N (5 lb.) weight from a height of 50 mm (2 in.).

e. Impact ten times by dropping a 31.2N (7 lb.) weight from a height of 50 mm (2 in.).

f. Impact ten times by a 40.1N (9 lb.) weight from a height of 50 mm (2 in.).

g. Stop the test, cool the rig, and examine and photograph the bearing surfaces.

h. Reassemble the bearing in the rig and run the bearing at room temperature at a shaft speed of 30,000 rpm to check the performance.

i. Heat the test rig to the maximum temperature.

j. Impact ten times by 48.9N (11 lb.) weight from a height of 50 mm (2 in.).

k. Impact ten times by 48.9N (11 lb.) weight from a height of 75 mm (3 in.).

l. Stop the test, cool the rig, and examine and photograph the bearing surfaces.

Severe shocks were repeated fewer times because an engine in practice would experience fewer of them.

The anticipated g level in the engine mounted in a vehicle is 6 g, but the testing was performed up to a level of 100 g's which corresponded to the eleven-pound load test (j). Bumps in the bump foil flattened at this load and further testing was stopped.

Results and Discussions

CdO-graphite-Ag on foil versus detonation gun Cr_3C_2 coating combination was tested at 427°C according to the load sequence presented earlier. The journal was reground in house, therefore, it was slightly rougher than the ones supplied by the vendor. The bumps were flattened at step (j) - 48.9N load X 50 mm so the testing was stopped. This represented a shock of about 100 g. The coating was very lightly polished over the bumps and there was minute wear over two bumps. No temperature increase during the shock was monitored by the thermocouple mounted in the bearing. The journal coating was virtually unchanged. The photographs of the bearing surfaces after the test and Talysurf traces of journal before and after the test are shown in Figures IV.29 and IV.30, respectively. The coatings were serviceable and would have taken higher levels of g. The results are tabulated in Table IV.7.

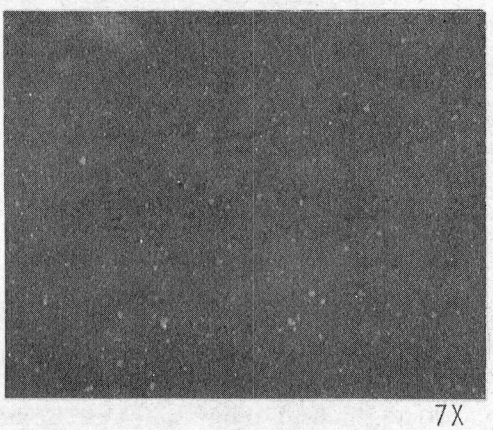

7X

CdO-GRAPHITE-Ag ON FOIL

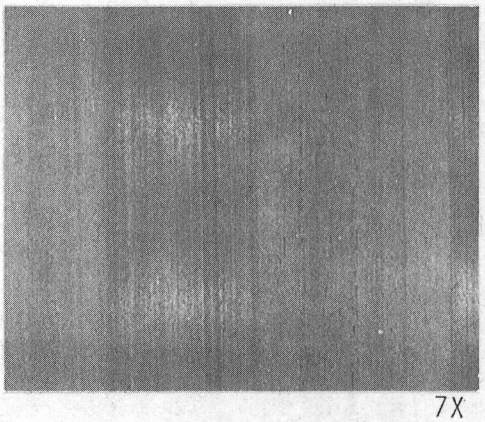

7X

Cr_3C_2 ON JOURNAL

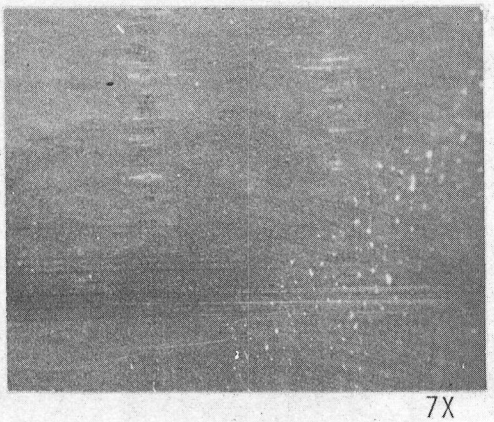

7X

Cr_2O_3 ON FOIL

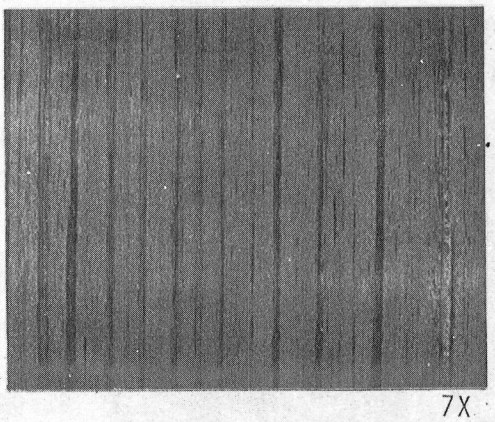

7X

Cr_3C_2 ON JOURNAL

Fig. IV.29 Photographs of Surfaces After High Speed Rub Tests (Tests Nos. 30 and 31)

793270

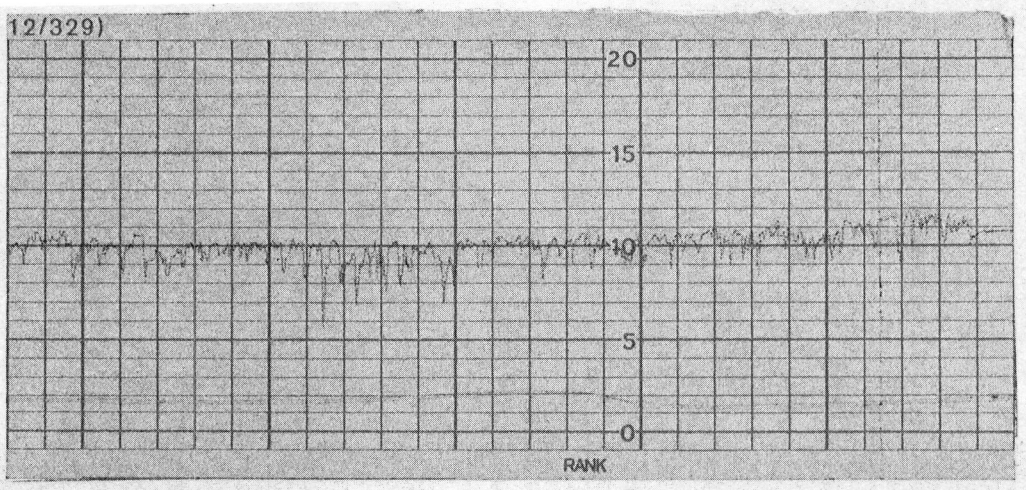

BEFORE TEST

CLA = 0.15μm (6μin.)

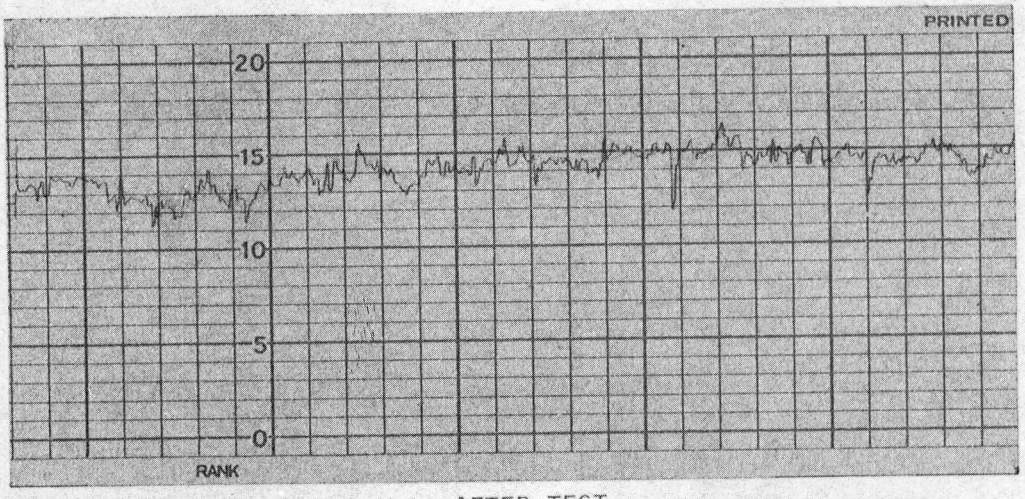

AFTER TEST

CLA = 0.15μm (6μin.)

VERTICAL MAG.: EACH SMALL DIV. = 0.25μm

HORIZONTAL MAG.: EACH SMALL DIV. = 250μm

Fig. IV.30 Talysurf Traces of Det. Gun Cr_3C_2 Coated Journal Tested Under Shock Load Against CdO-Graphite-Ag Coated Foil Bearing (Test 30)

793263

TABLE IV.7

HIGH SPEED RUB TEST DATA

Full Bearings

Steady State Load = 14 kPa (2 psi)
Speed = 30,000 rpm

Test No.	Foil and Journal Coating	Maximum Test Temp. °C	Breakaway Friction Coefficient		Surface Roughness of Journal μm (μin.)		Results
			At Start	At Stop	Before	After	
30	Air Sprayed CdO-Graphite-Ag versus Det. Gun Cr_3C_2	427	0.18	0.20	0.15 (6)	0.15 (6)	Completed test sequence with a maximum load of 49 N producing 100 g. There was no ambient temperature change during shocks. Some uniform polishing of foil coating over bumps. Coating serviceable. Rated - Successful.
31	Sputtered Cr_2O_3 (Run #56) versus Det. Gun Cr_3C_2	650	0.24	0.78	0.15 (6)	0.36 (14)	Completed test sequence with a maximum load of 49N producing 100 g. Temperature increased during a shock of more than 22.3N x 50 mm; duration of temperature rise < 0.4s. Polishing of foil coating over bumps, some bare spots. Journal coating lightly worn. Rated - Successful.

The next test (No. 31) consisted of sputtered Cr_2O_3 on foil against detonation gun Cr_3C_2 on journal (Test No. 31, Table IV.7). The test was again conducted up to step (j), i.e. 48.9N X 50 mm. The bearing was taken apart after step (f), i.e., after loading by 40.1N X 50 mm. The foil coating had some polishing over the bumps, but there was no visible wear.

After additional testing to step (j) (48.9N X 50 mm), there was some wear of the foil coating, but most of the coating was virtually unchanged. The polishing of the bump in shock tests was much more pronounced than in start/stop tests. Journal coating was worn and its surface became rougher. The photographs of the bearing surfaces after the test and Talysurf traces of the journal before and after tests are shown in Figures IV.29 and IV. 31.

During tests at a load of 22.3N X 50 mm there was a temperature increase recorded of about $5^{o}C$ during shock. The duration of the temperature rise was one count of instrument (it scans 2.5 times per second). At the maximum shock of 48.9N X 50 mm there was a temperature increase of about $20^{o}C$ for one count of instrument.

The coating would have taken more shocks since the bearing bumps did not deform. Both tests were rated very successful.

Why Does Cr_2O_3-Cr_3C_2 Work?

The results obtained with chrome oxide coating that were sputtered on Inconel X-750 foil, rubbing against nickel-chrome (80-20) bonded chrome carbide applied by detonation gun on A286 journal indicate that oxidation of the substrate, or of the coated surface or complex oxide formation, is also influencing the performance of the bearings. A characteristic pattern of friction versus temperature was obtained. Typical data illustrating this pattern are shown in Figures IV.18, IV.25, IV.26, and IV.27. The results show that the lowest coefficients of friction (0.3-0.4) were obtained at $650^{o}C$. When the test was cooled to an intermediate temperature or to room ambient, there was marked rise in friction to values of 0.6 to 0.8. Each time the test temperature was cycled from hot to cold: this frictional pattern was repeated.

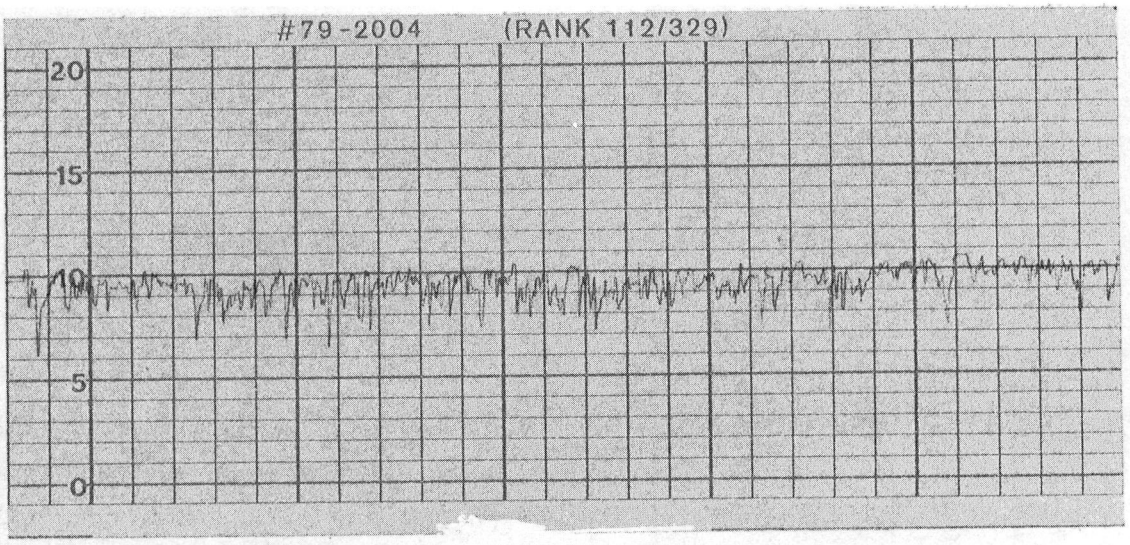

BEFORE TEST

CLA = 0.15μm (6μin.)

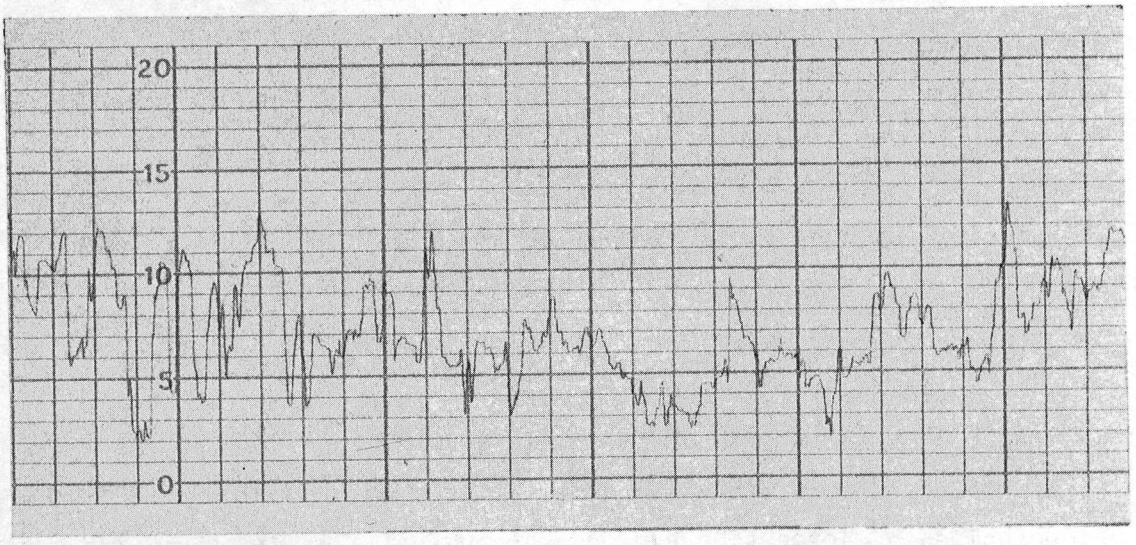

AFTER TEST

CLA = 0.36μm (14μin.)

VERTICAL MAG.: EACH SMALL DIV. = 0.25μm
HORIZONTAL MAG.: EACH SMALL DIV. = 250μm

Fig. IV.31 Talysurf Traces of Det. Gun Cr_3C_2 Coated Journal Tested Under Shock Load Against Sputtered Cr_2O_3 on Foil Bearing (Test No. 31)

793262

Similar results were reported by Peterson et. al. [4.2] in a study of the effect of temperature on the slow speed sliding behavior of certain metals and superalloys. Figure IV.32,which was taken from this reference, shows the frictional characteristics on Inconel X (70% Ni, 15% Cr) sliding on Inconel X and nickel sliding on nickel at various temperatures. As the sliding specimens were heated, the coefficient of friction increased slightly to a maximum value of about 0.85. At a temperature of about 704°C (1300°F), the coefficient of friction suddenly decreased to about 0.35. During the cooling cycle, the coefficient of friction remained low until a temperature of about 540°C (1000°F) has been reached. Below this temperature level, the friction increased rapidly to a value of about 0.8. Surface damage, in the form of numerous small welds, was also observed on the specimens that were run at the lower temperatures while the tests run at high temperature resulted in an oxidized area of contact that was smooth and polished. It should be noted that the temperature at which these frictional changes occurred were both load and time dependent. The use of lower loads or longer sliding times reduced the transition temperature. For example, a 30-hour run at 540°C (1000°F) also resulted in low friction.

There is substantial evidence to show that this effect of temperature on friction is due to the formation of oxide films on the sliding surfaces. At low temperatures, the friction is characteristic of rubbing coating surfaces or bare metal sliding on bare metal in the case of coating failure. When a certain transition temperature is reached, where the oxide film (could be eutectic or other complex oxides) is being replenished as rapidly as it is worn away, smooth sliding performance is obtained.

Table IV.8, which was taken from Peterson et. al. [4.2], shows the characteristic transition temperatures for several pure metals. When these metals are used as major alloying ingredients, various complex oxide films can be formed; some of which are even more effective than the single oxides [2.18]. Molybdenum, as an alloying element, is particularly effective since it forms soft protective molybdates with transition temperatures of about 427°C (800°F).

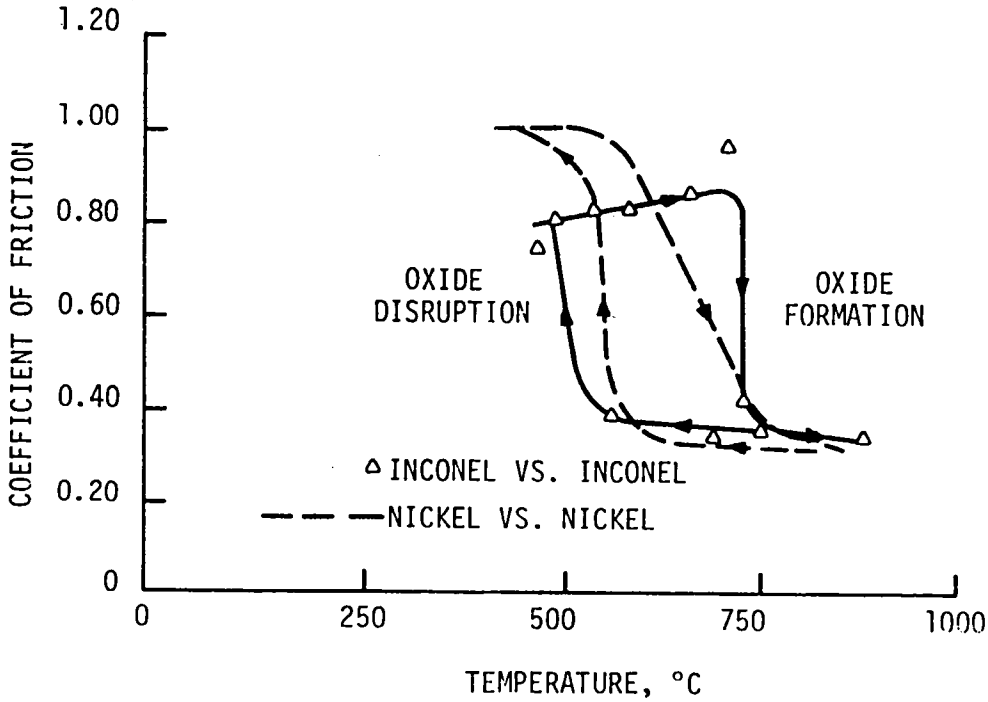

Fig. IV.32 Effect of Temperature on the Coefficient of Friction for Various Material Combinations during Material Cycling. Load, 1881g; velocity, 0.0076 $m.s^{-1}$

793303

TABLE IV.8

TRANSITION TEMPERATURES AND TYPICAL COEFFICIENTS OF FRICTION FOR SOME PURE METALS

Metal	$f<T_t$ (°C)	T_t (°C)	$f>T_t$ (°C)
Fe	0.98	38-93	0.45
Cu	0.78-1.4	204-260	0.50-0.70
Ni	0.92	650-760	0.22
Mo	1.0	427-482	0.28
Cr	0.50-0.60	427-593	0.28-0.32

In the foil bearing material evaluations described in this report, the results obtained with the sputtered chrome oxide coating also seem to be strongly influenced by oxidation effects. It should be noted that in these tests the coated specimens were preheated to 650°C (1200°F) before the first 500 start/stop cycles at 650°C were run. Experience had shown that preheating the specimens and running some start/stops at high temperature first generally had a very beneficial effect on performance. After this high temperature run, 500 start/stop cycles were run at an intermediate temperature and 500 cycles at room temperature. This temperature sequence was repeated until the required number of start/stop cycles had been achieved.

One major advantage of running some cycles at high temperatures first is that oxidation of the bearing surfaces during testing replenishes oxide layers continuously (reactive replenishment) where the coating has failed. This may be especially important during the run-in period. The foil bearings are compliant and there would be some microscopic high spots in the bearing from manufacturing which would experience extremely high loads and, the coating would probably wear. Continuous high temperature oxidation would replenish the oxide layer and prevent any catastrophic coating failure.

Since the sputtered chrome oxide was already in the most stable oxidation state, the oxidation that took place during heating (there is additional localized heating due to frictional energy) must have been oxidation of the substrate which in every case contained chrome and nickel as major alloying elements. These oxides probably diffused out into the coating. Even the detonation gun chrome carbide coating had a significant amount of chrome and nickel as the binder for the carbide. There could also be either eutectic or other complex oxide formation from interaction of bearing surfaces at high temperatures, which generally has low friction. The sputtered chrome oxide coating must still have been functioning on the surfaces in spite of replenishment oxidation. If this coating had been removed, severe welding and surface damage would have taken place when the bearing was run at intermediate or low temperatures where the oxide film was not effective. Running a bare Inconel X-750 foil against a bare A286 stainless journal would result in almost immediate

failure (see Test No. 4, Table IV.3). It should be noted that Ni-Cr bonded Cr_3C_2 has the beneficial ability to form surface oxides at high temperature (due to presence of Ni and Cr) and as well as providing a hard substrate (Cr_3C_2 is harder than Cr_2O_3).

The following tentative conclusions can be drawn from the results of these tests:

a) Sputtered chrome oxide is effective in preventing damage to the surfaces of the foil bearings over a wide temperature range, from 20°C to 650°C.

b) At 650°C, protective oxide films are formed, apparently by oxidation of the substrate alloys. These oxides significantly reduce the coefficient of friction.

c) In spite of the oxidation that occurs at 650°C, the sputtered chrome oxide films continue to protect the surfaces at lower temperatures where the oxide films cannot be replenished after they have been worn away.

V. CONCLUSIONS AND RECOMMENDATIONS

The most promising coating combinations found in this program to withstand start-stop cycles in a 427°-650°C (800°-1200°F) environment for an air-lubricated compliant journal bearing, are listed below:

Foil Coating	Journal Coating	Maximum Test Temperature °C (°F)
CdO-Graphite-Ag (HL-800-2) 8-10 μm thick	Det. Gun and Ground Ni-Cr bonded Cr_3C_2 60-90 μm thick	427 (800)
Sputtered Cr_2O_3 1 μm thick	Det. Gun and Ground Ni-Cr-bonded Cr_3C_2 60-90 μm thick	650 (1200) and 427 (800)

The combinations listed above have completed a total 9000 start-stop cycles (this represents useful engine life) each, consisting of 3000 cycles at the maximum test temperature, 3000 cycles at the intermediate temperature and 3000 cycles at the room temperature at a normal load of 14 kPa (2 psi) in partial arc bearing tests. Cr_2O_3 vs Cr_3C_2 coating combination was further successfully tested in full bearing tests to ensure that any wear debris generated would not give any problem. This coating combination has also been successfully tested for a total of 9000 start-stop cycles at a maximum test temperature of 427°C (800°F).

Both the coatings were also tested during start-stop cycles at a higher normal load of 35 kPa (5 psi) loading. The coatings were able to survive for 3000 start-stop cycles at this load.

Finally both the coatings were tested under shock loading with the journal running at 30,000 rpm. Contact resistance measurement between the bearing and the rotating journal verified that each shock level provided micro-contacts during shock application. Both the coatings survived 100 g's of impact and further testing was terminated because the foil bumps deformed at this loading level. It should be noted that the anticipated g level in the automotive gas turbine engine is six so we have far exceeded the requirements.

Hence the two coating combinations mentioned here can satisfy the functional requirements.

SPECIFIC CONCLUSIONS

Sputtered Cr_2O_3 Coating

This coating system was developed at MTI. We find that each coating system has to be optimized for best adherence. A parametric study provided an optimum Cr_2O_3. Low pressure in the sputtering system, high power, and water-cooled substrate improve the coating adhesion and its smoothness. Bias coatings were not as adherent (had residual stress) as the sputter-deposited coatings. One reason could be the absence in bias coatings of naturally occurring oxide layer present in the interface which may be responsible for increased adhesion. The cleanliness of the substrate, target, and the system was extremely crucial. The hardness of the substrate had an influence on the coating adherence. Inconel X-750 foil coated in the annealed condition and heat treated provided the optimum adherence. X-ray diffraction analysis showed that the applied coating was Cr_2O_3. The optimum thickness of the coating was found to be 1 μm.

The optimized sputtering parameters for Cr_2O_3 coating in our sputtering system were the following:

Spacing (mm)	Power (Watts)	Chamber P_r (microns)	Bias Sputter	Water-Cooled Substrate	Thickness (μm)(μin.)
41.3	390	6	No	Yes	1.02 (40)

The adhesion strength (in tension) of this coating was more than 68.9 MPa (10 ksi).

Sputtered Metallic Bonded and Multilayered Cr_2O_3 Coatings

Ni-Cr bonded Cr_2O_3 was found to have improved ductility as indicated by the bend tests. The coating did not perform very well during start-stop tests. Scratch tests indicated that the scratch resistance due to metallic binder addition did not change.

More work is needed to optimize sputtering parameters, its constituents and the coating thickness.

Sputtered Cr_3C_2 Coating

The coating applied using optimized parameters for Cr_2O_3 was highly stressed and additional work is needed. This demonstrates that parameters which were optimum for Cr_2O_3 are not necessarily right for Cr_3C_2.

CdO-Graphite-Ag (HL-800-2) Coating

A very fine silver grade was needed to obtain a uniformly dispersed coating and fine silver would not pull off easily during burnishing and the sliding. The coating has performed very well when tested against det. gun Cr_3C_2 and the wear has been less than a coating of Cdo-graphite without silver.

The CdO-graphite coating combination did not perform well when tested against itself at a maximum temperature of 427°C. However, elsewhere [4.1] it has been reported that coating performs better at 274°C when tested against itself. The reason is that when the coating combination has the CdO-graphite on both members, coupled thermal conductivity goes down thereby increasing the interface temperature. At 274°C, the total surface temperature probably remains below the temperature limit of CdO-graphite ($\sim$427°C).

PbO-SiO_2-Ag Coatings

The coating softens at a low temperature ($\sim$260°C) and thus is not suitable for the high temperature.

NASA PS Coatings

The coatings generally were quite porous. The high friction during sliding and relatively low hardness of the coating was responsible for the poor result.

Kaman DES Coating

The coating received in this program was very rough and our experience indicates that the coatings in dry lubrication have to be smooth in order to work satisfactorily.

Evaporated TiC and HfN Coatings

The coatings as applied were stressed, and means to reduce this were not too fruitful. The coatings also did not survive static oven tests at 540°C This temperature was high from an oxidation standpoint. ARE (activated reactive evaporation) technique is very attractive as it has high deposition rates and thick coatings can be applied with little loss in adhesion.

RECOMMENDATIONS FOR FUTURE RESEARCH

The successful Cr_2O_3 should be tested at room temperature without testing at high temperature first as done here to determine its suitability for low temperature applications. More work is needed to develop parameters to successfully apply Cr_2O_3 coating on A286 journals. Constituents and quantity of the metallic binders (e. g. Ni-Cr, and Co) should be tried to develop an adherent coating with improved ductility and minimal loss in the hardness.

Based on the work reported in References [4.2] and [2.18], any combination of foil and journal materials which contained molybdenum as a major alloying ingredient would provide low friction over a wider temperature range. For example, if the Inconel X-750 foil was coated with sputtered chrome oxide and was run against a molybdenum bonded chrome carbide coating on the journal (instead of the nickel chrome bonded chrome carbide), then low friction values should persist over the range from about 370°C (700°F) to 650°C (1200°F). However, oxidation of the molybdenum at 650°C (1200°F) might be so rapid that the coating on the journal would have a relatively short life.

Further work is needed to optimize parameters including thickness of each layer for multi-layered coatings. A soft lubricant, e. g. MoS_2 may be tried as a top layer to provide some lubrication during the run-in period.

Further improvement of CdO-Graphite-Ag coating may be accomplished by trying different graphite grades (e. g. synthetic or natural), by varying coating variables (thickness, density mixtures, etc.) and by changing surface preparation.

More work on process optimization on the unsuccessful candidates is needed to improve further their performance. In particular, CaF_2 based coatings (e.g., PS120) should be further optimized in order to reduce their porosity and improve hardness. A list of coatings and process variables for future development is shown in Table V.1.

TABLE V.1

SELECTION OF COATING SYSTEMS AND PROCESS VARIABLES FOR FUTURE DEVELOPMENT

	Coating System	Development Source	Composition and Process Variables
1.	Sputtered Chrome Oxide	MTI	• Make following changes: Metallic binder, Co or Ni-Cr mixtures to improve ductility of the coating and to better match the thermal expansion; interlayer to improve adhesion; and overlay of MoS_2 or gold to provide run-in lubricant.
2.	Sputtered Chrome Carbide	MTI	• Same as above • Optimize following parameters: Power level/gas pressure/substrate bias/target precleaning/substrate etching/preoxidation.
3.	CaF_2 Based Coatings	NASA	• Develop compositions of plasma sprayed fluoride coatings. • Add self lubricating materials to reduce friction. • Develop techniques to reduce porosity.
4.	CdO-Graphite-Ag	MTI	• Surface preparation. • Try other graphite grades.
5.	Commercial Coatings	Vendor	• Develop coatings tailored to the application.

REFERENCES

1.1 Ruscitto, D., McCormick, J., and Gray, S., "Development of a Hydrodynamic Air Lubricated Compliant Surface Bearing for an Automotive Gas Turbine Engine Part I - Journal Bearing Performance," Report on NASA Contract NAS3-19427, NASA Report CR-135368, April 1978.

1.2 Bhushan, B., Ruscitto, D., and Gray, S., "Hydrodynamic Air Lubricated Compliant Surface Bearing for an Automotive Gas Turbine Engine II - Materials and Coatings," Report on NASA Contract NAS3-19427, NASA Report CR-135402, July 1978.

2.1 Bowden, F. P. and Tabor, D., Friction and Lubrication of Solids, 2nd Edition, Clarendon Press, England, 1954.

2.2 Bhushan, B. and Gray, S., "Static Evaluation of Surface Coatings for Compliant Gas Bearings in an Oxidizing Atmosphere to 650°C," Thin Solid Films, Vol. 53, No. 3, 1978, pp. 313-331.

2.3 Bhushan, B. and Gray, S., "Development of Surface Coatings for Air-Lubricated Compliant Journal Bearings to 650°C," ASLE Trans. (in press).

2.4 Murray, S. F., "Selection of Gas Bearing Materials," Design of Gas Bearings Vol. II Ed. D. F. Wilcock, Mechanical Technology Inc. Latham, NY, 1972.

2.5 Perrot, M., "Augmentation Des Facteurs De Reflexion Par Une Couche Protectrice," Revue D' Optique, Vol. 26, 1947, pp. 202-204.

2.6 Sharma, N. K., Williams, W. S., and Gottschall, R. J., "Investigation of the Interlayers Between Cemented Carbides and Titanium Carbide Coatings Obtained by Chemical Vapor Deposition," Thin Solid Films, Vol. 45, 1977, pp. 265-273.

2.7 Brainard, W.A., and Wheeler, D.R., "An XPS Study of the Adherence of Refractory Carbide, Silicide, and Boride RF-Sputtered Wear Resistant Coatings," J. Vac. Sci. Tech. Vol. 15, No. 6, 1978, pp. 1800-1805.

2.8 Bunshah, R. F., Shabaik, A. H., Nimmagadda, R., and Covy, J., Machining Studies on Coated High Speed Steel Tools," Thin Solid Films, Vol. 45, 1977, pp. 453-462.

2.9 Kodama, M., Shabaik, A. H., and Bunshah, R. F., "Machining Evaluation of Cemented Carbide Tools Coated with HfN and TiC by the Activated Reactive Evaporation Process," Thin Solid Films, Vol. 54, 1978, pp. 353-357.

2.10 Engineering Properties of Selected Ceramic Materials, American Ceramic Society.

2.11 MacDonald, N. J. and Ransley, C. E., "The Oxidation of Hot Pressed Titanium Carbide and Titanium Boride in the Temperature Range 300-1000°C," Powder Metallurgy, Vol. 3, 1959, pp. 172-177.

2.12 Eser, E., Ogilvie, R. E., and Taylor, K. A., "Friction and Wear Results from WC + Co Coatings by-dc-biased rf-Sputtering in a Helium Atmosphere," J. Vac. Sci. Technol., Vol. 15, No. 2, 1978, pp. 401-405.

2.13 Spalvins, T., "Microstructural and Wear Properties of Sputtered Carbides and Silicides," Proceedings of the International Conference on Wear of Materials, St. Louis, Missouri, April 1977.

2.14 Zeman, K. P. and Coffin, L. F., "Friction and Wear of Refractory Compounds," ASLE Trans., Vol. 3, 1960, pp. 191-202.

2.15 Brainard, W. A., "The Friction and Wear Properties of Sputtered Hard Refractory Compounds," ASLE Proceedings: 2nd International Conference on Solid Lubrication, Denver, Colorado, August 15-18, 1978.

2.16 Sliney, H. E., "Plasma Sprayed, Self-Lubricating Coatings for Use from Cryogenic Temperatures to 870°C," NASA Technical Memorandum, NASA TM X-71798, 1971.

2.17 Lavik, M., Midwest Research Institute, Personal Communications.

2.18 Peterson, M. B., Murray, S. F., and Florek, J. J., "Consideration of Lubricants for Temperatures above 1000°F," ASLE Trans., 1959, pp. 225-234.

2.19 Murray, S. F., and Peterson, M. B., "Solid Lubricant Coatings and Coating Compositions," Patent No. 3,158,495, General Electric Company, November 1964.

2.20 Sliney, H. E., "Plasma Sprayed Metal-Glass and Metal-Glass Fluoride Coatings for Lubrication to 900°C," Presented at Annual Meeting of ASLE, Cleveland, Ohio, April-May 1974.

2.21 Sliney, H. E., "Solid Lubricants for Extreme Temperatures," NASA Technical Memorandum, NASA TMX-52214, 1966.

2.22 Olson, K. M. and Sliney, H. E., "Additions to Fused-Fluoride Lubricant Coatings for Reduction of Low Temperature Friction," NASA, TND-3793, January 1967.

2.23 Sliney, H. E., "Lubricating Properties of Lead-Monoxide-Base Coatings of Various Compositions at Temperatures to 1250°F," NASA 3-2-59E, February, 1959.

2.24 Materials Selector, 1973 and other issues.

3.1 Bhushan, B., "Surface Pretreatment of Thin Inconel X-750 Foils for Improved Coating Adherence," Thin Solid Films, Vol. 53, No. 1, 1978, pp. 99-107.

3.2 Sliney, H. E. and Johnson, R. L., "Bonded Lead Monoxide Films as Solid Lubricants for Temperatures up to 1250°F," NACA RM E57B15, May 1957.

3.3 Maissel, L. I. and Glang, R., Handbook of Thin Film Technology, McGraw Hill Book Company, 1970, Chapter 4.

3.4 Greene, J. E., Woodhouse, J., and Pestes, M., "A Technique for Detecting Critical Loads in the Scratch Test for Thin Film Adhesion," Rev. Sci. Instrum., Vol. 45, 1978, pp. 747-749.

3.5 Brainard, W. A., "The Friction and Wear Properties of Sputtered Hard Refractory Compounds," Proc. 2nd Int. Conf. on Solid Lubrication, Denver, Colorado, August, 1978, pp. 139-147.

3.6 Movchan, B. A. and Demchishin, "Study of the Structure and Properties of Thick Vacuum Condensates of Nickel, Titanium, Tungsten, Aluminum Oxide, and Zirconium Dioxide," Fiz. Met. Metalloved, Vol. 28, No. 4, 1969, pp. 653-660.

3.7 Thronton, J. A., "Influence of Substrate Temperature and Deposition Rate on Structure of Thick Sputtered Cu Coatings," J. Vac. Sci. Technol., Vol. 12, No. 4, 1975, pp. 830-835.

3.8 Taylor, K. A., High Vacuum Equipment Corp., Hingham, MA, personal communications.

4.1 Heshmat, H., and Bhushan, B., "Reliability Improvement Study for Compliant Foil Air Bearing in Chrysler Upgraded Automotive Gas Turbine Engine," MTI Technical Report 79TR73, 1979.

4.2 Peterson, M. B., Florek, J. J., and Lee, R. E., "Sliding Characteristics of Metals at High Temperatures," ASLE Trans., Vol. 3, No. 1, 1960, pp. 101-109.

APPENDIX A

METALLURGICAL ANALYSES OF RF-SPUTTERED CHROME OXIDE COATING

AES ANALYSIS OF SELECTED SAMPLES

Auger electron spectroscopy (AES) was conducted on a number of specimens. All of the spectra were taken with a primary electron beam energy of 2500 volts, and a beam current of 10μ amp. The analyzer modulation was at 16,000 Hz, 3 volts peak to peak. This technique measures the surface layer only 3 to 4 atomic layers (5 to 6 Å thick). During analysis, the coating was ion bombarded (sputtered) away, and the measurement of what was remaining on the substrate was made. Surface composition measurements of the Cr_2O_3 target chip (reference base line) and of substrate Inconel foil were conducted. Then surface composition and concentration depth profile were carried out on a number of rf sputter-deposited chrome oxide films on Inconel X-750 foils.

A spectrum taken of the as-received Inconel X-750 foil is shown in Figure A.1. This is a nickel base alloy (~73% Ni) with additions of Fe, Cr, Ti, Aℓ, Mn, Cb, and Si. It is apparent from Figure A.1 that the Ti has segregated preferentially to the surface, as the major peaks seen are those for Ti, plus the usually observed surface impurity peaks for C, O, and Cℓ. The Ar peak is due to argon uptake during the light ion bombardment used to remove gross surface contamination prior to making the Auger measurement.

The Auger spectrum of the Cr_2O_3 reference chip is shown in Figure A.2. Some difficulty was experienced with this sample due to surface charging, a common problem with thick insulating layers. The problem was circumvented by operating at reduced electron beam voltage, and allowing some residual surface carbon contamination to remain on the surface. The resulting spectrum shows the expected peaks for Cr and O; and in addition peaks for S, Cℓ, and C, presumably as surface impurities. The ratio of the Cr to O peak heights is consistent with the bulk composition Cr_2O_3.

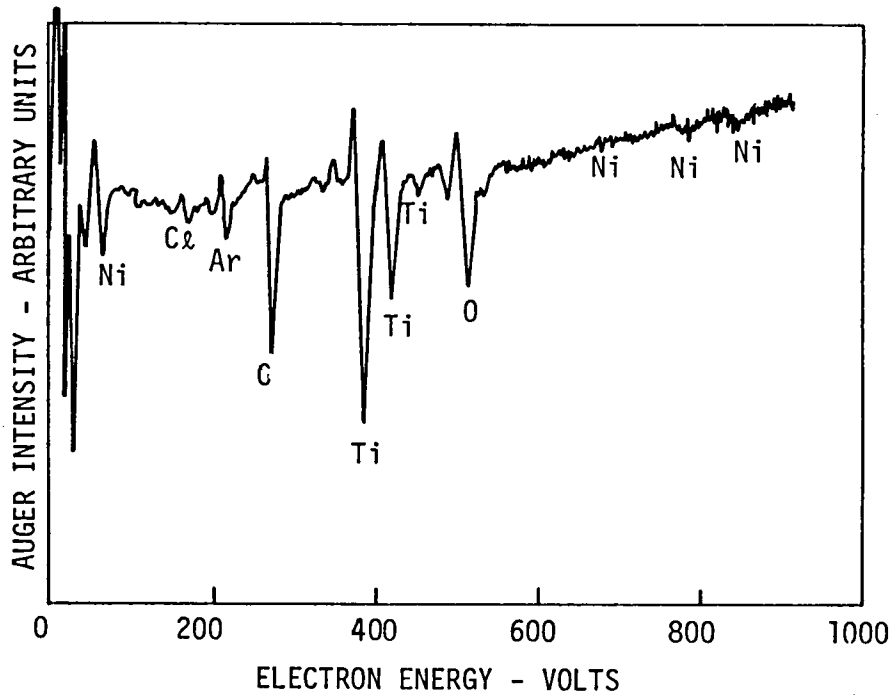

Fig. A.1 Auger Electron Spectra of Inconel X-750 Foil

793288

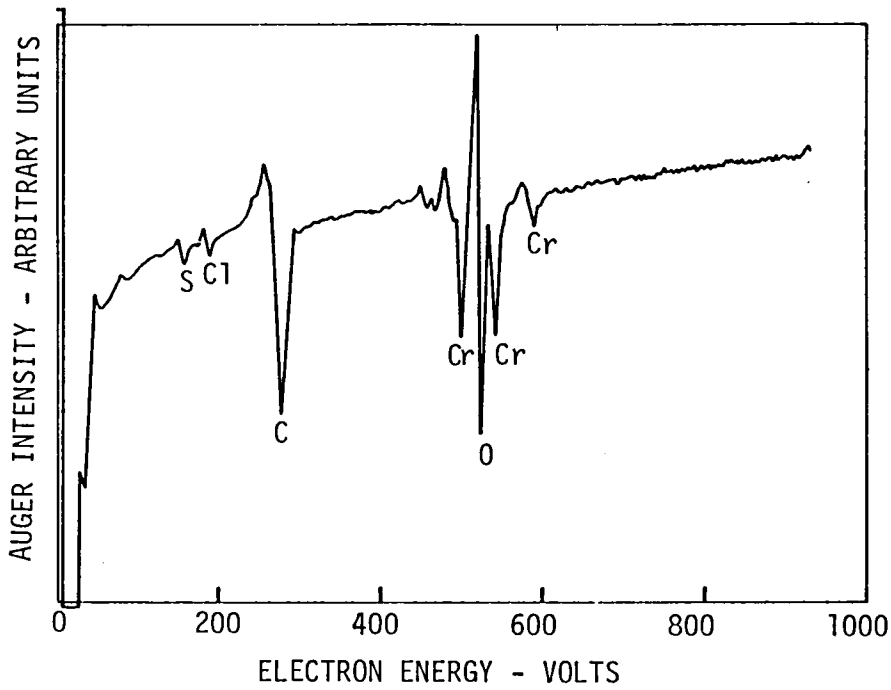

Fig. A.2 Auger Electron Spectra of Cr_2O_3 Target Chip (Reference)

A number of samples were selected to study any effect of sputtering parameters on the coating stoichiometry. Eight chrome oxide film samples numbered 2, 5, 8, 9, 12, 13A, 13B, and 13A after heat treatment, were analyzed to determine near-surface composition. In sample 13A, chrome oxide coating was sputtered on annealed Inconel X-750 foil. The foil has to be heat treated at 704°C for 20 hours and air cooled before it is used in the bearing application. Therefore, a 13A sample was heat treated and also examined for any stoichiometric change. Each of these samples was given an argon ion bombardment dose sufficient to reduce the surface carbon contaminant peak to a low level, and then an Auger spectrum was taken. The resulting spectra, after sputtering for about five minutes, are shown in Figure A.3 and A.4. All spectra show essentially the same ratio of O to Cr peak heights. The two peaks below 50eV probably arise from a splitting of the normal Cr peak at 36eV. Such splitting is often observed when a transition metal species is present in two different valence states, as is the likely case here. The small differences in the shape of the O and Cr peaks from sample to sample arise from very small changes in peak shape that are accentuated in the process of taking the derivative spectrum shown here, and are not thought to represent significant composition differences.

Peak height intensity ratios of selected Cr and O peaks were taken from the spectra and are presented in Table A.1. Based on the reference spectra available, the peak height intensity ratios were converted to atomic ratios. The atomic ratio of the target chip was found to be 1·81, where theoretically it should be 1·5 for Cr_2O_3. There is some interaction between Cr and O although it is low in high energy peaks. The experimental error in case of oxides could be as high as 10-20%. The interaction and the experimental error probably accounts for the discrepancy. Cr_2O_3 chip was also analyzed by Electron Microprobe Analysis (EMPA)*. X-ray counts/sec. of Cr and O were measured and compared with standard chromium to determine the weight % of Cr and remaining was assumed to be oxygen. With this analysis, the target chip was found to be pure Cr_2O_3. Assuming target to be Cr_2O_3, the O to Cr atomic ratio was revised as shown in the last column of the table. The results indicate that all eight coatings show essentially the same atomic ratio of O to Cr. The ratio observed is consistent with a composition close to Cr O, possibly with an oxygen deficiency. The color of the coating

*EMPA gives elemental distribution of about 200μm deep layer.

TABLE A.1

RESULTS OF AES STUDY OF COATED SAMPLES

Sample No.	Peak Height Intensity Ratios of Selected O to Cr Peaks (taken from Figs. III.11 to 13)	Atomic Ratio of O to Cr	
		Corrected Based on Reference Spectra	Corrected Based on Target Chip Taken as a Reference
Cr_2O_3 Target Chip	8.0	1.81	1.5
2	3.5	0.79	0.66
5	3.9	0.88	0.73
8	3.0	0.68	0.56
9	3.3	0.75	0.62
12	3.8	0.87	0.72
13A	3.6	0.82	0.68
13B	3.7	0.85	0.70
13A Coating heat treated 704°C/20 hrs/AC	4.0	0.91	0.76

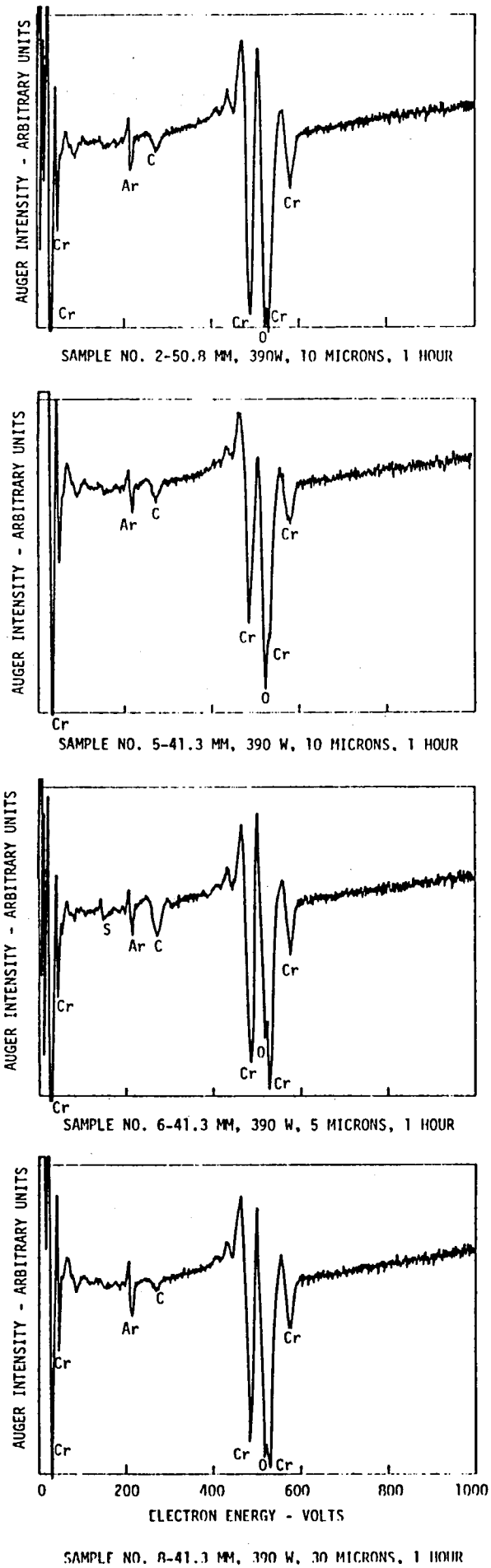

Fig. A.3 Auger Electron Spectra of rf Sputter-deposited Cr_2O_3 Coatings After Ion Bombardment of 5 min.

793281

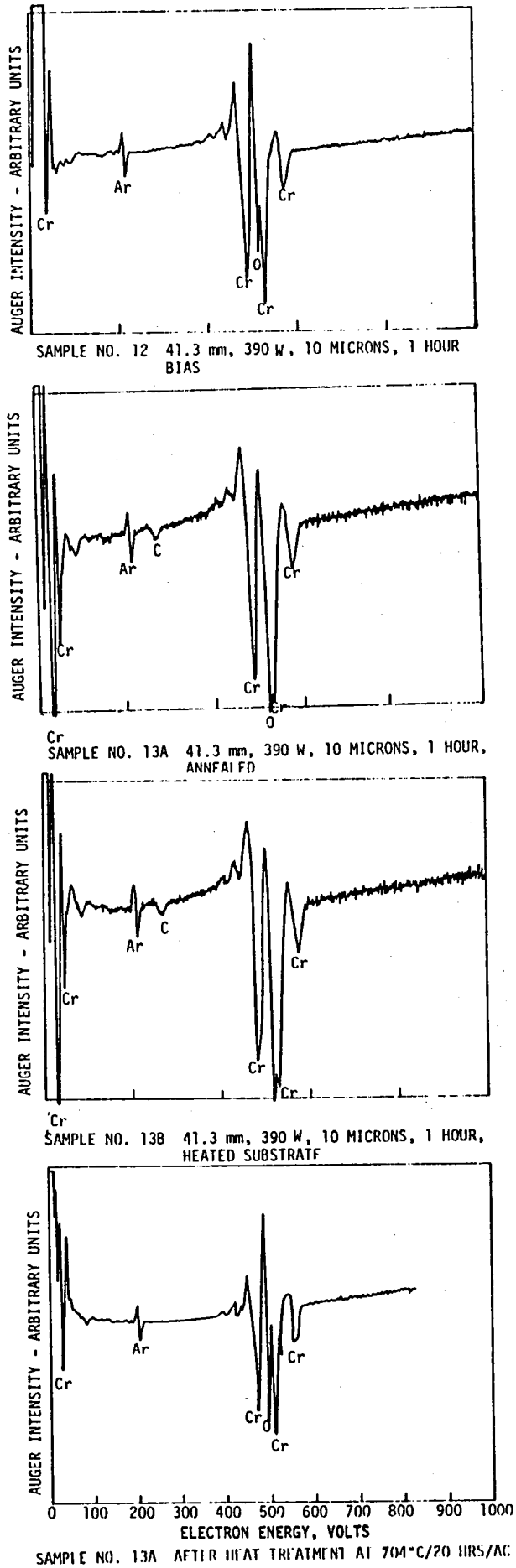

Fig. A.4 Auger Electron Spectra of rf Sputter-Deposited Cr_2O_3 Coating after Ion Bombardment of 5 minutes

793290

in most of the cases was grayish black, sometimes with green tint. The coatings after heat treatment were greener. The color of CrO, Cr_2O_3, and CrO_2 is supposed to be black, green, and brownish black, respectively. Therefore, the color of the coating probably indicates that it is either CrO or Cr_2O_3, or a mixture of both.

Concentration versus depth profile of sample Nos. 12 (bias sputtered), 5 (sputter deposit), and 13A after heat treated at 704°C/20 hours AC, were determined by taking Auger spectra in the course of an extended period of argon ion bombardment. In this study, the only species detected in the bulk of the film were Cr and O. As the film-substrate interface was approached, appreciable quantities of nickel and titanium were detected. The results of these measurements are presented in Figure A.5. The representative spectra showing bulk of coating, interface, and substrate are shown in Figure A.6 to A.8. The bombardment time to reach the first indication of the interface is identical for the first two cases, numbered 5 and 12, indicating virtually identical film thicknesses. The coating in sample 13A is probably thicker.

The small variation in Auger intensities for O and Cr in the bulk of the film are not thought to be significant. The observed decreases in intensity during the first hour of bombardment are probably due to slight changes in Auger electron detection efficiency due to surface roughening under the effects of the ion beam. The high concentration of Ti at the substrate surface, observed for the clean substrate material (Figure A.1) is not observed at the interface for either sample. It is possible that this layer was removed during sample conditioning (sputter etching) prior to the sputter deposition.

The only major peaks observed prior to reaching the interface were chromium, and oxygen, in an essentially constant atomic ratio. Peaks of Ti and Ni, and in one case Fe, appear as the film substrate is approached and the decrease in Cr and O is observed. It shows that the sputtering parameters in the range studied do not have significant influence on the coating stoichiometry.

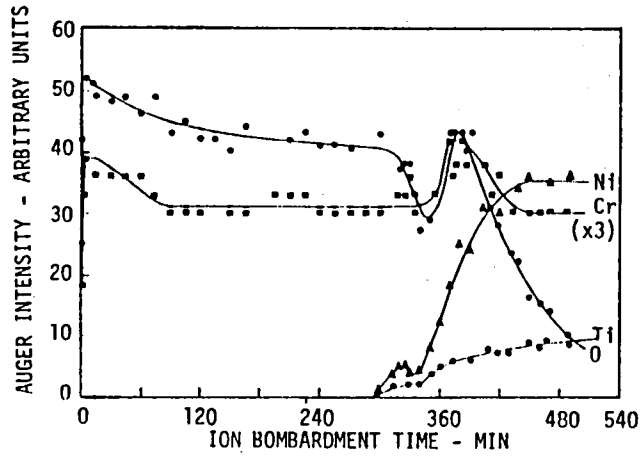

SAMPLE NO. 5 41.3 mm, 390 W, 10 MICRONS, 1 HOUR

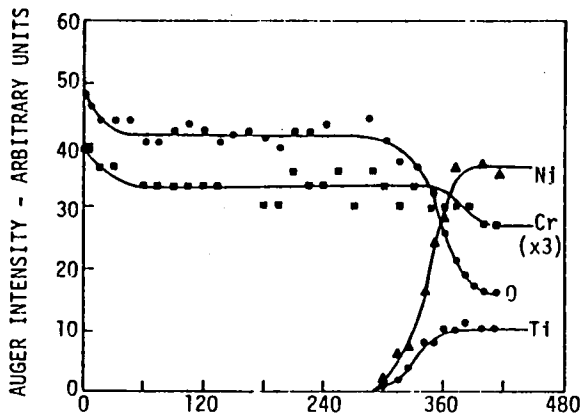

SAMPLE NO. 12 41.3 mm, 390 W, 1 HOUR, BIAS

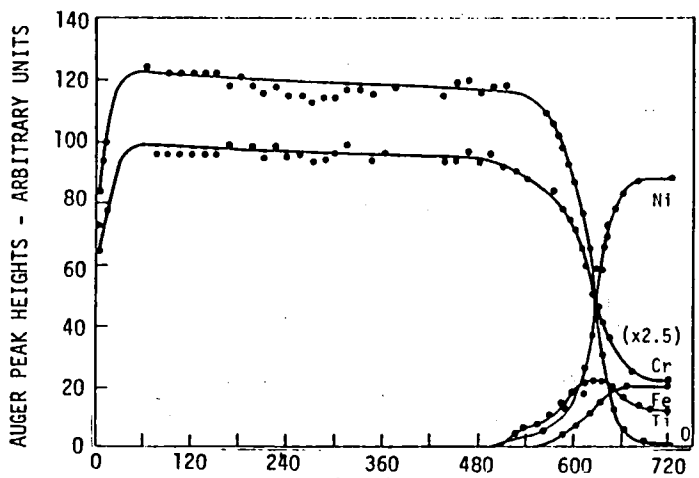

SAMPLE NO. 13A 41.3 mm, 390 W, 10 MICRONS, 1 HOUR ANNEALED AND HEAT TREATED AFTER COATING

Fig. A.5 Depth Profiling of the Sputter-Deposited Cr_2O_3 Coatings

793304

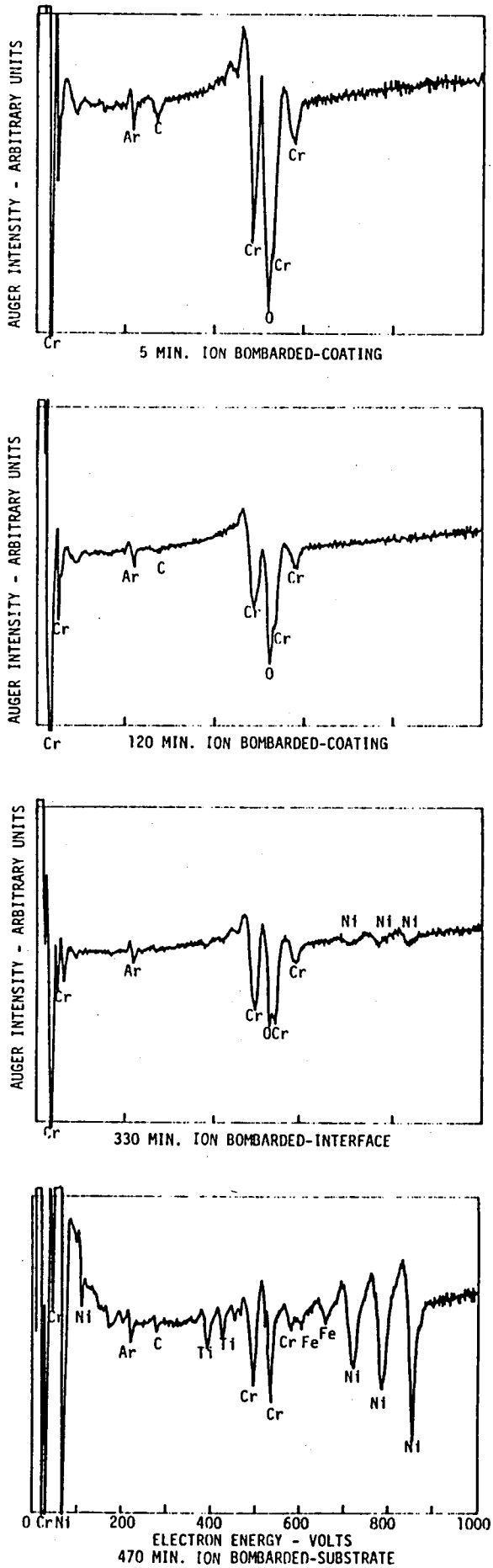

Fig. A.6 Auger Electron Spectra of rf Sputter-Deposited Cr_2O_3 Coating (Sample No. 5)

793284

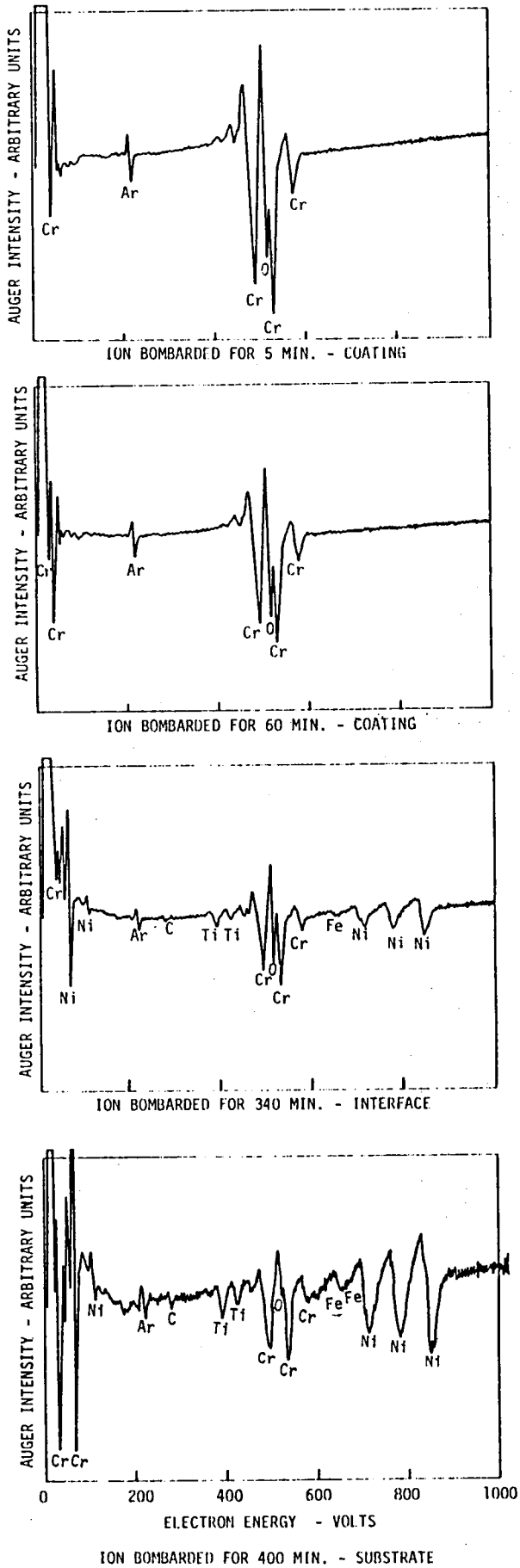

Fig. A.7 Auger Electron Spectra of rf Suptter-Deposited Cr_2O_3 Coating (Bias sputtered - No. 12)

793285

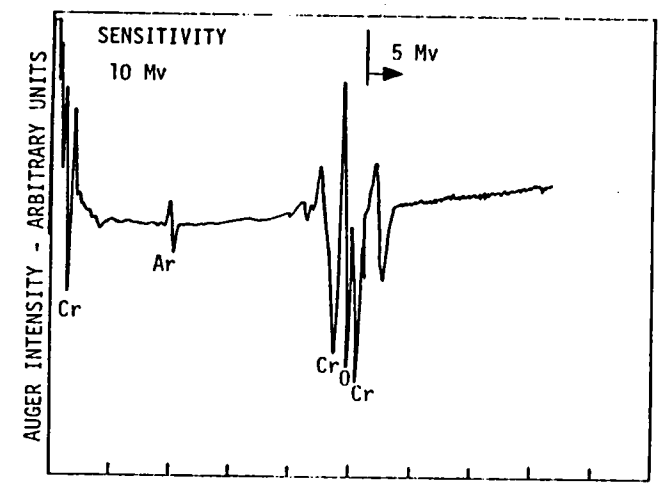

ION BOMBARDED FOR 330 MIN. - BULK OF COATING

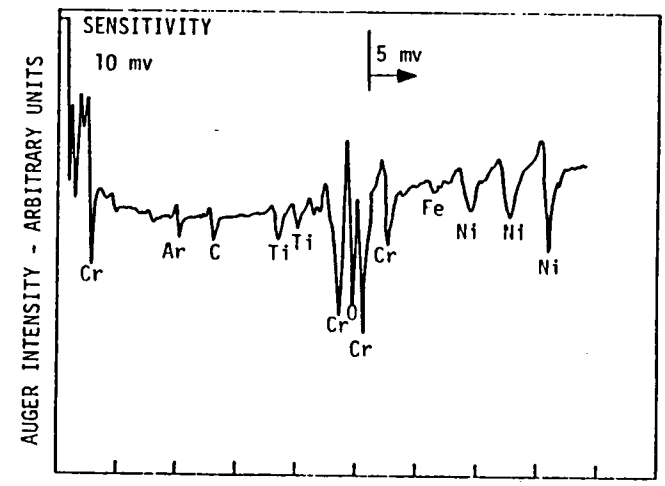

ION BOMBARDED FOR 625 MIN. - INTERFACE

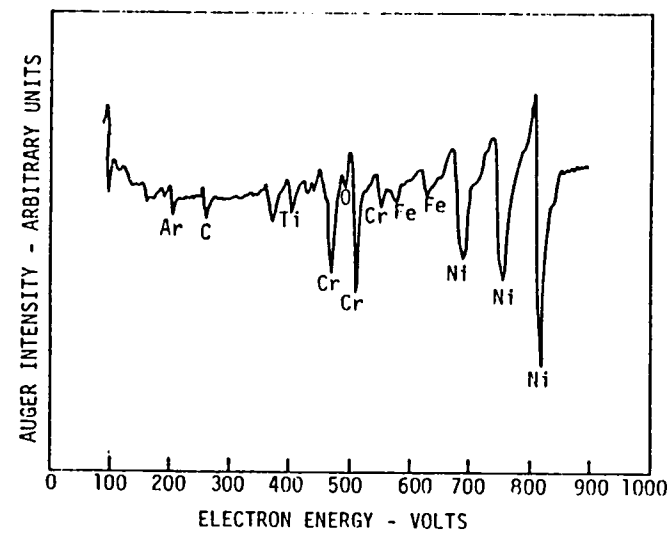

ION BOMBARDED FOR 720 MIN. - SUBSTRATE

Fig. A.8 Auger Electron Spectra of rf-Sputtered Cr_2O_3 Coating (No. 13A) after Heat Treatment

79328A

The only significant difference between the samples numbered 5 and 12 is that the "bias sputtered" sample shows a smooth transition in composition as the interface is traversed, while the "sputter deposited" sample shows a composition spike within the interfacial region. It is possible that this arises from a native chromium rich oxide layer present on the substrate which contains 15% Cr prior to film formation. This native chromium, rich oxide layer present at the interface may be responsible for improved bond in the case of sample 5. As it is discussed in Section 3, the sputter deposited coating had a better bond than bias sputtered coating. Bias sputtered coating was heavily stressed, and in some cases flaked off in handling. Similar results for other coating systems have been reported by Brainard and Wheeler [2.7].

Cr to O atomic ratio in coating No. 13A heat treated is the same as in sputtered coating No. 5. In the case of sample No. 13A after heat treatment, there is a smooth decrease in chromium and oxygen near the interface. However, the presence of Fe at the interface is noticed, probably resulting from diffusion of substrate element. Oscillations in the chromium and oxygen peak height with depth near the interface, that were observed in sample 5, were not observed in the sample No. 13A. It appears that the annealing associated with the heat treatment allowed any existing inhomogeneities to be relieved by diffusion. The final substrate ratios for the substrate are Ni: Cr: Fe: Ti = 1·00: 0·36: 0·13: 0·08. The results show that the coating stoichiometry from heat treatment is virtually unchanged and some diffusion at the interface has taken place which may result in improved adhesion.

X-RAY DIFFRACTION ANALYSIS OF SELECTED SAMPLES

Analysis determines the structure of the material to be examined. This technique penetrates through the sample several hundred microns. X-Ray diffraction study was done using a General Electric diffractometer at room temperature over an angle variation of $10^{o}<2\Theta<90^{o}$ using a Cr target with a Vd filter. X-ray diffraction plots were obtained for different samples. '2Θ' values and relative intensities of the peaks were read off from the plots. Using the formula $n\lambda = 2d \sin\Theta$, d-spacing was calculated where λ = wave length of chromium target (2.285 $\mathring{A}$), n - order of diffrac-

tion and θ = diffraction angle. Once d-spacing and relative intensities are known, search for ASTM cards is made which match calculated data. Primarily, matching of the d-spacing is done; intensities are usually slightly different due to the lack of randomness of the coating particles in the case of coating and some absorption of X-rays by the coating coming from the substrate in the case of substrate. However, the general pattern is still the same. Samples examined were: No. 5 (sputter deposited), 12 (bias sputtered), and 13A (sputter deposited on annealed foil) after heat treating the coating at 704°C/20 hours/AC. In the case of the first two samples, the coating was applied on Inconel X-750 foil and the microscope slide. Due to the possibility of diffusion during heat treatment in the third sample, it was tested only on Inconel X-750 foil.

In the process of analyzing samples Nos. 5, 12, and 13A after heat treatment, we have, in order to evaluate the effect of the substrate, started by conducting the X-ray analysis on Inconel X-750 foil and glass slide substrates. The measurements on the Inconel X-750 foil yielded the presence of 6 peaks with positions and intensities listed in the enclosed data sheets. The measurements on the glass slide substrate was marked by the absence of a diffraction pattern typifying the amorphous structure of the system. Having characterized the background pattern for the substrates, a series of runs were then conducted on sample Nos. 5 and 12 which consisted of sputtered Cr_2O_3 with and without a bias potential, and sample #13A which consisted of sputtered Cr_2O_3 (sp deposit) on annealed foil then heat treated. The first two samples exhibited after subtraction of the Inconel X-750 background pattern, a broad peak of very small intensity positioned at a 2θ of about 54.2 ± 0.8^{o}. The diffraction patterns are shown in Figure A.9 and data are tabulated in Table A.2. This single peak corresponding to a d-spacing of 2.51Å characterizes the presence of a microcrystalline structure of Cr-O within an amorphous matrix of the deposited film. This conclusion is reinforced in the observation of the deposited films on the glass substrate. For sample Nos. 5 and 12 deposited on glass, one notes the presence of that broad peak at 54.2^{o}. The diffraction patterns are shown in Figure A.10 and data are given in Table A.3 characterizing again the presence of some microcrystalline precipitates of Cr-O.

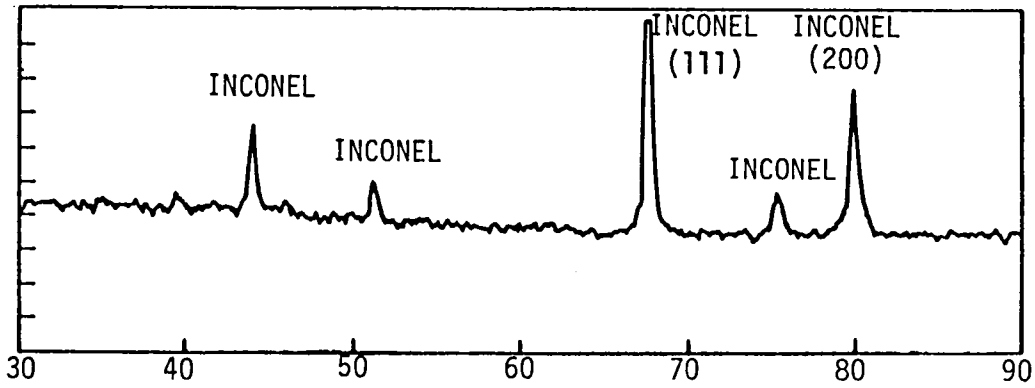

INCONEL X-750 SUBSTRATE

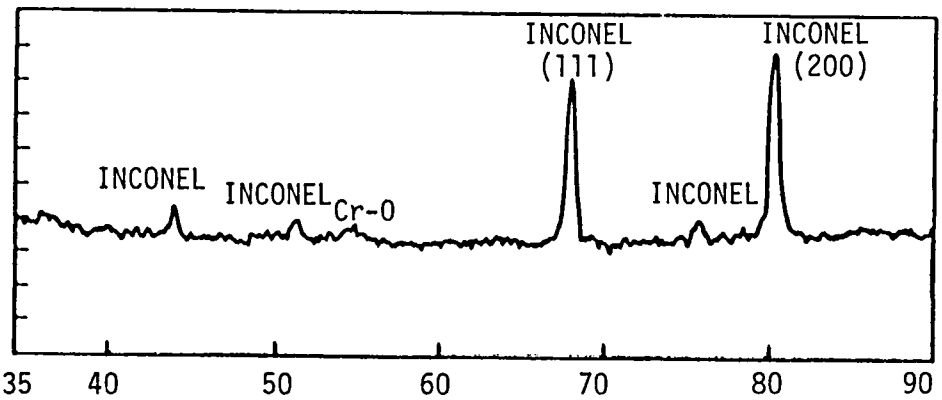

SAMPLE 5, SPUTTER DEPOSITED

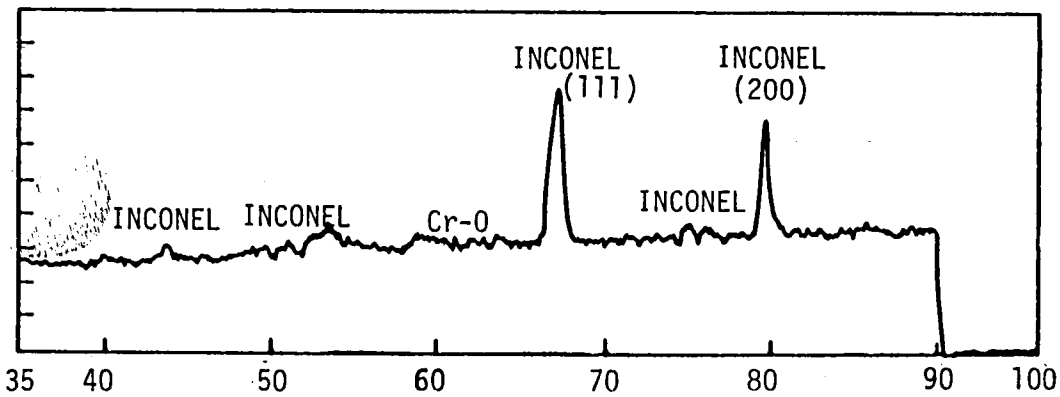

SAMPLE 12, BIAS SPUTTERED

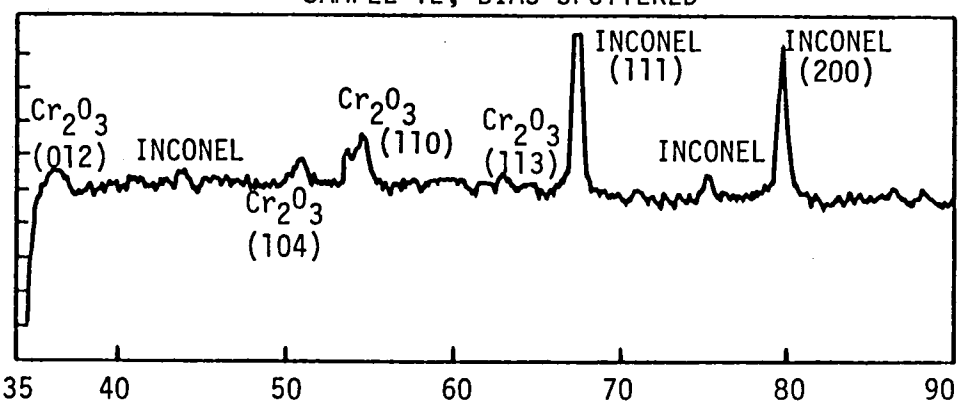

SAMPLE 13A, COATING APPLIED ON ANNEALED FOIL THEN HEAT TREATED (704°C/20 HRS/AC)

Fig. A.9 X-Ray Diffraction Data of the rf Sputter-Deposited Cr_2O_3 Coatings (41.3 mm, 390 W, 10 Microns, 1 hour) on Inconel X-750 Substrate

792855

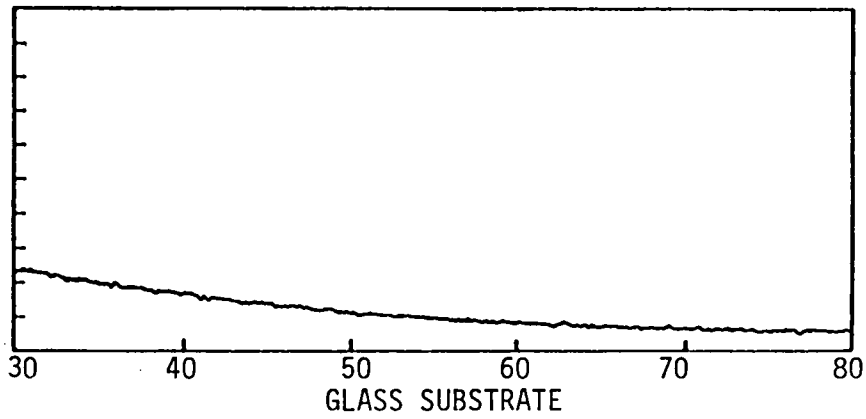

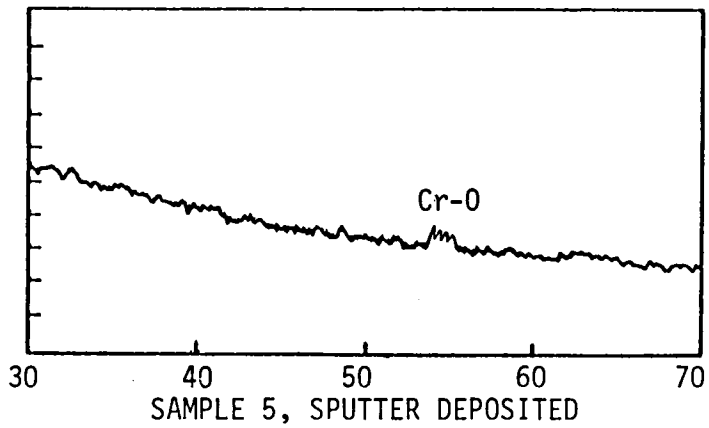

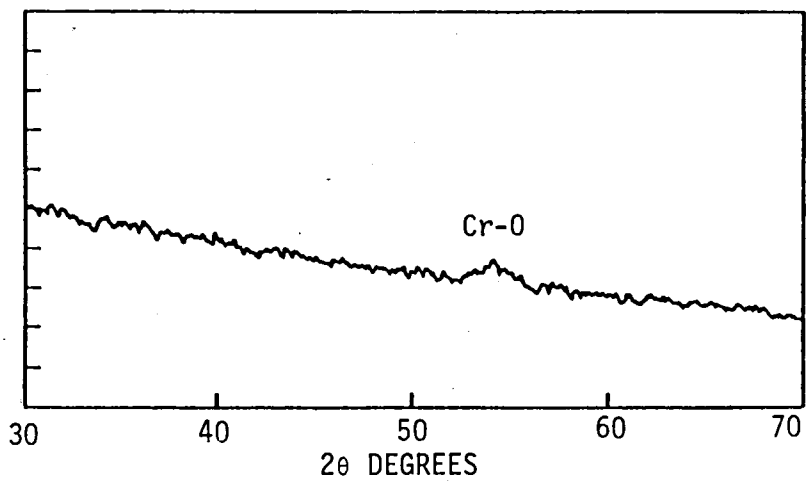

Fig. A.10 X-Ray Diffraction Data of the rf Sputter-Deposited Cr_2O_3 Coatings (41.3 mm, 390 W, 10 Microns, 1 hour) on Microscope Slide Substrate

792857

TABLE A.2

X-RAY DIFFRACTION DATA FOR Cr_2O_3 COATED INCONEL X-750 SUBSTRATE

X-Ray Run for Inconel X - 750 Substrate Using Cr Target with Vd Filter

2θ (degrees)	Intensity (Arbitrary Units)	d (Angstroms)	hkl
39.45	1.0	3.39	
43.95	5.0	3.06	
51.20	2.2	2.65	
67.60	Off Scale	2.06	Ni (111)
75.30	2.4	1.87	
79.90	8.5	1.78	(200)

X-Ray Run for Inconel X - 750 Substrate Coated with Cr_2O_3 (sputter deposited, Sample #5) using Cr Target with Vd Filter

2θ (degrees)	Intensity (Arbitrary Units)	d (Angstroms)	hkl
44.50	1.8	1.63	Inconel
51.80	1.4	2.61	Inconel
54.90*	1.0	2.47	CrO
68.10	9.7	2.04	Inconel
75.80	1.2	1.86	Inconel
80.40	12.0	1.77	Inconel

X-Ray Run for Inconel X - 750 Substrate Coated with Cr_2O_3 (bias sputtered, Sample #12) using Cr Target with Vd Filter

2θ (degrees)	Intensity (Arbitrary Units)	d (Angstroms)	hkl
43.95	0.9	3.06	Inconel
51.20	0.7	2.65	Inconel
53.40*	1.5	2.54	CrO
67.60	9.0	2.06	Inconel
75.30	0.9	1.87	Inconel
79.90	6.8	1.78	Inconel

*Asterisk indicates presence of additional broad peak in reference to Inconel substrate.

TABLE A.2 (Cont'd)

X-RAY DIFFRACTION DATA FOR Cr_2O_3 COATED INCONEL X-750 SUBSTRATE

X-Ray Run for Inconel X - 750 Substrate with Cr_2O_3 Coating on Annealed Foil (Sp. deposit, Sample #13A)

2θ (degrees)	Intensity (Arbitrary Units)	d (Angstroms)	hkl
36.2	1.8	3.67	Cr_2O_3 (012)
43.9	1.4	3.06	Inconel
50.9	1.7	2.66	(104)
54.5	3.5	2.50	(110)
63.1	1.1	2.18	(113)
67.4	Off Scale	2.06	Inconel
75.3	1.5	1.87	Inconel
79.9	11.5	1.78	Inconel

TABLE A.3

X-RAY DIFFRACTION DATA FOR Cr_2O_3 COATED GLASS SUBSTRATE

X-Ray Run for Glass Substrate using Cr Target with Vd Filter

No Peaks

X-Ray Run for Glass Substrate with Bias Sputtered Cr_2O_3 (Run No. 12) using Cr Target with Vd Filter

2θ (degrees)	Intensity (arbitrary units)	d (angstroms)
54.20	1.2	2.51

X-Ray Run for Glass Substrate with sp. deposted Cr_2O_3 (Run No. 5) using Cr Target with Vd Filter

2θ (degrees)	Intensity (arbitrary units)	d (angstroms)
54.20	0.8	2.51

It is worthwhile noticing at that point, by referring to the diffraction plots, the substantial simplification in the acquisition of the data and the interpretation of the results in the case of the films deposited on glass substrates. It was henceforth recommended for future research efforts that all X-ray work on these films be carried out on glass substrates.

The analysis of Run 13A heat treated, after the subtraction of the Inconel X-750 background exhibits four peaks at 36.2 ± 0.2^{o}, 50.9 ± 0.2^{o}, 54.5 ± 0.3^{o}, and 63.1 ± 0.3^{o}. These peaks correspond to d-spacings of 3.67, 2.66, 2.50, and 2.18Å, respectively; and characterize the crystalline compound Cr_2O_3 (see Figure A.9). The copy of ASTM cards corresponding to Cr-O and Cr_2O_3 are shown in Figure A.11.

d	2.67	2.48	1.67	3.633
I/I₁	100	96	90	74

Cr_2O_3

Chromium (III) Oxide

Rad. Cu λ 1.5405 Filter Coll.
Dia. Cut off d corr. abs.?
I/I₁
Ref. Swanson et al., NBS Circular 539 Vol. V (1955)

Sys. Hexagonal S.G. D_{3D}^6 - $R\bar{3}c$
a_o 4.954 b_o c_o 13.584 A C
α β γ Z 6
Ref. Ibid.

εα nωβ εγ Sign
2V Dx 5.23 mp Color
Ref.

Sample from Johnson, Matthey and Co. Ltd.
Spect. anal.: <0.001% Ca, Mg; <0.0001% Si, Cu.
X-ray pattern at 26°C. Fe_2O_3 structure type.

Replaces 1-1294, 2-1362, 3-1124, 4-0765

d Å	I/I₁	hkl	d Å	I/I₁	hkl
3.633	74	012	0.9370	12	410
2.666	100	104	.8357	14	1.3.10
2.480	96	110	.8883	7	1.0.12
2.264	12	006	.8658	23	416
2.176	38	113	.8425	8	4.0.10
2.048	9	202	.8331	11	1.0.16
1.8156	39	024	.8263	9	330
1.672	90	116	.7977	15	3.2.10
1.579	13	122			
1.465	25	214			
1.4314	40	300			
1.2961	20	1.0.10			
1.2398	17	220			
1.2101	7	306			
1.1731	14	128,312			
1.1488	10	0.2.10			
1.1239	10	134			
1.0874	17	226			
1.0422	16	2.1.10			
0.9462	13	324			

d	2.41	2.04	1.90	2.82
I/I₁	100	30	30	10

CrO

Chromium (II) Oxide

Rad. CoKα λ Filter Dia.
Cut off I/I₁
Ref. Luz, Z. anorg. Chemie 257 73-78 (1948)

Sys. S.G.
a_o b_o c_o A C
α β γ Z Dx
Ref.

εα nωβ εγ Sign
2V D mp Color
Ref.

d Å	I/I₁	hkl	d Å	I/I₁	hkl
2.82	10				
2.59	100				
2.44	10				
2.26	10				
2.04	30				
1.90	30				
1.77	10				

d 4-0854	2.034	1.762	1.246	2.036
I/I₁ 4-0850	100	42	21	100

Ni

Nickel

Rad. Cu λ 1.5405 Filter Ni
Dia. Cut off Coll.
I/I₁ d corr. abs.?
Ref. Swanson and Tatge, JC Fel. Reports, NBS 1951

Sys. Cubic (F.c.) S.G. O_h^5 - $Fm3m$
a_o 3.5238 b_o c_o A C
α β γ Z 4
Ref. Ibid.

εα nωβ εγ Sign
2V Dx 9.907 mp Color
Ref.

Spectrographic analysis ends <0.1% each of Mg, Si and Ca.
At 26°C
To replace 1-1258, 1-1260, 1-1266, 1-1272, 3-1043, 3-1051

d Å	I/I₁	hkl	d Å	I/I₁	hkl
2.034	100	111			
1.762	42	200			
1.246	21	220			
1.0624	20	311			
1.0172	7	222			
0.9810	4	400			
.8084	14	331			
.7880	15	420			

d	2.06	1.26	1.08	2.060
I/I₁	100	27	16	100

C

Carbon (Diamond)

Rad. Cu λ 1.5405 Filter Ni
Dia. Cut off Coll.
I/I₁ d corr. abs.?
Ref. NBS Circular 539 Vol II pp 5-6 (1953)

Sys. Cubic (F.c.) S.G. O_h^7 - $Fd3m$
a_o 3.5667 b_o c_o A C
α β γ Z 8
Ref. Ibid.

εα nωβ 2.4125 εγ Sign
2V Dx 3.515 mp Color
Ref. Ibid.

Sample was an industrial abrasive powder.
X-ray pattern at 27°C.

Replaces 1-1249, 2-1248

d Å	I/I₁	hkl	d Å	I/I₁	hkl
2.060	100	111			
1.261	27	220			
1.0754	16	311			
0.8916	7	400			
0.8182	15	331			

d	2.04	1.18	0.91	2.0390
I/I₁	100	29	21	100

Cr

Chromium

Rad. Cu λ 1.5405 Filter
Dia. Cut off Coll.
I/I₁ d corr. abs.?
Ref. Swanson et al., NBS Circular 539 Vol V (1955)

Sys. Cubic (s.c.) S.G. O_h^9 - $Im3m$
a_o 2.8839 b_o c_o A C
α β γ Z 2
Ref. Ibid.

εα nωβ εγ Sign
2V Dx 7.200 mp Color
Ref.

Spect. anal. of sample: <0.1% Si; 0.01% Cu, Mn, Sn; <0.001% Ag, Fe.
Hydrogen annealed; cooled in helium.
X-ray pattern at 25°C

Replaces 1-1250, 1-1251, 1-1261

d Å	I/I₁	hkl	d Å	I/I₁	hkl
2.0390	100	110			
1.4419	16	200			
1.1774	29	211			
1.0195	17	220			
0.9120	21	310			
0.8325	6	222			

Fig. A.11 ASTM Cards for Cr_2O_3, CrO, Ni, C and Cr

793255

APPENDIX B

METALLURGICAL ANALYSIS OF RF-SPUTTERED NICHROME-BONDED CHROME OXIDE COATING

AES ANALYSIS OF SELECTED SAMPLES

Auger electron spectroscopy was conducted on sample Nos. 30, as sputtered on annealed foil and the same coating after heat treatment and 31; and the reference target chip. The spectra were taken with a primary electron beam of 3000 eV energy, 20μA current, and a modulation voltage of 3V peak to peak.

The spectrum obtained from a Ni-Cr-Cr_2O_3 chip is shown in Figure B.1. Great difficulties were encountered with this specimen due to surface charging. Consequently, the electron energy scale is distorted and spurious peaks due to charging are present. It is possible, however, to obtain approximate relative concentration information from the spectrum. Using the techniques detailed in Appendix A, we obtain the ratios Cr: O: Ni = 1.00 : 1.16 : 0.04. The theoretically expected ratio, based on the nominal composition of the sample is Cr: O: Ni - 1.00: 1.28: 0.57. The sample surface is thus very deficient in nickel.

The Auger depth profile analysis was carried out to determine the composition as a function of depth within the film. The resulting depth profile for sample No. 30 (as coated) is shown in Figure B.2. This film was sputtered from the Ni-Cr-Cr_2O_3 target. Here the peak-to-peak heights of the Auger peaks for the various species detected are plotted as a function of ion bombardment time, which is proportional to etching depth. Throughout the bulk of the film, the only major peaks are those of chromium, oxygen, and nickel. The slight changes in peak height with time are most probably due to drift in Auger analyser sensitivity. Calculation of concentration ratios at various bombardment times gave consistent values of Cr: O: Ni = 1.00: 1.00: 0.38. The coating is slightly deficient in oxygen and nickel. A typical spectrum for the bulk of the film is shown in Figure B.3. As the film-substrate interface was approached, peaks typical of titanium and iron were observed; the nickel peaks increased and chromium and oxygen decreased. Spectra typical of the interfacial region and the substrate material are also shown in

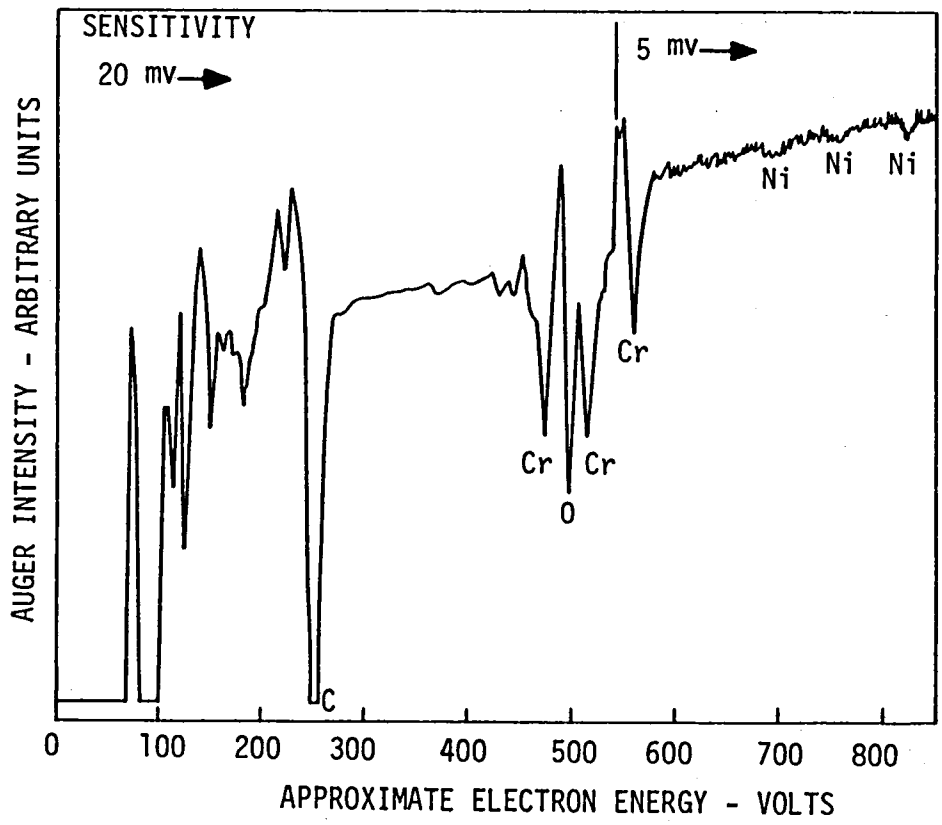

Fig. B.1 Auger Electron Spectrum of Ni-Cr-Cr_2O_3 Target Chip (Reference)

793289

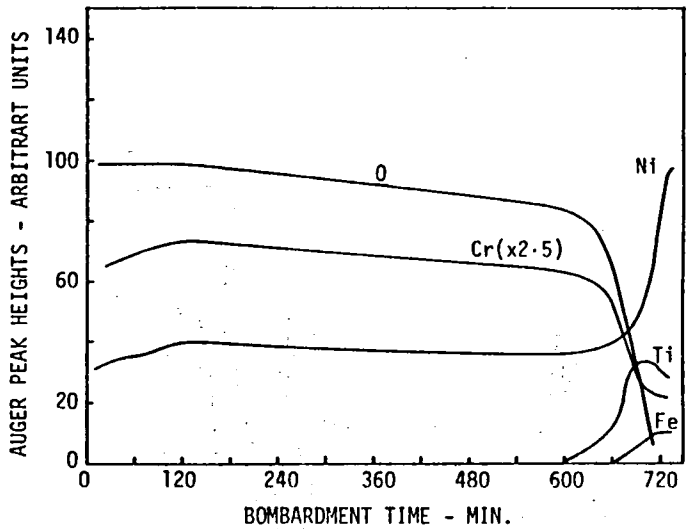

SAMPLE NO. 30 AS COATED

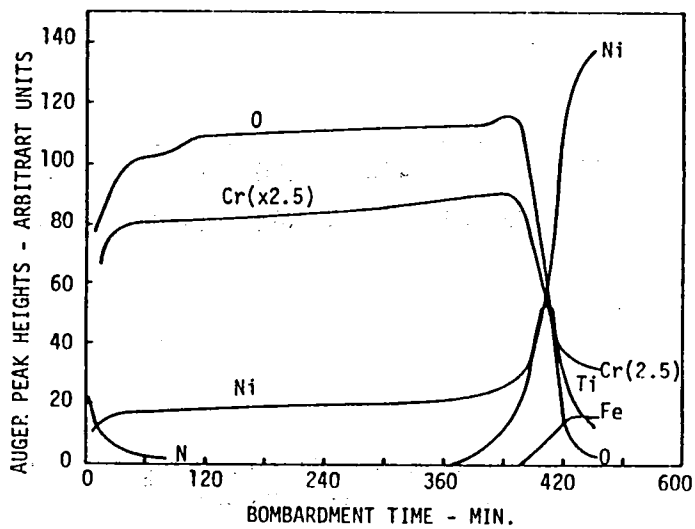

SAMPLE NO. 30 AFTER HEAT TREATMENT

Fig. B.2 Depth Profiling of the Sputter-Deposited Ni-Cr-Cr_2O_3 Coatings

793291

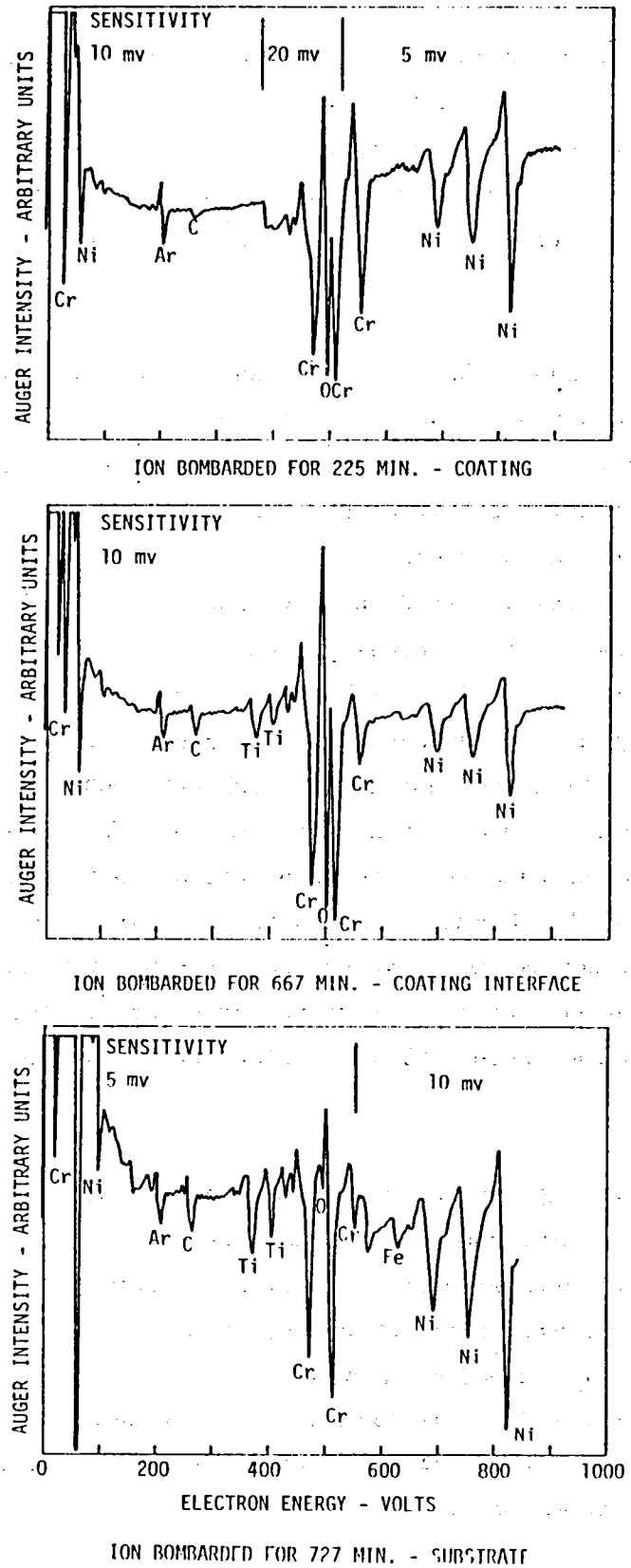

Fig. B.3 Auger Electron Spectra of rf Sputter-Deposited Ni-Cr-Cr_2O_3 Coating (Sample No. 30 as coated)

793286

Figure B.3. The concentration ratios calculated for the substrate material are Ni: Cr: Fe: Ti - 1.00: 0.34: 0.15: 0.09. These may be compared to the ratios expected from the bulk composition of the substrate material of Ni: Cr: Fe: Ti - 1.00: 0.21: 0.09: 0.03, indicating that the substrate surface is somewhat deficient in nickel. This is consistent with the results in Appendix A.

The depth profile of Sample No. 30, after an additional heat treatment in the nitrogen atmosphere is shown in Figure B.2. It differs from the profile obtained from the as-coated specimen primarily in that a significant concentration of nitrogen is found near the sample surface. This nitrogen concentration drops to a low value at a depth of roughly 1000Å. The nitrogen was diffused into the surface during heat treatment. The bulk of the film is of essentially constant composition, with observed concentration ratios of Cr: O: Ni - 1.00: 1.00: 0.16. That is, the chrome-to-oxygen ratio appears not to have been changed by the heat treatment, but the nickel concentration has been greatly reduced. As with the as-coated sample, peaks for titanium and iron appear as the film-substrate interface is approached, and the same increase in nickel and decrease in chromium and oxygen is observed. Typical spectra for the near-surface region, the bulk of the coating, and the coating substrate interface are shown in Figure B.4. The final concentration ratio in the substrate is Ni: Cr: Ti: Fe = 1.00: 0.33: 0.14: 0.06, essentially identical to the value for the as-coated sample.

The spectrum for bias sputtered coating (No. 31 as coated) is shown in Figure B.5. The spectrum shows large amounts of oxygen, chromium, and nickel; and small amounts of argon and carbon present as an impurity. The calculated concentration ratios are Cr: O: Ni = 1.00: 0.86: 0.35. The ratio of oxygen to chromium in this specimen is small compared to the ratio previously observed in the film prepared by sputter deposit mode (No. 30) or the target chip. It indicates that bias sputtering provides slightly oxygen-deficient coating.

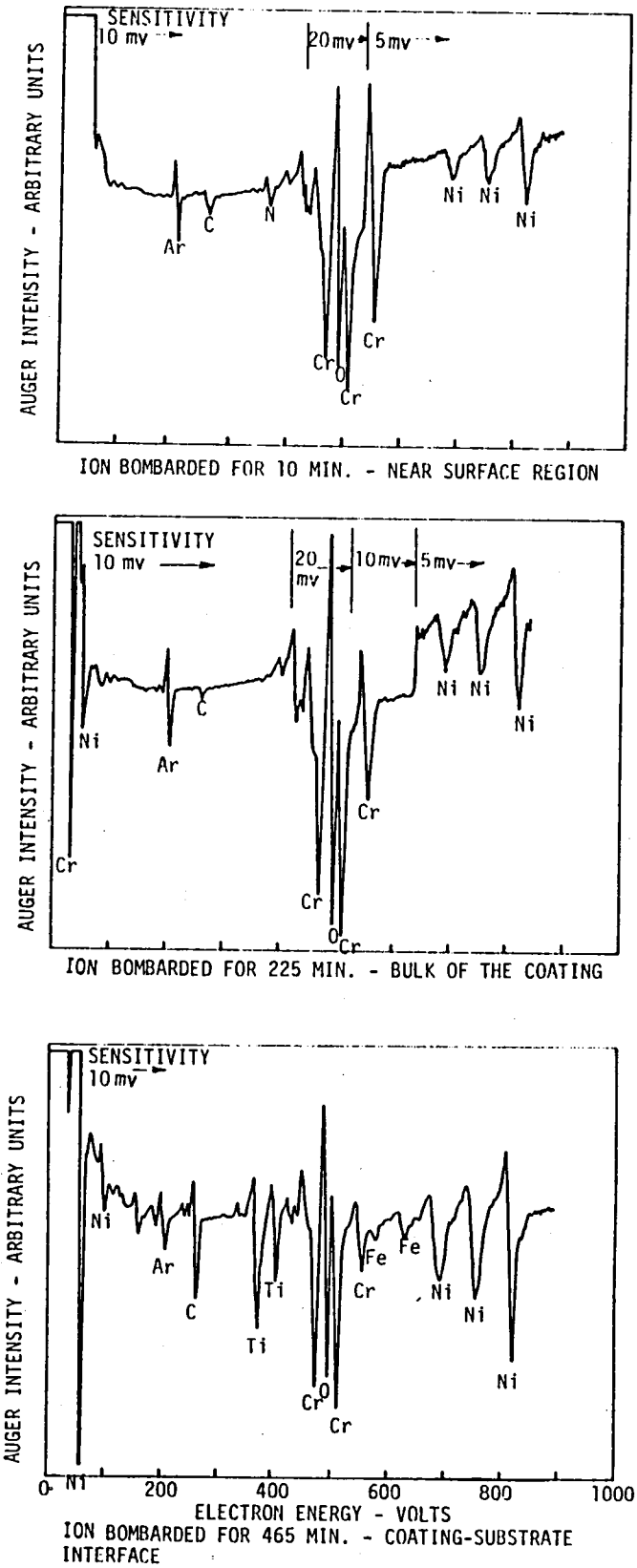

Fig. B.4 Auger Electron Spectra of rf Sputter-Deposited Ni-Cr-Cr_2O_3 Coating (sample No. 30, after heat treatment)

793282

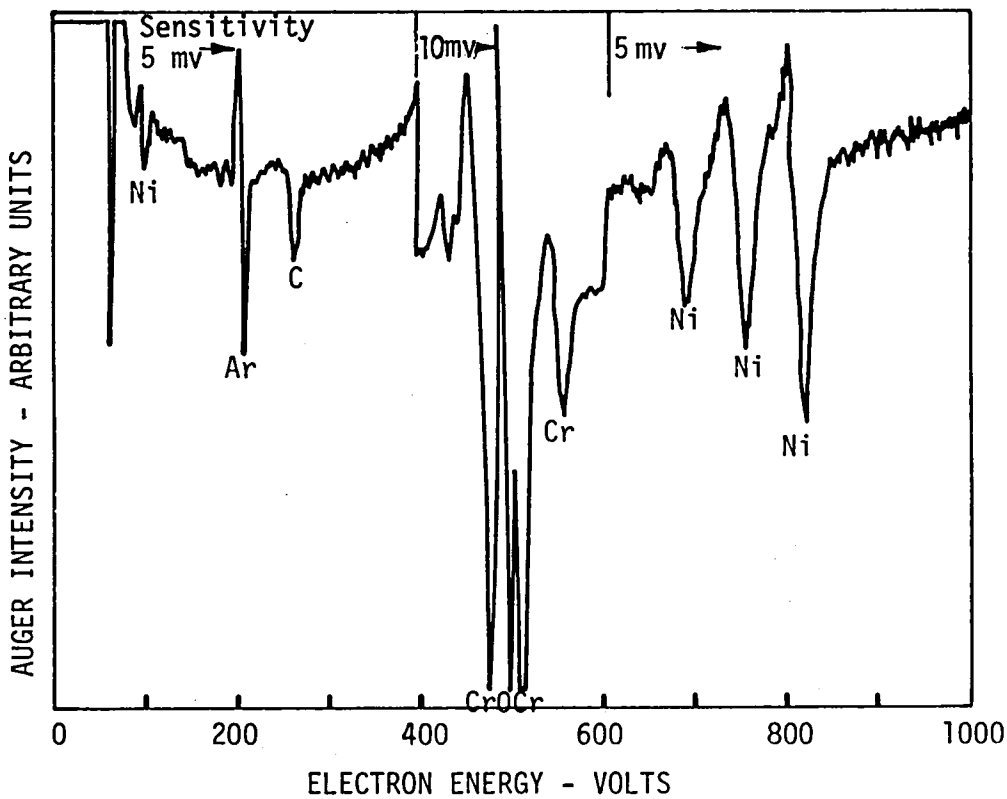

Fig. B.5 Auger Electron Spectrum of Ni-Cr-Cr_2O_3 Coating, Bias Sputtered (Sample No. 31 as coated)

793292

X-Ray Diffraction Analysis of Selected Samples

A series of X-ray measurements were conducted on the following specimens: sputter-deposited Ni-Cr-Cr_2O_3 as coated on annealed foil (No. 30) and No. 30 after heat treatment and bias sputtered Ni-Cr-Cr_2O_3 on unetched specimen (No. 31). 'As sputtered' coatings used for examination were applied on the glass substrate and carbon planchets. The coating after heat treatment for examination was applied on Inconel X-750 because interaction of the substrate with the coating needed to be studied. The results for the carbon blank, shown in the enclosed data sheets, yielded, within the range of angles investigated, twelve peaks which were used for background standard. The X-ray data for (Sample 30) and (Sample 31) yielded a pattern of peaks with identical positions to those of the carbon substrate but with varying intensities reflecting in this case the presence of coatings on the surface. The data are presented in Table B.1. The absence of any new lines for these coatings indicate unequivocally the amorphous nature of these two deposits. This conclusion is again reinforced when the X-ray data for the same two coating deposited on glass also yielded no diffraction patterns (see Table B.2).

Sample 30, after heat treatment revealed five peaks after the subtraction of the Inconel X-750 background. The five peaks corresponded to the compound Cr_2O_3 and were at 36.5 ± 0.3^o, 51.0 ± 0.2^o, 54.7 ± 0.4^o, 63.3 ± 0.2^o, and 86.3 ± 0.2^o corresponding to d-spacing of 3.65, 2.65, 2.49, 2.18, and 1.67 Å, respectively (Table B.3 and Figure B.6). Since substrate (Inconel X-750 has Ni and Cr, Ni and Cr in the coating cannot be positively identified. Nickel, chromium peaks, and Inconel X-750 peaks are overlapping, and varying intensities reflect the additional presence of nickel at 67.3^o and 79.8^o and of chromium at 67.3^o.

Thus, the analysis shows that the coating is Ni-Cr-Cr_2O_3 after heat treatment and it had amorphous structure before heat treatment.

TABLE B.1

X-RAY DIFFRACTION DATA FOR Ni-Cr-Cr_2O_3 COATED CARBON SUBSTRATE

X-Ray Run for Carbon Blank using a Cr Target with Vd Filter

2θ (degrees)	Intensity (Arbitrary Units)	d (Angstroms)	hkl
23.60	4.5	5.57	
26.20	Off Scale	5.02	
39.60	Off Scale	3.36	(002)
42.30	0.7	3.16	
43.40	0.9	3.08	
44.30	1.2	3.02	
54.20	0.6	2.50	
65.00	1.2	2.12	(100)
68.60	1.7	2.02	(101)
77.50	0.7	1.82	
83.60	0.2	1.71	
85.90	1.2	1.67	(004)

X-Ray for Sample #30 with Carbon Substrate using Cr Target and Vd Filter

2θ (degrees)	Intensity (Arbitrary Units)	d (Angstroms)
23.60	1.6	5.57
26.20	6.5	5.02
39.60	Off Scale	3.36
42.40	0.6	3.15
43.40	0.7	3.08
44.10	0.7	3.04
54.30	0.6	2.50
65.00	1.0	2.12
68.60	1.3	2.02
77.50	0.5	1.82
83.60	0.2	1.71
85.90	0.9	1.67

No New Peaks

TABLE B.1 (cont'd)

X-Ray for Sample #31 with Carbon Substrate using Cr Target and Vd Filter

2θ (degrees)	Intensity (Arbitrary Units)	d (Angstroms)
23.60	2.0	5.57
26.30	6.7	5.01
39.60	Off Scale	3.36
42.40	0.5	3.15
43.70	0.6	3.06
44.20	0.6	3.03
54.20	0.7	2.50
65.10	1.1	2.12
68.60	1.3	2.02
77.40	0.5	1.82
83.60	0.4	1.71
85.80	1.2	1.67

No New Peaks

TABLE B.2

X-RAY DIFFRACTION DATA FOR Ni-Cr-Cr_2O_3 COATED GLASS SUBSTRATE

X-Ray for Sample #30 (As Coated) with Glass Substrate
using Cr Target and Vd Filter

No Peaks

X-Ray for Sample #31 (As Coated) with Glass Substrate
using Cr Target and Vd Filter

No Peaks

TABLE B.3

X-RAY DIFFRACTION DATA FOR Ni-Cr-Cr_2O_3 COATED INCONEL X-750 SUBSTRATE

X-Ray Run for Inconel X - 750 Substrate Using Cr Target with Vd Filter

2θ (degrees)	Intensity (Arbitrary Units)	d (Angstroms)	hkl
39.45	1.0	3.39	
43.95	5.0	3.06	
51.20	2.2	2.65	Cr_2O_3 (104)
67.60	Off Scale	2.06	Ni (111)
75.30	2.4	1.87	
79.90	8.5	1.78	Ni (200)

X-Ray Run for Inconel X - 750 Substrate with Sample #30 After Heat Treatment using Cr Target with Vd Filter

2θ (degrees)	Intensity (Arbitrary Units)	d (Angstroms)	hkl
36.5	1.1	3.65	(012)Cr_2O_3
43.7	2.2	3.07	Inconel
51.0	1.6	2.65	(104)Cr_2O_3
54.7	0.7	2.49	(110)Cr_2O_3
63.3	1.3	2.18	(113)Cr_2O_3
67.3	7.5	2.06	Inconel, Ni, Cr
75.3	0.5	1.87	Inconel
79.8	9.3	1.78	Inconel, Ni
86.3	0.8	1.67	(116)Cr_2O_3

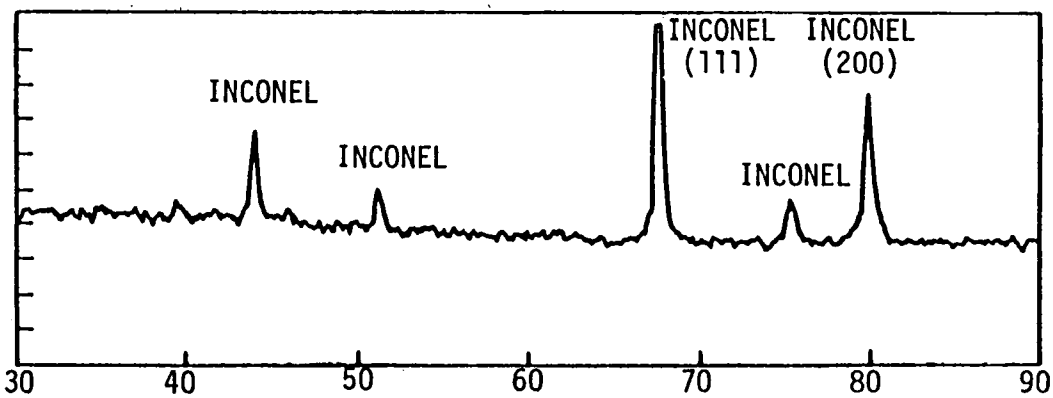

INCONEL X-750 SUBSTRATE

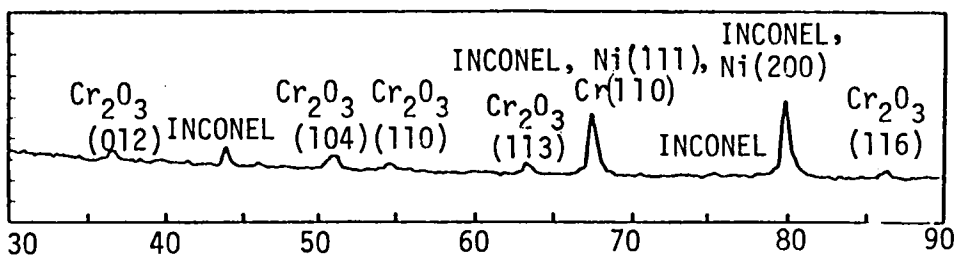

SAMPLE 30, SPUTTER DEPOSITED ON ANNEALED FOIL THEN HEAT TREATED (704°C/20 HRS/AC)

Fig. B.6 X-Ray Diffraction Data of the rf Sputter-Deposited Ni-Cr-Cr_2O_3 Coating on Inco X-750 Substrate

792856

APPENDIX C

METALLURGICAL ANALYSIS OF RF-SPUTTERED NICHROME COATING

AES ANALYSIS OF NICHROME

Auger electron spectroscopic analysis was carried out on Ni-Cr target chip and its coating (sample 33). The spectrum obtained are shown in Figure C.1. Here, as expected, the major peaks are for nickel and chromium with little amount of argon and carbon. The calculated ratio of Ni: Cr for the target chip is 1.00: 0.427, and for the coating is 1.00: 0.52. The ratio expected from the nominal composition is Ni: Cr = 1.00: 0.25. It thus appears that the sputter etching process used to clean the samples prior to the Auger measurement resulted in significant surface enrichment of the chromium component. However, the ratio for the coating and the targets are comparable.

X-Ray Diffraction Analysis of Ni-Cr

Nichrome coatings applied on carbon and glass substrates were analyzed. The results for the carbon blank, shown in the Table B.1, yielded, within the range of angles investigated, twelve peaks which we used for a background standard. The diffraction data patterns of Sample 33 are shown in Figure C.2 and data are given in Table C.1. Three-highly distinctive peaks appear both within the carbon and the glass diffraction patterns. These peaks positioned at approximately 39.60°, 44.20°, and 68.10° are indicative of the definite presence in this case of the Ni-Cr crystalline structure.

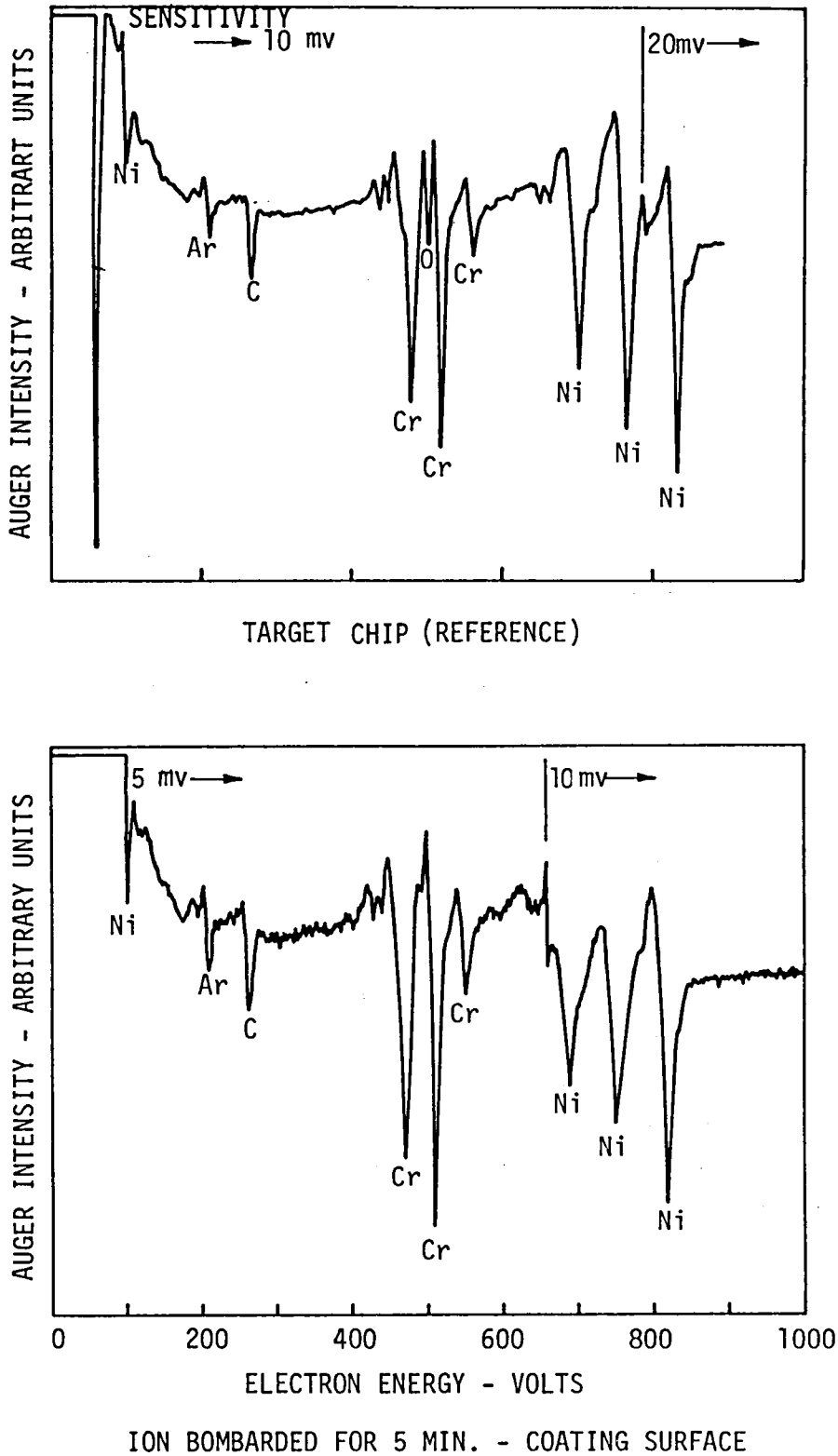

Fig. C.1 Auger Electron Spectra of rf Sputter-Deposited Ni-Cr Coating (Target chip and Sample 33)

793283

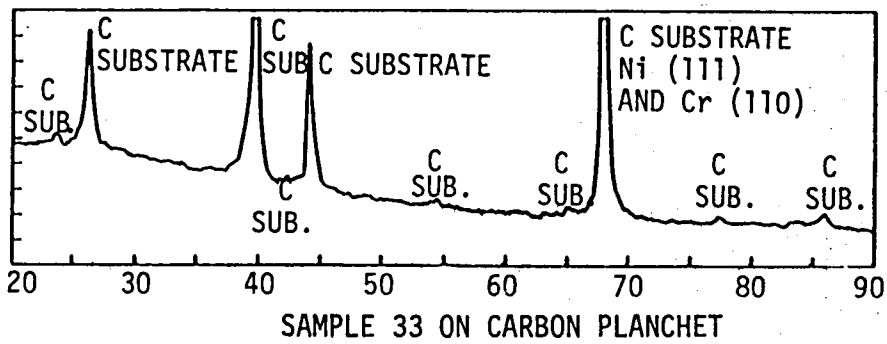

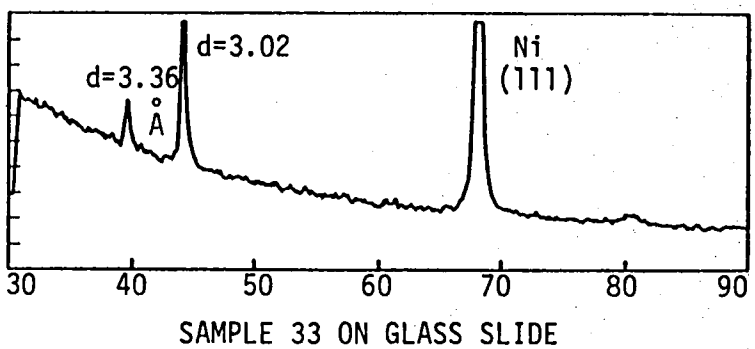

Fig. C.2 X-Ray Diffraction Data of the Sputter-Deposited Ni-Cr Coating on Carbon Planchet and Glass Slide

792858

TABLE C.1

X-RAY DIFFRACTION DATA FOR NICHROME COATING

X-Ray for Run #33 with Carbon Substrate using Cr Target and Vd Filter

2θ (degrees)	Intensity (Arbitrary Units)	d (Angstroms)	hkl
23.70	0.9	5.57	
26.30	9.0	5.01	
39.60*	Off Scale	3.36	(002)
42.30	0.6	3.16	
44.10*	11.3	3.03	
54.50	0.6	2.49	
65.10	0.7	2.12	(100)
68.00	Off Scale	2.03	(101)
77.40	0.5	1.82	
83.60	0.5	1.71	
85.90	1.1	1.67	(004)

*Asterisk shows additional peaks to carbon planchet

X-Ray for Run #33 with Glass Substrate using Cr Target and Vd Filter

2θ (degrees)	Intensity (Arbitrary Units)	d (Angstroms)	hkl
39.60	3.7	3.36	
44.20	Off Scale	3.02	
68.10	Off Scale	2.03	Ni (111), Cr(110)

APPENDIX D

METALLURGICAL ANALYSIS OF RF-SPUTTERED Ni-Cr-Cr_3C_2 COATING

AES ANALYSIS

AES analyses of the target chip and the coated sample (as coated, sample 42) were carried out using the technique described earlier. All of the spectrum were taken with a primary electron beam of 3000 eV energy, 20μA current, and a modulation voltage of 3V peak to peak.

The spectrum obtained from the target chip after light ion bombardment cleaning is shown in Figure D.1. The spectrum shows primarily carbon, chromium and nickel, with smaller peaks for argon, embedded in the cleaning process, and molybdenum, arising from the sample holder used. Concentration ratios were calculated using the relative sensitivity factors published in the Handbook of Auger Electron Spectroscopy. The resulting ratios are: C: Cr: Ni = 1.00: 0.60: 0.09. The theoritical ratios are: C: Cr: Ni = 1: 1.66: 0.66. The reason for the discrepancy is not very well understood. It is possible that the steady state surface composition may be different than that of the bulk. The spectrum of the coating shows major peaks of C, Cr, Ni, with the usual embedded carbon. Concentration ratios calculated are C: Cr: Ni = 1.00: 0.61: 0.07. The final film composition is thus very close to the composition of the target.

X-Ray Diffraction Study

X-ray diffraction analysis of Ni-Cr-Cr_3C_2 coated glass slide (sample 42, as sputtered) yielded no peaks when analyzed, indicating the presence of an amorphous coating on the surface.

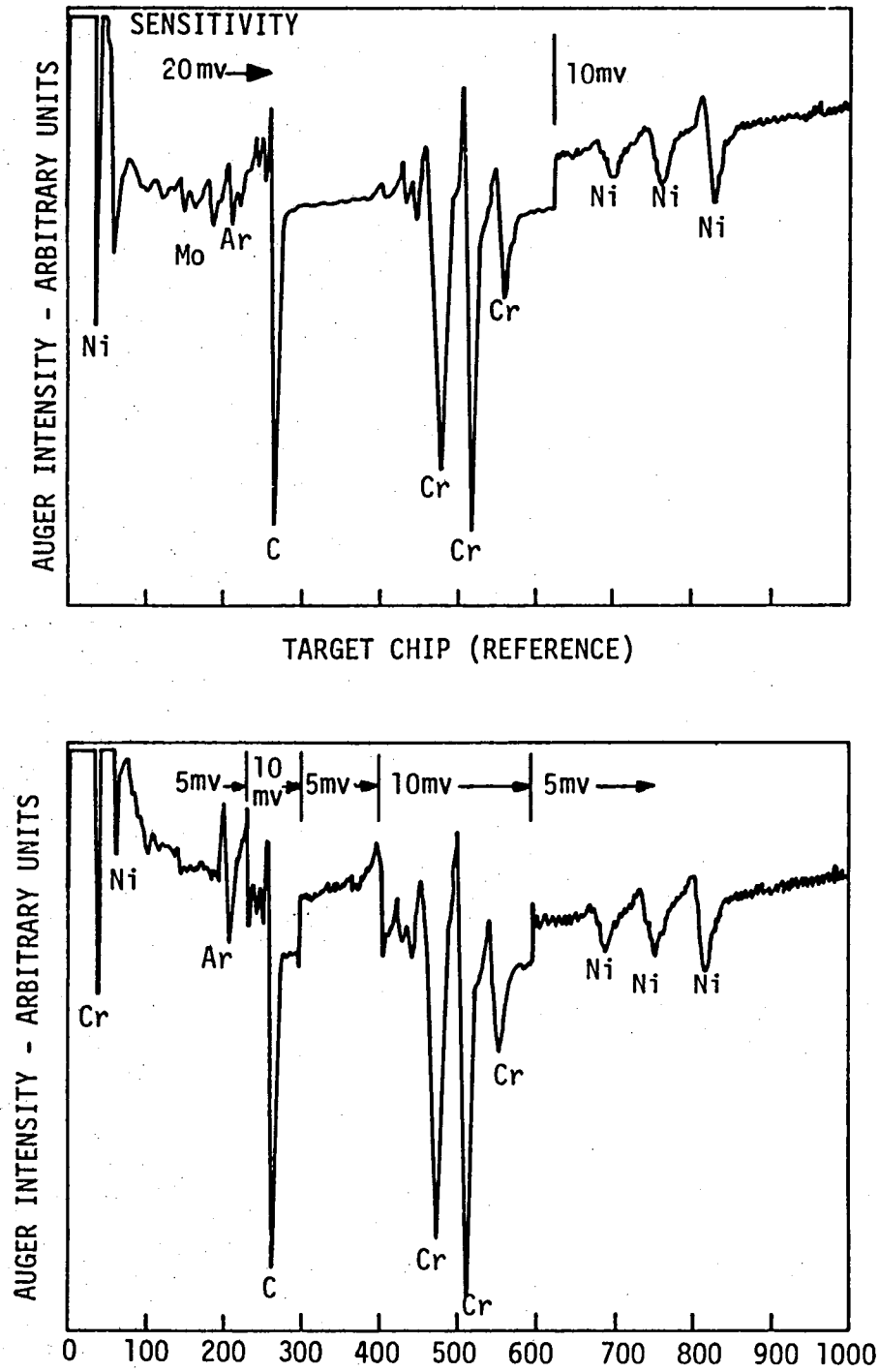

Fig. D.1 Auger Electron Spectra of rf Sputter-Deposited Ni-Cr-Cr_3C_2 (target chip and Sample 42)

APPENDIX E

THE EXAMINATIONS OF TEST SAMPLES BEFORE AND AFTER STATIC OVEN SCREENING

E-1 VISUAL INSPECTION

Table E.1 Examination of Coated A286 Coupons

Table E.2 Examination of Coated Inconel X-750 Coupons

TABLE E.1

EXAMINATION OF COATED A-286 COUPONS - OVEN SCREENING TEST

No.	Coating	Before/ After Oven Test	Max. Test Temp.	Color	Surface Adhesion Test by Scotch Tape	Scratch Test Under Microscope	Microscope Examination (X400 max)	Coating Hardness	Wt. Gain Gms	Thick-ness Gain mm	Comments	Selected for Start-Stop Test
1	Kaman DES	Before		Greenish Gray	Coating did not come off	Scratched with more loose particles on sides	Granular structure of the coating	-			Loose coating particles came off during first two tape pulls in after-oven samples. Color of coating became greenish after exposure; probably coating was deficient in O_2 and oxidized to stable Cr_2O_3.	Yes
		After	A	Grayish Green	Coating did not come off	Scratched with more loose particles on sides	Granular structure of the coating	-	0.0035	-		
2	Kaman SCA	Before		Dark Gray	Coating did not come off		Granular structure of the coating	-			Color of coating changed during oven test; probably coating was deficient in oxygen and oxidized to stable Cr_2O_3.	Yes
		After	A	Green	Coating did not come off	Scratched with more loose particles on sides than before oven samples	Granular structure of the coating	-	0.0085	-		
3	Linde Cr_3C_2 (D.G.)	Before		Light Gray	Coating did not come off			82 (15-N)≡			Surface of the coating oxidized. Light polishing removed the oxidized laver.	Yes
		After	A	Grayish black	Coating did not come off	Scratched same	Could not see due to poor reflection	82 (15-N)	0.0296	-		
4	71% PbO, 4% SiO_2, 25% Ag (fused) Run #5	Before		Black with silver spots	Coating did not come off	Scratched with very little loose wear debris	Could see silver particles in the coating	64-66 (15-N)			Surface became brownish, probably PbO converted to Pb_3O_4 at surface. Very light polishing removed this layer. Coating appearance underneath unchanged.	Yes
		After	A	Black with silver spots	Coating did not come off	Scratched with very little loose wear debris	Could see silver particles in the coating	72-74 (15-N)	0.0012	1		

TABLE E.1 (cont'd)

No.	Coating	Before/ After Oven Test	Max. Test Temp.	Color	Adhesion Test by Scotch Tape	Scratch Test Under Microscope	Microscope Examination (X400 max)	Coating Hardness	Wt. Gain Gms	Thick-ness Gain mm	Comments	Selected for Start-Stop Test
5	85.2% PbO, 4.8% SiO_2 & 10% Ag (Run #8)	Before		Black	Coating did not come off	-	Fairly smooth	42-47 (15-N)			Surface became brownish probably PbO converted to Pb_3O_4 at surface. Very light polishing removed this layer. Coating appearance underneath unchanged.	Yes
		After	A	Brown at top Black under-neath	Coating did not come off	-	Fairly smooth	60 (15-N)	-	-		
6	NASA PS120 (P.S.)	Before		Steel Gray	Coating did not come off		Fairly smooth, could see silver particles	60-65 (15-N)	-	-	Coating peeled off at the interface entirely.	No
		After	A	Black	Coating did not come off		Coating peeled off	-	-	-		
7	NASA PS122 (P.S.)	Before		Steel Gray	Nothing came off	-	Fairly smooth	69-72 (15-N)	-	-	Coating peeled off at the interface entirely	No
		After	A	Black	Nothing came off	-	Coating peeled off		-	-		
8	ZrO_2-CaF_2 (P.S.)	Before		Grayish White	Nothing came off	-	Coating porous	57-63 (15-N)	-	-	Coating separated at the interface during thermal cycling.	No
		After	A	Yellow-ish White	Nothing came off	-	Coating separated	-	-	-		
9	Cr_2O_3 (sp.)	Before		Dark Gray	Nothing came off	Crack with no branch cracking	Smooth, can see substrate topography	-	-	-	Coating unchanged.	Yes
		After	A	Dark Gray	Nothing came off	Crack with no branch cracking	Smooth, can see substrate topography	-	-	-		

TABLE E.1 (cont'd)

No.	Coating	Before/ After Oven Test	Max. Test Temp.	Color	Surface Adhesion Test by Scotch Tape	Scratch Test Under Microscope	Microscope Examination (X400 max)	Coating Hardness	Wt. Gain Gms	Thick-ness Gain mm	Comments	Selected for Start-Stop Test
10	NASA PS 122 (P.S.)	Before		Steel Gray	Nothing came off	-	Fairly smooth	69-72 (15-N)			Coating changed color otherwise unchanged.	Yes
		After	B	Dark Gray	Nothing came off	-	fairly smooth	67-78 (15-N)	0.18	<1		
11	NASA PS120 (P.S.)	Before		Steel Gray	Nothing came off	-	fairly smooth	60-65 (15-N)			Ag on the coating surface much more obvious and the coating feels rougher after oven test. Silver probably melted and agglomerated.	Yes
		After	B	Mostly Ag in black back-ground	Nothing came off	-	Silver much more prominent	59-66 (15-N)	0.33	1		
12	CdO-Graphite on Metco Cr_3C_2	Before		Black	Very little coating came off	-	Could see CdO par-ticles	-			Coating appearance unchanged.	Yes
		After	C	Black	Very little coating came off	Scratched same	Could see CdO particles	-	-0.0479	0.05		

A - 650°C/100 hrs/10 thermal cycles

B - 540°C/100 hrs/10 thermal cycles

C - 427°C/100 hrs/10 thermal cycles

TABLE E.2

EXAMINATION OF COATED INCO X-750 COUPONS OVEN SCREENING TEST

No.	Coating	Before/ After Oven Test	Maximum Test Temp.	Color	Flex Test 4×10^6 Cycles Total Flex 12.7 mm	Surface Adhesion Test by Scotch Tape	Scratch Test Under Microscope	Microscope Examination (x 400 max.)	Weight Gain Gms	Thickness Gain mm	Comments	Selected for Start-Stop Test
-		Before		Grayish black	OK	Coating did not come off	Scratched with some debris on sides	Could see substrate topography-smooth coating		-	Coating appearance unchanged	
1	Cr_2O_3 (bias sp.) Run #12	After	A	Dark gray with streaks of green	OK	Coating did not come off	Scratched with some debris on sides	Could see substrate topography-smooth coating	-0.0006	-		No
		Before		Grayish black with green tint	OK	Coating did not come off	Scratched with very little debris on sides	Could see substrate topography-smooth coating	-	-	Coating appearance unchanged	
2	Cr_2O_3 (sp. deposit) Run #15	After	A	Grayish black	OK	Coating did not come off	Scratched with very little debris on sides	Could see substrate topography-smooth coating	-0.0004	-		Yes
		Before		Grayish black	OK	Coating did not come off	Scratched with some debris on sides	Could see substrate topography-smooth coating		-	Coating appearance unchanged	
3	Cr_2O_3 (sp. deposit) Run #16	After	A	Black with green tint	OK	Coating did not come off	Scratched with some debris on sides	Could see substrate topography smooth coating	0.0002			Yes

TABLE E.2 (cont'd)

No.	Coating	Before/ After Oven Test	Maximum Test Temp.	Color	Flex Test $4x10^6$ Cycles Total Flex 12.7 mm	Surface Adhesion Test by Scotch Tape	Scratch Test Under Microscope	Microscope Examination (x 400 max.)	Weight Gain Gms	Thickness Gain mm	Comments	Selected for Start-Stop Test
4	Cr_2O_3 (sp. deposit) on annealed foil Run #13A	Before		Grayish black	OK	Coating did not come off	Scratched with some debris on sides	Could see substrate topography-smooth coating			Coating appearance unchanged	Yes
		After	A	Grayish black	OK	Coating did not come off	Scratched with some debris on sides	Could see substrate topography-smooth coating	-	-		
5	TiC (sp.) Quad Group	Before		Steel gray	OK	Coating did not come off	Scratched with some debris on sides	Could see substrate topography-coating uniform	0.0006	-	Coating was 3000°A thick. Coating completely oxidized during oven test.	No
		After	A	Substrate Color	OK	Coating did not come off	Scratched with some debris on sides	Could see substrate topography-				
6	Ag (sp.)	Before		Silver	OK	Coating did not come off	Scratched with some debris on sides	Smooth and uniform coating			Surface oxidized. Coating intact underneath	Yes
		After	A	Brownish black	OK	Coating did not come off	Could see silver under scratch		0.0069			

TABLE E.2 (cont'd)

No.	Coating	Before/ After Oven Test	Maximum Test Temp.	Color	Flex Test $4x10^6$ Cycles Total Flex 12.7 mm	Surface Adhesion Test by Scotch Tape	Scratch Test Under Microscope	Microscope Examination (x 400 max.)	Weight Gain Gms	Thick-ness Gain mm	Comments	Selected for Start-Stop Test
7	Kaman DES 50-100 µin. thick	Before		Irides-cence of brown, green, etc.	OK	Coating did not come off	Scratched with some debris on sides	Could see substrate topography-coating granular			No change in coating appearance after test	Yes
		After	A	Irides-cence of brown, green, etc.	OK	Coating did not come off	Scratched with some debris on sides	Could see substrate topography-coating granular				
8	Ni-Cr-Cr_2O_3 (sp. deposit) Run #38	Before		Dark steel gray	OK	Nothing came off	-	Smooth coating, can see substrate topography			Coating color changed. Free chromium in the coating oxidized to stable Cr_2O_3	Yes
		After	A	Irides-cence of green, red in grayish black	OK	Nothing came off	-	Microspots on the surface	- 0.0014			

TABLE E.2 (cont'd)

No.	Coating	Before/ After Oven Test	Maximum Test Temp.	Color	Flex Test 4×10^6 Cycles Total Flex 12.7 mm	Surface Adhesion Test by Scotch Tape	Scratch Test Under Microscope	Microscope Examination (x 400 max.)	Weight Gain Gms	Thickness Gain mm	Comments	Selected for Start-Stop Test
9	Ni-Cr (sp. deposit) Run #39	Before		Steel gray	OK	Nothing came off	-	Smooth coating can see substrate topography			Free chromium oxidized to stable Cr_2O_3. No other change in general appearance	Yes
		After	A	Iridescence of green and red	OK	Nothing came off	-	Surface spotty	-0.0020			
10	Ni-Cr-Cr_2O_3 w/Ni-Cr underlay on annealed foil (sp. deposit) Run #40	Before		Steel gray	OK	Nothing came off	-	Coating smooth, can see substrate topography			Coating color changed, appearance same otherwise	Yes
		After	A	Iridescence of green and red	OK	Nothing came off	-	Microspots on the surface	-0.0016			
11	Ni-Cr-Cr_2O_3 w/Ni-Cr underlay and Ag overlay (sp. deposit) Run #41	Before		Silver color	OK	Nothing came off.	-	Surface reflective, can see some substrate topography			Coating after oven test became spotty probably silver oxidized somewhat as expected	Yes
		After	A	Almost black	OK	Nothing came off	-	Surface has numerous microspots	-.0014	-		

TABLE E.2 (cont'd)

No.	Coating	Before/ After Oven Test	Maximum Test Temp.	Color	Flex Test 4×10^6 Cycles Total Flex 12.7 mm	Surface Adhesion Test by Scotch Tape	Scratch Test Under Microscope	Microscope Examination (x 400 max.)	Weight Gain Gms	Thickness Gain mm	Comments	Selected for Start-Stop Test
12	Ni-Cr-Cr_3C_2 (sp. deposit)	Before		Steel gray	OK	Nothing came off	-	Smooth, can see substrate topography			It seems coating reacted and became spotty	No
		After	A	Yellowish gray and spotty	OK	Nothing came off	-	Surface very spotty	-0.0017	-		
13	Ni-Cr Cr_3C_2 (bias sp.)	Before		Light gray	OK	Nothing came off	-	Smooth, can see substrate topography			It seems coating reacted and became spotty	No
		After	A	Yellowish gray and spotty	OK	Nothing came off	-	Surface very spotty	-0.0013	-		
14	Ni-Cr-Cr_3C_2 (sp. deposit) on annealed foil	Before		Light gray	OK	Nothing came off	-	Smooth can seen substrate topography			It seems coating reacted and became spotty	No
		After	A	Blue with spots	OK	Nothing came off	-		-.0020	-		

TABLE E.2 (cont'd)

No.	Coating	Before/ After Oven Test	Maximum Test Temp.	Color	Flex Test 4×10^6 Cycles Total Flex 12.7 mm	Surface Adhesion Test by Scotch Tape	Scratch Test Under Microscope	Microscope Examination (x 400 max.)	Weight Gain Gms	Thickness Gain mm	Comments	Selected for Start-Stop Test
15	61.5% PbO, 3.5% SiO_2-25% Ag, 10% Fe_3O_4 (fused) Run #6	Before		Black with Ag particles	OK	Nothing came off	Scratched with little debris	Coating porous			Top of the coating oxidized. When burnished, coating underneath OK	Yes
		After	A	Brownish black with Ag particles	OK	Nothing came off	Scratched with little debris	Coating became rougher				
16	CaF_2-BaF_2 eutectic + Ag OSF 6 (fused)	Before		Nearly black	OK	Nothing came off	-		-		Coating oxidized on surface with blisters. Coating intact underneath.	Yes
		After	A	Grayish black	OK	Nothing came off	-	Looks rough				
17	75.8% PbO, 4.2% SiO_2, 10% Ag, 10% Fe_3O_4 (Run #7) (fused)	Before		Black	OK	Nothing came off	-	Smooth			Can see some coating on edges of uncoated side. Probably melted and flowed somewhat. Coating recrystallized probably due to melting. After polishing, original coating can be recovered.	Yes
		After	A	Black	OK	Nothing came off	-	Forms a crystalline structure-surface rougher	0.003	1		

TABLE E.2 (cont'd)

No.	Coating	Before/ After Oven Test	Maximum Test Temp.	Color	Flex Test $4x10^6$ Cycles Total Flex 12.7 mm	Surface Adhesion Test by Scotch Tape	Scratch Test Under Microscope	Microscope Examination (x 400 max.)	Weight Gain Gms	Thickness Gain mm	Comments	Selected for Start-Stop Test
18	85.2% PbO, 4.8% SiO_2, 10% Fe_3O_4 (Run #9) (fused)	Before		Black	OK	Nothing came off	-	Smooth			Coating surface appearance unchanged	Yes
		After	A	Black	OK	Nothing came off	-	Smooth	0.0002	-		
19	TiC (ARE)	Before		Gray	OK	Nothing came off	Scratched with very little debris	Coating smooth and uniform			Coating foil as received was stressed. Coating in more than half of the foil was oxidized.	No
		After	B	Gray where coating survived	OK	Nothing came off	Scratched with very little debris	Coating in most of the area oxidized	0.005	-		
20	HfN (ARE)	Before		Gray	OK	Nothing came off		Coating smooth and uniform			Coating oxidized. The surface had interference pattern due to thin coating left after oxidization.	No
		After	B	Almost black Iridescence of blue, red and purple	OK	Nothing came off		Coating oxidized	0.007	-		

TABLE E.2 (cont'd)

No.	Coating	Before/ After Oven Test	Maximum Test Temp.	Color	Flex Test 4×10^6 Cycles Total Flex 12.7 mm	Surface Adhesion Test by Scotch Tape	Scratch Test Under Microscope	Microscope Examination (x 400 max.)	Weight Gain Gms	Thickness Gain mm	Comments	Selected for Start-Stop Test
21	CdO-Graphite (Air sprayed)	Before		Black	OK	Very little coating came off	Scratched with some debris on sides	Dark with visible CdO particles			Coating appearance unchanged	Yes
		After	C	Black	OK	Very little coating came off	Scratched with some debris on sides	Dark with visible CdO particles	-0.0085	-		
22	CdO-Graphite Ag (Air sprayed)	Before		Black with silver spots	OK	Very little coating came off	Scratched with some debris on sides	Dark with visible Ag particles			Coating turned yellowish at spots	Yes
		After	C	Black with silver spots	OK	Very little coating came off	Easier to flake off coating	Dark with visible Ag particles	-0.028	-0.2		

*Heated in a metal muffle

TABLE E.2 (cont'd)

No.	Coating	Before/ After Oven Test	Maximum Test Temp.	Color	Flex Test 4×10^6 Cycles Total Flex 12.7 mm	Surface Adhesion Test by Scotch Tape	Scratch Test Under Microscope	Microscope Examination (x 400 max.)	Weight Gain Gms	Thickness Gain mm	Comments	Selected for Start-Stop Test
23	CdO-Graphite Ag* (Air sprayed)	Before		Black with silver spots	OK	Very little coating came off					Coating unchanged in color and general appearance	Yes
		After	C	Black with silver spots	OK	Very little coating came off	Easier to flake off coating	Dark with visible Ag particles	-.0119	-		
24	Kaman DES+ SCA (C.A.)	Before		Greenish black	OK	Nothing came off	Scratched with some debris on sides	Can't see any structure			Coating became greener after oven test probably oxygen deficient chrome oxide turned to most stable oxide-Cr_2O_3	Yes
		After	A	Greenish dark gray	OK	Nothing came off	Scratched with some debris on sides	Can't see any structure	-0.0027			

* Heated in a metal muffle.

A - 650°C/100 hours/10 thermal cycles

B - 540°C/100 hours/10 thermal cycles

C - 427°C/100 hours/10 thermal cycles

APPENDIX F

PHOTOGRAPHS OF BEARING SURFACES AFTER START/STOP TESTS

The Appendix includes the photographs (Figures F.1 to F.15) of the journal and foil surfaces after partial arc start/stop tests, not included in Section IV.

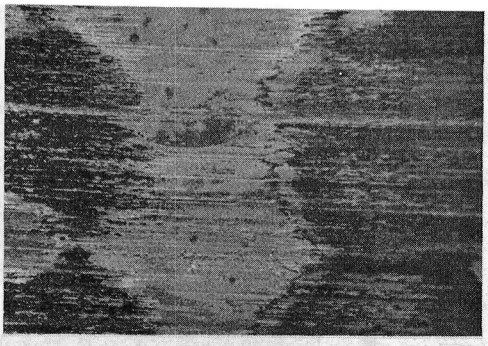

7X

PREOXIDIZED FOIL

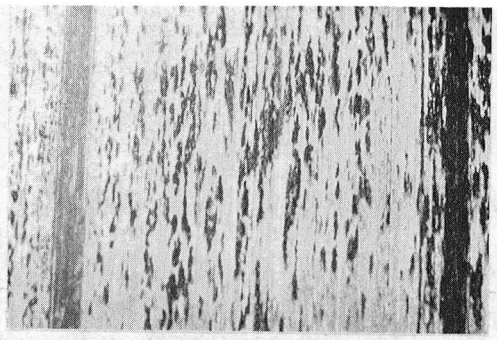

7X

PREOXIDIZED JOURNAL

Fig. F.1 Photographs of Surfaces After 1500 Cycles
(Max. Temp.-650°C, Test No. 4)

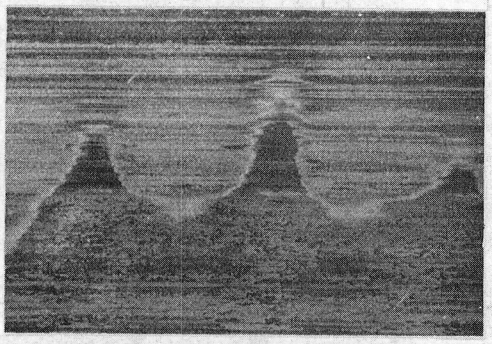

7X

CdO-GRAPHITE ON FOIL

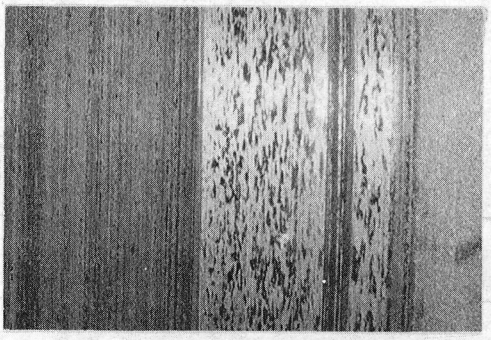

7X

CdO-GRAPHITE ON JOURNAL

Fig. F.2 Photographs of Surfaces After 3000 Cycles
(Max. Temp.-427°C, Test No. 8)

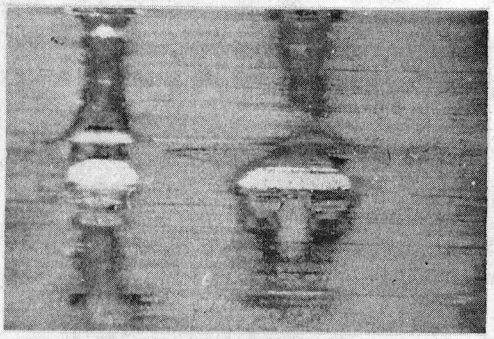

7X

CdO-GRAPHITE ON FOIL

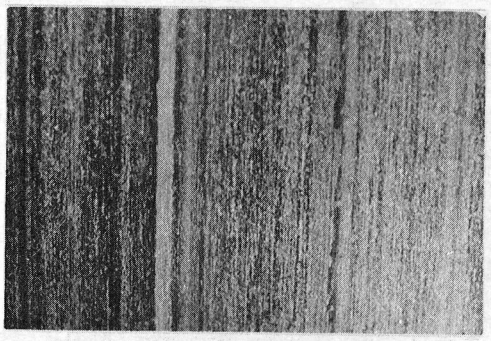

7X

CdO-GRAPHITE + METCO Cr_3C_2
ON JOURNAL

Fig. F.3 Photographs of Surfaces After 3000 Cycles
(Max. Temp.-650°C, Test No. 5)

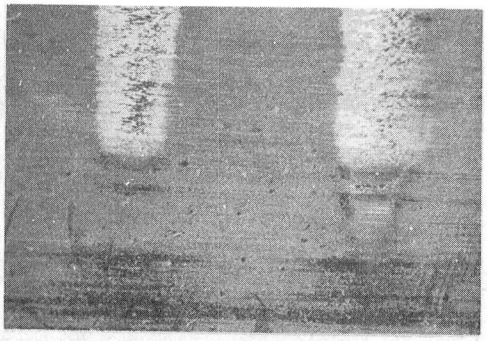

7X

CdO-GRAPHITE-Ag ON FOIL

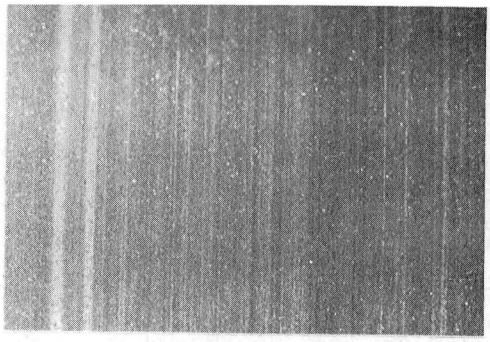

7X

Cr_3C_2 ON JOURNAL

Fig. F.4 Photographs of Surfaces After 3000 Cycles
(Max. Temp.-427°C, Test No. 3)

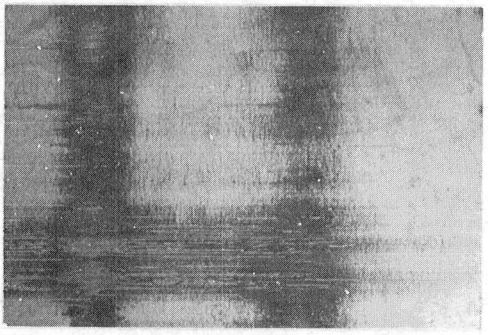

7X

PREOXIDIZED FOIL

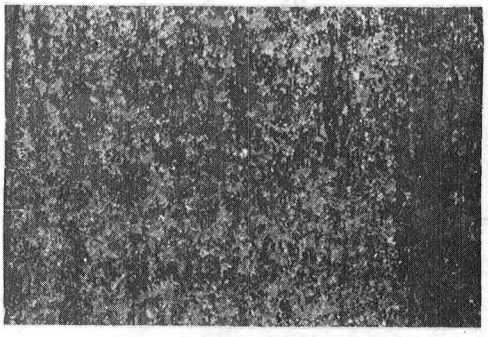

7X

NASA PS 120 ON JOURNAL

Fig. F.5 Photographs of Surfaces After 3000 Cycles
(Max. Temp. - 540°C, Test No. 13)

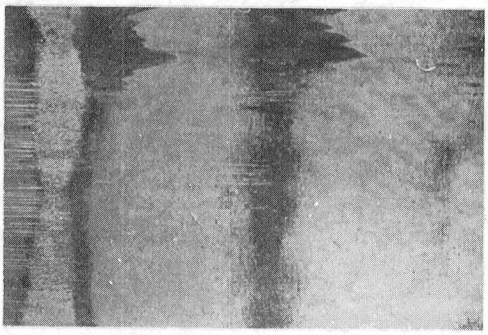

7X

PREOXIDIZED FOIL

7X

NASA PS 122 ON JOURNAL

Fig. F.6 Photographs of Surfaces After 4500 Cycles
(Max. Temp. - 540°C, Test No. 15)

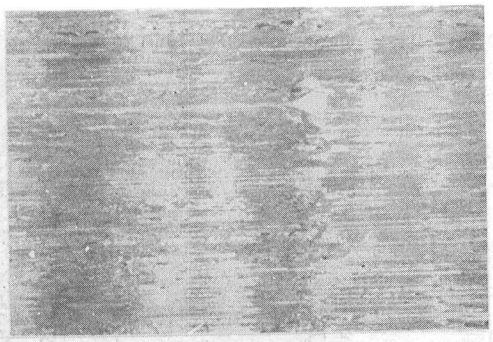

7X

PREOXIDIZED FOIL

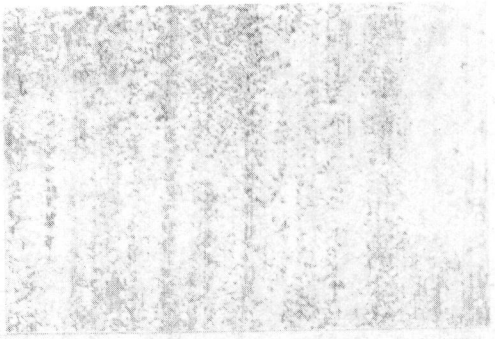

7X

ZrO_2 - CaF_2 ON JOURNAL

Fig. F.7 Photographs of Surfaces After 600 Cycles
(Max. Temp. - 650°C, Test No. 26)

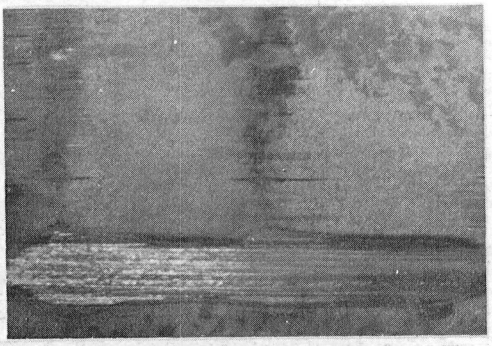

7X

PbO-SiO_2-Ag-Fe_3O_4 ON FOIL

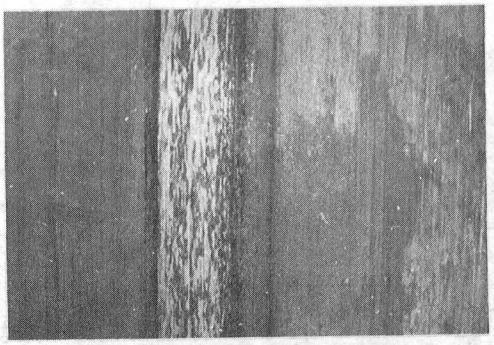

7X

PREOXIDIZED JOURNAL

Fig. F.8 Photographs of Surfaces After 1000 Cycles
(Max. Temp. - 260°C, Test No. 9)

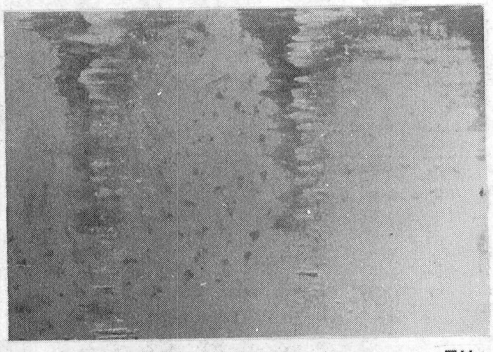

7X

PREOXIDIZED FOIL

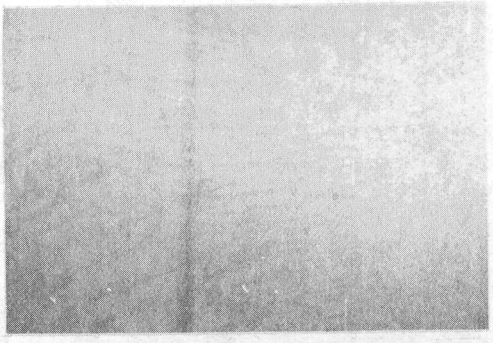

7X

PbO-SiO_2-Ag ON JOURNAL

Fig. F.9 Photographs of Surfaces After 1000 Cycles
(Max. Temp. - 260°C, Test No. 10)

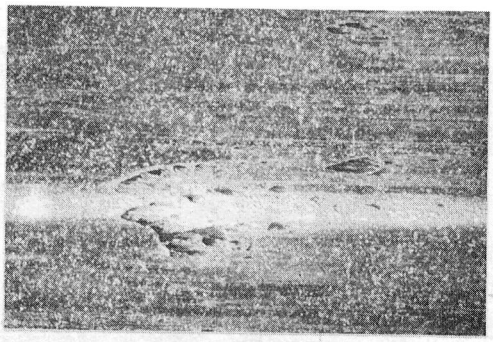

7X

$PbO-SiO_2-Ag-Fe_3O_4$ ON FOIL

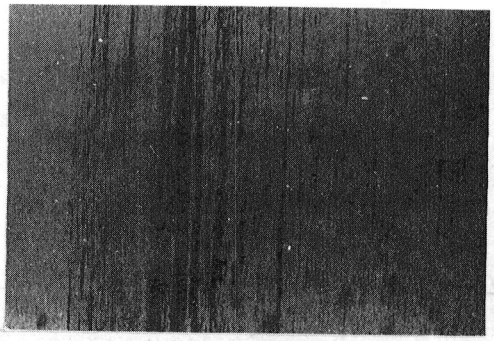

7X

PREOXIDIZED JOURNAL

Fig. F.10 Photographs of Surfaces After 50 Cycles
(Max. Temp. - 260°C, Test No. 17)

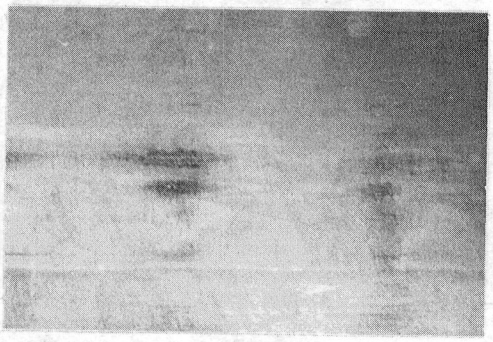

7X

PREOXIDIZED FOIL

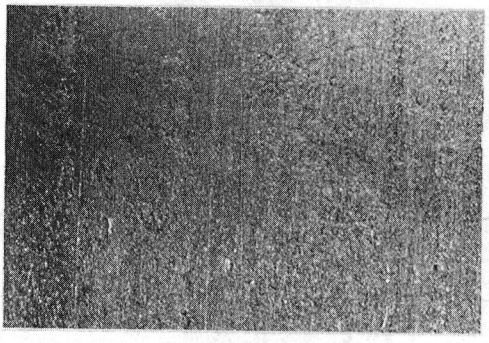

7X

$PbO-SiO_2-Ag$ ON JOURNAL

Fig. F.11 Photographs of Surfaces After 100 Cycles
(Max. Temp. - 260°C, Test No. 18)

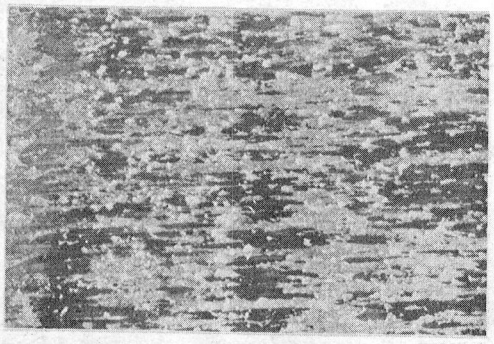

7X

$PbO-SiO_2-Fe_3O_4$ ON FOIL

7X

PREOXIDIZED JOURNAL

Fig. F.12 Photographs of Surfaces After 150 Cycles
(Max. Temp. - 370°C, Test No. 21)

7X

CaF_2-B_aF_2-Ag ON FOIL

7X

PREOXIDIZED JOURNAL

Fig. F.13 Photographs of Surfaces After 100 Cycles
(Max. Temp. - 650°C, Test No. 16)

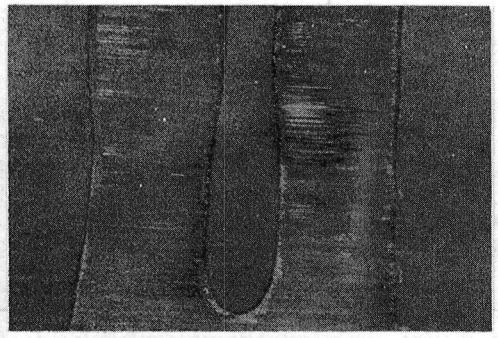

7X

Ni-Cr-Cr_2O_3 ON FOIL

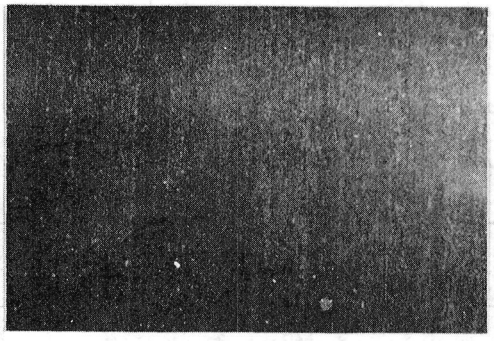

7X

Cr_3C_2 ON JOURNAL

Fig. F.14 Photographs of Surfaces After 3000 Cycles
(Max. Temp. - 650°C, Test No. 7)

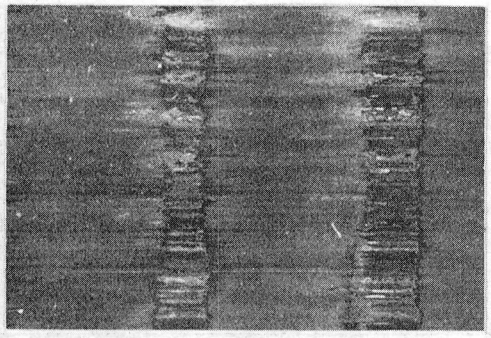

7X

Cr_2O_3 ON FOIL

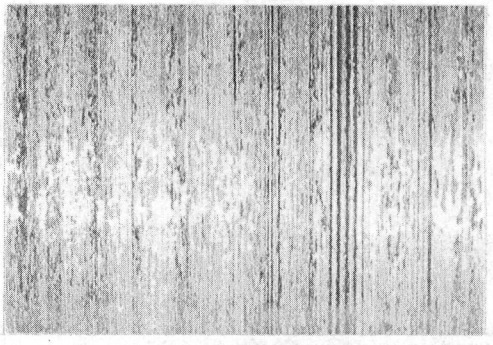

7X

Cr_2O_3 ON JOURNAL

Fig. F.15 Photographs of Surfaces After 3000 Cycles
(Max. Temp. - 650°C, Test No. 24)

1. Report No.	2. Government Accession No.	3. Recipient's Catalog No.
NASA CR-159848		

4. Title and Subtitle	5. Report Date
HIGH TEMPERATURE SELF-LUBRICATING COATINGS FOR AIR LUBRICATED FOIL BEARINGS FOR THE AUTOMOTIVE GAS TURBINE ENGINE	April 1980
	6. Performing Organization Code
7. Author(s)	8. Performing Organization Report No.
Bharat Bhushan	MTI 79TR76
	10. Work Unit No.
9. Performing Organization Name and Address	
Mechanical Technology Incorporated 968 Albany-Shaker Road Latham, New York 12110	11. Contract or Grant No. DEN 3-43
	13. Type of Report and Period Covered
12. Sponsoring Agency Name and Address	Contractor Report
U.S. Department of Energy Division of Transportation Energy Conservation Washington, D.C. 20545	14. Sponsoring Agency Code DOE/NASA/0043-2

15. Supplementary Notes

Final report. Prepared under Interagency Agreement EC-77-A-31-1040. Project Manager, Harold E. Sliney, Structures and Mechanical Technologies Division, NASA Lewis Research Center, Cleveland, Ohio 44135.

16. Abstract

The objective of this program was to further develop the coating combinations identified in a previous program for compliant surface bearings and journals to be used in an automotive gas turbine engine. The coatings should be able to withstand the sliding start/stops during rotor liftoff and touchdown and occasional short-time, high speed rubs under representative loading of the engine - 14 kPa and at 35 kPa if possible, and at a maximum temperature of 427° - 650° C. Some dozen coating variations of CdO-graphite, Cr_2O_3 (by sputtering) and CaF_2 (plasma sprayed) were identified. The coatings were optimized and they were examined for stoichiometry, metallurgical condition, and adhesion. Sputtered Cr_2O_3 was most adherent when optimum parameters were used and it was applied on an annealed (soft) substrate. Metallic binders and interlayers have been used to improve the ductility and the adherence. The following coating combinations have satisfied the above requirements: CdO-graphite-Ag (HL-800-2^{TM}) on foil versus det. gun Cr_3C_2 good up to 427° C and sputtered Cr_2O_3 versus det. gun Cr_3C_2 good from RT to 427° - 650° C.

17. Key Words (Suggested by Author(s))	18. Distribution Statement
Gas bearings; Sputtering; Foil bearings; Detonation gun; Coatings; Air spray; Materials; Plasma spray	Unclassified - unlimited STAR Category 27 DOE Category UC-96

19. Security Classif. (of this report)	20. Security Classif. (of this page)	21. No. of Pages	22. Price*
Unclassified	Unclassified	231	A11

* For sale by the National Technical Information Service, Springfield, Virginia 22161

*USGPO: 1980 — 657-145/5229